CORRELATING CHROMATIN STATES WITH SILENCING PHENOTYPES IN *SACCHAROMYCES CEREVISIAE*

Thesis submitted for the degree of
Doctor of Philosophy
at the University of Leicester

by

Esther R. Loney

Department of Genetics
University of Leicester

August 2005

ProQuest LLC
789 East Eisenhower Parkway
P.O. Box 1346
Ann Arbor, MI 48106-1346

Declaration

The work reported in this thesis was performed by myself, Esther Loney, in the Department of Genetics at the University of Leicester.
Except where acknowledgement is made, the work is my own and has not been submitted for any other degree.

Acknowledgments

First I would like to thank Ed for his supervision and enthusiasm to sponsor me to pursue my D. Phil in his lab. I have appreciated your willingness to let me pursue my own path over the last several years and for your advice and friendship along the way. I would also like to thank the entire yeast group and everyone I have worked with in Leicester for their scientific advice, training and friendship. I certainly could never have done this without the help of so many of you. Special thanks to Peter and Marcus for training, scientific discussions and of course your friendship; Pat for always agreeing to my endless special requests with a smile and for invaluable training on the squash court, you're one of a kind!; Alex for your friendship and humour, I'll miss the whistles!; and of course to Rob and Stu for believing that as a proud Canadian I really do live in an igloo, club seals and go polar bear hunting. I have enjoyed your endlessly creative jokes!; and particular thanks to Rhona for her friendship, scientific advice and especially for reading this thesis which is definitely beyond the call of duty!; and to all other members of the yeast labs past and present for your friendship, its been a great three years.

To all my friends in Leicester that aren't members of the yeast group, thank you so much for making my time in England wonderful, for your support, particularly during my first year alone and for your continuing friendship. You've all got a place to stay if you ever come to Canada. For my Canadian friends, in particular Shereen and Erin, I can only say thank you for always standing with me and encouraging me, your friendship over the years has been invaluable.

Emmet, thank you for everything! You've supported my pursuit of this degree from the beginning, you even moved countries for me. I never could have done it without you beside me, keeping me sane and happy. I know its been a long year but hopefully you can have your wife back now!

And finally to my family who have supported me in all my pursuits. In particular to my parents and my sister for your constant love, friendship and encouragement, and for even pretending you're interested in telomeres now and then! All I can say is thank you for everything and for making this possible.

CONTENTS

Figures and Tables

CHAPTER 1

CHAPTER 2

CHAPTER 3

CHAPTER 4

CHAPTER 5

CHAPTER 6

CHAPTER 7

APPENDIX

Correlating chromatin states with silencing phenotypes in *Saccharomyces cerevisiae*

Esther Loney, University of Leicester
A thesis submitted for the degree of Doctor of Philosophy, August, 2005

Abstract

The structure of chromatin is indicative of its expression status. This work explores the structure of repressive and non-repressive subtelomeric regions at native telomeres and the effect of both cis- and trans-acting factors on these regions.

The region adjacent to the subtelomeric core X element exhibited a heterochromatic MNase digestion pattern, indicative of phased nucleosomes, at the repressive telomere and a euchromatic structure at the non-repressive telomere. *SIR2*, *SIR3* and *SIR4*, but not *SIR1* were all required for formation of the heterochromatic structure in addition to the gene repression. However, deletion mutants of several histone modifiers (*SET1*, *DOT1*, *BRE1*, *SAS2* and *BDF1*) disrupted silencing of the *URA3* marker without affecting the heterochromatic structure. Deletion of *yKU80*, known to be essential for TPE, moderately disrupted the heterochromatic features. Therefore, formation of a heterochromatic structure is required but insufficient for silencing. Mutations in the ACS and Abf1p binding element in core X, known to decrease TPE, also caused a moderate disruption of the heterochromatic features. Therefore, core X is proposed to be required for the establishment but not maintenance of TPE.

A loop model of the telomere structure involving a telomere-core X interaction, stabilized by factors bound to both loci (ORC, Abf1p, Rap1p, Sir's and yKu), was previously proposed to explain the discontinuous nature of silencing close to telomeres. In this study, yKu80p is found to associate with core X elements at repressive and non-repressive telomeres, in addition to its known association with the telomere repeats. Disruption of the ORC and Abf1p binding sites in core X was insufficient to disrupt yKu binding. Therefore, the loop is proposed to be present at all telomeres, not just those with regions of repression around core X. The loop is primarily stabilized by yKu and is independent of ORC association and perhaps other silencing factors. It is therefore proposed that the function of the loop structure is primarily to protect the telomere and the silencing effects due to the associated silencing factors are secondary.

Abbreviations

ACS	ARS consensus sequence
ARS	autonomous replication sequence
COMPASS	complex associated with Set1p
DNA-PK	DNA protein kinase
DSB	double strand break
E(var)	enhancer of variegation
HAT	histone acetyltransferase
HDAC	histone deacetylase
HMTase	histone methyltransferase
MNase	micrococcal endonuclease
NHEJ	non-homologous end-joining
ORC	origin recognition complex
ORF	open reading frame
PcG	polycomb group protein
PEV	position effect variegation
PRE	PcG response element
SIR	Silent information regulator
STAR	Subtelomeric anti-silencing regions
STR	subtelomeric repeat
Su(var)	suppressor of variegation
TAS	telomere associated sequences
TPE	telomere position effect
UAS	upstream activating sequence
Xic	X-inactivation centre

CHAPTER 1

1 Introduction

1.1 Telomeres

Telomeres are specialized structures at the ends of chromosomes that serve two major roles in eukaryotic cells; end protection and end replication (Blackburn and Greider, 1995). Telomeres prevent loss of genetic information from exonucleolytic degradation and incomplete replication by DNA polymerases and also prevent detrimental end-to-end fusions.

The most common telomere structure consists of a simple G-rich repeat sequence, maintained by the telomerase ribonucleoprotein complex, which terminates in a G-rich single-stranded overhang (reviewed in Lingner and Cech, 1998). In most unicellular organisms, including *Saccharomyces cerevisiae,* telomerase is a constitutively expressed enzyme but it is strongly suppressed in human somatic tissue (reviewed in Smogorzewska and de Lange, 2004). Some organisms have alternate means of maintaining chromosome ends such as the arrays of retrotransposons (*HeT-A* and *TART*) in *Drosophila* (Biessmann and Mason, 1997) and long tandem repeats in *Chironomus* and *Alliaceae* (Fig. 1.1) (Lopez *et al.*, 1996; Pich *et al.*, 1996). The length of the telomere is heterogeneous and varies considerably between species and strains, from approximately 350bp in *S. cerevisiae* to over a hundred kilobases in some higher organisms.

The subtelomeric regions of most eukaryotes consist of a mosaic of repetitive elements (Fig. 1.1) that are usually highly variable in sequence, copy number and location. These elements are known as the telomere associated sequences (TAS) (Flint *et al.*, 1997; Mefford *et al.*, 2001; Pryde *et al.*, 1997). In recent years it has become apparent that both telomeres and the TAS are specialized areas of the genome that may serve a number of functions in nuclear architecture, transcriptional control, DNA repair and genome stability, aging and the generation of genetic diversity through interactions with a variety of proteins including chromatin remodeling, double-strand break repair and replication factors.

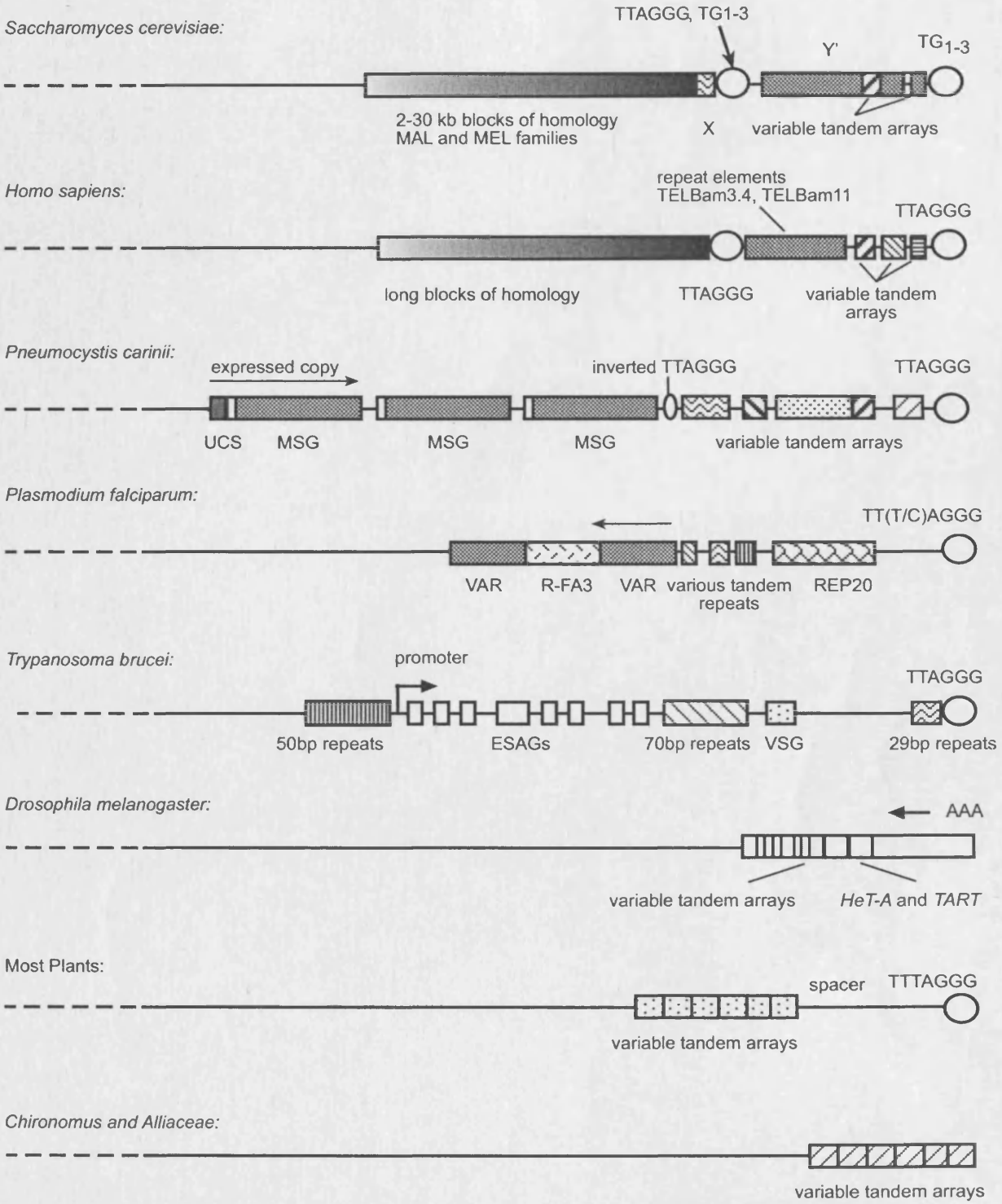

Figure 1.1. Eukaryotic chromosome ends.

1.1.1 Telomeres in *S. cerevisiae*

The telomeres of *S. cerevisiae* are relatively short consisting of 300 ± 50bp of a variable TG_{1-3} repeat, maintained by the yeast telomerase complex (see Section 1.2). In addition to telomerase, yeast telomeres are protected by formation of the telosome, a unique non-nucleosomal chromatin structure. The telosome is formed by the binding and interaction of a number of proteins with the telomere repeats, including Rap1p, the silent information regulators (Sir1-4p), yKu, and Rif1p and Rif2p (Rap1p interacting factors) (Gravel *et al.*, 1998; Wotton and Shore, 1997; Wright *et al.*, 1992; Wright and Zakian, 1995).

The TAS varies in composition between chromosome termini and yeast strains but contain a number of common elements (Fig. 1.2). The most telomere proximal element is the highly conserved Y' element that has similarities to transposable elements and is found in two classes, Y'-long (6.7kb) or Y'-short (5.2 kb) (Louis and Haber, 1990; Louis and Haber, 1992). The haploid S288C sequencing strain has up to four tandem copies of Y' at approximately 70% of the telomeres (Chan and Tye, 1983a; Chan and Tye, 1983b; Louis, 1995; Louis *et al.*, 1994). The function and origin of Y' elements is unknown, but they contain an autonomous replication sequence (ARS), degenerate telomere repeats and encode a helicase protein, indicating they may play an active role in the cell (Pryde and Louis, 1997; Yamada *et al.*, 1998). Centromere proximal to Y' are the small (45-150bp) subtelomeric repeats elements (STRA-D) and the 473bp core X element (Fig. 1.2) (Louis *et al.*, 1994; Pryde *et al.*, 1995). Similar to Y', the STR elements are present at some, but not all, ends and are found in differing arrangements. STR-A also contains degenerate telomere repeats that are binding sites for Tbf1p (Liu and Tye, 1991; Louis *et al.*, 1994; Pryde and Louis, 1997).

The core X subtelomeric element is the only one found at all ends in S288C. The overall degree of homology for core X is approximately 80% although several regions share almost perfect homology including an ARS consensus sequence (ACS), found at all ends, and a potential Abf1p binding site, found at all but one telomere (Fig. 1.2) (Pryde and Louis, 1997). The core X element affects gene expression near telomeres and may also aid in telomere protection via its ACS and Abf1p binding site (Pryde and Louis, 1997; Pryde and Louis, 1999). Abf1p is a transcription factor and essential DNA binding protein that also functions in repression of specific loci while the ACS element is a binding site for the yeast origin

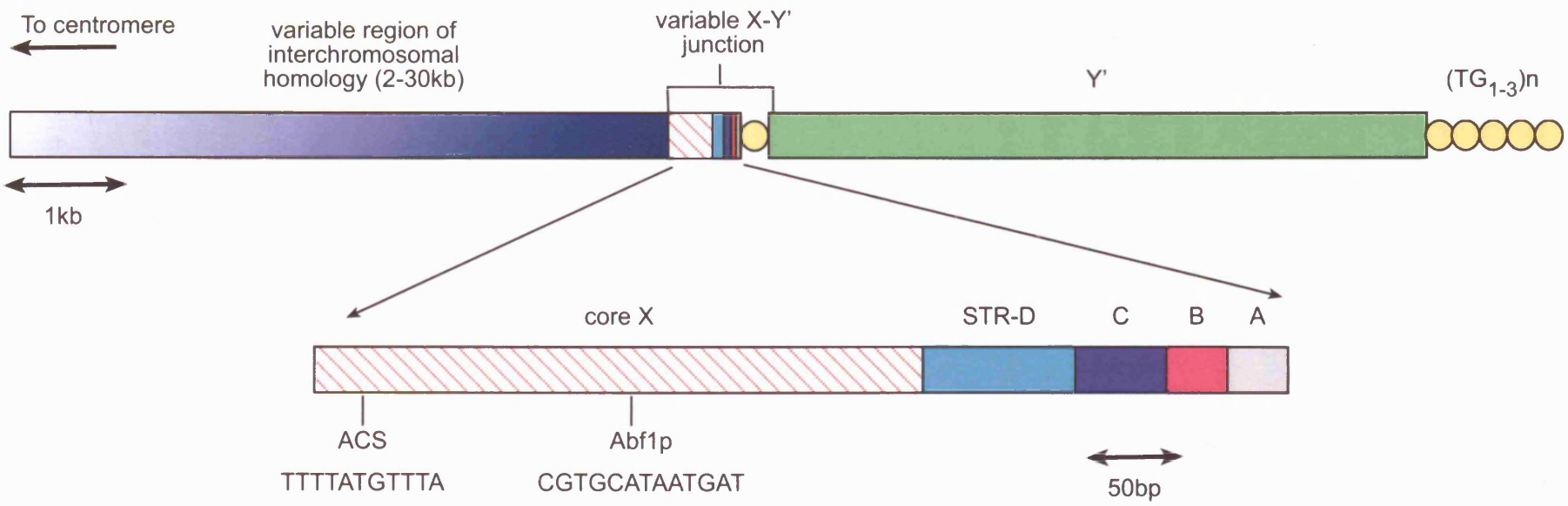

Figure 1.2 Chromosome ends in *Saccharomyces cerevisiae* with core X and STR elements shown in detail. The Y' element is present in 1-4 tandem copies at many telomeres. The arrangement and number of STR elements varies between telomeres. The core X element is present at all ends and usually contains both the ACS and Abf1p binding site.

recognition complex (ORC) (Loo *et al.*, 1995b). ORC, composed of six subunits (ORC1-6), is essential for initiation of replication and is also involved in transcriptional repression (Bell and Dutta, 2002; Bell *et al.*, 1993; Bose *et al.*, 2004; Dillin and Rine, 1997; Fox *et al.*, 1995; Micklem *et al.*, 1993). All six subunits are highly conserved in eukaryotes from yeast to humans (reviewed in Bell and Dutta, 2002).

Internal to core X are blocks of homology (2-30kb) shared by a few subtelomeres that often contain members of repetitive multigene families such as the *SUC*, *MAL* and *MEL* families (reviewed in Zakian, 1996). These gene families exist predominantly, and in some cases exclusively, in the subtelomeric domains of yeast and many are involved in sugar metabolism (see Louis, 1995; Pryde and Louis, 1997 for review). Recombination between subtelomeric domains of non-homologous chromosomes is believed to facilitate the accumulation and spread of these gene families and to generate potentially adaptive gene variants similar to parasites (see Section 1.1.3) (Michels *et al.*, 1992; Naumov *et al.*, 1996). The positioning of these families within subtelomeric domains may also have an adaptive advantage for different environments as some strains possess either *SUC* or *MEL* genes but not both (Naumov *et al.*, 1996).

1.1.2 Human telomere structure

In contrast to the short, variable-repeat telomeres of yeast, telomeres of human chromosomes are long tracts (5-15kb) of the tandem repeat sequence TTAGGG. In addition, the telomeres of mammals are nucleosomal (Makarov *et al.*, 1993). Interestingly, the nucleosome DNA repeat of telomeres is ~40bp shorter than in bulk chromatin in all animal species examined, including humans, indicating a specialized chromatin structure perhaps analogous to the yeast telosome (Lejnine *et al.*, 1995; Makarov *et al.*, 1993).

Sequence comparisons of the subtelomeric regions show striking structural similarities between yeast and humans (Flint *et al.*, 1997; Pryde *et al.*, 1997). The human TAS contain two large blocks of homology, one adjacent to the telomere and one more internal, separated by a tract of telomere repeats and a putative origin of replication (Fig. 1.1) (Flint *et al.*, 1997; Macina *et al.*, 1994; Riethman *et al.*, 2004). The telomere-adjacent homologous regions are common to many telomeres while the internal elements are only shared between a few telomeres, remarkably similar to the yeast structure (Coleman *et al.*, 1999; Flint *et al.*, 1997). These homologous regions in humans also contain genes from multigene families including the large

olfactory receptor family (Glusman *et al.*, 2001; Mefford *et al.*, 2001; Trask *et al.*, 1998). The similarity of human and yeast subtelomeric regions suggests that this structure may be required for a function of the telomere or is possibly the result of a similar process that results in the formation and maintenance of these features.

1.1.3 Chromosome ends in parasites and pathogens

Parasites and pathogens appear to make use of special properties of subtelomeric regions to facilitate evasion of host immune responses via antigenic variation (reviewed in Barry *et al.*, 2003). Many of the surface-antigen genes are located in the subtelomeres of organisms such as *Trypanosoma brucei* (Borst *et al.*, 1996; Eid and Sollner-Webb, 1995) and the malaria parasite *Plasmodium falciparum* (Rubio *et al.*, 1996) in addition to tandem arrays of repeat sequences (Fig. 1.1). *Pneumocystis carinii*, a fungal pathogen, encodes virtually all its major surface glycoproteins, which are also thought to be involved in host immune invasion, near the tandem repeat sequences of the subtelomeric regions (Underwood *et al.*, 1996; Wada and Nakamura, 1996). Subtelomeric regions of most organisms are known to be very dynamic with a high turnover and significant sequence exchange. These properties are believed to be important in generating variation in sequence and expression of the surface antigen genes of these organisms, providing an adaptive flexibility (Freitas-Junior *et al.*, 2000; Lanzer *et al.*, 1995; McCulloch *et al.*, 1997). In addition, the TAS are subject to transcriptional repression in many organisms, a property that appears to facilitate control of the expression of the many antigen genes in *T. brucei* and *P. falciparum* (reviewed in Barry *et al.*, 2003; Freitas-Junior *et al.*, 2005).

1.2 Telomere length regulation

The telomerase reverse-transcriptase is responsible for extending telomeres in most organisms, including *S. cerevisiae,* by adding *de novo* telomere repeats using its own RNA component as a template. In yeast, *TLC1* encodes this RNA template (Singer and Gottschling, 1994) while the reverse-transcriptase is encoded by *EST2* (Lingner *et al.*, 1997). In the absence of telomerase, telomeres can be maintained by recombination-based mechanisms such as ALT (alternative lengthening of telomeres) in humans or the survivor pathways in yeast (Bryan *et al.*, 1997; Huang *et al.*, 2001; Lundblad and Blackburn, 1993). These alternative pathways result in highly variable telomere lengths in contrast to telomerase-mediated length control, which

acts preferentially on the shortest telomeres (Hemann *et al.*, 2001; Smogorzewska and de Lange, 2004; Teixeira *et al.*, 2004).

In yeast, telomerase action is modulated by a variety of positive and negative regulators that often affect multiple aspects of telomere and cell biology. Mutations in some of these genes, including *TLC1* or any of the *EST* genes (*EST1-4*), causes progressive telomere shortening leading to cell death. *EST1* and *EST4* (*CDC13*) are both single-stranded DNA binding proteins and are thought to regulate telomerase access to the telomere overhang (reviewed in Smogorzewska and de Lange, 2004). The current model proposes that Est4p binds the telomere single-stranded overhang and interacts with Est1p, an accessory factor bound to telomerase, thus recruiting telomerase to the telomere (Smogorzewska and de Lange, 2004).

Although most yeast cells with mutations leading to ever shorter telomeres eventually die, some are able to survive via alternate 'survivor' pathways, that can involve *RAD52*-dependent accumulation of Y' elements at their chromosome ends or an abrupt elongation of telomere repeats (Huang *et al.*, 2001; Lundblad and Blackburn, 1993). Similar mechanisms for unconventional telomere elongation have also been observed in human ALT cells (Marciniak *et al.*, 2005; Reddel, 2003). In other mutants, such as *TEL1* or *TEL2* mutants, telomeres are shortened but are stably maintained at the shorter length (Kota and Runge, 1999; Lustig and Petes, 1986). This stable length reduction also occurs in *Ku* mutants in both yeast and humans (see Section 1.4.6).

The major regulator of telomere length in yeast is Rap1p which binds directly to telomere repeats and negatively regulates telomere extension (reviewed in Smogorzewska and de Lange, 2004). There is approximately one Rap1p binding site every 18bp in yeast telomere tracts (Gilson *et al.*, 1993; Marcand *et al.*, 1997b). Studies have shown that telomere length is 'counted' by the number of bound Rap1p molecules and not by the actual length of telomere repeats (Marcand *et al.*, 1997a; Ray and Runge, 1999). Similar mechanisms of length control, by counting the number of a telomere bound protein, are observed in other organisms including humans (Loayza and De Lange, 2003). When a threshold number of Rap1p molecules are bound the telomere is thought to fold back on itself allowing the end to interact with the telomere-subtelomere junction, thereby preventing further elongation (see also Section 1.5.1) (Marcand *et al.*, 1997a; Ray and Runge, 1999). This model is supported by evidence that sequences internal to the telomere and at the telomere-nontelomere junction affect telomere length suggesting an interaction

between the TAS and telomere termini (Ray and Runge, 1999). In addition, mutations of proteins not found in the telosome, including histones, also affect telomere length (Venditti *et al.*, 1999b). The telomere folding may be caused directly by Rap1p, which causes a 90° to 100° bend in DNA *in vitro* (Gilson *et al.*, 1993), and a similar function has been observed for human *TRF1* (Bianchi *et al.*, 1997).

The Rif1p/Rif2p complex mediates the Rap1p counting mechanism (Hardy *et al.*, 1992; Wotton and Shore, 1997) and appears to compete with the Sir complex for binding to Rap1p (Buck and Shore, 1995; Hardy *et al.*, 1992; Marcand *et al.*, 1997b). Both Rap1p binding complexes affect control of telomere length. Deletion of either of the *RIF* genes causes extensive elongation of the telomere (reviewed in Smogorzewska and de Lange, 2004) while deletion of *SIR* genes causes telomere shortening (Palladino *et al.*, 1993a; Venditti *et al.*, 1999b). A recent study has confirmed it is the number of Rif factors bound to Rap1p that determines the telomere length, rather than direct Rap1p counting (Levy and Blackburn, 2004). The human homologue, hRap1p, also appears to function in telomere length control through interactions with Trf1p and Trf2p, which may serve analogous roles to the yeast Rif complex (Broccoli *et al.*, 1997; Chong *et al.*, 1995; Karlseder, 2003; Karlseder *et al.*, 2003; Li and de Lange, 2003; O'Connor *et al.*, 2004). *RAP1* homologues are also found in many other organisms (Park *et al.*, 2002b; Tan *et al.*, 2003).

1.3 Silencing

Silencing, or gene repression, is present in all eukaryotes and is essential for a variety of processes including cell differentiation and regulation of development (Grewal and Moazed, 2003). Developmental regulation requires controlled silencing of developmental genes in *Drosophila* and other multicellular organisms (Muller, 1995; Muller *et al.*, 1995). This type of expression control is also known as an epigenetic effect; a heritable change in gene expression that is not due to the DNA sequence. The term silencing describes the reversible repression of genes in a given chromosomal domain, rather than of a single gene. These silenced domains are believed to form through protein-mediated chromatin compaction to create a specialized chromatin structure, termed heterochromatin, which limits the access of transcription factors (Section 1.6). The epigenetic silencing of genomic regions occurs in mammalian imprinting and, on a large scale, in X-chromosome inactivation in females of higher organisms. In *Drosophila,* silencing was first described in

position effect variegation (PEV) and similar effects are observed in *Schizosaccharomyces pombe*. Gene repression is also a well characterized phenomenon in *S. cerevisiae* in mating type regulation and telomere position effect (TPE).

1.3.1 Genomic imprinting

Imprinting is the specialized expression pattern in which the gene is expressed from only one of the two parental alleles and results from one copy of the gene being inherited in the silent state while the other is inherited in the expressed state. Their imprinted state and resulting expression status must be maintained in every cell. Imprinted genes are often found in large clusters in the genome. The role of imprinting appears to be primarily in development as most of the imprinted genes are developmental regulators. The method of differentiating the two alleles is believed to be an epigenetic marking of one or both parental alleles. In addition to the differential expression, the alleles exhibit differences in DNA methylation, histone modification, chromatin structure and replication timing (reviewed in Verona *et al.,* 2003). The DNA methylation is a strong candidate for the epigenetic mark used to distinguish alleles. In most instances of endogenous imprinting, the parental alleles are differentially methylated at CpG dinucleotides (Razin and Cedar, 1994). This DNA methylation mark is recognized by methylCpG-binding proteins (MBD1 through MBD4 and MeCP2) which bind and initiate repression by recruiting other silencing and chromatin remodelling factors to create the silenced loci (reviewed in Li, 2002 and Mukai and Sekiguchi, 2002).

The mouse insulin-like growth factor 2 (*Igf2*) was the first endogenous mammalian imprinted gene discovered (DeChiara *et al.*, 1991). A mutated copy inherited from the father resulted in a 40% decrease in the size of the fetus but had no effect if inherited from the mother, indicating that *Igf2* is paternally expressed. The *Igf2* inhibitor, *H19*, is located proximal to *Igf2* and is oppositely imprinted, resulting in expression of only the maternal allele (Fig. 1.3). The imprinting of both genes is determined by the imprinting control region (ICR) 5' of *H19* (Leighton *et al.*, 1995). The ICR of the maternal allele is unmethylated and acts to block enhancers 3' of *H19* that are required for *Igf2* expression (Fig. 1.3) (Bell and Felsenfeld, 2000; Kaffer *et al.*, 2000). Methylation of the paternal ICR spreads into the *H19* promoter resulting in gene silencing. In addition the methylated ICR is unable to block the *Igf2* enhancers

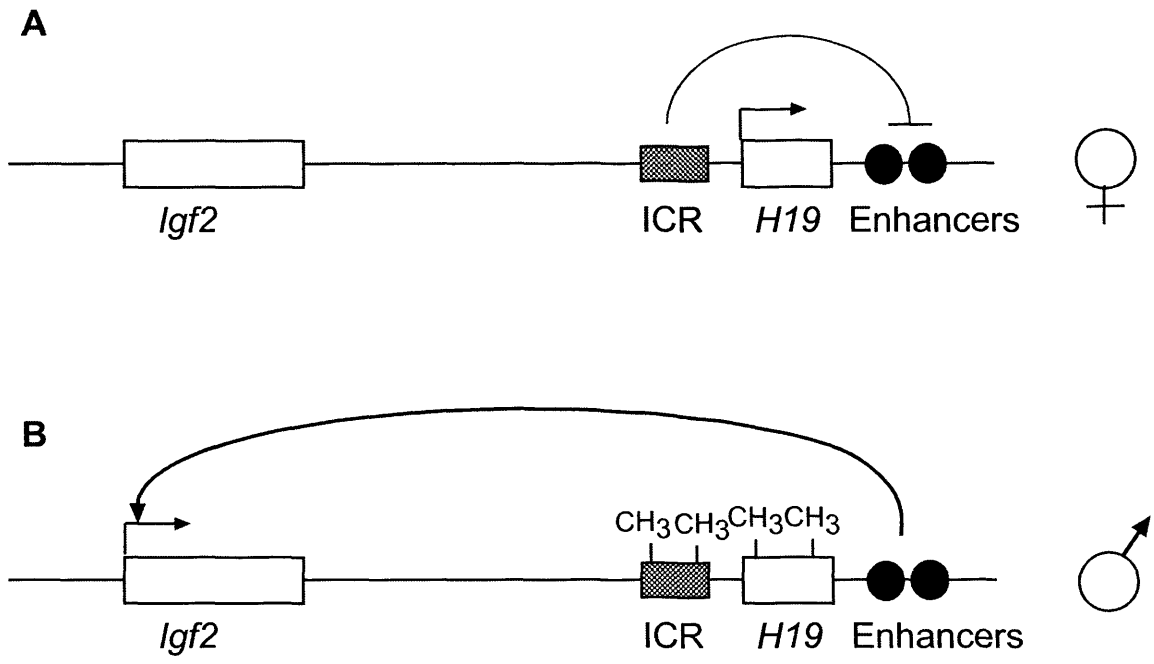

Figure 1.3. DNA methylation and imprinting of the *H19* and *Igf2* loci. A) The unmethylated ICR on the maternal chromosome acts to block the *Igf2* enhancers. B) The DNA methylation of the paternal ICR spreads into the *H19* locus, preventing expression. The enhancers are able to activate *Igf2* expression.

allowing the paternal *Igf2* allele to be expressed (Bell and Felsenfeld, 2000; Drewell *et al.*, 2002).

Although many lower organisms, including budding yeast, lack DNA methylation, differential histone modification is often used to differentiate silenced and expressed genes. DNA methylation has been linked with histone methylation in fungi and plants, suggesting a related role for these modifications in gene silencing and formation of heterochromatin (Jackson *et al.*, 2002; Tamaru and Selker, 2001). Many imprinted loci also have a heterochromatin-like structure on the silenced alleles similar to other types of repressive domains (reviewed in Recillas-Targa, 2002; see also Section 1.6).

1.3.2 X-chromosome inactivation

Genomic imprinting is believed to be a process of dosage compensation in cases where expression of both alleles would be harmful to the organism. It bears a high degree of similarity to the equalization of X-linked gene dosage between males and females by inactivation of one X-chromosome in females. Many strategies are utilized in this equalization but in mammals one chromosome is transcriptionally silenced through formation of extensive heterochromatic regions along the chromosome. The choice of which X chromosome to inactivate in a cell can be random, as in most mammals, or can be an imprinting effect with either the paternal or maternal chromosome being silenced in every cell (reviewed in Lee, 2003).

Repression is initiated at the X-inactivation centre (Xic) which encodes the non-translated Xist RNA (reviewed in Lee, 2003). Xist is repressed on the active X chromosome but is one of the few transcribed sequences from the inactive homologue (reviewed in Brockdorff and Duthie, 1998). The RNA transcript of Xist coats the chromosome and induces chromatin compaction through recruitment of other silencing factors, including the PcG proteins (reviewed in Heard, 2004). As in imprinting, the choice of active versus inactive chromosome appears to involve DNA and histone methylation. The inactive X chromosome also has heterochromatic features including hypoacetylated histones, heterochromatic histone methylation marks and late replication (reviewed in Lee, 2003).

1.3.3 PEV in *Drosophila*

Position effect variegation (PEV) was originally identified in *Drosophila* strains containing an X chromosome inversion in which the *white* gene, required for the red eye colour, was translocated adjacent to centromeric heterochromatin. This

translocation resulted in clonally heritable but reversible repression of the white gene, as evidenced by mottled eye pigmentation (reviewed in Weiler and Wakimoto, 1995). Silencing through PEV involves over 150 gene products, only a few of which have been extensively analyzed. PEV is dependent on the Suppressor of variegation [*Su(var)*] and Enhancer of variegation [*E(var)*] genes, many of which are involved in the heterochromatin formation (Boivin and Dura, 1998; Wallrath and Elgin, 1995). Most of the *E(var)* gene group, for example the GAGA protein encoded by the *E(var)* gene *Trithorax-like,* are transcriptional activators which also repress transcription in silenced domains. This is similar to Rap1p in yeast that has both positive and negative transcription regulatory functions (Section 1.4.3) (reviewed in Schotta and Reuter, 2003).

More is known about the *Su(var)* genes, in particular *Su(var)2-5* and *Su(var)3-9,* both of which are important for heterochromatin formation. *Su(var)2-5* encodes the heterochromatin-associated protein HP1 (Eissenberg *et al.*, 1990). HP1 is highly conserved with homologues from *S. pombe* to humans (reviewed in Grewal and Elgin, 2002). The chromodomain (chromatin organization modifier domain; often involved in targeting proteins to chromatin) of HP1 specifically binds histone H3 methylated on lysine 9, and appears to be the major factor in initiating heterochromatin formation (Bannister *et al.*, 2001; Jacobs *et al.*, 2001; Lachner *et al.*, 2001). The ability of HP1 to self-associate suggests a mechanism through which chromatin may be compacted, similar to the self-association of yeast Sir3p (Section 1.4.4) (Brasher *et al.*, 2000).

Su(var)3-9 also contains a chromodomain in addition to the evolutionarily conserved SET catalytic domain, commonly found in histone methyltransferases (HMTase) (Jenuwein *et al.*, 1998). *Su(var)3-9* is selective for methylation of lysine 9 in histone H3 (H3-K9), the essential modification for HP1 chromatin association (reviewed in Schotta and Reuter, 2003). The *Su(var)3-9* homologues of humans and fission yeast have also been shown to have HMTase activity required for association of the HP1 homologues with heterochromatin (Nakayama *et al.*, 2001; Rea *et al.*, 2000).

PEV is not the only form of silencing in *Drosophila*. The regulation mechanism for the expression of homeotic genes in different domains may be related to PEV and also bears similarities to Sir-mediated silencing in yeast. Homeotic gene silencing is established in the embryo and maintained though further development by the Polycomb Group (PcG) proteins (reviewed in Pirrotta, 1999 and 2003). The PcG's

are recruited by the PcG response elements (PREs), similar to yeast silencers (Section 1.4.1). Association of the PcG's with chromatin and subsequent silencing also involves histone modifications, such as specific methylation and deacetylation of lysine residues common to heterochromatic regions. PcG silencing can occur at sites more than 30kb from the PRE but the PcG proteins don't appear to spread away from the PRE's (Strutt *et al.*, 1997). Therefore a looping mechanism has been proposed that would allow the PRE-bound PcG silencing factors to interact cooperatively with each other or with other weaker PcG-binding elements to silence a distance locus (Fig. 1.4) (reviewed in Pirrotta and Gross, 2005).

In addition to homeotic gene regulation, PcG proteins also affect TPE in *Drosophila* (Ronsseray *et al.*, 2003). TPE was identified by observation of a variegated phenotype for a *white* transgene when it was inserted into the telomere associated sequences (TAS), similar to PEV, suggesting the TAS are also heterochromatic (Karpen and Spradling, 1992; Levis *et al.*, 1985). PcG proteins are also located close to TAS in hybridization experiments suggesting that TAS contain PRE's and share a similar method of silencing to the homeotic genes (Ronsseray *et al.*, 2003). Although very little work has been done on TPE in humans, one study identified a telomere linked gene that was expressed at a 10-fold lower rate than the same gene at an internal location in HeLa cells, suggesting TPE may also occur in higher organisms (Baur *et al.*, 2001).

1.3.4 Silencing in *Schizosaccharomyces pombe*

In *S. pombe*, similar to *S. cerevisiae* (Section 1.4), repression is observed at the silent mating type loci, the rDNA repeats and near centromeres and telomeres (reviewed in Huang, 2002). Both yeast species are able to exist as either haploid or diploid organisms. The two mating types of *S. pombe* haploids are M (minus) and P (plus), expressed from the *mat1* locus. Silenced copies of the M and P information are encoded at the donor *mat2* and *mat3* loci respectively. As in *S. cerevisiae*, wild-type homothallic strains switch to the opposite mating type in the majority of cell divisions via gene conversion using the donor loci (reviewed in Huang, 2002). The repression of the *mat2* and *mat3* loci is controlled by cis-acting elements. Silencing extends from these elements into the neighbouring regions, facilitating the repression of marker genes inserted nearby (Grewal and Klar, 1997).

Many of the trans-acting factors which affect silencing in *S. pombe* have been identified. Several of the more important factors, including Swi6p, Clr4p and Clr6p

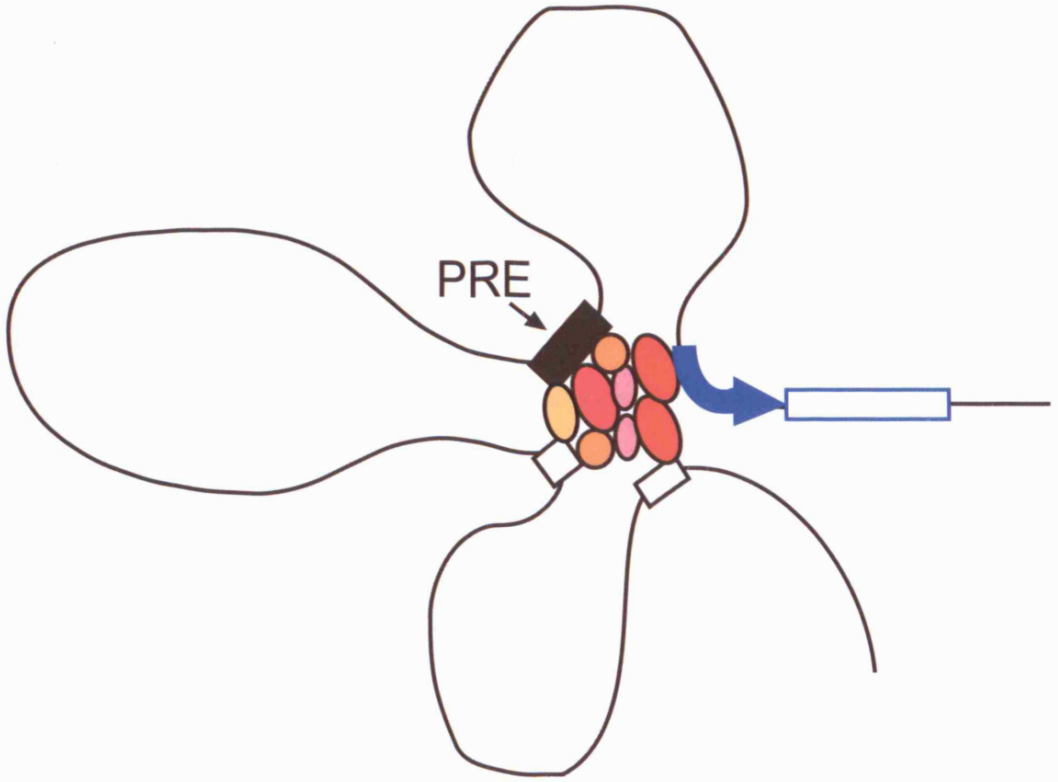

Figure 1.4. PcG-mediated silencing at a distance in *Drosophila*. PcG complexes (filled ovals) assemble at PRE elements. Interactions with PcG factors bound at other weak silencing elements facilitate interaction at a distance on a gene promoter (blue arrow) to initiate gene silencing.

are required for silencing of all loci. Clr6p is a histone deacetylase (HDAC) required to specifically deacetylate lysine 9 of H3 (Nakayama *et al.*, 2001) to allow the subsequent methylation of this residue by Clr4p (Ivanova *et al.*, 1998). The Clr4p HMTase, containing the conserved SET domain, is specific for methylation of H3-K9 and is a homologue of the *Drosophila Su(var)3-9* HMTase (Cavalli and Paro, 1998; Ivanova *et al.*, 1998; Jenuwein *et al.*, 1998). The chromodomain Swi6p factor shares homology with both HP1 and the PcG *Drosophila* proteins and serves an analogous structural function to these proteins at most silenced loci in *S. pombe* (Lorentz *et al.*, 1994; Nakayama *et al.*, 2000). As its localization requires Clr4p (Ekwall *et al.*, 1996), Swi6p likely binds specifically to histones with the heterochromatic H3-K9 methylation mark, similar to HP1. In addition, telomeric silencing in *S. pombe* is specifically affected by Taz1p, a member of the telomere-associated TRF family that regulate telomere length in yeast and humans (Cooper *et al.*, 1997; reviewed in Huang, 2002).

1.4 Silencing in *S. cerevisiae*

Gene silencing in *S. cerevisiae* occurs at a few specialized loci near telomeres (TPE), the *HML/HMR* silent mating type loci and the rDNA repeats (Lustig, 1998; Sherman and Pillus, 1997). Silencing at the *HM* loci and telomeres is controlled by many shared silencing factors including the Sir proteins (Sir1-4p), Rap1p, histone modifiers and the histones themselves (Table 1.1) (reviewed in Moazed *et al.*, 2004). rDNA silencing however, is controlled by a different set of factors although it still requires the Sir2p histone deacetylase as a member of the RENT complex (Straight *et al.*, 1999). Silencing of the very repetitive rDNA loci inhibits recombination to stabilize this genome region (Guarente and Kenyon, 2000; Smith and Boeke, 1997). Repression of the silent mating type loci and TPE are discussed in further detail below.

1.4.1 Silencing of *HML* and *HMR*

The two haploid states in *S. cerevisiae* are determined by the expression of genes from the *MAT* locus. The **a** mating type requires the *MAT***a** allele while the α mating type requires the *MAT*α allele. Diploid **a**/α cells are formed by conjugation of an **a** and α cell and express both *MAT* alleles. Diploid cells are consequently unable to mate. Conversion from one mating type to the other in haploid cells is initiated by cleavage at the *MAT* locus by the HO endonuclease followed by copying the information from one of the silent mating type loci, *HML*α or *HMR***a**. The *HM* loci are

Table 1.1. Selection of genes involved in silencing in *S. cerevisiae.*

		Position of Action			
Effect	**Gene**	***HM* loci**	**Telomere**	**rDNA**	**Reference**
Required for silencing	*ABF1*	+	?	?	(Kimmerly *et al.*, 1988)
	H2A	?	?	+	(Bryk *et al.*, 1997)
	H2B	?	?	+	(Bryk *et al.*, 1997)
	H3	+	+	?	(Thompson *et al.*, 1994)
	H4	+	+	?	(Aparicio *et al.*, 1991)
	yKU70	-	+	?	(Boulton and Jackson, 1998; Laroche *et al.*, 1998; Nugent *et al.*, 1998; Pryde and Louis, 1999)
	yKU80	-	+	?	
	NET1	-	-	+	(Straight *et al.*, 1999)
	NAT1	+	+	?	(Aparicio *et al.*, 1991)
	ORC2	+	+	?	(Fox *et al.*, 1997; Fox *et al.*, 1993)
	ORC5	+	+	?	(Fox *et al.*, 1997; Fox *et al.*, 1993)
	ORC1	+	+	?	(Triolo and Sternglanz, 1996)
	RAP1	+	+	?	Reviewed in Shore, 1994
	RIF1	+	-	+	(Hardy *et al.*, 1992; Smith *et al.*, 1998)
	RIF2	+	-	?	(Wotton and Shore, 1997)
	SET1	+	+	+	(Bryk *et al.*, 2002; Nislow *et al.*, 1997)
	SIR1	+	modest	-	(Aparicio *et al.*, 1991; Pillus and Rine, 1989; Pryde and Louis, 1999; Rine and Herskowitz, 1987; Smith and Boeke, 1997)
	SIR2	+	+	+	
	SIR3	+	+	-	
	SIR4	+	+	-	
	RAD6	+	+	+	(Bryk *et al.*, 1997; Huang *et al.*, 1997; Wood *et al.*, 2003a)
	SUB2	?	+	?	(Lahue *et al.*, 2005)
	SIT4	?	+	?	(Hayashi *et al.*, 2005)
	SAS2	+	+	+	(Ehrenhofer-Murray *et al.*, 1997; Kimura *et al.*, 2002; Meijsing and Ehrenhofer-Murray, 2001; Suka *et al.*, 2002)
	BDF1	+	+	?	(Ladurner *et al.*, 2003)
	SET1	+	+	+	(Briggs *et al.*, 2001; Bryk *et al.*, 2002; Nislow *et al.*, 1997)
	DOT1	?	+	?	(Ng *et al.*, 2002a; Singer *et al.*, 1998)
	BRE1	+	+	?	(Huang *et al.*, 1997; Wood *et al.*, 2003a)
	UBP10	?	+	?	(Emre *et al.*, 2005)
Abrogate silencing	*HTZ1*	+	+	?	Reviewed in Hild and Paro, 2003
	MEC3	?	+	?	(Corda *et al.*, 1999)
	RIF1	-	+	-	(Kyrion *et al.*, 1993)
	RIF2	-	+	?	(Marcand *et al.*, 1997b)
	SAS10	+	+	+	(Kamakaka and Rine, 1998)
	SAS2	+	?	?	(Ehrenhofer-Murray *et al.*, 1997)
	SIR4	-	-	+	(Smith and Boeke, 1997)

located near either end of chromosome III (12 and 25kb from the telomeres respectively) which also carries the expressed *MAT* locus (reviewed in Gartenberg, 2000). If the *HM* loci are derepressed in haploids, the cells are also unable to mate as they simultaneously express **a** and α mating type information and therefore appear phenotypically as diploids (reviewed in Herskowitz, 1989 and Herskowitz, 1988). Most lab strains contain a mutated HO gene to prevent mating type switching.

The *HM* loci are normally in a repressed state which involves the Sir proteins, Rap1p, Abf1p, the ORC complex and flanking silencer elements that encode binding sites for Rap1p, ORC and Abf1p (Fig. 1.5) (reviewed in Moazed *et al.*, 2004). *HMR* is the most extensively studied locus and has two flanking silencers, *HMR-E* which is essential for repression and contains all three binding sites, and *HMR-I* which is only required for complete repression (Abraham *et al.*, 1984). The *HML* locus is also flanked by *E* and *I* silencers (Fig. 1.5). The repressed domain is able to spread several kilobases from the silencer elements (Loo and Rine, 1994). The requirement for the silencers in repression is bypassed by direct tethering of Sir proteins near the *HM* loci, indicating that their primary function is to recruit the Sir complex (Chien *et al.*, 1993; Marcand *et al.*, 1996). There is also a degree of redundancy as studies of *HMR-E* have shown that any two of the three binding elements are sufficient for silencing (Brand *et al.*, 1987; Kimmerly *et al.*, 1988; Loo *et al.*, 1995a). Of the four Sir proteins, only Sir2p, Sir3p and Sir4p are required for silencing at *HMR* and *HML*.

ORC, Rap1p and Abf1p act cooperatively to recruit and stabilize the Sir2/3/4p complex at the silencers which then spreads across the *HM* loci (reviewed in Rusche *et al.*, 2002). Although ORC is essential for replication, its role in silencing is separable (Dillin and Rine, 1997; Foss *et al.*, 1993; Loo *et al.*, 1995a; Micklem *et al.*, 1993) and its functions in both replication and silencing appear to be conserved (Bell and Dutta, 2002; Pak *et al.*, 1997). ORC acts by recruiting Sir1p via a direct interaction between the Orc1p subunit and Sir1p (Gardner and Fox, 2001; Gardner *et al.*, 1999; Hsu *et al.*, 2005; Triolo and Sternglanz, 1996; Zhang *et al.*, 2002). This interaction is also facilitated by an interaction with Sir4p (Bose *et al.*, 2004; Gardner and Fox, 2001) which is believed to bind to the silencers though a Rap1p interaction (Cockell *et al.*, 1995; Moretti *et al.*, 1994; Moretti and Shore, 2001). This Sir1p-Sir4p interaction appears to confine the interaction of Sir1p to silencer-bound ORC's (Bose *et al.*, 2004; Gardner and Fox, 2001). The binding of Sir4p to Rap1p is essential for association of Sir2p and Sir3p with the silencer, indicating that Sir4p is central to recruiting and stabilizing the Sir complex (Rusche *et al.*, 2002). Sir1p, although not

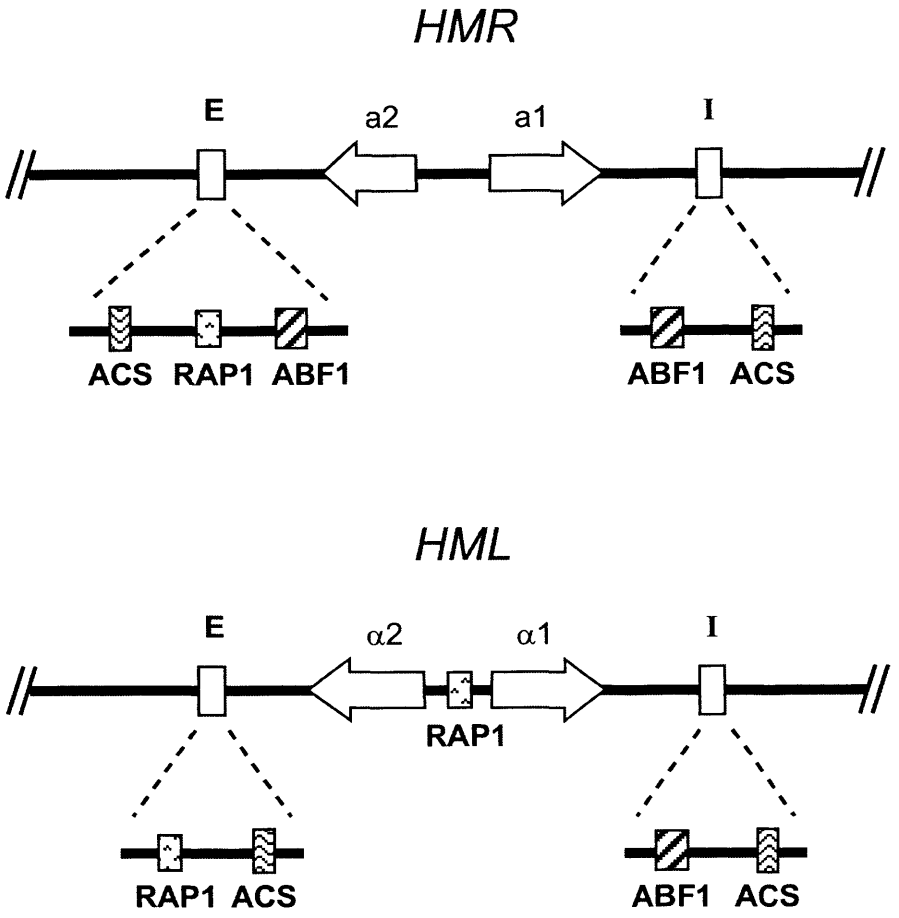

Figure 1.5. The *HMR* and *HML* loci. The E silencers (E), I silencers (I), open reading frames of the **a**1, **a**2, α1 and α2 mating type genes and Rap1p (RAP1) binding site between α1 and α2 are indicated. The ORC (ACS), Rap1p and Abf1p (ABF1) binding sites at each silencer are shown in the expanded silencers.

essential, functions in the establishment of the silenced state by recruiting the other Sir proteins and stabilizing the complex at the silencer elements (reviewed in Moazed *et al.,* 2004).

Following Sir complex assembly, the Sir's spread and form the repressive domain which involves the formation of a heterochromatic region, similar to silencing in other organisms (Hoppe *et al.*, 2002; Rusche *et al.*, 2002). Both *HM* loci exhibit several hallmarks of heterochromatin including a compact, ordered nucleosome array, decreased accessibility to nucleases and hypoacetylated histones (see also Section 1.6) (Bi *et al.*, 1999; Braunstein *et al.*, 1993; Ravindra *et al.*, 1999; Weiss and Simpson, 1998).

1.4.2 TPE

Genes placed adjacent to telomeres or within the subtelomeric regions of *S. cerevisiae* are subject to a silencing effect that, as in *Drosophila*, is known as TPE (reviewed in Rusche, 2003). TPE in yeast is mediated by the concentration of silencing proteins that are recruited to the telomere clusters that form near the nuclear periphery (Section 1.5). Silencing is nucleated by the binding of Rap1p that, similar to *HM* silencing, directly recruits Sir4p and subsequently the rest of the Sir silencing complex (Lustig *et al.*, 1996; Marcand *et al.*, 1996). Unlike the silent mating type loci, the yKu complex is also involved in TPE and Sir recruitment to the telomere repeats (Boulton and Jackson, 1998; Maillet *et al.*, 2001; Pryde and Louis, 1999). Tethering either Sir3p or Sir4p directly to the telomere overcomes the silencing defect of *rap1* mutants lacking the Sir interaction domain (Lustig *et al.*, 1996; Marcand *et al.*, 1996).

A critical factor in TPE is the competition between the Sir4p silencing factor and the Rif1p/Rif2p telomere length proteins for binding to Rap1p. Rif1p and Rif2p antagonize silencing by competing with the Sir proteins for binding to the C-terminus of Rap1p (Hardy *et al.*, 1992; Marcand *et al.*, 1997a; Wotton and Shore, 1997). Deletion of Rif1p and Rif2p removes the requirement for yKu in TPE, suggesting the role of yKu may be to promote the Sir4p-Rap1p interaction (Mishra and Shore, 1999). The lengthening of the telomere in *rif* mutants may also increase TPE due to increasing the number of Rap1p binding sites. However, other models for yKu's role in TPE are described in Section 1.4.6. Once the full Sir2-4p silencing complex is recruited it is able to spread from the telomere repeats to silence subtelomeric regions.

In the original studies of TPE, a modified telomere was used in which the subtelomeric DNA was deleted and a reporter gene was placed adjacent to a newly formed telomere, known as a truncated telomere. In this arrangement the reporter gene was observed to have a variegated expression pattern in which the gene switched between the silenced and expressed states, similar to PEV (Gottschling *et al.*, 1990). The degree of silencing and the spread of the Sir complex from truncated telomeres is continuous and decreases steadily toward the centromere (Gottschling *et al.*, 1990; Hecht *et al.*, 1996; Renauld *et al.*, 1993).

However, further studies using native telomeres showed a different picture. A reporter gene placed at a variety of subtelomeric loci revealed silencing in the native subtelomeric regions to be discontinuous (Fourel *et al.*, 1999; Pryde and Louis, 1999). Peaks of silencing were found near the core X element and the telomere repeats but reporter constructs were well expressed from positions in Y' elements (Louis and Haber, 1990; Pryde and Louis, 1997; Pryde and Louis, 1999). The expression variegation observed in truncation studies was not observed at the native telomeres. In addition only about half of the telomeres tested exhibited significant repression of the marker when inserted adjacent to core X. TPE was very low at IIIR, IVL and XR, but was quite high at IIR, XIL and XIIIR. So far, there is no clear difference in sequence or structure between the silenced and unsilenced ends (Pryde and Louis, 1999).

The discontinuous nature of TPE is related to the subtelomeric elements. The STR repeats, telomere-proximal to core X, and the telomere-proximal portion of Y' elements have barrier functions. These regions, termed STARs (subtelomeric anti-silencing regions), prevent the silencing of regions located between them without interfering with repression of genes located centromere-proximal to core X (Fourel *et al.*, 1999; Lebrun *et al.*, 2001). The binding sites for Tbf1p and Reb1p found in the STR repeats appear to be responsible for their STAR activity (Fourel *et al.*, 1999; Liu and Tye, 1991). In contrast, the ACS and Abf1p binding site in the core X element have protosilencer function; they act cooperatively to enhance silencing of subtelomeric regions and promote the discontinuous silencing beyond STAR elements, but are unable to silence independently (Lebrun *et al.*, 2001). Discontinuous silencing is proposed to occur through the formation of a loop structure at chromosome ends as described in Section 1.5.1 (see also Fig. 1.6). Although the ORC and Abf1p binding sites are also important elements of the *HM* silencers, their function in TPE is still unclear. Mutation of either site reduces TPE,

but although the role of ORC in *HM* silencing is to recruit Sir1p, deletion of Sir1p has very little effect on TPE at native ends (this study; Pryde and Louis, 1999).

Many of the endogenous subtelomeric genes are members of repetitive multigene families, complicating analysis of their expression. However, analysis of four unique subtelomeric genes showed that only one, of unknown function located near the VIR telomere and less than 1kb from the core X element, exhibited Sir-dependent silencing (Vega-Palas *et al.*, 2000). The other three ORFs examined were located beyond the reported spread of the Sir complex at their respective ends and therefore were not expected to be repressed (Vega-Palas *et al.*, 2000). A Ty5-1 retrotransposon located 1.8kb from the silencing-competent IIIL telomere also exhibited Sir-dependent silencing effects (Vega-Palas *et al.*, 2000; Vega-Palas *et al.*, 1997). These studies indicate that silencing of endogenous subtelomeric genes is rare and unlikely to be the function of TPE. Silenced telomeric regions also exhibit heterochromatic features including hypoacetylation of histones, reduced nuclease accessibility and some initial work has also indicated heterochromatic nucleosome spacing (reviewed in Rusche, 2003). The function of TPE is still elusive although proteins involved in silencing also affect telomere structure and maintenance as well as other processes such as DNA repair and aging.

1.4.3 *RAP1*

Rap1p is a multifunction protein that appears to act both as a transcriptional activator and a repressor depending on its location within the genome. Homologues are found in many species of yeast (Wahlin *et al.*, 2003), vertebrates (Tan *et al.*, 2003) and also in humans (Li *et al.*, 2000). In yeast, Rap1p binds to the upstream activation site (UAS) at ~5% of all promoters where it activates transcription (Graham *et al.*, 1999; Lieb *et al.*, 2001; Sussel and Shore, 1991). However, when bound to the silent mating type loci or the telomere repeats, Rap1p represses transcription and it is also an essential structural component of telomeres (reviewed in Pina *et al.*, 2003). It is still unclear how Rap1p fulfills its many roles. It may provide a DNA-bound platform to which many other factors can bind; alternatively, binding of Rap1p may induce a structural change to allow only a subset of its potential partners to bind (Pina *et al.*, 2003).

At both the telomeres and silent mating type loci in yeast, Rap1p is believed to initiate the gene repression and heterochromatin formation (Moretti *et al.*, 1994; Moretti and Shore, 2001) and is also important in telomere length maintenance

(Conrad *et al.*, 1990; Marcand *et al.*, 1997b; Ray and Runge, 1999). Rap1p has a loosely defined binding sequence of 12-14bp in length (Pina *et al.*, 2003). Interestingly, Rap1p has a higher affinity for the telomeric binding sites than for those located elsewhere in the genome (Gilson *et al.*, 1993).

Rap1p is comprised of three domains; a non-essential N-terminal domain, a central DNA binding domain and a C-terminal activation/repression domain (Li and de Lange, 2003). The DNA binding domain is similar to the Myb-repeat of telobox proteins and similar domains are found in the yeast Tbf1p, the human telomere-binding proteins Trf1p and Trf2p and the *S. pombe* telomere-associated Taz1p. The C-terminal domain interacts with the various Rap1p-binding partners, including the Rif and Sir proteins, and is critical for silencing and telomere length maintenance. C-terminal deletion mutants can also disrupt the heterochromatic nature of silenced regions (reviewed in Pina *et al.*, 2003). Although Sir3p and Sir4p are both able to interact with Rap1p, only the Sir4p interaction is independent of other silencing factors (Cockell *et al.*, 1995; Liu and Lustig, 1996; Luo *et al.*, 2002; Moretti and Shore, 2001; Roy *et al.*, 2004). The interaction between Rap1p and the Sir complex is essential for TPE (Luo *et al.*, 2002).

1.4.4 The Sir complex

In *S. cerevisiae*, the major silencing factors are the four silent information regulators, *SIR1-4* (Aparicio *et al.*, 1991; Rine and Herskowitz, 1987). Sir2p, Sir3p and Sir4p form the silencing complex which spreads across the silent mating type loci and repressed subtelomeric domains to form the heterochromatic regions (reviewed in Rusche *et al.*, 2002). Sir3p and Sir4p bind to hypoacetylated and hypomethylated N-terminal histone tails associated with heterochromatic regions to stabilize and spread the silencing complex. The Sir2p histone deacetylase facilitates the spread of the complex by deacetylating adjacent histones to create the Sir3p and Sir4p binding substrates. All three of the Sir's are required for establishment and maintenance of silencing at both the *HM* loci and telomeres (reviewed in Rusche *et al.*, 2003). In contrast, the role of Sir1p appears to be restricted to the establishment of silencing at the silent mating type loci. Sir1p is found associated primarily with the silencer elements and does not spread across the silenced domains with the Sir silencing complex (Rusche *et al.*, 2002). Deletion of Sir1p has no effect on TPE at truncated telomeres (Aparicio *et al.*, 1991) and only a small effect on TPE at native

ends (Fourel *et al.*, 1999; Pryde and Louis, 1999; Vega-Palas *et al.*, 2000), although tethering of Sir1p near telomeres increases silencing (Chien *et al.*, 1993).

Numerous studies have elucidated the interactions of the Sir proteins with each other, the histones and with other silencing factors. There is a binding hierarchy in Sir complex assembly at the *HM* loci and telomeres. At the *HM* loci, Sir1p is the first Sir factor to bind through its association with Orc1p bound at the silencers (Gardner *et al.*, 1999; Geissenhoner *et al.*, 2004; Hsu *et al.*, 2005; Triolo and Sternglanz, 1996). At the telomeres, Sir4p is the first factor to bind through its interaction with the telomere-bound Rap1p (Luo *et al.*, 2002). Rap1p-bound Sir4p acts together with yKu at the telomeres and with Sir1p at the *HM* silencers to recruit Sir2p and Sir3p (Martin *et al.*, 1999; Roy *et al.*, 2004; Tsukamoto *et al.*, 1997). Interestingly, Sir2p and Sir4p associate constitutively, an interaction that inhibits Sir3p association (Moazed *et al.*, 1997). yKu is proposed to initiate a conformation change in Sir4p at the telomere to allow Sir3p to bind (Roy *et al.*, 2004), and perhaps Sir1p has the same function at the silencers. Upon full assembly, the Sir complex spreads and represses the nearby regions (Rusche *et al.*, 2002).

Formation of silenced domains is believed to involve construction of higher order chromatin structures in addition to the ordered nucleosome arrays. Sir3p may be able to crosslink nucleosome arrays into such supramolecular complexes via its known ability to self-associate (Georgel *et al.*, 2001). The recent discovery that multiple Sir3p proteins can associate with a single Sir2p/Sir4p heterodimer, facilitating a structural change in the Sir complex, also suggests a role for Sir3p in higher order structure and chromatin crosslinking (Liou *et al.*, 2005). In addition to alleviating silencing, loss of Sir3p or Sir4p causes telomere shortening and an increase in chromosome loss, indicating they are involved in the telosome structure required to protect the telomere (Huang, 2002; Palladino *et al.*, 1993a)

Of the four Sir proteins, only Sir2p has homologues in higher organisms (North *et al.*, 2003). However, Sir3p and Sir4p may be considered orthologues of the heterochromatin-binding HP1 protein, despite a lack of sequence similarity. The Sir2p family is characterized by a highly conserved core domain that is essential for silencing (Brachmann *et al.*, 1995). Members of the *SIR2* gene family exist from archaebacteria to eukaryotes (Frye, 2000). In addition, Sir2p is the only one of the four Sir's to participate in rDNA silencing through interactions with Net1p and the RENT complex (Bryk *et al.*, 1997; Ghidelli *et al.*, 2001; Smith and Boeke, 1997;

Straight *et al.*, 1999) and also appears to be important in cellular aging (Bitterman *et al.*, 2002; Kaeberlein *et al.*, 1999; Tissenbaum and Guarente, 2001).

The yeast Sir2p is a nicotinamide adenine dinucleotide (NAD)-dependent histone deacetylase, a unique class of HDAC's that hydrolyze the NAD substrate resulting in synthesis of O-acetyl-ADP-ribose (AAR) (Imai *et al.*, 2000b; Landry *et al.*, 2000; Smith *et al.*, 2000b). Sir2p specifically deacetylates the H4-K16 residue which is essential for Sir complex association (Liou *et al.*, 2005). The acetylation state of other histone lysine residues appears to have no effect on binding of Sir3p and Sir4p (Venditti *et al.*, 1999a). Acetylated histones may be required for the spread of the Sir complex as AAR, generated by the Sir2p deacetylation reaction, promotes Sir3p association with the silencing complex and between adjacent complexes (Liou *et al.*, 2005). Thus the role of Sir2p is not solely to deacetylate histones but is also important to generate AAR.

1.4.5 Telomeres and DNA repair

Paradoxically, a number of studies in recent years have implicated components of DNA repair pathways in telomere maintenance and silencing. Although these proteins function to recognize and process broken DNA ends, for some reason they are also able to actively prevent telomeres from being recognized as breaks. The repair of DNA double-strand breaks (DSBs) occurs either through homologous recombination or non-homologous end-joining (NHEJ). It is predominantly the proteins involved in NHEJ, in particular the yKu heterodimer and the Rad50p-Mre11p-Xrs2p complex, that also have telomere and silencing functions in yeast. Mutations in either yKu subunit causes a dramatic loss of repression near both native and truncated telomeres (Boulton and Jackson, 1998; Laroche *et al.*, 1998; Nugent *et al.*, 1998). However, this effect appears specific to telomeres as mutations of *yKU70* have little effect on *HM* silencing (Laroche *et al.*, 1998). yKu mutations also disrupt the perinuclear localization of telomeres (Laroche *et al.*, 1998) and cause a stable shortening of the telomere repeats (Boulton and Jackson, 1996; Porter *et al.*, 1996). Both the human and *Drosophila* Ku homologues also affect telomere length (d'Adda di Fagagna *et al.*, 2001; Melnikova *et al.*, 2005). The association of yKu with the telomere is independent of the Sir proteins, although spreading of yKu into subtelomeric regions is Sir-dependent (Martin *et al.*, 1999) and likely involves the yKu-Sir4p interaction (Luo *et al.*, 2002). Studies conducted to generate *yKU80* separation-of-function mutants indicate the role of the Ku complex in

silencing and telomere maintenance is independent of its NHEJ role (Bertuch and Lundblad, 2003; Roy *et al.*, 2004; Stellwagen *et al.*, 2003).

The Rad50p-Mre11p-Xrs2p DNA repair complex, which has endo- and exonucleolytic activities (Martin *et al.*, 1999), also acts in the telomere length pathway in yeast (Boulton and Jackson, 1998; Nugent *et al.*, 1998). Unlike yKu, mutations of this complex do not affect TPE (Boulton and Jackson, 1998). The Rad50 complex primarily functions in the telomerase-mediated pathway for telomere replication while the yKu heterodimer has an end-protection role (reviewed in Bertuch and Lundblad, 1998). Interestingly, the human Ku homologue binds to Trf1p and the Rad50p/Mre11p/Nbs1p repair complex associates with Trf2p (reviewed in Shore, 2001) indicating the association between DNA repair proteins and telomeres is not limited to yeast.

All of these proteins localize to telomeres in the absence of DNA damage but are rapidly dissociated once a DSB is detected, suggesting that telomeres act as a reservoir for DNA repair proteins (Martin *et al.*, 1999). However, the significance of this association has yet to be determined. The Sir silencing complex may play a reciprocal role with yKu in NHEJ as the Sirs also re-localize from the telomeres to DSBs with yKu (Martin *et al.*, 1999). It has been suggested that the Sirs function in break repair by forming a silenced region (Martin *et al.*, 1999). However, some studies indicate an effect of Sir mutants on NHEJ while other studies do not (Astrom *et al.*, 1999; Boulton and Jackson, 1998; Lee *et al.*, 1999; Mills *et al.*, 1999), leaving the role of Sir proteins in DNA repair unresolved. In addition to the Sir proteins, other chromatin remodeling factors, such as Cbf1p (Ferreiro *et al.*, 2004; Kent *et al.*, 2004) and the CAF-1 complex (Enomoto and Berman, 1998; Kaufman *et al.*, 1997; Monson *et al.*, 1997), have also been implicated in both DNA repair processes and regulation of gene expression.

1.4.6 The Ku heterodimer

The Ku complex (Ku) is a heterodimer composed of two subunits of approximately 70 and 80kDa, known as Ku70p and Ku80p respectively (Gottlieb and Jackson, 1993). Homologues of Ku have been identified throughout eukaryotes and even in some prokaryotes, all of which appear to have DNA repair functions (Downs and Jackson, 2004). In higher eukaryotes, Ku is a component of DNA-PK, composed of the Ku heterodimer and the DNA-PK_{cs} catalytic subunit. Ku appears to first bind DNA breaks and subsequently recruit DNA-PK_{cs}. In lower organisms, including *S.*

cerevisiae, the DNA-PK_{cs} subunit isn't found although it is likely that the binding of Ku to break sites still acts to recruit other repair components (reviewed in Downs and Jackson, 2004).

Ku was first recognized for its role in NHEJ and has subsequently been shown to have telomere-related roles. Localization of the Ku heterodimer to telomeres has been observed by both direct immunofluorescence and chromatin-immunoprecipitation (ChIP) in *S. cerevisiae* (Gravel *et al.*, 1998; Martin *et al.*, 1999) and humans (Bianchi and de Lange, 1999; d'Adda di Fagagna *et al.*, 2001; Hsu *et al.*, 1999). Ku also associates with the telomeres of human ALT cells (d'Adda di Fagagna *et al.*, 2001) which maintain their telomeres by a telomerase-independent recombination mechanism (Dunham *et al.*, 2000; Varley *et al.*, 2002). The Ku heterodimer is able to bind in a sequence-independent manner to all double-stranded DNA ends from overhangs, blunt ends and stem-loops to telomeres. The crystal structure of human Ku reveals a ring formation through which a DNA molecule can be bound (Walker *et al.*, 2001). Ku is also able to translocate along DNA after binding (reviewed in Hopfner *et al.* 2002 and Tuteja and Tuteja, 2000). Binding of Ku is thought to prevent DNA degradation, aid in alignment of broken ends and in recruitment of other factors for DNA repair or telomere maintenance. The *S. cerevisiae KU80* (*yKU80*, also known as *HDF2*) and *KU70* (*yKU70*, also known as *HDF1*) homologues have also been shown to stimulate NHEJ and to have telomere-related roles (Boulton and Jackson, 1996; Boulton and Jackson, 1998; Feldmann *et al.*, 1996; Feldmann and Winnacker, 1993; Milne *et al.*, 1996).

Mutation of Ku often has contrasting effects in different organisms. In most organisms including *S. cerevisiae* (Boulton and Jackson, 1998; Porter *et al.*, 1996), *S. pombe* (Baumann and Cech, 2000; Manolis *et al.*, 2001), trypanosomes (Conway *et al.*, 2002) and humans (d'Adda di Fagagna *et al.*, 2001; Jaco *et al.*, 2004; Myung *et al.*, 2004) inactivation of Ku results in stably shortened telomeres, while in plants it results in telomere lengthening (reviewed in Riha and Shippen, 2003). In both mice and humans, Ku appears to stabilize chromosomes and prevent telomeric fusions (Bailey *et al.*, 1999; Jaco *et al.*, 2004; Samper *et al.*, 2000), in contrast to yeast, where yKu deletion results in shorter but protected telomeres (Boulton and Jackson, 1996; Porter *et al.*, 1996). However, yKu-deficient yeast strains exhibit a temperature sensitivity (Boulton and Jackson, 1996; Feldmann and Winnacker, 1993), caused by the activation of the Rad53p-dependant DNA damage checkpoint; thus end-protection is defective in yKu mutants but is only observed at increased temperatures

(Teo and Jackson, 2001). An extension of the G-strand overhang is also observed in several organisms, including yeast, suggesting that Ku protects telomeres from exonucleolytic activity (Gravel *et al.*, 1998; Polotnianka *et al.*, 1998; Riha and Shippen, 2003a). Recent studies have shown Ku binds the RNA component of telomerase in yeast (Stellwagen *et al.*, 2003) and humans (Ting *et al.*, 2005), and also interacts physically with telomerase in other mammals (Chai *et al.*, 2002; Hsu *et al.*, 1999) suggesting that Ku's roles in telomere protection and length maintenance may be mediated through recruitment of telomerase.

The effect of Ku on transcriptional repression of subtelomeric genes is also varied as it is required for repression in *S. cerevisiae* (Boulton and Jackson, 1998; Nugent *et al.*, 1998) but not in *S. pombe* (Manolis *et al.*, 2001). The repression of telomere-proximal genes in *S. cerevisiae* appears to depend on both the ability of the trans-acting silencing factors to associate with the telomere and on the localization of telomeres to the nuclear periphery (see Section 1.5). In yeast, telomere-bound yKu tethers telomeres to the nuclear envelope, resulting in the peripheral telomere localization. yKu mutants exhibit both telomere localization and TPE defects (Galy *et al.*, 2000; Laroche *et al.*, 1998; Pryde and Louis, 1999; Taddei *et al.*, 2005). Ku also appears to function in TPE through recruitment of the Sir complex to the telomere (Luo *et al.*, 2002; Roy *et al.*, 2004).

Separation-of-function studies in yeast demonstrating that yKu's telomere-related roles and NHEJ functions are separable are beginning to shed light on how yKu can protect telomeres without initiating DNA end-joining (Bertuch and Lundblad, 2003; Roy *et al.*, 2004; Stellwagen *et al.*, 2003). These groups isolated NHEJ-proficient mutants with defects in some or all of yKu's telomere-related roles. Silencing mutations within an evolutionarily conserved domain of yKu80p, part of its structural core, disrupted the yKu80p-Sir4p interaction and impaired Sir3p recruitment to the telomere, showing that this interaction is critical for the establishment of the silenced domain (Roy *et al.*, 2004). The roles of Ku in silencing and telomere tethering have also been shown to be separable (Taddei *et al.*, 2004).

1.4.7 Organization of silenced DNA and competition

Silencing is restricted to defined loci by competition for a limiting amount of silencing factors, in particular for Sir2p, Sir3p and Sir4p (Buck and Shore, 1995; Cockell *et al.*, 1995; Maillet *et al.*, 1996; Sussel and Shore, 1991). The silenced *HM* loci and telomeres in particular share many of the essential trans-acting silencing

factors and their relative degrees of silencing are determined by competition for these factors. For example, mutations of Rap1p in the region critical for Rif1p/Rif2p interaction increases telomere length and TPE, but also results in a decrease in *HM* silencing. The increase in TPE is thought to be due to increased binding of the Sir proteins to Rap1p due to decreased competition with the Rif complex, thus resulting in a reduction of the Sir factors at *HM* loci (Buck and Shore, 1995; Sussel and Shore, 1991). The overexpression of Sir factors, resulting in dispersement throughout the nucleus, or alterations in the relative amounts of each of the Sir factors can alter silencing at both normally repressed and normally expressed loci (Cockell *et al.*, 1995; Maillet *et al.*, 1996; Smith *et al.*, 1998). Therefore, the stoichiometry of the Sir proteins is also a critical factor in silencing (Maillet *et al.*, 1996). *HM* repression can be decreased by overexpression of Sir1p or Sir4p alone, believed to be a result of titrating away Sir2p and Sir3p into incomplete silencing complexes (Cockell *et al.*, 1998a). Even overexpression of either the N-terminal or C-terminal region of Sir4p is sufficient to decrease *HM* repression and TPE (Cockell *et al.*, 1998b; Singer *et al.*, 1998). In addition, if regions of the genome at which the Sir complex is not normally found suddenly become able to recruit the complex, the strength and spread of silencing at the normally silenced loci will decrease. This is observed in aging yeast where the Sir complex relocates to the nucleolus resulting in a disruption of TPE (Kennedy *et al.*, 1997).

Chromosomal context is also important. The majority of Rap1p, Sir3p and Sir4p are concentrated with telomeric foci, resulting in subnuclear silencing compartments (Gotta *et al.*, 1996; Marcand *et al.*, 1996). Even flanking a euchromatic reporter gene with the *HML* silencers is insufficient to cause repression. However silencing of the gene construct can be improved by increased proximity to the telomere silencing compartments or overexpression of the Sir proteins (Maillet *et al.*, 1996).

1.5 Nuclear architecture and silencing

Chromosomes of interphase nuclei are non-randomly distributed (reviewed in Marshall, 2002). Although the function of the spatial compartmentalization of chromosomes and different chromatin domains is largely unknown, there is evidence to suggest that formation of specialized subnuclear compartments may allow specific epigenetic control of these regions (reviewed in Fisher and Merkenschlager, 2002). An example of this is the subnuclear silencing compartments that are found in

several organisms, including *S. cerevisiae, Drosophila* and *P. falciparum,* in which transcriptionally inactive chromatin regions are associated with the nuclear periphery (Figueiredo *et al.*, 2002; Klein *et al.*, 1992; Marshall *et al.*, 1996; Palladino *et al.*, 1993a). Peripherally-associated telomeres cluster together in several foci in yeast (Funabiki *et al.*, 1993; Gotta *et al.*, 1996; Laroche *et al.*, 1998; Palladino *et al.*, 1993a), trypanosomes (Chung *et al.*, 1990; Perez-Morga *et al.*, 2001) and *P. falciparum* (Figueiredo *et al.*, 2002), allowing specific gene regulation of these specialized regions. Cytological and biochemical experiments in higher eukaryotes, including human cells (Balajee *et al.*, 1996; de Lange, 1992; van Dekken *et al.*, 1989), *Drosophila* (Gruenbaum *et al.*, 1984), hamsters (Balajee *et al.*, 1996) and plants (Rawlins and Shaw, 1990) also indicate the telomeres are closely associated with the nuclear periphery or the nuclear matrix, which may provide an analogous organization function to the periphery of lower organisms.

In *S. cerevisiae*, the clustering of telomeres and centromeres to opposite sides of the nuclear periphery and the restriction of their movement is proposed to facilitate chromosome alignment, pairing and recombination during cell division (Dresser and Giroux, 1988; Hediger *et al.*, 2002; Heun *et al.*, 2001a; Rockmill and Roeder, 1998; Trelles-Sticken *et al.*, 1999). It is still unclear how telomeres associate and locate to the periphery; DNA-DNA, DNA-protein and protein-protein interactions between telomeres and nuclear membrane components may all be involved. Tethering of telomeres near the periphery occurs via two overlapping pathways which require either yKu or Sir4p. Fusion proteins with yKu or Sir4p silencing-deficient mutants targeted to an internal locus were able to localize it to the nuclear periphery without nucleating silencing (Taddei *et al.*, 2004). Peripheral localization by Sir4p required either yKu or Esc1p (a protein localized to the nuclear periphery). Both the yKu and Esc1p-dependent tethering pathways mediate the anchoring of natural telomeres *in vivo* (Hediger *et al.*, 2002; Laroche *et al.*, 1998; Maillet *et al.*, 2001; Taddei *et al.*, 2005; Taddei *et al.*, 2004).

The 64 telomeres of an *S. cerevisiae* diploid cluster into 5-8 foci located primarily at the periphery of the nucleus (Gotta *et al.*, 1996; Klein *et al.*, 1992; Louis, 1995; Palladino *et al.*, 1993a; Palladino *et al.*, 1993b; Pryde and Louis, 1997). This nuclear architecture is separable from silencing but the two processes are interrelated and reinforce each other (Taddei *et al.*, 2004). The peripheral localization of a telomere is insufficient for silencing (Tham *et al.*, 2001) but a cluster of telomeres does facilitate the recruitment of a high concentration of silencing factors; in turn, the

silencing factors, which include the yKu80p and Sir4p anchoring components, reinforce the peripheral localization and clustering (reviewed in Taddei *et al.*, 2005). Deletion of *yKU80* increases the number of telomeric foci in addition to delocalizing the telomeres from the periphery, implicating yKu80p in cluster formation (Hediger *et al.*, 2002; Laroche *et al.*, 1998). Mutations of the other silencing factors, including Rap1p, Sir2p and Sir3p, delocalize the silencing factors from the telomeres but do not affect the nuclear architecture (Gotta *et al.*, 1997; Laroche *et al.*, 1998). The clustering of telomeres has been proposed to be related to the degree of homology between the TASs, but has recently been shown to be unrelated to the amount of homology (Bystricky *et al.*, 2005).

One apparent function of localizing telomeres at the periphery is to prevent their dynamic recombination from destabilizing the rest of the genome by restricting their degree of movement through the nucleus (Hediger and Gasser, 2002; Heun *et al.*, 2001b). Telomeric regions are highly polymorphic and are capable of both meiotic and mitotic ectopic recombination in many organisms, resulting in translocations of telomeric regions that would be detrimental at interstitial locations. However, the genome of the organism remains highly stable, indicating the presence of a barrier to sequester the telomeres from the rest of the genome (Fischer *et al.*, 2000; Pryde *et al.*, 1997). In *S. cerevisiae*, the Y' subtelomeric elements are nearly identical to each other, suggesting sequence homogenization through frequent ectopic recombination. However, core X elements show a much greater divergence (10-20%), indicating this recombination barrier may lie within the X-Y' junction in yeast (Louis, 1995). Many mutations can disrupt this barrier. Notably, mutations of yKu result in significantly increased recombination between internal and telomeric loci, presumably due to the delocalization from the periphery (Eyre, 2001). The role of this protein in preserving genome stability appears to be conserved in humans as a loss of *KU80* results in end-to-end fusions of telomeres (Kass-Eisler and Greider, 2000).

1.5.1 Telomere folding: the structure of TPE?

In addition to the clustering and peripheral localization of telomeres into subnuclear silencing compartments, the higher order structure of telomeric regions is also believed to affect silencing. Rap1p associates *in vivo* not only with the telomere repeats (Conrad *et al.*, 1990) but also with the subtelomeric region despite a lack of Rap1p binding sites in the TAS (de Bruin *et al.*, 2000; Hecht *et al.*, 1996; Strahl-Bolsinger *et al.*, 1997). This Rap1p binding within the TAS appears to require

association with the Sirs. yKu also associates with the subtelomeric domains in a Sir-dependent manner, suggesting a relationship with the spread of silencing (Martin *et al.*, 1999). These observations resulted in a model whereby the telomere folds back on the subtelomeric domain to form a core heterochromatin region through interactions between Rap1p, the Sir complex and histones (Fig. 1.6). This folded structure would account for the association of Rap1p and yKu with the subtelomeric loci (Strahl-Bolsinger *et al.*, 1997). In addition, folding of the telomere has been demonstrated genetically using gene activation by a downstream UAS at a truncated telomere. The UAS is the yeast equivalent of an enhancer but can only act when positioned upstream of the gene promoter. However, placing the UAS downstream of a gene located near the telomere allowed activation of the gene, indicating that the telomere folded back on the subtelomeric region (de Bruin *et al.*, 2001). This activation was also Sir3p-dependent, implicating the Sir's in the folded telomere structure (de Bruin *et al.*, 2001). Interestingly, an earlier study showed that deletion of *SIR3* did not disrupt the subnuclear Rap1p associations (de Bruin *et al.*, 2000). Therefore the requirement for, and role, of the Sir proteins in telomere folding is still unclear.

The folding of telomeres is proposed to facilitate the continuous silencing of telomere adjacent regions observed in studies at truncated ends (Park and Lustig, 2000). However, the studies of silencing at native telomeres demonstrated silencing to be discontinuous, and centred around core X, in contrast to the folded telomere model (Pryde and Louis, 1999). Therefore, a modified structure was proposed in which the telomere repeats are bound by the telosome and silencing factors (Rap1p, yKu and the Sir's), that in turn interact with proteins recruited to core X (ORC, Abf1p), causing the silencing of the regions around core X and the telomere (Fig. 1.6) (Pryde and Louis, 1999). In this model the non-repressive Y' elements are excluded from the tight region of heterochromatin, resulting in a loop structure (Fig. 1.6). The loop model is also supported by a silencing study in which a 6.7kb Y' element extended silencing of a marker gene several kilobases further from the telomere than unique sequences (Renauld *et al.*, 1993).

Telomere loops have also been found in mammals (Griffith *et al.*, 1999), ciliates (Murti and Prescott, 1999) and trypanosomes (Munoz-Jordan *et al.*, 2001) where they are believed to be important for telomere end-protection. These loops are distinct from yeast loops however, as they form by invasion of the 3' overhang into the duplex telomeric DNA whereas there is no evidence of a similar invasion in yeast.

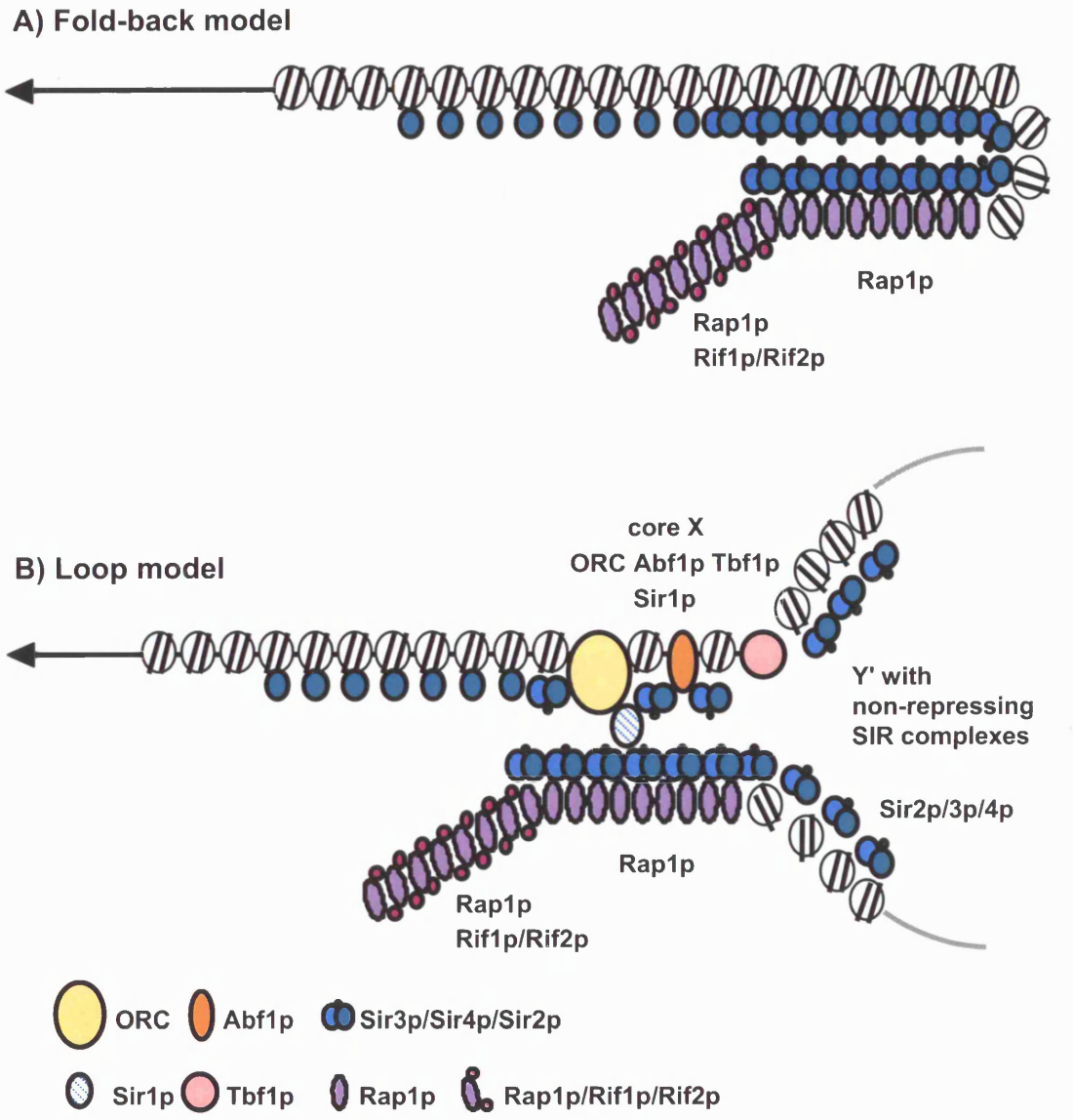

Figure 1.6. Models for formation of repressive chromatin at telomeres. A) Truncated telomeres fold-back on the subtelomeric region creating a continuous region of core heterochromatin and silencing. B) Native telomeres interact with the subtelomeric core X element creating a tight domain of repression at the telomere-core X junction. The exclusion of the unsilenced Y' elements from this domain results in a loop structure.

1.6 Heterochromatin

Chromatin has been described as a means of formatting the genome (Paro, 2000) into either transcriptionally permissive (euchromatin) or non-permissive (heterochromatin) domains through alteration in the degree of nucleosome spacing and packing. Such formatting allows certain gene expression profiles to be followed, as in the case of maintaining cell types in higher organisms, and to establish and maintain specialized regions of the genome including centromeres, telomeres and, in yeast, the silent mating type loci (reviewed in Grewal and Moazed, 2003). Maintaining these domains requires stable chromatin modifications while other less stable modifications allow the cell to adjust gene expression for changing conditions (Jenuwein, 2001). Such control of gene expression through non-genetic modifications is known as epigenetic regulation.

In mammals, heterochromatic domains can be visualized as dark bands on stained metaphase chromosomes corresponding to highly condensed chromatin. Heterochromatin is more broadly defined as gene-poor regions consisting predominantly of repetitive DNA elements. It is typically late-replicating, exhibits reduced meiotic recombination, decreased sensitivity to endonucleases and modifying enzymes, and contains closely spaced nucleosomes. The closely spaced, or 'phased', nucleosomes are further packaged into compacted chromatin fibers resulting in the dark bands (reviewed in Grewal and Elgin, 2002). This higher order compaction imposes topological constraints on the access of other factors, including transcription factors, resulting in the observed gene repression in these domains. The correlation between decreased gene expression and the condensed chromatin is supported by studies of *Drosophila* PEV showing that a variegated gene adjacent to a heterochromatin domain is only repressed when it is also packaged into the condensed structure (Cryderman *et al.*, 1999). Heterochromatin can be classified as constitutive or facultative. Constitutive heterochromatin is found in large blocks such as near centromeres and telomeres while facultative heterochromatin refers to the silencing of one of the two chromosome homologues, as occurs in X-inactivation. Interestingly, some species contain naturally heterochromatic genes whose native expression is dependent on the heterochromatic localization (Lu *et al.*, 2000). Although heterochromatic regions in yeast cannot be visualized, silenced regions at the silent mating type loci and near telomeres are classified as heterochromatic based similarities to that of higher organisms. These similarities include compact,

phased nucleosomes, reduced nuclease accessibility and heterochromatic histone modifications in addition to the characteristic gene silencing (reviewed in Moazed *et al.,* 2004).

1.6.1 Genetic control

The spread of natural heterochromatic regions is regulated by several mechanisms; genetic elements, primarily silencers and barriers, often define the initiation and termination sites of the domain while epigenetic modifications are involved in spreading of the silenced region and can also have barrier function. Silencers, such as the telomeres and *E* and *I* silencers in *S. cerevisiae,* are defined by their ability to silence a region independently. Other elements, termed protosilencers, have been identified which act cooperatively with silencers to enhance repression (reviewed in Fourel, 2002). Protosilencers are often individual binding sites for silencing factors, for example the Rap1p binding site in the promoter of *α1/α2* genes between the two *HML* silencers (see Fig. 1.5) which contributes to the silencing of this locus (Boscheron *et al.*, 1996). As mentioned previously, the core X element at yeast telomeres is also classed as a protosilencer. Silencers and protosilencers can interact, despite the presence of intervening barrier elements or expressed domains, resulting in a discontinuity in the silenced domain and propagation of the silenced region to larger distances from the canonical silencer elements. (Fourel *et al.*, 2002; Fourel *et al.*, 1999; Lebrun *et al.*, 2001). Compelling evidence for such long range interactions is presented by the visualization of heterochromatin looping in *Drosophila* that arises from physical interactions between protosilencers and known heterochromatic domains (Csink and Henikoff, 1996; Seum *et al.*, 2001). Concatamerization of individual protosilencers can also generate an independent silencer; artificially combining an ORC, Rap1p and Abf1p binding site generates functional silencers that are otherwise unrelated to the *HM* silencers (McNally and Rine, 1991).

Barrier elements, also termed insulators, are able to block the spread of heterochromatin and the associated transcriptional silencing. In budding yeast, the STAR elements (Fourel *et al.*, 1999), the right boundary of *HMR* (Donze *et al.*, 1999; Donze and Kamakaka, 2001) and a number of promoters (Bi and Broach, 1999; Yu *et al.*, 2003) have been shown to function as barriers. PRE-initiated silencing in *Drosophila* can also be blocked by insulator DNA elements (Sigrist and Pirrotta, 1997). Many of these barriers contain binding sites for transcriptional activators,

believed to interrupt the ordered nucleosome array of heterochromatic domains, thereby preventing the spread of the Sir complex (Bi and Broach, 1999; Morse, 2000; Yu *et al.*, 2003). The binding of the Ctf-1p transcription factor to H3 is able to block the spread of the Sir complex (Ferrari *et al.*, 2004). Other models propose that the barrier elements recruit chromatin remodeling factors, such as histone acetyltransferases (HATs), to create an open chromatin conformation that counteracts heterochromatin formation (Donze and Kamakaka, 2001; Oki and Kamakaka, 2002). Removal of barrier elements can result in the spread of the heterochromatic structure from its normal locus as observed in PEV, where chromosome rearrangements with one breakpoint within a heterochromatic domain allows silencing of adjacent and normally active genes (reviewed in Grewal and Elgin, 2002).

1.6.2 Epigenetic control and the nucleosome

The nucleosome is the fundamental building block of chromatin and consists of 147 base pairs of DNA wrapped around two sets of the four histones, H2A, H2B, H3 and H4 (reviewed in Kornberg and Lorch, 1999). Adjacent nucleosomes are connected by linker DNA that varies in length in different organisms, tissues, and different nucleosomes with an average nucleosome repeat length of 170-240bp in metazoans. A fifth histone, H1, is found only in higher eukaryotes and binds to the linker DNA (reviewed in Van Holde, 1989; Thoma *et al.*, 1993). Yeast nucleosomes are more closely spaced with a repeat length of ~160bp and a linker of 15-20bp (White *et al.* 2001). With the published structures of *Xenopus laevis* and *S. cerevisiae* nucleosomes (Luger *et al.*, 1997; White *et al.*, 2001), the role of the N-terminal histone tails has become more evident. These tails appear to be important in connecting nucleosomes, with the H4 tails contacting the neighbouring H2A-H2B dimer (Luger and Richmond, 1998). These interactions likely facilitate nucleosome positioning, particularly in the ordered arrays of heterochromatic domains, and may also play a role in higher order chromatin compaction. Epigenetic histone modifications including acetylation, methylation and ubiquitination, occur primarily in the N-terminal tails and are believed to destabilize the inter-nucleosome interactions (Luger and Richmond, 1998). Thus the reduction in histone modification observed for heterochromatic regions is likely to be required for the chromatin compaction. A histone variant, Htz1 in yeast and H2A.Z in higher organisms, is thought to act as a barrier and counteracts Sir-mediated repression in yeast (reviewed in Hild and Paro,

2003). This variant has been proposed to be defective in these inter-nucleosome interactions therefore preventing heterochromatin formation.

Nucleosome positioning is described in terms of the 'translational positioning', or location on the DNA sequence, and 'rotational setting', referring to the orientation of the DNA on the nucleosome surface (reviewed in Travers and Klug, 1987). Micrococcal nuclease (MNase), which cuts the nucleosome linker, is used to map the translational positioning while digestion of chromatin with DNaseI, which cuts exposed DNA on the nucleosome surface, allows determination of the rotational setting. MNase analysis of heterochromatic domains, including artificial (as occur in PEV or transposon insertion in heterochromatin) and endogenous (such as telomeres) heterochromatin in *Drosophila*, and the *HM* loci in yeast, have revealed specialized nucleosome arrays of phased and closely spaced nucleosomes (Wallrath and Elgin, 1995; Weiss and Simpson, 1998; Cryderman *et al.*, 1999; Ravindra *et al.*, 1999; Sun *et al.* 2001). In contrast, nucleosomes within the expressed *MAT* locus in yeast were randomly distributed and the **a**1 TATA box showed increased accessibility to MNase compared to the *HM* copy (Ravindra *et al.*, 1999; Weiss and Simpson, 1998). The precise positioning of nucleosomes at the *HM* loci is disrupted by both *sir3* and H4 amino-tail mutations (Ravindra *et al.*, 1999; Weiss and Simpson, 1998), confirming the importance of the Sir-complex and histone tails in establishing heterochromatin. Higher order chromatin structures, such as the 30nm fibre and tertiary structures of higher organisms, are also more condensed in heterochromatic regions, presumably due to the shorter linkers and more compact and regular nucleosome spacing (reviewed in Adkins *et al.*, 2004 and Grigoryev, 2004).

The epigenetic control of chromatin structure to alter gene expression is accomplished by two main mechanisms: ATP-dependent chromatin remodeling by factors such as the Swi-Snf and Isw1/2 remodeling complexes, and covalent histone modifications (reviewed in Workman and Kingston, 1998). In higher eukaryotes, DNA methylation of cytosine residues in CpG islands is also used to mark differentially expressed regions (reviewed in Richards and Elgin, 2002, also Section 1.3.1). The chromatin remodelors appear to act locally by repositioning nucleosomes to make promoter regions more or less accessible to transcription factors. However, the effect of histone modifications on chromatin structure and gene expression, while often affecting large domains, is only beginning to be understood. The histone tails, in contrast to the core, are relatively unstructured (Luger *et al.*, 1997) and are accessible for a variety of modifications including acetylation, methylation,

ubiquitination, phosphorylation, and ADP ribosylation (Luger and Richmond, 1998). A few core residues have also been shown to undergo modification. The specific combinations of these modifications are believed to constitute a 'histone code' that can be interpreted by other proteins to effect given molecular processes including chromatin structure and gene transcription (Jenuwein and Allis, 2001; Strahl and Allis, 2000).

Acetylation and methylation are the best understood of the various modifications. Histone acetylation was the first histone modification to be associated with gene regulation through identification a histone acetyltransferase (HAT) and deacetylase (HDAC) in yeast with opposite effects on gene expression (Kuo and Allis, 1998). In general, the lysine residues on the four histones are hypoacetylated in the heterochromatin regions, including the yeast *HM* loci and telomeres (Braunstein *et al.*, 1993; Braunstein *et al.*, 1996; Suka *et al.*, 2001), while histones in euchromatic regions contain numerous acetylated lysines (Grunstein, 1997; Struhl, 1998; Suka *et al.*, 2001). The effect of methylation, in contrast, is dependent on the specific residue that is modified. Euchromatic regions are specifically methylated on K4 of histone H3 while heterochromatin, in contrast, is methylated on K9 and K27 of H3. Methylation of H3-K9 serves as a heterochromatic mark that attracts heterochromatin proteins such as *HP1* and its homologues (Bannister *et al.*, 2001; Lachner *et al.*, 2001). It is perhaps the acetylation of H3-K9 within barrier elements that blocks the spread of heterochromatin by preventing methylation of this residue (Litt *et al.*, 2001). However, the H3-K27 and H3-K9 methylation marks are absent in *S. cerevisiae* which also lacks an HP1 homologue (Suka *et al.*, 2002). *S. cerevisiae* instead appears to regulate the spread of heterochromatin from the telomere by maintaining a balance between the modified and unmodified nucleosomes (Suka *et al.*, 2002).

1.7 Acetylation

Histone acetylation appears to be the major epigenetic regulator in yeast transcriptional control (Grunstein, 1997). Nucleosomes at the silent mating type loci and telomeres are hypoacetylated (Braunstein *et al.*, 1993) and are more compact (Chen *et al.*, 1991; Chen-Cleland *et al.*, 1993) than euchromatin nucleosomes and mutations in the N-terminal tails of H3 or H4 causes derepression of these loci (Johnson *et al.*, 1990; Laurenson and Rine, 1992; Park and Szostak, 1990; Thompson *et al.*, 1994). The majority of acetylated lysines are within the N-terminal tails of H3 (K9, 14, 18, 23 and 27) and H4 (K5, 8, 12 and 16) (Suka *et al.*, 2001).

Acetylation of H4-K16, in particular, is critical for silencing in budding yeast while the other lysine residues have less important functions in silencing (Imai *et al.*, 2000a; Liou *et al.*, 2005). The binding of Sir3p and Sir4p to the nucleosome requires hypoacetylation of H4-K16, but not the other H4 lysine residues (Carmen *et al.*, 2002; Liou *et al.*, 2005; Venditti *et al.*, 1999b). The spread of the silenced domains appears to be regulated by competition between HATs and HDACs for modification of this residue. HDAC's are correlated with repression (Kuo and Allis, 1998; Rundlett *et al.*, 1998; Struhl, 1998) and HATs are often required for transcription activation (Agalioti *et al.*, 2000; Allard *et al.*, 1999; Ikeda *et al.*, 1999; Utley *et al.*, 1998). The Sir2p HDAC is specific for acetylated H4-K16 (Imai *et al.*, 2000a; Suka *et al.*, 2002). The *S. pombe* and *Drosophila* Sir2p homologues also have conserved deacetylase activities that are essential for the formation of heterochromatin (Parsons *et al.*, 2003; Shankaranarayana *et al.*, 2003). Preventing the spread of the Sir complex into active regions of the genome appears to involve both active, opposing acetylation of H4-K16 by Sas2p and the protection of acetylated residues from Sir2p activity by Bdf1p (see below).

1.7.1 *SAS2*

SAS2 is an orthologue of the *MOF* acetyltransferase, a member of the MYST family that is specific for H4-K16 in *Drosophila* and *S. cerevisiae* (Akhtar and Becker, 2000; Reifsnyder *et al.*, 1996; Shia *et al.*, 2005; Smith *et al.*, 2000a; Suka *et al.*, 2002). *SAS2* mutants affect silencing at telomeres, the *HM* loci and rDNA in yeast (Ehrenhofer-Murray *et al.*, 1997; Kimura *et al.*, 2002; Meijsing and Ehrenhofer-Murray, 2001; Osada *et al.*, 2005; Suka *et al.*, 2002). Sas2p is part of the SAS trimeric complex composed solely of Sas2p, Sas4p and Sas5p (Shia *et al.*, 2005) and also interacts with chromatin assembly factor 1 (CAF-1) and nucleosome assembly factor Asf1p which have similar effects on silencing (Meijsing and Ehrenhofer-Murray, 2001). Mutating the K14-K16 residue to arginine phenocopies a *SAS2* deletion, indicating the acetylation of the residue is required for Sas2p's role in silencing (Suka *et al.*, 2002). Both the arginine substitution and the *SAS2* deletion decreased the acetylation of the other lysine residues within both the H3 and H4 tails specifically near the telomere, indicating a cooperative effect in histone acetylation (Suka *et al.*, 2002). Deletion of Sas2p allows Sir3p to spread beyond the normal silencing boundary and silence normally expressed genes (Kimura *et al.*, 2002; Suka

et al., 2002). Sas2p therefore appears to prevent the spread of the Sir complex from silencers by counteracting Sir2p histone deacetylation (Fig. 1.7).

1.7.2 *BDF1*

The bromodomain was originally identified in the *Drosophila* Brahma protein (Tamkun *et al.*, 1992) and is conserved in eukaryotes. Bromodomain factors have been shown to specifically recognize acetylated histone tails and are found in many transcriptional coactivators including HAT complexes (e.g. SAGA, P/CAF) and chromatin remodeling complexes (e.g. Swi/Snf, RSC) (Dhalluin *et al.*, 1999; Hassan *et al.*, 2002; Hudson *et al.*, 2000; Jacobson *et al.*, 2000; Jeanmougin *et al.*, 1997; Ornaghi *et al.*, 1999; Owen *et al.*, 2000; Pamblanco *et al.*, 2001). HAT bromodomains may provide a feedback mechanism to maintain acetylated histones in appropriate chromatin domains (Matangkasombut *et al.*, 2000). In yeast, the bromodomain-containing Bdf1p binds acetylated H3 and H4 histones *in vivo* and is required for the association of the TFIID transcription complex with chromatin containing acetylated histones (Lygerou *et al.*, 1994; Martinez-Campa *et al.*, 2004; Matangkasombut *et al.*, 2000; Matangkasombut and Buratowski, 2003; Pamblanco *et al.*, 2001). Bdf1p may have both TFIID-dependent and independent roles as studies looking for Bdf1p-TFIID interactions have produced mixed results (Gavin *et al.*, 2002; Matangkasombut *et al.*, 2000; Sanders *et al.*, 2002). In agreement with this proposal, Bdf1p was found to bind chromosomes throughout the nucleus, with the exception of the nucleolus, and did not show the promoter-specific binding pattern that was expected from its association with TFIID, although it is involved in gene specific regulation (Chua and Roeder, 1995; Matangkasombut and Buratowski, 2003). Bromodomains have been proposed to bind with low affinity to their unacetylated target proteins and with higher affinity upon recognition of a specific acetylation modification. This implies Bdf1p may act as a signaling molecule to recognize the acetylation signals for transcription and recruit binding partners such as TFIID (Winston and Allis, 1999).

A role in anti-silencing and maintenance of euchromatin for Bdf1p has also been recently discovered (Ladurner *et al.*, 2003). Bdf1p competes with Sir2p for binding to acetylated histones at the heterochromatin boundaries near the silent mating type loci and telomeres. Significantly, acetylation of the H4-K16 residue is both required and sufficient for Bdf1p binding (Ladurner *et al.*, 2003). Mutations in *BDF1* that abrogated its histone binding activity resulted in decreased expression of genes close to heterochromatin domains (Ladurner *et al.*, 2003). Therefore, Bdf1p

appears to shield the acetylated H4-K16 residue from Sir2p deacetylation, thereby limiting the spread of the Sir complex (Fig. 1.7). By comparison, one of the roles of Sir3p and Sir4p in repression may be to protect the hypoacetylated histones of heterochromatin from HATs (Ladurner *et al.*, 2003).

1.8 Methylation

Histones can also be modified by methylation of either lysine or arginine residues. Arginine methylation, although not observed in yeast, is found in transcriptionally active regions while the function of lysine methylation appears to be dependant on which histone residue is altered (reviewed in Jenuwein and Allis, 2001; Zhang and Reinberg, 2001). Lysine methylation occurs predominantly on residues K4, K9, K27 and K36 of histone H3, and on K20 of H4 and each residue can be mono-, di-, or trimethylated (Jenuwein, 2001). Histone methylation is a highly stable modification and may serve as a transcriptional memory to mark long term patterns of expression (Jenuwein, 2001; Krogan *et al.*, 2003) or play a more direct role in transcription elongation (Bernstein *et al.*, 2002). Although methylation has been proposed to be a permanent mark, the recent discovery of a histone demethylase conserved from yeast to humans shows that, although it is stable, methylation is reversible (Shi *et al.*, 2004). The *Drosophila Su(var)3-9* suppressor of variegation was one of the first identified lysine-specific HMTases (K-HMT), most of which contain the SET domain, and orthologues have been identified from yeast to mammals (Rea *et al.*, 2000). In mammals, *Drosophila* and *S. pombe,* K-HMTs that methylate H3-K9 are important for the formation of heterochromatin (Lachner and Jenuwein, 2002; Nielsen *et al.*, 2001). In contrast, other K-HMTs methylate K4 of histone H3, a modification associated with gene activation (Briggs *et al.*, 2001; Nishioka *et al.*, 2002; Noma and Grewal, 2002; Strahl *et al.*, 1999; Wang *et al.*, 2001).

1.8.1 *SET1*

In *S. cerevisiae,* H3-K9 methylation is not observed and H3-K4 is the predominant site for histone methylation (Strahl *et al.*, 1999). In contrast to higher organisms, this modification is required for both gene expression and maintenance of silenced domains in yeast (Corda *et al.*, 1999; Nislow *et al.*, 1997). Seven genes containing SET domains have been found in budding yeast (Schultz *et al.*, 2000). *SET1*, part of the multiprotein COMPASS complex (in addition to Swd1p, Swd2p,

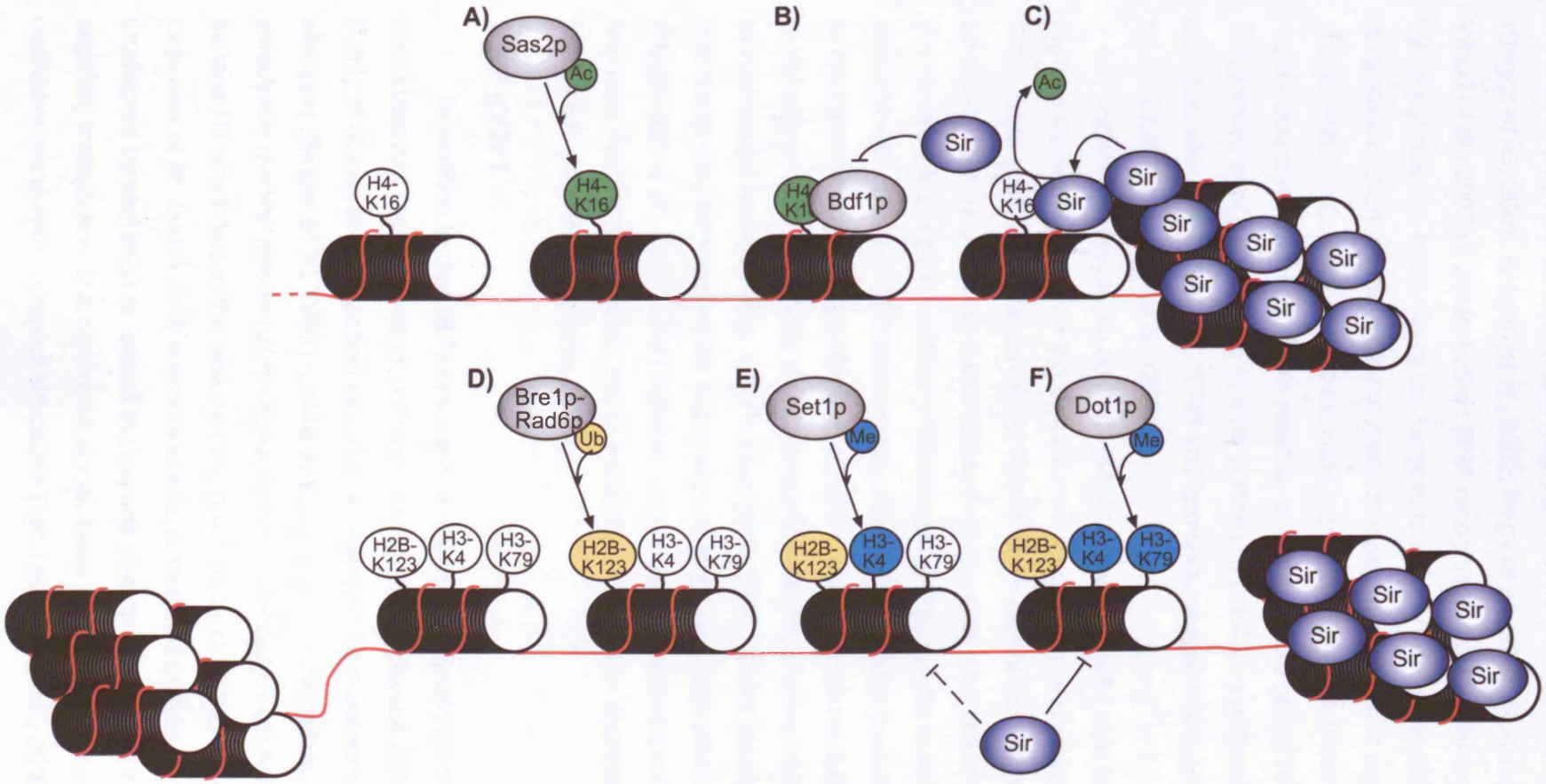

Figure 1.7. Euchromatic histone modifications prevent Sir-mediated heterochromatin formation. A) Acetylation of H4-K16 by Sas2p and (B) the binding of Bdf1p to nucleosomes acetylated at H4-K16 prevents (C) deacetylation by Sir2p and the subsequent spreading of the Sir complex. D) Bre1p directs the ubiquitination of H2B-K123 by Rad6p. This facilitates the methylation of lysine residues H3-K4 by Set1p (E) and H3-K79 by Dot1p (F), inhibiting association of the Sir complex.

Swd3p, Bre2p, Sdc1p, Spp1p and Shg1p), is responsible for H3-K4 methylation (Briggs *et al.*, 2001; Krogan *et al.*, 2002; Nagy *et al.*, 2002; Roguev *et al.*, 2001; Wood *et al.*, 2003a). Set1p has an RNA recognition motif at the amino terminus and the conserved SET domain at the carboxy terminus. The N-terminal region is specific for tri-methylation of H3-K4, found predominantly in the 5' gene regulatory regions (Fingerman *et al.*, 2005; Schlichter and Cairns, 2005). The full Set1p is important for mono- and di-methylation of this residue, which are more global histone modifications (Fingerman *et al.*, 2005). The tri-methylation of H3-K4 is specifically required to maintain silencing at the *HM*, rDNA and telomeric domains (Briggs *et al.*, 2001; Bryk *et al.*, 2002; Fingerman *et al.*, 2005).

Initially, it was proposed that H3-K4 methylation was able to both promote and repress transcription, given the disruption of silencing in *set1* mutants (Briggs *et al.*, 2001; Bryk *et al.*, 2002; Nislow *et al.*, 1997). More recent studies have revealed that removal of the euchromatin-associated tri-methylation mark allows components of the Sir silencing complex to bind promiscuously. This results in decreased association of the Sirs with the normally silenced loci which presumably is sufficient to disrupt silencing (Santos-Rosa *et al.*, 2004; van Leeuwen and Gottschling, 2002). In agreement with this, Sir3p binds unmodified histones but is unable to bind H3-K4 tri-methylated histones (Fig. 1.7) (Santos-Rosa *et al.*, 2004). Another possibility is that Set1p may be required for expression of other essential silencing factors (Fingerman *et al.*, 2005). *Set1* deletion also causes a modest shortening of the telomere tract (Roguev *et al.*, 2001), most likely due to the decreased association of the Sir complex with telomeres.

1.8.2 *DOT1*

In addition to the SET-containing and arginine-specific methyltransferases, a third class has recently been identified. The methyltransferase *DOT1* (also known as Pch1) of *S. cerevisiae* was first identified in a screen for disruptors of telomeric silencing (Singer *et al.*, 1998). Unlike any previously characterized HMTs that selectively modify histone tail residues, Dot1p specifically methylates lysine 79 of histone H3 which lies in the histone core (Lacoste *et al.*, 2002; Ng *et al.*, 2002a; van Leeuwen *et al.*, 2002). One outcome of this, is that methylation by Dot1p is unaffected by alteration or loss of the histone tails (van Leeuwen *et al.*, 2002). In addition, methylation of a core residue may have a greater effect on the ability of nucleosomes to form compact structures (van Leeuwen *et al.*, 2002). Dot1p contains

a methylase fold, lacks the characteristic SET domain (Ng *et al.*, 2002a) and only acts in the context of the nucleosome as its methylation activity is not detected on free histone H3 (van Leeuwen *et al.*, 2002). H3-K79 methylation and *DOT1* homologues have subsequently been observed in many species from flies to humans (Feng *et al.*, 2002; Min *et al.*, 2003; Zhang *et al.*, 2004). Deletion of *DOT1*, while it fails to alter Set1p-mediated H3-K4 methylation levels, does provoke a significant increase in bulk histone acetylation. Interestingly, the level of H4-K16 acetylation is unchanged in a *dot1* mutant (Lacoste *et al.*, 2002).

Similar to *SET1*, methylation by Dot1p was originally thought to be required for silencing as *dot1* mutants disrupted silencing and decreased association of the Sir proteins near telomeres (Ng *et al.*, 2002a; Singer *et al.*, 1998). Intriguingly, although the Sir complex is thought to associate with histones via interactions with the histone tails, the H3-K79 residue does affect Sir association (Park *et al.*, 2002a; Smith *et al.*, 2002). Dot1p is recruited with COMPASS to RNA polymerase II and therefore appears to have a role, together with Set1p, in gene activation (Krogan *et al.*, 2003; Wood *et al.*, 2003b). Dot1p methylation of H3-K79 is now proposed to also act to restrict binding of the Sir-silencing complex to the silenced domains by methylating this residue in euchromatic domains and preventing Sir-association (Fig. 1.7) (van Leeuwen *et al.*, 2002; Wood *et al.*, 2003b).

1.8.3 *BRE1* and ubiquitination

Histone ubiquitination affects 10-15% of histone H2A in most eukaryotic organisms (Jason *et al.*, 2002). However, the role of this modification is still poorly understood although it has been linked with transcribed regions and expression regulation (Barsoum and Varshavsky, 1985; Wood *et al.*, 2003b). The yeast Rad6p is a ubiquitin-conjugating enzyme involved in many diverse processes including DNA repair (Hishida *et al.*, 2002; Jentsch *et al.*, 1987), meiosis (Kupiec and Simchen, 1986), Ty transposition (Kang *et al.*, 1992), DNA damage-induced mutagenesis (Hishida *et al.*, 2002) and gene silencing at both the *HM* loci and telomeres (Huang *et al.*, 1997). The specific activity of Rad6p in these processes is directed by various interacting proteins. *BRE1* encodes a RING finger-containing protein, characterized by a C3HC4 or C3H2C3 motif that binds a zinc ion, and recruits Rad6p to promoters in active chromatin regions where it mono-ubiquinates K123 of histone H2B (Muren *et al.*, 2001; Wood *et al.*, 2003a). Bre1p therefore specifically directs the activity of Rad6p in transcriptional regulation (Fig. 1.7) (Wood *et al.*, 2003a; Wood *et al.*,

2003b). This ubiquitination of H2B-K123 is essential for subsequent H3 methylation by Dot1p and Set1p (Fig. 1.7) (Briggs *et al.*, 2002; Dover *et al.*, 2002; Ng *et al.*, 2002b; Robzyk *et al.*, 2000; Sun and Allis, 2002). Interestingly, the H2B-K123 residue is in a region important for internucleosomal contacts and the addition of the bulky ubiquitin group would be expected to disrupt these contacts, in correlation with the association of this mark with open, euchromatic regions (White *et al.*, 2001). Both Rad6p and Bre1p are essential for maintenance of the silent domains, presumably by maintaining the Set1p and Dot1p euchromatic methylation marks that prevent promiscuous Sir complex binding (Huang *et al.*, 1997; Wood *et al.*, 2003a). The Ubp10p ubiquitin protease localizes to telomeres and specifically removes the H2B-K123 ubiquitin mark to facilitate association of the Sir complex (Emre *et al.*, 2005).

1.9 Aims of this project

This study examines the chromatin structures of truncation, and native repressive and non-repressive telomeres in *S. cerevisiae*, using MNase chromatin analysis, in order to establish a link between the underlying nucleosome positioning and the silencing states of telomeres. The roles of the Sir factors and the histone modifiers, Sas2p, Bdf1p, Set1p, Dot1p and Bre1p in the silencing and chromatin structures of a native repressive and non-repressive telomere are examined. The contribution of the core X element, and in particular the bound ORC and Abf1p factors, in chromatin structure and stabilization of the proposed telomere loop structure at a repressive end is also examined. The involvement of yKu in the stabilization of the telomere loop, silencing and chromatin structure is assessed to gain insight into the role of TPE and the structure and function of the loop in telomere biology.

CHAPTER 2

2 Materials and Methods

2.1 Materials

2.1.1 Antibiotics and other drugs

Ampicillin, L-canavanine and cyclohexamide were obtained from Sigma. Geneticin (G418) was purchased from Gibco (BRL) and hygromycin was purchased from Invitrogen. 5-flouro-orotic acid (FOA) was obtained from Apollo Scientific.

2.1.2 Chemicals

General laboratory chemicals were bought from Sigma and BDH laboratory supplies unless otherwise stated. Ultrapure grades of phenol and 20% sodium dodecyl sulphate (SDS) were purchased from USB.

2.1.3 Competent cells

DH5α *Escherichia coli* competent cells were purchased from Gibco (BRL) or made competent for transformation by treatment with calcium chloride. DH5α cells were grown overnight at 37°C in a shaking incubator in 5ml of SOB (2% bacto-tryptone, 0.5% yeast extract, 0.5% NaCl). Following autoclaving and cooling, 10ml 1M $MgCl_2$ and 10ml 1M $MgSO_4$ per litre was added. A fresh 250ml of SOB was inoculated with the 5ml overnight culture and grown as before for approximately 16hrs to an OD_{600} of 1. The cells were harvested by centrifugation at 5000rpm (0°C) for 10 minutes and resuspended in 125ml of ice cold 50mM calcium chloride, incubated on ice for 20 minutes and harvested as before. The cells were resuspended in 20ml ice cold $CaCl_2$ and stored at 0°C for 4 hours to overnight. Following addition of 7ml of cold 50% glycerol (in 50mM $CaCl_2$) the cells were aliquoted on dry ice into eppendorf tubes and stored at -80°C.

2.1.4 DNA molecular weight markers

Bacteriophage λ DNA digested with *Bst*EII (λ*Bst*EII) or *Hind*III (λ*Hind*III) and 1kb DNA ladder were obtained from New England Biolabs (NEB) and used at a concentration of 50ng/μl. 100bp DNA ladder was purchased from Gibco BRL and used at a concentration 0.5ng/μl for chromatin gels.

2.1.5 Media

Yeast extract, bacto-peptone, yeast nitrogen base without amino acids, bacto-agar and bacto-tryptone were purchased from Difco/Becton Dickinson. α-amino acids were obtained from Sigma.

2.1.6 Microscopes

Yeast cells were examined for spheroplasting and counting under phase contrast using an Olympus BH-2 microscope.

2.1.7 Oligonucleotides

Oligonucleotides used in this study were purchased from Invitrogen.

2.1.8 PCR

All standard PCR amplification reactions were performed in a Peltier Thermal Cycler-225 (MJ Research). Quantitative PCR reactions were carried out in a Stratagene MX3000 thermal cycler (Stratagene).

2.1.9 Plasmids

Plasmids used in this study are listed in Table 2.1. Plasmids created during this study are described in Section 2.3.7. Plasmids pFA6a-*kanMX4,* pAG32 and pFA6a-13Myc-*kanMX6* were provided by the Eurofan Yeast Sequencing Project (Goldstein and McCusker, 1999; Longtine *et al.*, 1998; Wach *et al.*, 1994). All pAB plasmids (109, 110, 111 and 117) were kindly provided by Allison Bertuch (Baylor College of Medicine, Texas). p306-*ORC1*-HA was kindly provided by Ann Ehrenhofer-Murray and Stephen Bell.

pFA6a-*kanMX4* was used as the template for most gene deletions and confers resistance to kanamycin. pAG32, which encodes for resistance to hygromycin and is otherwise the same as pFA6a-*kanMX4*, was used as the template for gene deletions in strains already containing the kanamycin resistance gene. For gene tagging of *yKU80* pFA6a-13Myc-*kanMX6* (Longtine *et al.*, 1998) was used as the PCR template. It contains 13 Myc tags at the 5' end of the PCR cassette followed by the *S. cerevisiae ADH1* terminator and the *kanMX6* selectable marker.

Table 2.1. Plasmids used in this study.

Plasmid	Description	Reference (Source)
pFA6a-*kanMX4*	*kan*^{R} ORF from *E. coli Tn*903 plus control sequences from *Ashbya gossypii TEF* gene cloned into pSP72 (Promega)	Eurofan Yeast Sequencing Project (Wach et al., 1994)
pFA6a-13Myc-*kanMX6*	pFA6a-*kanMX4* with 13 Myc epitopes followed by the *ADH1* terminator inserted 5' of the *kan*^{R} ORF.	Eurofan Yeast Sequencing Project (Longtine et al., 1998)
pAG32	pFA6a-*kanMX4* with the kanMX4 gene replaced with *hph*, encoding resistance for hygromycin	Eurofan Yeast Sequencing Project (Goldstein and McCusker, 1999)
pEL13	*LEU2 Xho*I/*Sal*I fragment cloned into pGEM3 (Promega).	E. Louis, this lab
p306-*ORC1*-HA	Integrating plasmid to form one function copy of *ORC1* tagged with HA at the C-terminus, and one truncated copy of *ORC1*.	A. Ehrenhofer-Murray S. Bell
pAB109	CEN *LEU2 yKU80*$_{Myc18}$	A. Bertuch (Bertuch and Lundblad, 2003)
pAB110	CEN *LEU2 yku80-1*$_{Myc18}$	A. Bertuch (Bertuch and Lundblad, 2003)
pAB111	CEN *LEU2 yku80-4*$_{Myc18}$	A. Bertuch (Bertuch and Lundblad, 2003)
pAB117	CEN *LEU2 yku80-8*$_{Myc18}$	A. Bertuch (Bertuch and Lundblad, 2003)
pFEP43	Contains *URA3::yEGFP* construct	F. Pryde, this lab
pEL30	Contains the telomere-proximal *Xho*I Y' fragment and TG_{1-3} repeats.	E. Louis, this lab

2.1.10 Restriction and modifying enzymes

Restriction enzymes, Klenow DNA polymerase I fragment, T4 DNA ligase, and Proteinase K were purchased from Boehringer Mannheim/Roche Molecular Biochemicals or NEB. RNase A was purchased from Sigma and Taq DNA polymerase from ABgene. Shrimp alkaline phosphatase (SAP) was purchased from USB. Zymolyase-20T was obtained from ICN Biomedicals. Micrococcal endonuclease (MNase) was purchased from Sigma and 100T zymolyase for chromatin analysis was obtained from Seikagaku Corp. Sybr Green PCR master mix for quantitative PCR was purchased from Sigma.

2.1.11 Yeast strains

The *S. cerevisiae* strains used in this thesis are isogenic derivatives of strain S288C (Winston *et al.*, 1995). All strains created for this thesis are fully described in the appropriate chapter and those not specific to this thesis are listed in Table 2.2.

FEP100-10 contains *URA3::yEGFP* integrated at a VII-L terminal truncation within the *ADH4* gene locus of strain FEP91-1a (*MAT**a**, leu2Δ1, ura3-52, can1-1, ade2Δ*). All other strains listed in Table 2.2 contain *URA3::yEGFP* integrated centromere-proximal to core X of strain FYBL1-8B (*MAT**a**, ura3Δ851, leu2Δ1, his3Δ200, lys2Δ202*) at the indicated chromosome termini. Additionally, FEP270-1 contains a mutated core X element with an *Nde*I and *Sph*I restriction site introduced in the ACS and Abf1p binding site respectively. PIY133 was derived from FEP314-19 by deletion of *yKU80* by one-step gene replacement with *kanMX4*. PIY134 was created by mating of FEP314-23 and PIY133 and selection for the appropriately marked telomere and *yKU80* disrupted haploid after dissection of the diploid. PIY180 was derived from FEP100-10 by *NatMX* deletion-disruption of the native *ura3Δ851*.

2.2 General Methods

2.2.1 Agarose gel electrophoresis

Agarose gel electrophoresis was performed using appropriate percentage agarose gels in 1X TBE buffer containing 0.2µg/ml ethidium bromide. 10X TBE is 0.89 M Tris-HCL, 0.89 M boric acid and 100mM EDTA. Standard agarose (Seakem LE Agarose) was purchased from Cambrex. SeaPlaque low melting point (LMP) agarose was purchased from BioWhittaker.

Table 2.2. *S. cerevisiae* strains used in this study.

Strain	Genotype and relevant modifications	Source
FYBL1-8B	*MATa, lys2Δ202, leu2Δ1, ura3Δ851, his3Δ200*	F. Pryde (Pryde, 1999)
FEP91-1a	*MATa, leu2Δ1, ura3-52, can1-1, ade2Δ*	F. Pryde (Pryde, 1999)
FEP311-14	FYBL1-8B with *URA3::yEGFP* inserted at the chromosome VII truncation end	F. Pryde (Pryde, 1999)
FEP318-19	FYBL1-8B with *URA3::yEGFP* inserted at core X of chromosome XIL	F. Pryde, this lab
FEP318-23	FYBL1-8B with *URA3::yEGFP* inserted at core X of chromosome IIIR	F. Pryde, this lab
FEP100-10	FEP91-1a with *URA3* integrated centromere-proximal to core X at XIL	F. Pryde (Pryde, 1999)
PIY180	*MATa, leu2Δ1, ura3Δ, can1-1, ade2Δ*	P. Inglis, this lab
FEP270-1	Isogenic to FYBL1-8B, contains mutations in the ACS and Abf1p binding site of the XIL core X.	F. Pryde (Pryde, 1999)
FEP100-40	FEP91-1a with *URA3* integrated centromere-proximal to core X at XIIIR	F. Pryde (Pryde, 1999)
FEP229-4	FEP91-1a with *URA3* integrated centromere-proximal to core X at IVL	F. Pryde (Pryde, 1999)
PIY133	Isogenic to FEP318-19, except for *ura3-52, yku80::kanMX* disruption	P. Inglis, this lab
PIY134	Isogenic to FEP318-23 except for *MATα, yku80::kanMX* disruption	P. Inglis, this lab
PIY125	*MATα, leu2Δ, his3Δ, URA3::yEGFP* replacing native *URA3* on chromosome V	P. Inglis, this lab
PIY138	FEP311-14 with an *isw1::kanMX* disruption	P. Inglis, this lab
M107	*MATα, ura3-52, trp1Δ*	F. Winston (Winston *et al.*, 1995)
FEP131	FEP100-10 with a *sir1::kanMX4* disruption	F. Pryde (Pryde, 1999)
FEP236	FEP100-10, with a *sir4::kanMX4* disruption	F. Pryde (Pryde, 1999)

2.2.2 CHEF gel analysis

Clamped Homogenous Electric Field (CHEF) gel electrophoresis was performed using a BioRad CHEF DRIII system. Gels were prepared with 1% agarose in 0.5%TBE, without ethidium bromide. For routine separation of yeast chromosomes the following conditions were used:

Block 1	Initial time	60 seconds
	Final time	60 seconds
	Run time	15 hours
Block 2	Initial time	90 seconds
	Final time	90 seconds
	Run time	9 hours

The chromosomal bands were visualized after separation by soaking the gel in 500ml of H_2O containing 50µl of 10mg/ml ethidium bromide for 20 minutes and visualization on a UV transilluminator.

2.2.3 Cloning of DNA fragments

Cloning of DNA fragments was performed using standard techniques as described (Sambrook *et al.*, 1989). A four times molar excess of insert to vector was typically used for ligations. Sticky-ended ligations were carried out for 1 hour and blunt-ended ligations were done overnight at room temperature. For transformation into yeast, the ligation reactions were precipitated and resuspended in 1XTE pH 8.0 (10X TE is 0.1M Tris-HCL, 10mM EDTA, adjusted to the appropriate pH with HCL) buffer prior to transformation. For transformation of pEL*ORC1*-HA into yeast, the plasmid was digested with *Xba*I prior to transformation. Ligation mixes were transformed directly into *E. coli* using standard techniques and plated on LB media (1% bacto-tryptone, 0.5% yeast extract, 0.5% NaCl, 2% bacto-agar, pH 7.5) plates containing 50µg/ml ampicillin. Yeast transformants were plated onto appropriate media

2.2.4 Diploid selection

Strains used in this study all contained a non-functional HO allele. Therefore, they were incapable of switching mating type, allowing them to be propagated as stable **a** or α mating type haploids. Diploids were created by mixing approximately equal amounts of an **a**-mating and an α-mating strain on a YPD plate. Mating

proceeded for a minimum of six hours at 30°C. Following mating, diploids were selected by growth on minimal media (supplemented with amino acids as appropriate) to select for auxotrophic complementation.

2.2.5 DNA extraction

i) Plasmid DNA extraction

Small scale plasmid DNA purification (~2-20µg) from *E. coli* cultures was performed using Quiagen miniprep kit (Quiagen).

ii) Extraction of yeast genomic DNA

Yeast cultures were grown overnight in 5ml of liquid media (YPD or minimal media supplemented with appropriate amino acids) at 30°C in a shaking incubator. Cells were harvested by centrifugation at 3600 rpm for five minutes and resuspended in 0.5ml spheroplasting solution (1.2M sorbitol, 200mM Tris-HCl pH 7.5, 20mM EDTA, 0.1% β-mercaptoethanol). Cell suspensions were transferred to eppendorf tubes containing 50µl of 20T-zymolyase (10mg/ml, made up in spheroplasting solution lacking β-mercaptoethanol) and spheroplasted for 30 minutes at 37°C. Spheroplasts were harvested by centrifugation at 13000rpm for two minutes and gently resuspended in 50µl 1M sorbitol and 0.5ml lysis solution (50mM Tris-HCl pH 7.5, 100mM NaCl, 100mM EDTA, 0.5% SDS). Following addition of 20µl of Proteinase K (10mg/ml in 1X TE buffer, pH 7.5) and 50µl of RNase solution (1mg/ml), the extracts were incubated at 65°C for a minimum of 2 hours. The preparations were extracted twice with 0.5ml phenol/chloroform, 1:1 v/v pH 8.0 (Phenol was obtained from Appligene). DNA was spooled by addition of 1ml of ethanol to the supernatant (transferred to a new eppendorf) and mixing by inversion. After removal of the supernatant, the DNA spool was washed with 70% ethanol, air-dried and resuspended in 100-300µl 1X TE buffer, pH 8.0.

iii) Preparation of whole chromosomal DNA for CHEF gel analysis

Yeast genomic DNA was prepared for CHEF gel analysis in agarose plugs as described previously (Louis, 1998). Overnight yeast cultures were grown in 5ml YPD at 30°C. 1ml aliquots of the culture were transferred to eppendorf tubes and harvested by centrifugation at 13000rpm for 10 seconds. The cells were washed with 1ml of 50mM EDTA, harvested as before and resuspended in 200µl of 50mM EDTA. Addition of 100µl SCE/Zymolyase (1M sorbitol, 0.1M sodium citrate, 10mM EDTA, 5% β-mercaptoethanol, 9mg/ml 20T-zymolyase) was quickly followed by mixing with 0.5ml molten LMP agarose (1% LMP agarose in 0.125M EDTA,

melted and cooled to 50°C) and pipetting of the solution into 100µl plug formers (BioRad) on ice. The set plugs were transferred to eppendorf tubes and covered with 0.5ml Overlay 1 (0.45M EDTA, 0.1M Tris-HCl pH 8.0, 5% β-mercaptoethanol) and incubated for four hours at 37°C. Subsequently, Overlay 1 was removed and replaced by 0.5ml Overlay 2 (0.4M EDTA, 1% sodium sarcosyl, 10mg/ml Proteinase K, 0.1mg/ml RNase), and plugs were incubated overnight at 37°C. After incubating, Overlay 2 was removed and plugs were washed at room temperature for one hour in 1ml 1X TE buffer, pH 8.0. Plugs were stored at 4°C in 0.5ml of storage buffer (0.45M EDTA, 0.1M Tris-HCl, pH 8.0). Approximately 1/3 of a plug was loaded per lane on a CHEF gel.

2.2.6 DNA modification

i) Blunting DNA fragments

DNA fragments with non-compatible single-stranded overhangs were modified to produce blunt ends by treatment with the Klenow (large) fragment of DNA polymerase I. Reactions were carried out by incubating 1-5µg of DNA in a 100µl reaction of 1X Klenow buffer (10mM Tris-HCL pH 7.5, 5mM $MgCl_2$, 7.5mM DTT), 33µM dNTPs and 1 unit of Klenow per microgram of DNA for 20 minutes at room temperature. Subsequently, the enzyme was inactivated by incubation at 65°C for 20 minutes followed by ethanol precipitation.

ii) Vector dephosphorylation

As appropriate, the 5' phosphate groups of linearized vectors were removed by treatment with SAP to prevent re-circularization of the vector during cloning experiments. Typically, 1µl of SAP was added to the 20µl vector restriction digest after the restriction enzyme was deactivated by heating at the indicated temperature for the enzyme. This SAP reaction was incubated for 30 minutes at 37°C followed by inactivation of SAP at 65°C for 20 minutes.

2.2.7 Mating type testing

To determine the mating phenotype of strains, the haploid strain to be tested was streaked onto a YPD plate and overlain with *MATa* and *MATα* tester strains. These tester strains contain *ura2* and *tyr1* mutations not present in most other lab strains. Following a minimum of 6 hours mating at 30°C, the mating plates were replicated to minimal media to look for auxotrophic complementation. The mating type of the tested haploid is opposite that of the tester strain with which it successfully complements.

2.2.8 DNA gel purification

Where appropriate, DNA fragments for cloning were excised from agarose gels after separation by electrophoresis and purified from the gel fragment using the MinElute Gel Extraction kit (Quiagen) following the manufacturers instructions.

2.2.9 Restriction enzyme digests

Restriction enzyme digestion of DNA was performed according to manufacturers recommendations. Normally, 1-5µg of plasmid DNA was digested for 2 hours to overnight in a 20µl volume with 5-10units of the restriction enzyme(s) in 1X reaction buffer, as supplied. Digestions of yeast genomic DNA and chromatin samples were always carried out overnight.

2.2.10 Southern blot analysis

Southern transfers were performed as described (Sambrook *et al.*, 1989). DNA separated on agarose gels was transferred to Hybond-N+ (Amersham) or Osmonics nylon membrane using 20X SSC (0.15M NaCl, 0.015M sodium citrate). DNA fragments were detected using either fluorescein (Amersham) or radio-labeled (Stratagene Prime-It II Random Primer Labeling Kit) probes prepared as described in the manufacturers protocols. Radio-labeled probes were cleaned using NucTrap Probe Purification Columns (Stratagene). Hybridization with fluorescein probes were performed at 60°C overnight in hybridization buffer (5X SSC, 5% liquid block (Amersham), 0.1% SDS, 5% w/v Dextran sulphate). CDP-Star was used for detection as per manufacture's instructions. Hybridization with radio-labeled probes was performed at 65°C overnight in Church and Gilbert buffer (0.25M Na_2HPO_4, 1mM EDTA, 7% SDS). Excess blot was removed by four 30 minutes washes at 65°C in 3XSSC, 1%SDS. Super RX Fugi Medical X-Ray film was used to detect positions of probe hybridization.

2.2.11 Sporulation and tetrad dissection

Diploids were grown on minimal KAc media (2% KOAc, 2% bacto-agar) and incubated at room temperature for four to five days to induce sporulation by starving cells for nitrogen. Following sporulation, tetrads were prepared by incubation in 100µl of dissection buffer (1M sorbitol, 10mM EDTA, 10µM sodium-phosphate, pH 7.2) plus 10µl zymolyase (5mg/ml) and incubating at 37°C for 30 minutes. Tetrads were separated and arrayed onto YPD using a Zeiss Axioscope microscope and

micromanipulator. Separated spores were grown for three days at 30°C. Haploid phenotypes were determined by replica plating to appropriate selective media.

2.2.12 Transformation

A modified lithium acetate procedure (Gietz *et al.*, 1992) was used for yeast transformations. Yeast cells were grown at 30°C overnight in 5ml YDP, diluted 1:10 in YDP and grown for a further 4 hours at 30°C with shaking. The cells were harvested by centrifugation at 3600rpm for five minutes, resuspended in 2ml dH_2O and divided into two 1.5ml eppendorf tubes for separate transformations. The cells were washed again in another 1ml of dH_2O, and then washed twice in 1ml of 0.1M LiAc, pH7.5. Following the washes the transformation mixture of 240µl 50% PEG, 36µl 1M LiAc, 25µl denatured 2mg/ml salmon sperm DNA and 0.1-1ug of transforming DNA in 50µl dH_2O was added to each tube of cells. The cells were resuspended by vortexing, incubated at 30°C for 30 minutes followed by a 20 minute heat shock at 42°C. The cells were washed once in 1ml dH_2O and plated on the appropriate selective media. For *kanMX* or *hphMX4* selection, the cells were allowed to recover either for 4 hours at 30°C or at 4°C overnight to allow expression of the resistance gene prior to plating on selective media containing geneticin (G418) or hygromycin.

2.2.13 Temperature sensitivity analysis

To ascertain if mutations conferred temperature sensitivity, yeast strains were streaked onto two plates of the appropriate media. One plate was placed at 30°C and the other was placed and 37°C. Both plates were grown for 2-3 days and analyzed for colony growth.

2.2.14 Yeast media

All strains were grown at 30°C on YPD, minimal media, synthetic complete media and drop out media (synthetic media lacking one or more amino acid) unless otherwise indicated. YPD media is 1% yeast extract, 2% bacto-peptone and 2% dextrose. Following sterilization of the media by autoclaving, 10ml/L of 0.5% adenine hemisulphate (dissolved in 0.05M HCL, filter sterilised and stored at room temperature) was added. Synthetic complete media is 0.67% nitrogen base, 2% glucose and a mixture of all amino acids in the amounts listed below. For drop out media, the appropriate amino acids are omitted and all amino acids are omitted for minimal media.

Amino Acids	mg/L
Adenine	800
Arginine	800
Aspartic Acid	4000
Histidine	800
Leucine	800
Lysine	1200
Methionine	800
Phenylalanine	2000
Threonine	8000
Tryptophan	800
Tyrosine	1200
Uracil	800

Yeast media was adjusted to pH 6.5 prior to autoclaving and for solid media, 2.5% bacto-agar was added. Threonine and aspartic acid drop-out mixes were used at 540mg/l while all other drop-out mixes were used at 870mg/l. Following autoclaving, 6ml/l of a sterile 1% leucine solution was added as some lab strains require more than is present in the standard drop-outs.

Plates for cyclohexamide and canavanine resistance selection were made by adding 1ml/l of 1% cyclohexamide (in dH_2O) and 2ml/l of 2% canavine (in dH_2O) respectively, to YPD media after autoclaving. FOA media was made by adding 50mg/l of uracil to uracil drop out media and after autoclaving, adding 1g/l of 5-fluororotic acid to the media. Hygromycin plates were made by adding 300mg/l of hygromycin (50mg/ml in PBS) to YPD media after autoclaving and geneticin plates contained 400mg/l of geneticin.

Yeast strains were kept on plates for up to three weeks. For longer term storage, a small patch of cells (~2 cm^2) was suspended in 1ml of 25% glycerol and stored at -80°C.

2.3 Methods and Materials specific to this thesis

2.3.1 Chromatin analysis using micrococcal nuclease

Chromatin preparation and micrococcal nuclease digestion was performed as described previously (Kent *et al.*, 1993; Kent and Mellor, 1995; Wu and Winston, 1997). Overnight cultures were grown in YPD media and subcultured into 200mls of YPD for growth to mid-log phase. Nuclei were prepared by harvesting 1.2 x 10^9 cells and sphereoplasting with 100T zymolyase for 5 minutes at room temperature. The spheroplasted cells were permeabilized with NP-40, and digested with micrococcal

nuclease (MNase). Three samples from each nuclei preparation, containing chromatin from 2.0 x 10^8 cells, were digested with 2, 10 or 20 U/mL of MNase at 37°C for 4 minutes. An equivalent amount of purified DNA was digested with 5U/ml of MNase for 35 seconds at 37°C to yield "naked" DNA digestion patterns. All samples were purified and analyzed by indirect end labeling as described in Section 2.3.5.

2.3.2 Chromatin immunoprecipitation (ChIP)

ChIP was performed as described by Meluh and Broach (1999). Cells were fixed for two hours at room temperature in 1% formaldehyde. The fixed cells were washed and converted to spheroplasts using zymolyase. Spheroplasts were washed and resuspended in lysis buffer (1%SDS, 10mM EDTA, 50mM Tris-HCl pH8.1, supplemented with protease inhibitors; 1mM PMSF, 0.6µg/ml leupeptin, 0.8µg/ml pepstatin A) then sonicated to fragment chromosomal DNA to an average size of ~300-1000bp. The sonicated chromatin from 3.0x10^8 cells was diluted into immunoprecipitation buffer (final concentration 0.1%SDS, 1%Triton X-100, 150mM NaCl, 2mM EDTA, 20mM Tris pH 8.0) and incubated with (IP) or without (NoAb) antibody for 15 hours at 4°C. The anti-Myc monoclonal antibody from clone 9E10 (Sigma) was used at 1:200 final dilution. Monoclonal HA.11 antibody (Eurogentec) was used at 1:150 final dilution. Immune complexes were harvested by 1-2 hours incubation with protein A-sepharose CL-4B beads (Amersham). Beads were washed followed by elution of the immunoprecipitated material with 1%SDS, 01M Na_2CO_3, heated at 65°C overnight to reverse crosslinks and ethanol precipitated overnight. Precipitates were resuspended in 40µl of dH_2O. 1:20 dilutions of DNA from input chromatin (TOT) were analyzed by quantitative PCR as described in Section 2.3.8.

2.3.3 Myc tagging of *yKU80*

The genomic copy of *yKU80* was tagged in-frame at its carboxy terminus with 13 Myc epitope tags using the method of Longtine *et al.* (Longtine *et al.*, 1998). PCR fragments were generated using primers *yKU80* F2 (CGCGGTGAACAACACAGTAGGGGAAGTCCAAACAATAGCAATAATCGGATCCC CGGGTTA) and *yKU80* R1 (AACTGTGGTGACGAAAACATAACTCAAGATGTTAGA CCTTTTATCCATGAATTCGA). Reaction volumes and conditions were the same as for PCR amplification of the disruption cassettes (Section 2.3.4) using plasmid pFA6a-13Myc-*kanMX6* as the template. Selection of *kanMX6* transformants was performed as described for *kanMX4* transformants in Section 2.3.4. Correct transformants were confirmed by colony PCR as described in Section 2.3.10 using

the K2, K3 and A4 primers listed in Table 2.6 in addition to the *yKU80* A2 oligonucleotide (GATCCTCTTAGAATACCCACGG) upstream of the construct insertion site. Silencing phenotypes of tagged strains were comparable to the parental strains.

2.3.4 Disruption of genes with *kanMX4* or *hphMX4*

SIR1-4, BDF1, BRE1, SAS2, DOT1, SET1, yKU80, yKU70, and *ura-52* were disrupted with *kanMX4* or *hphMX4* by one-step PCR-mediated gene transplacement using regions of short flanking homology to the target locus (Longtine *et al.*, 1998; Wach *et al.*, 1994). PCR products were generated using primers as indicated in Table 2.3. Plasmids pFA6a-*kanMX4* and pAG32 were used as the templates for *kanMX4* and *hphMX4* disruptions respectively, with the exception of *kanMX4* disruptions of *SIR1*, *SIR4*, *yKU80* and *yKU70*. For these disruptions, DNA extracted from lab strains already disrupted for the appropriate gene was used as the template. For all templates, the PCR reaction was carried out in a total volume of 50µl containing approximately 100ng of template and 1mM of each dNTP, 0.2µM of each primer, 45mM Tris-HCl (pH 8.8), 11mM ammonium sulphate, 4.5mM magnesium chloride, 6.7mM β-mercaptoethanol, 4.4µM EDTA, 113µg/ml BSA and 2.5units of Taq DNA polymerase. Reaction parameters were as follows: 2 minutes at 95°C followed by 34 cycles of 45 seconds at 95°C, 45 seconds at 55°C and 2 minutes at 72°C.

Transformants containing *kanMX4* were selected for on plates containing G418 and *hphMX4* transformants were selected on plates containing hygromycin. To confirm resistance, *kanMX4* transformants were streaked onto plates containing 200mg/l G418 and *hphMX4* transformants were streaked onto the hygromycin containing media. All disruptions were confirmed by colony PCR as described below. Additionally, *SIR2, 3* and *4* disruptions were confirmed by loss of mating type and *yKU80* and *yKU70* disruptions were confirmed by temperature sensitivity at 37°C.

2.3.5 Indirect end labeling

Indirect end labeling was performed as described previously (Wu, 1980). Purified MNase-treated chromatin samples (see Section 2.31) were cut to completion with either *Stu*I or *Bst*XI and fractionated on a 1.5% agarose gel overnight, Southern blotted onto Osmonics nylon membrane and hybridized to radioactively labelled probes of ~200bp. The probes were oriented either towards the centromere or telomere from the site of digestion and were prepared using Stratagene oligolabeling

Table 2.3. Oligonucleotides used for complete ORF replacement by *kanMX4* and *hphMX4*

SIR1	F1	ggcaaacgataactgatcct
	R1	aggagttactctggagtgta
SIR2	F1	agacacattcaaaccatttttccctcatcggcacattaaagctggCGTACGCTGCAGGTCGAC
	R1	attgatattaatttggcacttttaaattattaaattgccttctacATCGATGAATTCGAGCTCG
SIR3	F1	tctatggcggaagtgaaaatgaatgttggtggtcaaatgcagtccATCGATGAATTCGAGCTCG
	R1	caattggattagctaaaatggctaaaacattgaaagatttggacggCGTACGCTGCAGGTCGAC
SIR4	F1	acatgtgcactgccattaag
	R1	ttatactgatccgcatgcca
BDF1	F1	agctaaaaggcggtcgaatctcaacggctctgataaacgtacgtaCGTACGCTGCAGGTCGAC
	R1	gctcattcttctcagtcgttgaagataatcaaattcaaaattcagATCGATGAATTCGAGCTCG
BRE1	F1	tttcaccgtttttatgctaatcgtgctagctgataataatcagatCGTACGCTGCAGGTCGAC
	R1	ggaggatataacacaaacagtggaaaagtggtagaataattagtaATCGATGAATTCGAGCTG
DOT1	F1	ggtcaccagtaattgtgcgctttggttacattttgttgtacagtaCGGATCCCCGGGTTAATTAA
	R1	ctacttagttattcatactcatcgttaaaagccgttcaaagtgccGAATTCGAGCTCGTTTAAAC
SAS2	F1	aggctcctattttctagttgctttttgttttcactcgcaaaaaaaCGGATCCCCGGGTTAATTAA
	R1	tatcctgaaatacatatgccattaagttacatcctgaatagattcGAATTCGAGCTCGTTTAAAC
SET1	F1	ttccttatttgttgaatctttataagaggtctctgcgtttagagaCGGATCCCCCCCTTAATTAA
	R1	cgatatgttaaatcaggaagctccaaacaaatcaatgtatcatcgGAATTCGAGCTCGTTTAAAC
yKU80	F1	gtagccttgttggcgcaatcg
	R1	ctgtttgttcctggaactgc
yKU70	F1	acaacaggtcacttctgc
	R1	gggacccacaaagtaattgtc
ura3-52	F1	acccaactgcacagaacaaaaacctgcaggaaacgaagataaatcCGTACGCTGCAGGTCGAC
	R1	aatttgtgagtttagtatacatgcatttacttataatacagttttATCGATGAATTCGAGCTCG

F1 is the upstream end and R1 is the downstream end of the genes. Upper case bases are the sequences homologous to the template plasmid and lower case letters are sequences homologous to the target gene.

kits. The $URA3_{cen}$, $URA3_{tel}$, GFP_{cen} and GFP_{tel} probes were generated by PCR using standard reaction conditions and oligonucleotides listed in Table 2.4. pFEP43 was used as the template. A 100bp ladder was used for calibration of distances between hypersensitive sites. Radioactive banding patterns were detected using Super RX Fugi Medical X-ray films and enhancer screens. Band intensities were analyzed using a KODAK 2000 Image Station with the KODAK 1D v3.5 program.

Table 2.4. Oligonucleotides used to generate $URA3_{cen/tel}$ and $GFP_{cen/tel}$ probes.

UraStuI-ds-F	Tel-F	CCTTTTGATGTTAGCAGAATTGTC
UraStuI-ds-R	Tel-R	ATGCGTCTCCCTTGTCATCTAAAC
UraStuI-us-F	Cen-F	GCTAAAGGCATTATCCGCCAAGTA
UraStuI-us-R	Cen-R	CCTCTAGGTTCCTTTGTTACTTCT
yEGFP-ds-F	Tel-F	CCAACCTTAGTCACTACTTTC
yEGFP-ds-R	Tel-R	GTGACCTAAAATGTTACCATCT
yEGFP-us-R	Cen-R	CAGTAGTACAAATAAATTTTAAGGTC
yEGFP-us-F	Cen-F	ATGTCTAAAGGTGAAGAATTATTC

F is the upstream and R is the downstream primer for each probe. Tel and Cen indicate the direction of the probe (either on the telomere or centromere-proximal side of the *StuI* or *Bst*XI digestion sites).

2.3.6 Measurement of silencing

The level of *URA3* or *URA3::yEGFP* repression in each strain was determined by measuring the percentage of cells able to grow on media containing 5-fluororotic acid (FOA) compared to growth on complete synthetic media (COM). Cells expressing *URA3* cannot grow in the presence of FOA, a uracil analogue that is lethal to cells able to synthesize uracil (Boeke *et al.*, 1984). Therefore, strains exhibiting TPE are able to grow either in the presence or absence of 5-FOA as *URA3* is not highly expressed.

Haploid strains were grown on complete synthetic media for 2-3 days. Single colonies were selected and resuspended in 100µl dH_2O. Several ten-fold serial dilutions were made in dH_2O and 8µl of each dilution was spotted onto both complete synthetic and FOA media. The percentage of FOA-resistant colonies after growth at 30°C for three days was calculated. FOA-resistant colonies were only counted if they were able to grow after replica plating onto media lacking uracil, confirming the FOA resistance was due to gene silencing rather than loss of *URA3*.

For a more accurate measurement of FOA resistance in *sir1*Δ strains, single colonies grown as above were resuspended in 350µl of dH_2O, ten-fold serial dilutions made and 100µl of each dilution was spread onto complete synthetic and FOA media followed by growth and calculation of FOA-resistance as above. Synthetic and FOA media lacking leucine was used to maintain plasmid selection for analysis of the plasmid-containing *yku80*^{tel} mutant strains.

2.3.7 Plasmids

Plasmid pEL*ORC1*-HA was derived from p306-*ORC1*-HA (Table 2.1), which contains an *ORC1* integration construct for creating a truncation of the native *ORC1* gene and a second, functional, copy of *ORC1* with three in-frame HA-epitope tags at the C-terminus. pEL*ORC1*-HA was constructed by excising the *ORC1* integration construct from p306-*ORC1*-HA by *Ava*I digestion, followed by filling in the DNA overhangs. This *Ava*I fragment was subsequently ligated into the *Sma*I site of the pEL13 polylinker to generate pEL13-*ORC1*. As digestion with *Xba*I is used to linearize the integration plasmid within the cloned *ORC1* sequence prior to transformation, the *Xba*I site in the polylinker of pEL13 was removed by partial digestion of pEL13-*ORC1* with *Xba*I followed by blunting, re-ligation and selection for pEL*ORC1*-HA, that retained only the *Xba*I site internal to the *ORC1* sequence.

2.3.8 Quantitative PCR (QPCR)

Quantitative PCR and real-time detection (QPCR) were performed on ChIP samples (see Section 2.3.2) using the Mx4000 PCR machine (Stratagene) and Sybr Green PCR master mix (Stragene) according to the manufacturer's instructions. The centromere-proximal end of the core X element at the marked telomere (either XIL or IIIR) was amplified with a primer (*URA3*-endF) to the *URA3* termination sequence adjacent to the core X element and a core X primer (CoreXIL-R). Analysis of all core X elements was performed with generic core X primers (CoreX-F and CoreX-R). Primers to the *SEO1* gene (*SEO1*-F and *SEO1*-R), located approximately 8kb from the left telomere of chromosome I, were used as a control. Primer sequences are listed in Table 2.5. Reaction parameters for amplification of the specific core X elements and the *SEO1* gene were as follows: 95°C for 10 minutes followed by 40 cycles of 94°C for 30 seconds, 50°C for 60 seconds, 68°C for 60 seconds. Similar reaction conditions were used for amplification with the generic core X primers with an annealing temperature of 57°C.

Table 2.5. Oligonucleotides used for QPCR analysis.

URA3-end	F	ATGCATGTATACTAAACTCAC
CoreXXIL	R	CACTTATTTCAATATACCCAC
CoreX	F	GTGTTTATGTATTATTGTTGAA
CoreX	R	CTCATTCGGCGGCCCCAA
SEO1	F	GCTATTGTGTCTGTCGTAGT
SEO1	R	CCTCGCCAACCTAATTTCAT

F primers are at the 5' end and R primers are at the 3' end of the amplified region.

2.3.9 Telomere length analysis

Bulk telomere lengths were analyzed by extracting DNA from three or more single colonies of each strain followed by *Xho*I digestion of 5µl of each DNA extraction. The digests were run on 0.5% agarose gels for ~16 hours, Southern transferred and probed with randomly-labeled pEL30. *Xho*I cuts once within Y' elements and pEL30 contains the telomere proximal Y' fragment and TG_{1-3} repeats. This technique therefore predominantly detects the telomere length of Y' containing ends that account for approximately half the telomeres of S288C. The lengths of the individually marked core X-only telomeres in each strain were analyzed by digestion of the DNA extractions with *Stu*I and probing with the $URA3_{tel}$ probe also used in chromatin analysis.

2.3.10 Verification of disruptions by colony PCR

Correct disruptions of the targeted genes was confirmed by colony PCR using oligonucleotides internal to the disruption cassette (K2 and K3 for *kanMX4*; H2 and H3 for *hphMX4*) paired with oligonucleotides flanking the targeted loci (A1 and A4) as listed in Table 2.6. PCR reactions and conditions were as described in Section 2.3.4 using an annealing temperature of 52°C. Cells picked from a fresh colony were resuspended in the PCR reaction mixture and subsequently heated at 95°C for 5 minutes prior to cycling.

2.3.11 Yeast strains

The hERL3 strain, containing the *URA3::yEGFP* construct integrated at the truncated VIIL telomere was derived by crossing PIY138 with M107. The resulting diploids were sporulated and dissected spores were analyzed to identify those that were able to stably retain the *URA3::yEGFP* construct at the truncated VIIL telomere and that also lacked the *isw1::kanMX* mutation of PIY138. One haploid strain that

Table 2.6. Oligonucleotides used for confirmation of disruptions.

kanMX4	K2	TTCAGAAACAACTCTGGCGCA
	K3	CATCCTATGGAACTGCCTCGG
hphMX4	H2	CGGCGGGAGATGCAATAGG
	H3	TCGCCCGCAGAAGCGCGGCC
SIR1	A1	TTACTACGATGAGCTCCCAA
	A4	AAGAACTGGAGCTGTTGCTT
SIR2	A1	TGCAACTCCTCAATGTGTCA
	A4	GAGATTCTGAGGCTATACCA
SIR3	A1	CCAGGGGAACAAAGTATTCGG
	A4	CCTGGAATTTCCAGCGGATGG
SIR4	A1	ACTGTTTGGGCTGACATCTT
	A4	ATGAGCATTTGGACTGGCAT
BDF1	A1	TCGTGTTTGTATTACCCAGC
	A4	TCGTCCGTCGTGATATCATT
BRE1	A1	TGAAGCACCAACTGATCGTA
	A4	AGGACTGCAGTAGAAGAGTT
DOT1	A1	CTGCTGACGCCTTCGCAC
	A4	TACCTGGTCCACGGCGC
SAS2	A1	ATCATGATATGTTAGGCGCG
	A4	GGAAACTTTTGCAGCAAAACAA
SET1	A1	CTGTTTCGTGCTGCTTTCAC
	A4	GCCGAGATTACTTATAGATGTA
yKU80	A1	CTATGAGACCTTGAACCAGT
	A4	ACCAGGCTTTTGGTCTTCAT
yKU70	A1	ACAACAGGTCACTTCTGC
	A4	GGGACCCACAAAGTAATTGTC
ura3-52	A1	GTGGCTGTGGTTTCAGGGT
	A4	GTTCTTGATTTGTGCCCCG

A1 is upstream and A4 is downstream of the targeted loci.

matched these criteria, hERL1 (*MATa, lys2Δ202, leu2Δ1, ura3-52)* was chosen and the *ura3-52* allele was replaced with the *hphMX4* gene for hygromycin resistance by one step gene replacement to create hERL3.

Strains containing *kanMX4* deletion-disruptions were created by one step gene replacement of the wild-type loci. Parental strains and relevant modifications are detailed in the appropriate chapters. Strains containing genomic $yKU80_{Myc}$ constructs were created by one step integration of the Myc tagging construct from pFA6a-13Myc-kanMX6 at the wild-type loci in the parental strains. Strains containing *ORC1* tagged with HA at the C-terminal end were created by transformation of the parental strains with *Xba*I-linearized pEL*ORC1*-HA. Integration of this plasmid results in one functional copy of *ORC1* with three in-frame HA epitope tags at the C-terminus and a second non-functional copy of *ORC1* lacking 500bp at the ORF amino terminus. Correct transformants were identified initially by selection on media lacking leucine, to select for cells containing the *LEU2* selectable marker encoded by pEL*ORC1*-HA. Secondary selection was performed by southern analysis to confirm integration at the *ORC1* locus using *Bgl*II/*Acc65*I-digested DNA preps and probing with a 1kb radio-labeled probe to the Amp^R gene that integrates with the plasmid. The Amp probe was generated by PCR using primers AmpF (ACGCTGTAGGTATCTCAGTT) and AmpR (AGAGAATTATGCAGTGCTGC). pFA6a-*kanMX4* was used as the template with standard PCR conditions.

Strains containing the pAB109, pAB110, pAB111 and pAB117 plasmids were selected and maintained on media lacking leucine.

CHAPTER 3

3 Different Endings

3.1 Introduction

Telomere position effect has been most extensively studied at truncated telomeres which lack the native subtelomeric element, including core X and Y's (Gottschling *et al.*, 1990). While information obtained from truncation studies has proved important to our understanding of silencing, studies of silencing at native telomeres have highlighted important differences. Silencing at truncation ends is initiated by recruitment of the Sir protein complex to the TG_{1-3} repeats followed by the uninterrupted spread of the silencing complex toward the centromere (Hecht *et al.*, 1996; Renauld *et al.*, 1993). Telomere position effect (TPE) at native ends, in contrast, is discontinuous. Strongly silenced domains are observed near core X and immediately adjacent to the telomere repeats. The Y' and STR repeats that lie between core X and the telomere exhibit a much lower degree of silencing (Fourel *et al.*, 1999; Pryde and Louis, 1999). Importantly, there are also two classes of native ends that lack the Y' element ("core X-only" ends); those with strong and those with weak silencing (Pryde and Louis, 1999). There is also more than one class of Y'-containing ends. This contrasts with truncated telomeres, which are always strongly silenced (Gottschling *et al.*, 1990; Pryde and Louis, 1999; Renauld *et al.*, 1993), suggesting the mechanisms of silencing at native and truncated ends may be significantly different.

Heterochromatic regions exhibit silencing of genes within the region in addition to decreased accessibility to nucleases, heterochromatic nucleosome modifications and condensed nucleosome structures. Silenced regions in yeast are also defined as heterochromatic as these regions exhibit the reduced nuclease accessibility and the characteristic nucleosome modifications (Braunstein *et al.*, 1996; Loo and Rine, 1994; Suka *et al.*, 2001). In addition, studies of the *HML* and *HMR* loci have revealed regularly spaced, or phased, nucleosome arrays typical of heterochromatic regions (Ravindra *et al.*, 1999; Weiss and Simpson, 1998). For the purposes of this study, heterochromatin in *S. cerevisiae* is defined as regions that are capable of repression in the wild-type state and exhibit the hallmarks of phased nucleosome spacing and decreased nucleosome acetylation and methylation.

This chapter describes investigations of the chromatin structure of two native core X-only ends. One of these represses expression of a marker gene placed centromere-proximal to core X and the other one does not. This comparison will determine if there is a correlation between the observed degrees of silencing and chromatin structure at *S. cerevisiae* telomeres. In this chapter, the chromatin structure was examined both over the promoter of the marker gene and the subtelomeric region toward the centromere, as well as over the telomere-proximal regions from core X element to the telomere. The structure at a truncated telomere was also analyzed to address the differences between TPE at native and truncated ends. The differences observed for the two native ends were confirmed by analysis of a second pair of repressive and non-repressive core X-only telomeres. In addition, the relationship between telomere length and silencing was investigated at the native telomeres.

3.2 Materials and Methods

With the exception of hERL3, all strains used in this chapter were previously created by F. Pryde or P. Inglis and are listed in Table 2.2. FEP318-19 and FEP318-23 are isogenic S288C strains containing the *URA3::yEGFP* marker construct inserted centromere-proximal to core X (Fig. 3.1) at the left telomere of chromosome XI (XIL) and the right telomere of chromosome III (IIIR) respectively. XIL and IIIR are both core X-only ends. FEP100-40 and FEP229-4 contain the *URA3* marker in the same position (Fig. 3.1) at the XIIIR and IVL telomeres respectively. The ends and positions marked are illustrated in Fig. 3.2. The hERL3 strain, containing the *URA3::yEGFP* construct integrated at the truncated VIIL telomere was constructed as described in Chapter 2 (Fig. 3.2). PIY125 is an isogenic S288C strain and contains the *URA3-yEGFP* construct at the native *URA3* locus (Table 2.2).

Silencing, chromatin and telomere length analyses were performed as described in Chapter 2. In this chapter, all chromatin structures were analyzed by indirect end labeling with either the centromere-proximal $URA3_{cen}$ or telomere-proximal $URA3_{tel}$ probe (Fig. 3.1).

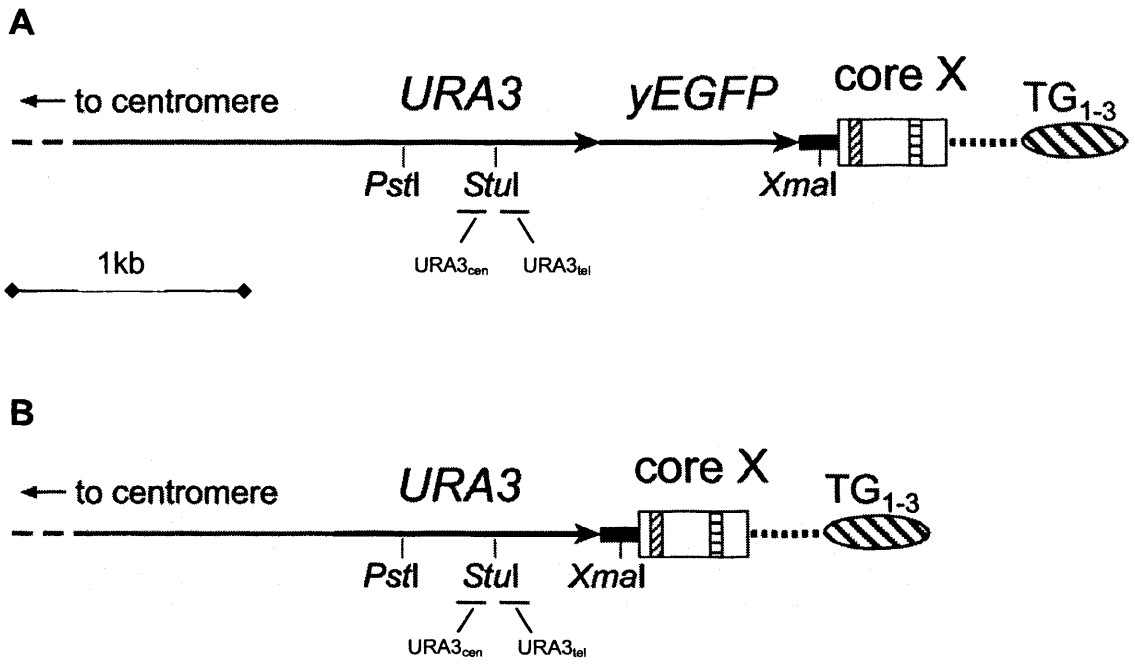

Figure 3.1. Schematic of the *URA3* and *URA3-yEGFP* marked native telomeres. A) The position of *URA3-yEGFP* (black arrows) and the *URA3* terminator (filled black rectangle) relative to core X (large open rectangle) at a native core X-only end is illustrated. The *Stu*I site within the *URA3* ORF and the *Pst*I and *Xma*I sites, used to generate the centromere and telomere-proximal marker bands respectively, are also indicated. Black bars under the *Stu*I site indicate the positions of the $URA3_{cen}$ and $URA3_{tel}$ probes used for chromatin analysis. The position of the ACS sequence in core X is shown by the diagonal lines while the horizontal lines indicate the Abf1p binding site. B) Schematic of a native telomere marked with *URA3*. Symbols are as described for A. All elements are drawn to scale.

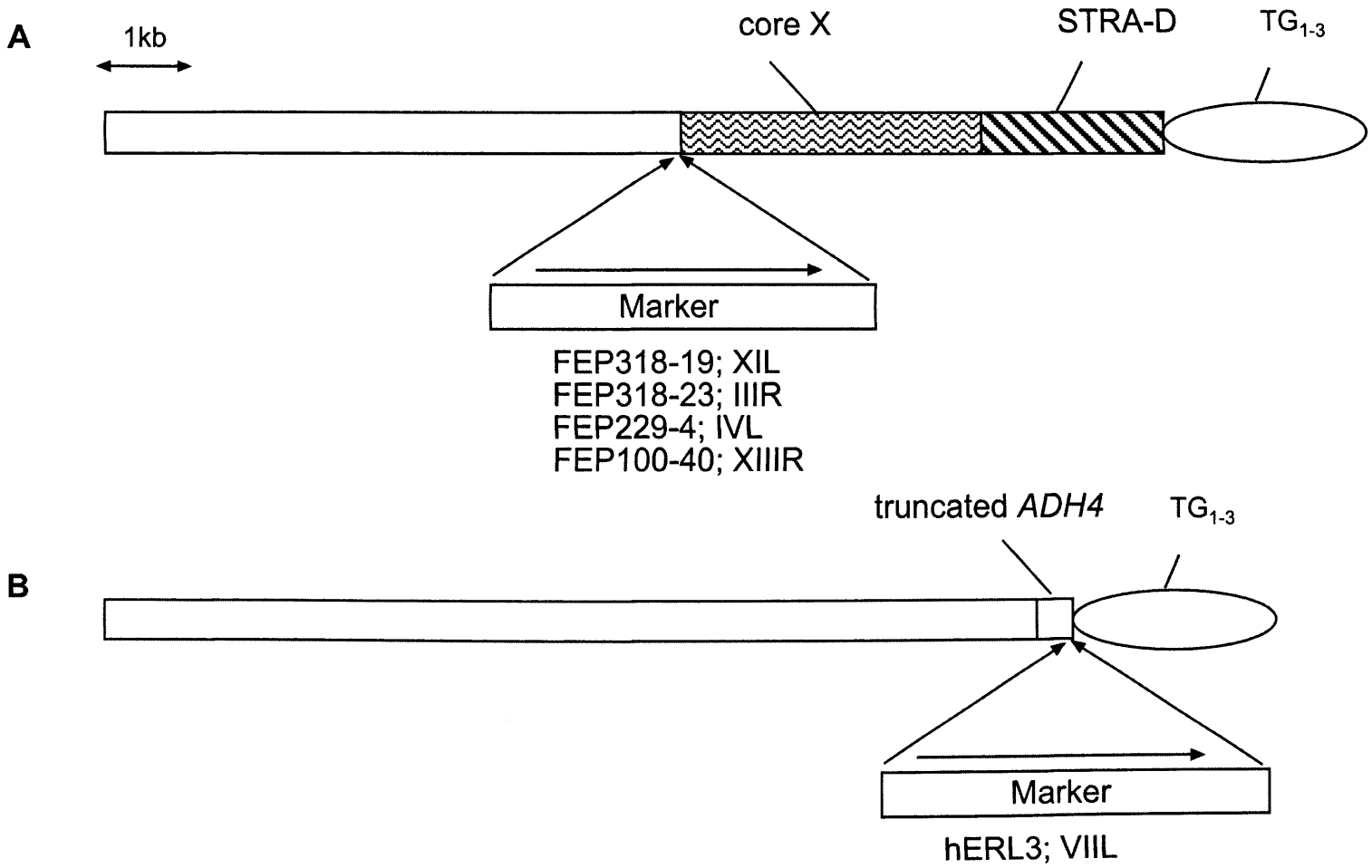

Figure 3.2. Marked telomeres. A) The structure of a native telomere lacking Y' elements. The insertion point of the marker constructs centromere-proximal to core X is shown and the specific telomere marked in each strain is indicated. B) The structure of the truncated VIIL telomere indicating the insertion point of the marker construct.

3.3 Results and Discussion

3.3.1 Comparison of silencing reveals alternative silencing states

Telomeric silencing at four native core X-only ends and at a truncated telomere was measured. FEP318-19 and FEP318-23 are marked with a *URA3-yEGFP* reporter immediately adjacent to core X, while FEP229-4 and FEP100-40 are marked with only *URA3* at the same position (Fig. 3.1 and 3.2). The truncated left telomere of chromosome VII (VIIL) in hERL3 lacks all subtelomeric elements and is marked with *URA3-yEGFP* immediately adjacent to the TG_{1-3} repeats. Previous examination of silencing at native core X-only ends, utilizing a *URA3* reporter gene inserted centromere-proximal to core X at the left telomere of chromosome XI (XIL), revealed a high degree of silencing (79% FOA^R) (Pryde and Louis, 1999). Similarly, *URA3* inserted at the same position on telomere XIIIR was also highly repressed (57% FOA^R). However, at IIIR and IVL, *URA3* silencing was reduced more than 100-fold (<1%). These four core X-only telomeres have no obvious sequence or compositional differences to account for the dramatic differences in silencing of the *URA3* promoter. The insertion of *URA3* in these strains placed the promoter approximately 1kb from the core X ACS element. At XIL, the degree of repression dropped by 4-5 orders of magnitude per kb that the reporter was moved away from core X.

For the purposes of this study, repression was examined at the XIL, IIIR, XIIIR and IVL native telomeres and the VIIL truncated end. The XIL and XIIIR telomeres strongly repressed the reporter constructs (Table 3.1). In contrast, both strains with the reporter construct at a non-repressive telomere (IIIR and IVL) had only slightly higher levels of growth on FOA than a strain expressing the *URA3-yEGFP* marker from the native *URA3* locus (Table 3.1). Therefore, *URA3* is almost completely derepressed at IIIR and IVL. These results are in agreement with previous repression analyses of these telomeres (Pryde and Louis, 1999). The truncated telomere also had a high degree of repression similar to observations of repression at truncated ends in other studies (Gottschling *et al.*, 1990; Renauld *et al.*, 1993). The ability of strains to grow on FOA is shown in Fig. 3.3.

Although the *URA3-yEGFP* marked telomeres showed the same pattern of high and low repression previously observed by F. Pryde (1999) for strains marked only with *URA3* at the same telomeres, the repression levels were reduced

compared to the *URA3* marked ends. At the *URA3* marked XIL telomere, *URA3* repression was 79% while the average at the *URA3-yEGFP* marked XIL was 25%, an approximately 3-fold reduction. This reduction is consistent with the increased distance of the *URA3* promoter from core X in the *URA3-yEGFP* strains due to the addition of the 800bp *yEGFP* ORF and, interestingly, is also observed at the non-repressive end (reduced from 0.31% repression to 0.02% by inclusion of *yEGFP*). This indicates that even the 'non-repressive' telomeres are still able to exert a silencing effect on a core X-adjacent marker.

Table 3.1. Frequency of FOA resistance for the *URA3-yEGFP* or *URA3* marker inserted at various telomeres and the native *URA3* locus.

Strain	Chromosome	%FOA^R	
hERL3	VIIL (truncated)	27 – 35	(31)
FEP318-19	XIL	10 – 42	(25)
FEP318-23	IIIR	0.002 – 1.6	(0.02)
FEP229-4	IVL	1.25 – 2.7	(1.79)
FEP100-40	XIIIR	38-39	(38.5)
PIY125	Native *URA3* (V)	0	(0)

The range of FOA resistance values from a minimum of three independent measurements is shown with the average value given in parenthesis. FOA resistance was analyzed as described in Chapter 2.

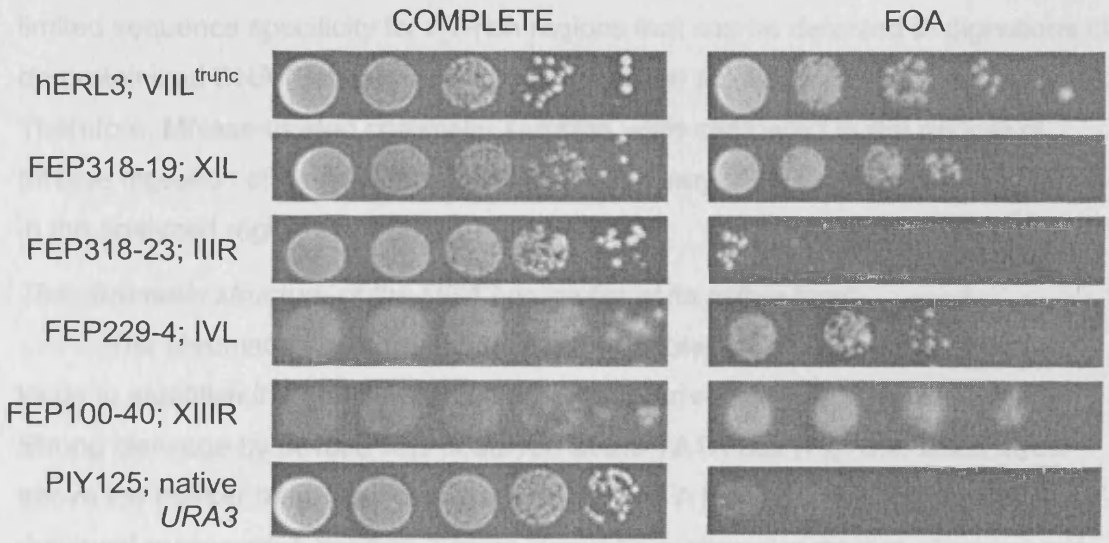

Figure 3.3. Representative examples of *URA3* repression assays at the native *URA3* locus, a truncated telomere and at native telomeres. The position of the *URA3* or *URA3-yEGFP* marker in each strain is indicated. Ten-fold serial dilutions of single colonies were plated on complete synthetic media or media containing FOA and grown for three days at 30°C as described in Chapter 2.

3.3.2 The chromatin structure of native and truncated subtelomeric regions is different

The subtelomere chromatin structure of the three *URA3-yEGFP* marked telomeres was analyzed by MNase digestion (as described in Chapter 2) to determine if there was a correlation between the silencing phenotypes of these three ends and their chromatin structures. The chromatin structure at the native *URA3* locus was also analyzed. Preliminary chromatin analyses indicated significant differences in the chromatin structure of *URA3* and the subtelomeric domains between the marked telomeres (P. Inglis, personal communication). MNase preferentially introduces DNA double-strand cuts in the linker DNA between histones, resulting in MNase hypersensitive sites in regions of phased nucleosomes (Tanaka *et al.*, 1996). However, MNase can also cut on the nucleosome surface and has limited sequence specificity for AT-rich regions that can be detected in digestions of de-proteinized DNA (Bellard *et al.*, 1989; Cockell *et al.*, 1983; Dingwall *et al.*, 1981). Therefore, MNase-treated chromatin samples were compared to the pattern of MNase digestion of de-proteinized DNA to detect any sequence specificity of MNase in the analyzed region as described in Chapter 2.

The chromatin structure of the URA3 promoter at its native locus

The chromatin structure of the *URA3* promoter was analyzed at its native locus to establish the structure of the expressed promoter (Fig. 3.4, *URA3* lanes). Strong cleavage by MNase was observed at the TATA box (Fig. 3.4, black arrow above the marker band), indicating the *URA3* TATA box is located on the edge of a dominant nucleosome position. Strong cleavage in promoter regions of expressed genes is commonly observed; the binding of the transcription factors appears to exclude nucleosomes (Becker, 1994). The UAS in the *URA3* promoter, located above this strong hypersensitive site, showed no indication of being nucleosomal; the MNase hypersensitivity sites in this region were not spaced a nucleosome apart and there was a degree of MNase digestion between the stronger bands (Fig. 3.4, this study; Tanaka *et al.* 1996). Therefore the region lacked the protection from MNase digestion that would occur in the presence of a positioned nucleosome. There were two other promoter-associated sites of interest below the marker band in Fig. 3.4, denoted by the two lower black arrows. The central of the three sites, just below the marker band, was protected from MNase cleavage at the native *URA3* locus, as it showed relatively little digestion in the chromatin samples compared to the naked

DNA sample. This protected region correlates with the presence of a nucleosome over the 5' end of the *URA3* ORF. The lower band was a hypersensitive site and therefore the lower limit of the nucleosome located over the *URA3* start site (Fig. 3.5, nucleosome 'b' at the IIIR end). The pattern of MNase sensitivity of these three promoter-associated sites at the native *URA3* locus (three black arrows in Fig. 3.4) is the 'open' chromatin structure, or the structure of the expressed *URA3* gene. The chromatin structure upstream of *URA3* was euchromatic with few prominent hypersensitive sites, none of which were spaced a nucleosome-length apart. The pattern of hypersensitive sites within the native *URA3* sequence at its native locus was similar to previously reported chromatin structures for *URA3* at its native locus, on minichromosomes and for *URA3* placed near a truncated telomere (Tanaka *et al.*, 1996; Thoma, 1986; Wright *et al.*, 1992).

The chromatin structure of URA3 correlates with silencing states at native telomeres

Several striking features were revealed by comparison of the chromatin structures of the *URA3* promoter at the native telomeres with the structure observed at the *URA3* locus (Fig. 3.4). The three promoter-associated bands (black arrows, Fig. 3.4), had different MNase sensitivity patterns at each telomere. At the non-repressive IIIR end, the pattern closely resembled the open promoter structure observed at the native *URA3* locus. The upper and lower bands exhibited increased MNase accessibility in comparison to the naked DNA digest ('N', Fig. 3.4). The distance between the upper and lower bands is equivalent to one nucleosome as shown in Fig. 3.5 (nucleosome 'b'). However, at the repressive XIL telomere the sensitivity of all three sites was different. In particular, the site closest to the TATA box was protected as it showed decreased cleavage both in relation to IIIR and to the naked DNA sample (top black arrow, Fig. 3.4). This indicates an altered nucleosome position to cover the TATA box at XIL in comparison to IIIR (Fig. 3.5, nucleosome '*b*'). The increased hypersensitivity of the middle band and decreased MNase digestion of the lower band also corresponds to the altered position of this promoter-proximal nucleosome at XIL (black arrows, Fig. 3.4). This pattern of MNase hypersensitivity and inferred alterations in nucleosome positioning over the *URA3* promoter at XIL is the closed, or repressive, promoter structure. A similar chromatin structure was observed by Tanaka *et al.* (1996) at the native *URA3* locus in a small fraction of the population (Tanaka *et al.*, 1996). The positioning of the nucleosome over the TATA box presumably interferes with the ability of transcription factors to bind, correlating with the reduced *URA3* expression from XIL. Therefore, the *URA3* promoter

Figure 3.4. Comparison of chromatin structures toward the centromere by indirect end label analysis. The subtelomeric chromatin structures of the *URA3-yEGFP* marked truncated VIIL, native XIL and native IIIR telomeres of *S. cerevisiae* (in strains hERL3, FEP318-19 and FEP318-23 respectively) were analyzed by digestion of permeabilized cells with 2, 10 and 20 U/mL of MNase (indicated by black triangle). The chromatin structure was also analyzed in the isogenic PIY125 strain with the *URA3-yEGFP* construct at the native *URA3* locus (*URA3*). The purified samples were end labeled at the *Stu*I site and resolved on an agarose gel with MNase-treated naked (N) DNA and the 456bp marker (M) DNA, generated by digestion of purified DNA with *Stu*I and *Pst*I. The marker indicates the position of the *URA3* TATA box. The MNase hypersensitivity patterns were detected by hybridization with the 200bp $URA3_{cen}$ probe (as indicated in Fig. 3.1). Black arrows indicate sites of interest close to the *URA3* promoter while grey arrows highlight prominent subtelomeric bands. A 100bp ladder (L), probed separately, is provided for an indication of the distance between hypersensitive sites. Positions of *Stu*I and *Pst*I on the blot relative to the inserted marker at native ends is indicated by the diagram on the right.

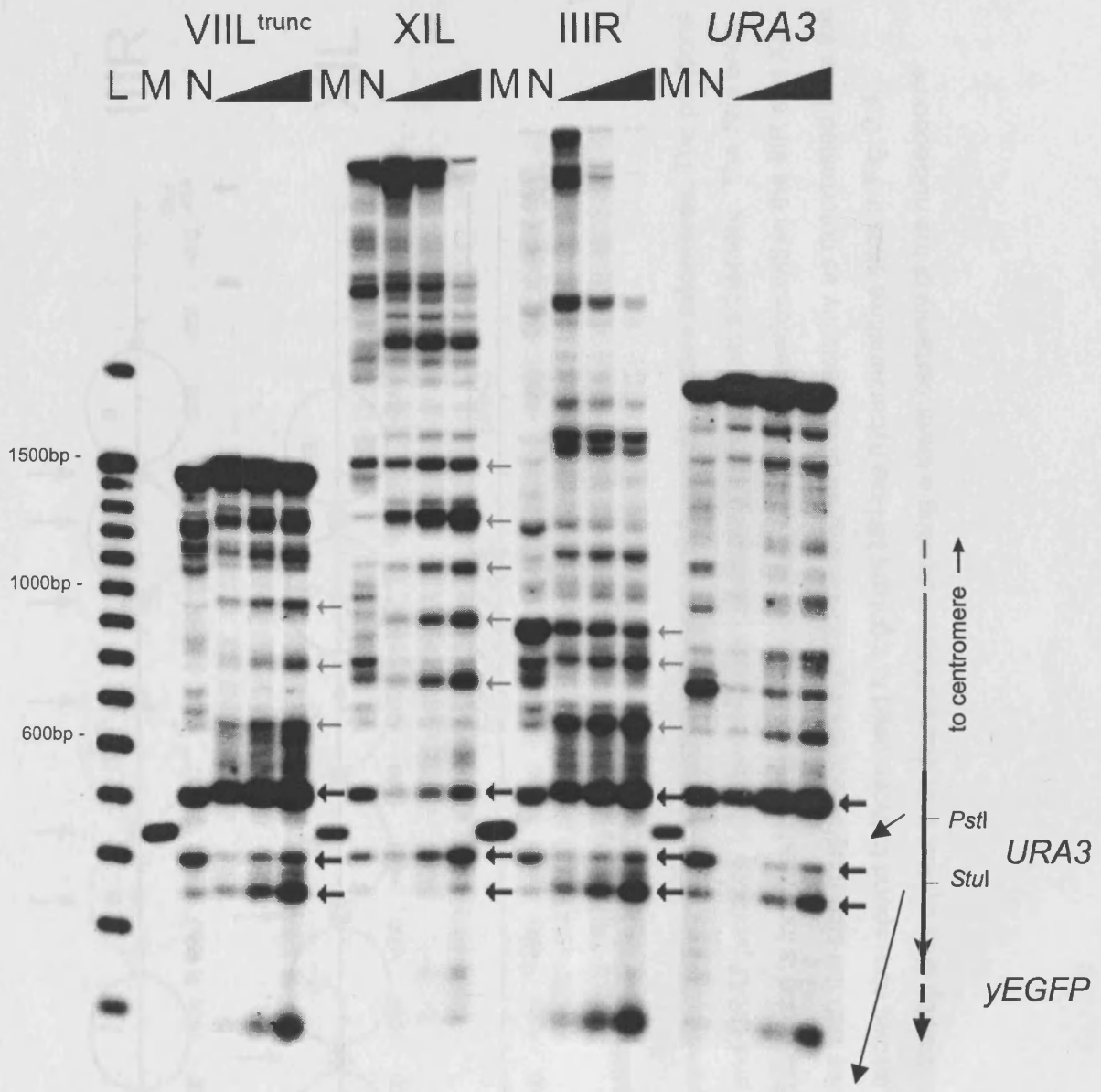

Figure 3.4. Comparison of chromatin structures toward the centromere by indirect end label analysis.

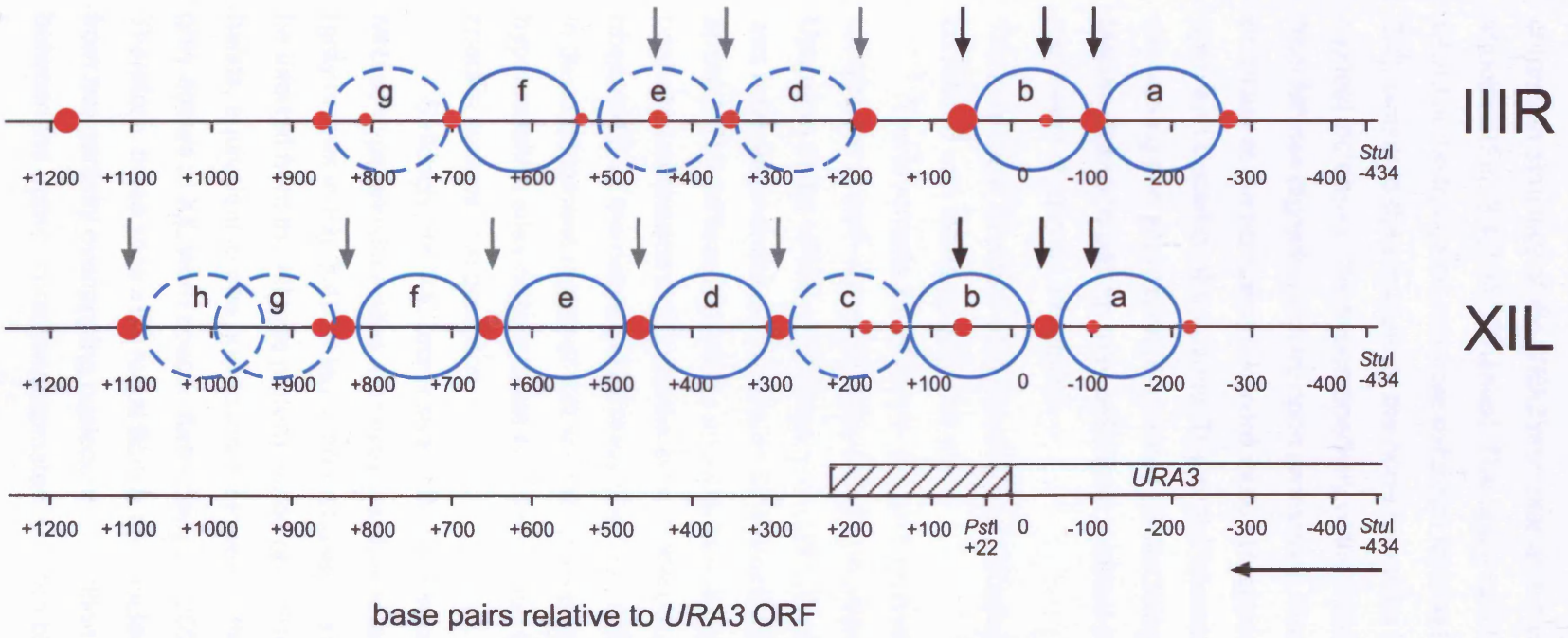

Figure 3.5. Inferred nucleosome positions toward the centromere from the IIIR and XIL native telomeres. The positions of the *URA3* ORF (open rectangle) and *URA3* promoter (diagonal lines) are indicated in the bottom schematic. The *Stu*I and *Pst*I sites are marked and the $URA3_{cen}$ probe is indicated by the black arrow. Sites of MNase digestion within the IIIR and XIL sequences are indicated by red circles with the size roughly correlating with the degree of accessibility as determined from the chromatin analysis. Black and grey arrows correspond to those used to highlight MNase hypersensitive sites in Fig. 3.4. Inferred nucleosome positions are shown by blue circles, with dashed lines indicating a lower certainty of the nucleosome placement.

structures observed for the two native ends correlated with the levels of repression observed at XIL and IIIR.

Although the truncated telomere exhibited high levels of repression, the chromatin structure of the *URA3* promoter at this end closely resembled the open structure (Fig. 3.4, VIIL^{trunc} lanes). The upper and lower promoter-associated sites of *URA3* at the truncated telomere exhibited MNase hypersensitivity (black arrows, Fig. 3.4), similar to the structure at the non-repressive IIIR end. However, there was a modest increase in the hypersensitivity of the middle band, which is well protected from MNase digestion at fully open promoters. The chromatin structure of the promoter at the truncated telomere therefore appears to be intermediate between the open and closed conformations. Truncated telomeres are known to switch between expressing and non-expressing states (Gottschling *et al.*, 1990), suggesting this MNase digestion pattern may arise from a mixed population of repressive and non-repressive chromatin structures.

The chromatin structure of the centromere-proximal subtelomeric domains is correlated with silencing at native ends

The chromatin structures of the endogenous subtelomeric regions toward the centromere of both native telomeres also correlated with the silencing states. Upstream of the *URA3-yEGFP* marker at IIIR, the MNase hypersensitivity pattern was irregular and was characterized by smearing between the bands (Fig. 3.4, grey arrows). This MNase digestion pattern is indicative of euchromatic domains with unphased nucleosomes (Ravindra *et al.*, 1999). A similar euchromatic pattern was observed 5' of the native *URA3* locus (Fig. 3.4, *URA3* lanes). Nucleosome positions in the subtelomeric region of IIIR are therefore uncertain (Fig. 3.5) and the hypersensitive sites observed are more likely due to site specificity of MNase than to specific nucleosome positions.

Strikingly, the XIL repressive end had a strong pattern of evenly spaced MNase hypersensitive sites, consistent with a heterochromatic chromatin structure (gray arrows in Fig. 3.4). At least three phased nucleosomes (*d*, *e* and *f*, Fig. 3.5) can be inferred from the MNase pattern based on a distance of ~150bp between the bands, equivalent to one nucleosome. However, the upper two sites indicated by grey arrows at XIL were spaced further apart (~200bp) than a typical nucleosome. Therefore, these sites may result from a non-nucleosomal feature of the chromatin or from two partially overlapping nucleosome positions (*g* and *h*, Fig. 3.5). The region between the upper promoter-associated site (top black arrow, Fig 3.4) and the first

hypersensitive site of the phased region (bottom grey arrow) was also well protected at XIL. This contrasts to IIIR which had a strong hypersensitive site in this region. Therefore, although the UAS element of the *URA3* promoter was not observed to be nucleosomal at an expressed location (this study; Tanaka *et al.*, 1996), the strong protection of the region at a repressive locus may indicate the presence of a second promoter-associated nucleosome, further facilitating the exclusion of transcription factors from the promoter ('c', Fig. 3.5).

Interestingly, the subtelomeric region at the truncated VIIL telomere had similarities to both the XIL heterochromatic structure and the euchromatic structure at IIIR (Fig. 3.4). There were three MNase hypersensitive sites spaced ~150bp apart, similar to XIL, indicating a repressive structure but there was more digestion between these bands, similar to IIIR (grey arrows, Fig. 3.4). In addition, the UAS region of the *URA3* promoter exhibited strong MNase hypersensitivity in contrast the XIL repressive structure. These features, in addition to the *URA3* promoter structure of the truncated end, indicate a chromatin region that is not fully repressive. This correlates with the expression variegation of truncated ends, and highlights the significant differences between repression at truncated and native telomeres.

Analysis of the centromere-proximal chromatin structure at the IVL and XIIIR native telomeres

The chromatin structures of the native IVL and XIIIR telomeres were examined by MNase to confirm that the features observed at XIL and IIIR are related to the degree of repression and not simply a feature of the subtelomeric sequence at these ends. IVL is non-repressive and XIIIR represses the *URA3* marker. Both ends are marked with *URA3* at the same position relative to core X as the *URA3-yEGFP* marker at the XIL and IIIR telomeres (Fig. 3.1). The chromatin analysis of IVL revealed a pattern nearly identical to the non-repressive IIIR end (Fig. 3.6). The *URA3* promoter at IVL was in the open configuration, with the upper and lower sites exhibiting MNase hypersensitivity and the central band being protected (three black arrows, Fig. 3.6). In addition, the chromatin structure of the endogenous subtelomeric sequence toward the centromere was euchromatic, with no regular pattern of MNase digestion.

The chromatin structure of the repressive XIIIR telomere yielded a pattern nearly identical to XIL (Fig. 3.6). There was more digestion by MNase between the hypersensitive sites at XIIIR in comparison to the XIL MNase pattern however. The pattern around the *URA3* promoter, while clearly in a closed configuration, was also

less distinct. However, these differences between the XIL and XIIIR structures are due to the presence of a mutant *ura3-52* allele at the native *URA3* locus in the strain carrying the marked XIIIRL telomere. The $URA3_{cen}$ probe used in the chromatin analysis is also able to bind this mutant allele. The heterochromatic banding pattern in the subtelomeric region, similar to that observed at XIL, was still distinct though. This heterochromatic pattern is very dissimilar from the chromatin structure 5' of the native *URA3* locus. Therefore, it is clear this pattern is a feature of the XIIIR subtelomeric domain and not a result of cross-hybridization with *ura3-52*.

With the exception of the core X and STR subtelomeric elements, the subtelomeric regions of these four native ends share no homology (Louis, 1995; http://www.leicester.ac.uk/genetics/ejl12). Therefore, together with the results for IIIR and XIL, the analysis of the subtelomeric regions of IVL and XIIIR toward the centromere confirms that the observed heterochromatic and euchromatic patterns at native telomeres are correlated with the silencing phenotypes of these ends and not merely a result of specific subtelomeric sequences.

Figure 3.6. Comparison of chromatin structures toward the centromere by indirect end label analysis at the XIIIR and IVL telomeres of *S. cerevisiae*. The subtelomeric chromatin structures of the *URA3* marked native XIIIR and IVL telomeres of *S. cerevisiae* were analyzed by digestion of permeabilized cells with increasing concentrations of MNase (indicated by black triangle). The purified samples were end labeled at the *Stu*I site and resolved on an agarose gel with MNase-treated naked (N) DNA. The 456bp marker (M) DNA, generated by digestion of purified DNA with *Stu*I and *Pst*I, is placed to indicate the position of the *URA3* TATA box. The MNase hypersensitivity patterns were detected by hybridization with the $URA3_{cen}$ probe. Black arrows indicate sites of interest close to the *URA3* promoter while grey arrows highlight prominent subtelomeric bands. A 100bp ladder (L), probed separately, is provided for an indication of the distance between hypersensitive sites. Positions of *Stu*I and *Pst*I on the blot relative to the inserted marker is indicated by the diagram on the right.

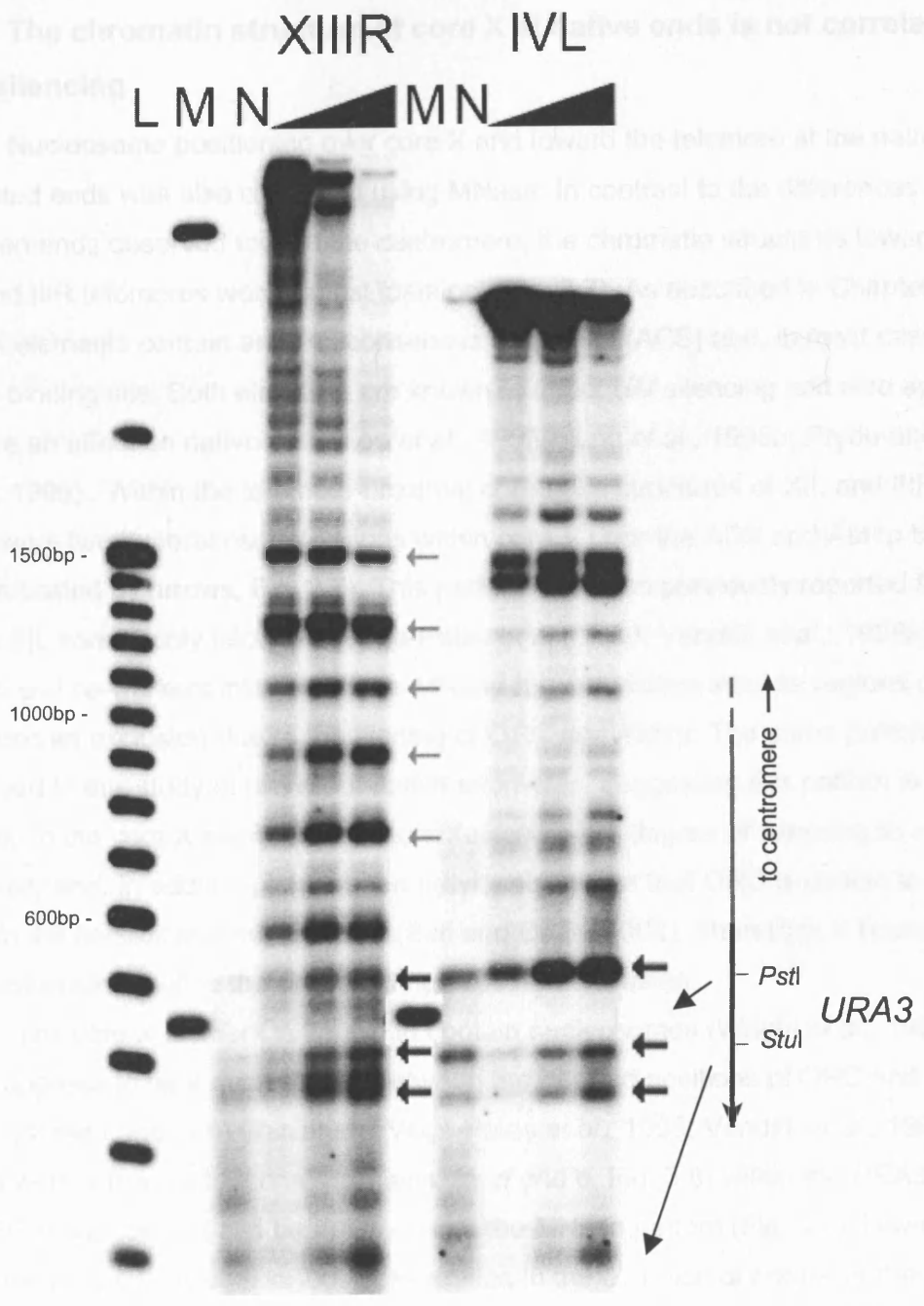

Figure 3.6. Comparison of chromatin structures toward the centromere by indirect end label analysis at the XIIIR and IVL telomeres of *S. cerevisiae*.

3.3.3 The chromatin structure of core X at native ends is not correlated with silencing

Nucleosome positioning over core X and toward the telomere at the native and truncated ends was also examined using MNase. In contrast to the differences between ends observed toward the centromere, the chromatin structures toward the XIL and IIIR telomeres were almost identical (Fig. 3.7). As described in Chapter 1, core X elements contain an ARS consensus sequence (ACS) and, in most cases, an Abf1p binding site. Both elements are known to affect *HM* silencing and also appear to have an effect on native TPE (Loo *et al.*, 1995a; Loo *et al.*, 1995b; Pryde and Louis, 1999). Within the telomere-proximal chromatin structures of XIL and IIIR, there were two hypersensitive regions within core X near the ACS and Abf1p binding site (indicated by arrows, Fig. 3.7). This pattern has been previously reported for the native IIIL core X-only telomere (Vega-Palas *et al.*, 1998; Venditti *et al.*, 1999a). Di Mauro and co-workers interpreted the MNase hypersensitive sites as regions of nucleosome exclusion due to the binding of ORC and Abf1p. The same pattern was observed in this study at two other native telomeres, suggesting this pattern is specific to the core X element and is unaffected by the degree of silencing at a particular end. In addition, it has been previously shown that ORC is unable to bind DNA in the context of a nucleosome (Bell and Dutta, 2002). Therefore, a bound ORC element would result is the proposed nucleosome exclusion.

The core X element is known to contain nucleosomes (Wright *et al.*, 1992) and there appears to be a nucleosome between the inferred positions of ORC and Abf1p (nucleosome *f*, Fig. 3.8) (this study; Vega-Palas *et al.*, 1998; Venditti *et al.*, 1999). There were a few nucleosome positions, (*a*, *d* and *e*, Fig. 3.8) within the *URA3-yEGFP* sequence that can be inferred from the MNase pattern (Fig. 3.7). However, there were no clearly positioned nucleosomes in the 3' region of core X or the STRs, indicating any nucleosomes in these regions are unphased. Regions of MNase digestion within the STRs may correspond to binding sites for Tbf1p, several of which are found in the STRs (Fig. 3.7 and Fig. 3.8). The unphased pattern of MNase digestion over the region between the Abf1p binding site and the telomere repeats is in agreement with previous observations that this region is not silenced (Pryde and Louis, 1999). The heavy band at the top of each chromatin lane (Fig. 3.7) corresponds with the telosome, which is non-nucleosomal and is not digested by MNase (Wright *et al.*, 1992).

Figure 3.7. Comparison of chromatin structures toward the telomere by indirect end label analysis. The subtelomeric chromatin structures of the *URA3-yEGFP* marked truncated VIIL and native XIL and IIIR telomeres of *S. cerevisiae* and at the native *URA3* locus were analyzed by MNase digestion and indirect end labeling at the *Stu*I site as described previously using the $URA3_{tel}$ probe (as indicated in Fig. 3.1). The 1171bp marker (M) bands were generated by digestion with *Stu*I and *Xma*I. Black arrows indicate sites of interest close to the ACS and Abf1p binding site in the core X elements and a hypersensitive region specific to the native *URA3* locus. A 100bp ladder (L), probed separately, is provided for an indication of the distance between hypersensitive sites. Positions of *Stu*I, *Xma*I and the telomere on the blot relative to the inserted marker at native ends is indicated by the diagram on the right (symbols are as given in Fig. 3.1).

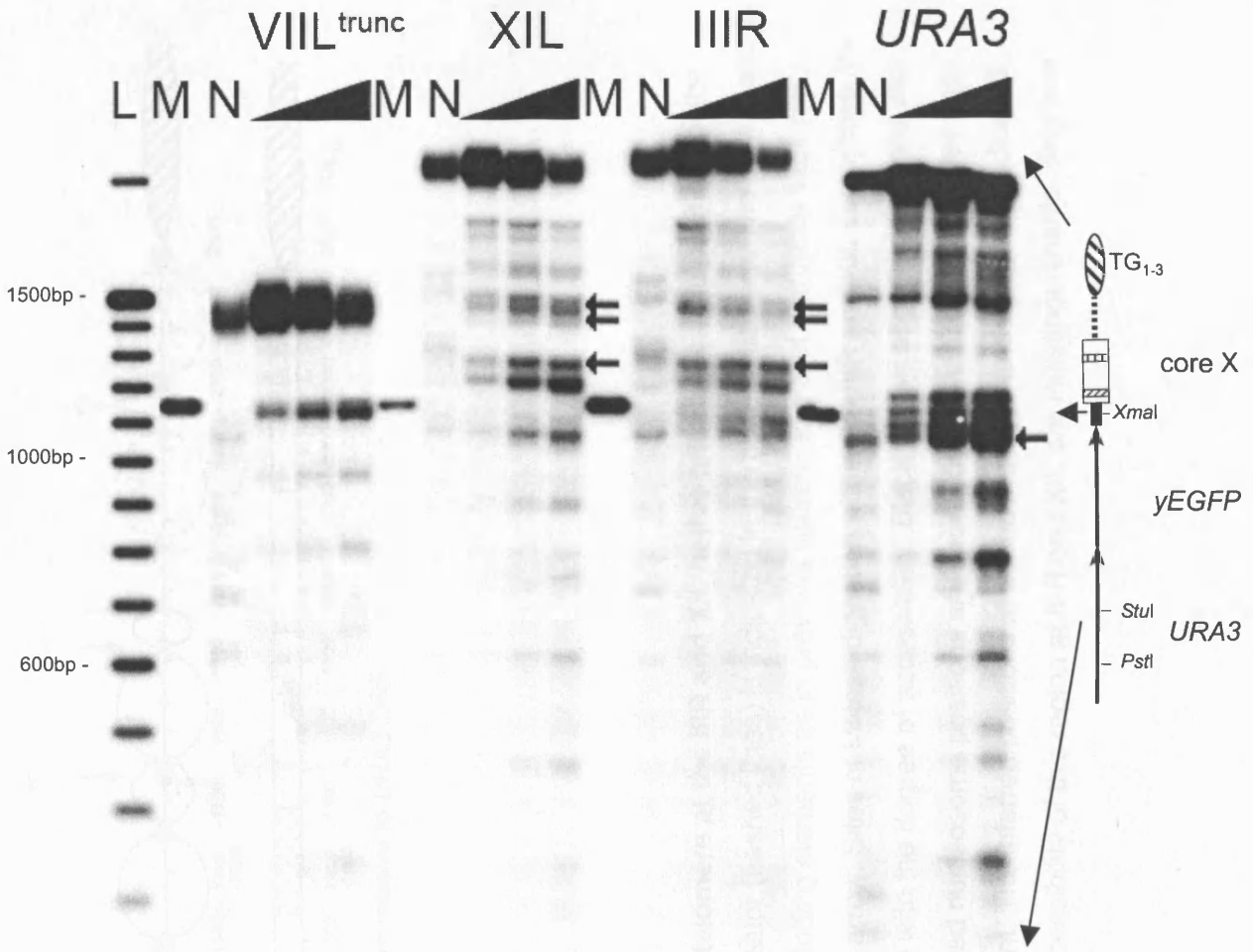

Figure 3.7. Comparison of chromatin structures toward the telomere by indirect end label analysis.

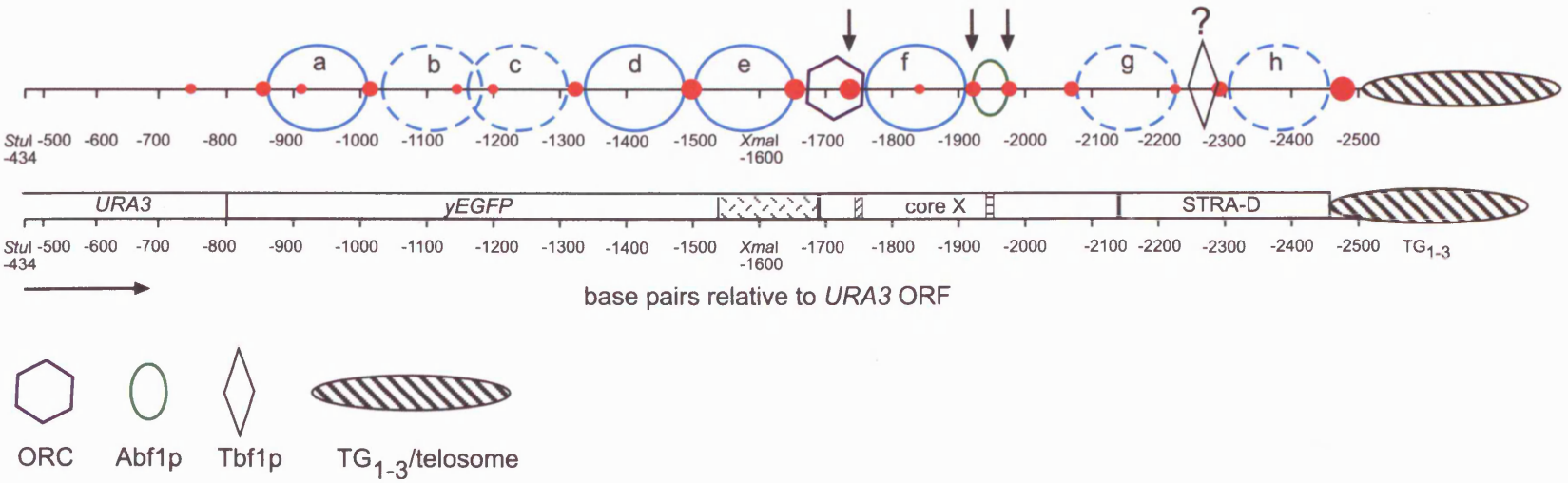

Figure 3.8. Inferred chromatin structure toward the telomere at the IIIR and XIL native telomeres. The positions of the *URA3-yEGFP* ORF (open rectangles) and *URA3* terminator (hashed lines) is indicated in the bottom diagram. The core X and STR repeats are also shown with the ACS and Abf1p binding elements as in previous figures. The *Stu*I and *Xma*I sites are marked and the $URA3_{tel}$ probe is indicated by the black arrow. Sites of MNase digestion within the IIIR and XIL sequences are indicated by red circles with the size roughly correlating with the degree of accessibility. Black arrows above correspond with those shown on the chromatin analysis (Fig. 3.7). Inferred nucleosome positions are shown by blue circles with dashed lines indicating a lower certainty of the nucleosome placement. The inferred positions of the bound ORC and Abf1p are indicated as is a possible site for bound Tbf1p. As the MNase accessibility of this region at IIIR and XIL are indistinguishable, only one inferred chromatin structure is illustrated.

Unsurprisingly, the pattern of digestion toward the telomere of the truncation end, which lacks core X, is very different from the native ends. A heterochromatin-like banding pattern persists from within *URA3-yEGFP* through to the telosome (Fig. 3.7), consistent with the continuous spread of the Sir complex at truncated telomeres (Renauld *et al.*, 1993).

Although the chromatin structure 3' of the native *URA3* locus is of little interest for comparison to the structure of subtelomeric elements, one notable feature was the strong hypersensitive region around the marker band, within the *URA3* termination sequence (black arrow in *URA3* chromatin lanes, Fig. 3.7). This MNase hypersensitive region was also observed in studies at the native *URA3* locus by Thoma *et al.* (1986) and Tanaka *et al.* (1996). Although the *URA3* termination sequence is also present at the marked telomeres, this strong hypersensitivity was almost entirely absent at XIL and there was only a small increase in MNase digestion at IIIR relative to XIL. This region of MNase sensitivity at the native *URA3* locus may be a feature of the *URA3* terminator of the unsilenced gene that is masked at IIIR due to non-native downstream sequence. Alternatively, the MNase sensitivity may be specific to the native *URA3* locus and unrelated to the degree of silencing. The chromatin structures of the telomeres and native *URA3* locus were consistent with preliminary analyses (P. Inglis, personal communication).

The telomere-proximal chromatin pattern was also examined at the IVL and XIIIR native telomeres. The hypersensitive regions close to the ACS and Abf1p binding sites were still present at IVL (Fig. 3.9). The specific core X chromatin structure was not clearly observed at XIIIR, however (Fig. 3.9). This was most likely due to the presence of a second mutant copy of *URA3* in the strain to which the probe binds. The pattern at XIIIR appears to be the sum of the normal telomere-proximal pattern observed at other ends, combined with the structure 3' of the native *URA3* locus.

Figure 3.9. Comparison of chromatin structures toward the telomere by indirect end label analysis at the XIIIR and IVL telomeres of *S. cerevisiae*. The subtelomeric chromatin structures of the *URA3* marked native XIIIR and IVL telomeres of *S. cerevisiae* were analyzed by MNase digestion and indirect end labeling at the *Stu*I site as described previously. The 445bp marker (M) DNA, generated by digestion of purified DNA with *Stu*I and *Xma*I, is placed to indicate the position of the *URA3*-coreX junction. MNase hypersensitivity patterns toward the telomere were detected by hybridization with the 200bp $URA3_{tel}$ probe. Black arrows indicate sites of interest close to the ACS and Abf1p binding site in the core X elements. A 100bp ladder (L), probed separately, is provided for an indication of the distance between hypersensitive sites. Positions of *Stu*I, *Xma*I and the telomere on the blot relative to the inserted marker is indicated by the diagram on the right (symbols are as given in Fig. 3.1).

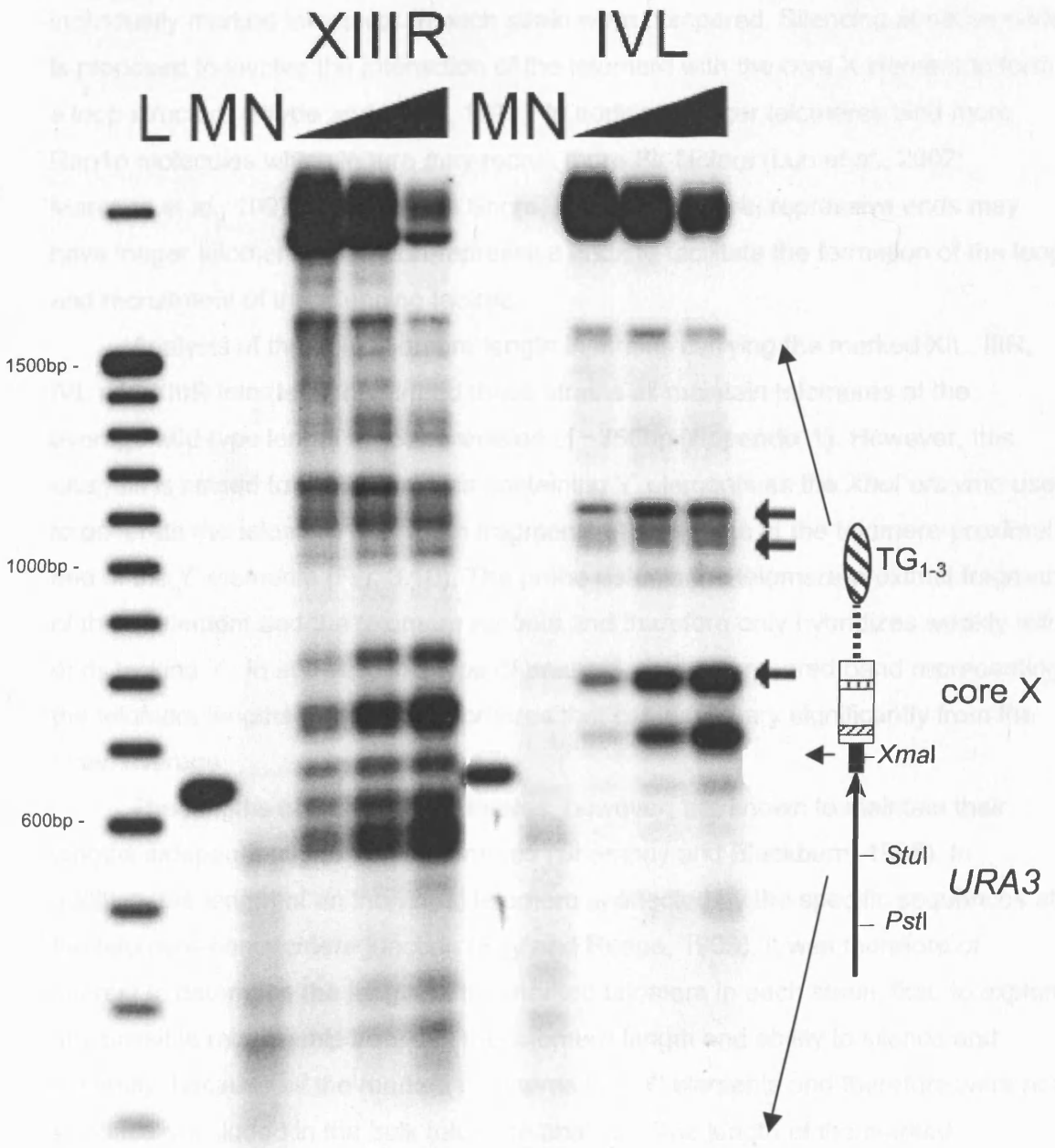

Figure 3.9. Comparison of chromatin structures toward the telomere by indirect end label analysis at the XIIIR and IVL telomeres of *S. cerevisiae*.

3.3.4 Telomere length effects in silencing

To assess the effect of telomere length on silencing, the lengths of the individually marked telomeres in each strain were compared. Silencing at native ends is proposed to involve the interaction of the telomere with the core X element to form a loop structure (Pryde and Louis, 1999). In addition, longer telomeres bind more Rap1p molecules which in turn may recruit more Sir factors (Luo *et al.*, 2002; Marcand *et al.*, 1997a; Moretti and Shore, 2001). Therefore, repressive ends may have longer telomeres than non-repressive ends to facilitate the formation of the loop and recruitment of the silencing factors.

Analysis of the bulk telomere length in strains carrying the marked XIL, IIIR, IVL and XIIIR telomeres confirmed these strains all maintain telomeres at the average wild-type length for *S. cerevisiae* of ~350bp (Appendix 1). However, this analysis is biased toward telomeres containing Y' elements as the *Xho*I enzyme used to generate the telomere restriction fragments (TRF's) cuts at the telomere-proximal end of the Y' elements (Fig. 3.10). The probe detects the telomere-proximal fragment of the Y' element and the telomere repeats and therefore only hybridizes weakly with ends lacking Y'. In addition, this type of analysis yields a smeared band representing the telomere lengths of multiple telomeres that can each vary significantly from the strain average.

The lengths of individual telomeres, however, are known to maintain their lengths independently of other telomeres (Shampay and Blackburn, 1988). In addition, the length of an individual telomere is affected by the specific sequences at the telomere-nontelomere junction (Ray and Runge, 1999). It was therefore of interest to determine the length of the marked telomere in each strain, first, to explore any possible relationship between the telomere length and ability to silence and secondly, because all the marked telomeres lack Y' elements and therefore were not specifically included in the bulk telomere analysis. The length of the marked telomeres was measured by digestion of three independent DNA preps for each strain with *Stu*I as described in Chapter 2. The *Stu*I-generated TRF for the *URA3-yEGFP* marked XIL and IIIR telomeres was expected to be ~2350bp. The TRF size expected for the *URA3*-only marked XIIIR and IVL strains was approximately 1620bp. The lengths of the telomere fragments for XIL and IIIR were indistinguishable from each other and were close to the expected size (Fig. 3.11). Similarly, although the telomere fragments for XIIIR and IVL were slightly larger than

predicted (~1750bp) both telomeres were of a similar length (Fig. 3.11). It therefore appears that differences in telomere lengths do not correlate with silencing differences between telomeres. All four telomeres analyzed had lengths close to the 350bp average and, in direct comparisons, the lengths of the repressive and non-repressive ends containing the same marker were indistinguishable. The telomere length of the truncated telomere was not analyzed as it has been previously shown that the length regulation of a truncated telomere is different from that of native ends (Craven and Petes, 1999).

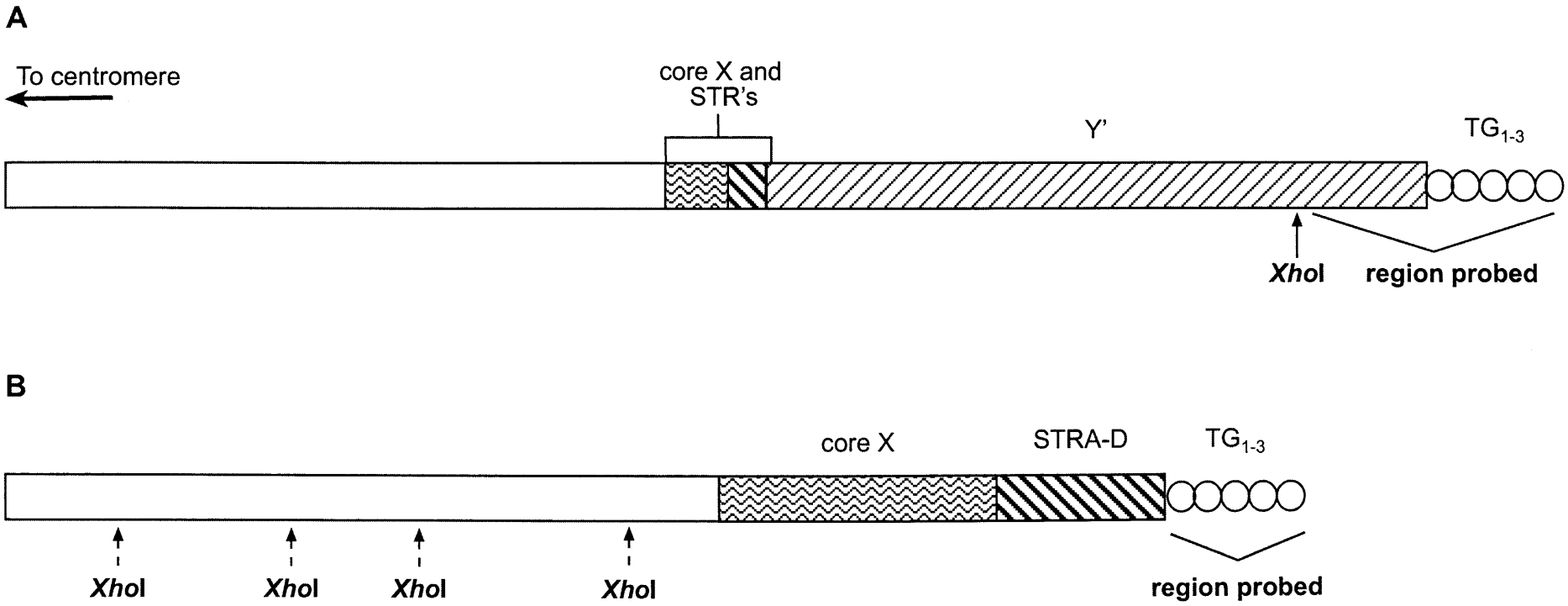

Figure 3.10. Positions of *Xho*I sites near yeast telomeres. A) *Xho*I cuts within Y' elements close to the telomere repeats. B) *Xho*I sites within the subtelomeric region are variable between different core X-only telomeres. The regions homologous to the pEL30 probe are indicated for both types of telomeres.

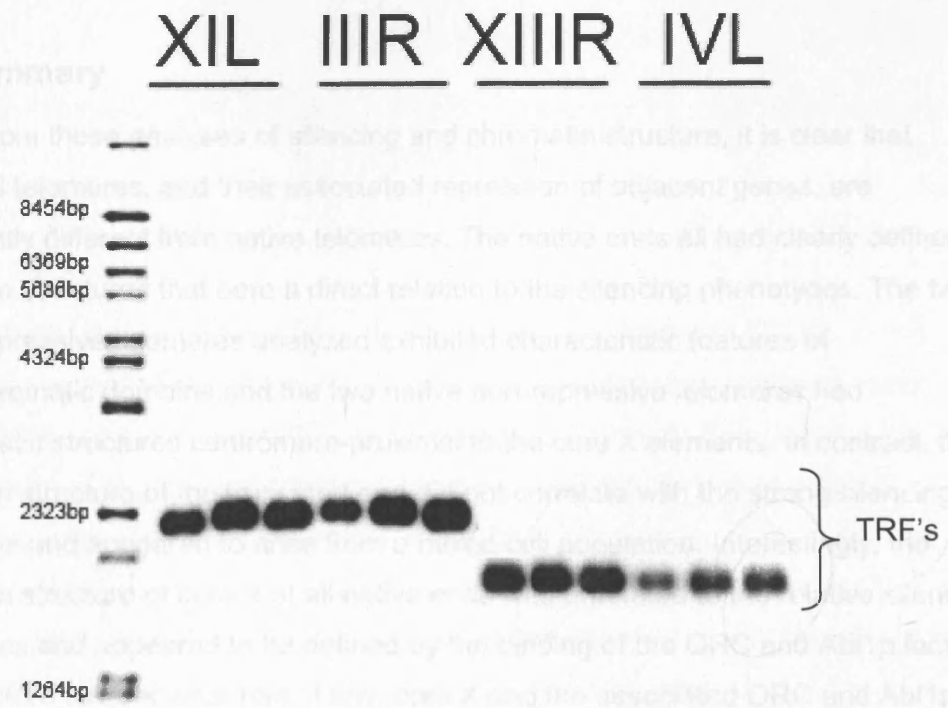

Figure 3.11. Analysis of individual telomere lengths in four *S. cerevisiae* strains. DNA preps from three individual colonies each of the four strains FEP318-19, FEP318-23, FEP100-40 and FEP229-4, containing the *URA3-yEGFP* or *URA3* marked XIL, IIIR, XIIIR or IVL telomeres, were digested with *Stu*I. Digestion fragments were separated on a 0.5% agarose gel, blotted and detected with the radio-labeled $URA3_{tel}$ probe. For determination of fragment size the _*Bst*EII ladder was also run on the gel and ladder fragments were detected by probing with labeled lambda DNA.

3.4 Summary

From these analyses of silencing and chromatin structure, it is clear that truncated telomeres, and their associated repression of adjacent genes, are significantly different from native telomeres. The native ends all had clearly defined chromatin structures that bore a direct relation to the silencing phenotypes. The two native repressive telomeres analyzed exhibited characteristic features of heterochromatic domains and the two native non-repressive telomeres had euchromatic structures centromere-proximal to the core X elements. In contrast, the chromatin structure of the truncated end did not correlate with the strong silencing phenotype and appeared to arise from a mixed cell population. Interestingly, the chromatin structure of core X at all native ends was unrelated to the relative silencing efficiencies and appeared to be defined by the binding of the ORC and Abf1p factors. It is therefore unclear what role, if any, core X and the associated ORC and Abf1p play in silencing. Although telomere length could potentially alter the ability of an end to form the loop structure, the lengths of the repressive and non-repressive telomeres were indistinguishable. Therefore, telomere length regulation at individual telomeres does not appear to affect the degree of silencing.

CHAPTER 4

4 Chromatin Modifiers, Silencing and Heterochromatin Formation

4.1 Introduction

This chapter investigates the roles of trans-acting silencing factors on the chromatin structure of native telomeres. Numerous factors have previously been identified that affect both silencing and chromatin structure. In *S. cerevisiae*, the Sir proteins are well known silencing factors that are essential for maintenance of repression at the silent mating type loci and at telomeres. Sir2p, Sir3p and Sir4p are essential for silencing and are directly involved in chromatin structure either through histone modification, in the case of the Sir2p histone deacetylase, or through direct binding to histones (Hecht *et al.*, 1995; Imai *et al.*, 2000b). In contrast, Sir1p is important for recruitment of the other Sir proteins to the *HML* and *HMR* silencers but is not known to directly affect chromatin (Pillus and Rine, 1989; Triolo and Sternglanz, 1996). In addition, Sir1p has only a very small effect on TPE at native ends, (Fourel *et al.*, 1999; Pryde and Louis, 1999; Vega-Palas *et al.*, 2000). Sir1p is recruited to the *HM* silencers by an interaction with the ORC complexes bound at the ACS sites (Triolo and Sternglanz, 1996). The subtelomeric core X element also contains an ACS that may be able to recruit ORC and subsequently Sir1p (Pryde and Louis, 1997).

In addition to the Sir proteins, other chromatin-modifying factors have also been shown to facilitate silencing. Bre1p, Dot1p and Set1p act together in a histone methylation pathway. Bre1p is an essential co-factor in the recruitment of Rad6p to ubiquitinate histone H2B (Wood *et al.*, 2003a). This ubiquitination, in turn, is required for the methylation of histone H3 at an internal and N-terminal lysine residue by the histone methytransferases Dot1p and Set1p respectively (Dover *et al.*, 2002; Ng *et al.*, 2002b; Sun and Allis, 2002). Mutation of any of these three histone modifiers alleviates repression at truncated telomeres (Dover *et al.*, 2002; Ng *et al.*, 2002a; Nislow *et al.*, 1997; Singer *et al.*, 1998; Wood *et al.*, 2003a). However, their effect on TPE at native ends is unknown.

Sas2p is a histone acetyltransferase that restricts the spread of the Sir complex by counteracting the Sir2p histone deacetylase (Ehrenhofer-Murray *et al.*, 1997; Kimura *et al.*, 2002). Deletion of Sas2p alleviates repression near truncated

telomeres and also results in moderately increased repression of loci further from the telomeric regions (Kimura *et al.*, 2002; Suka *et al.*, 2002). Bdf1p also appears to restrict the spread of the Sir complex from repressed domains. Bdf1p contains a bromodomain, allowing it to bind acetylated histones (Pamblanco *et al.*, 2001). The binding of Bdf1p is thought to protect histones from Sir2p-mediated deacetylation, thus preventing the Sir complex from continuing to spread (Ladurner *et al.*, 2003). Similar to Sas2p, deletion of Bdf1p alleviates repression near the telomere (Ladurner *et al.*, 2003). Mutations of histone N-terminal lysine residues and Sir proteins have been shown to affect chromatin structure at the silent mating type loci (Ravindra *et al.*, 1999), and the repressive IIIL telomere (Venditti *et al.*, 1999b). However, chromatin changes at silenced loci due to mutations of other histone modifiers have yet to be analyzed. This chapter investigates the effect of the four Sir proteins and the histone modifying factors, Bre1p, Dot1p, Set1p, Sas2p and Bdf1p on silencing and chromatin structure of the repressive XIL and non-repressive IIIR native telomeres. The strains used in this chapter are listed in Table 4.1 and were created as described in Chapter 2.

Table 4.1. *S. cerevisiae* strains used in Chapter 4.

Strain[a]	Genotype	Relevant Modifications	
hERL5	*MAT**a**, lys2Δ202, leu2Δ1, ura3Δ851, his3Δ200*	*URA3::yEGFP* on XIL	*sir1::kanMX*
hERL6	*MAT**a**, lys2Δ202, leu2Δ1, ura3Δ851, his3Δ200*	*URA3::yEGFP* on IIIR	*sir1::kanMX*
hERL7	*MAT**a**, lys2Δ202, leu2Δ1, ura3Δ851, his3Δ200*	*URA3::yEGFP* on XIL	*sir2::kanMX*
hERL8	*MAT**a**, lys2Δ202, leu2Δ1, ura3Δ851, his3Δ200*	*URA3::yEGFP* on IIIR	*sir2::kanMX*
hERL9	*MAT**a**, lys2Δ202, leu2Δ1, ura3Δ851, his3Δ200*	*URA3::yEGFP* on XIL	*sir3::kanMX*
hERL10	*MAT**a**, lys2Δ202, leu2Δ1, ura3Δ851, his3Δ200*	*URA3::yEGFP* on IIIR	*sir3::kanMX*
hERL11	*MAT**a**, lys2Δ202, leu2Δ1, ura3Δ851, his3Δ200*	*URA3::yEGFP* on XIL	*sir4::kanMX*
hERL12	*MAT**a**, lys2Δ202, leu2Δ1, ura3Δ851, his3Δ200*	*URA3::yEGFP* on IIIR	*sir4::kanMX*
hERM211	*MAT**a**, lys2Δ202, leu2Δ1, ura3Δ851, his3Δ200*	*URA3::yEGFP* on XIL	*sas2::kanMX*
hERM212	*MAT**a**, lys2Δ202, leu2Δ1, ura3Δ851, his3Δ200*	*URA3::yEGFP* on IIIR	*sas2::kanMX*
hERM230	*MAT**a**, lys2Δ202, leu2Δ1, ura3Δ851, his3Δ200*	*URA3::yEGFP* on XIL	*bfd1::kanMX*
hERM231	*MAT**a**, lys2Δ202, leu2Δ1, ura3Δ851, his3Δ200*	*URA3::yEGFP* on IIIR	*bdf1::kanMX*
hERM214	*MAT**a**, lys2Δ202, leu2Δ1, ura3Δ851, his3Δ200*	*URA3::yEGFP* on XIL	*set1::kanMX*
hERM215	*MAT**a**, lys2Δ202, leu2Δ1, ura3Δ851, his3Δ200*	*URA3::yEGFP* on IIIR	*set1::kanMX*
hERM208	*MAT**a**, lys2Δ202, leu2Δ1, ura3Δ851, his3Δ200*	*URA3::yEGFP* on XIL	*dot1::kanMX*
hERM209	*MAT**a**, lys2Δ202, leu2Δ1, ura3Δ851, his3Δ200*	*URA3::yEGFP* on IIIR	*dot1::kanMX*
hERM227	*MAT**a**, lys2Δ202, leu2Δ1, ura3Δ851, his3Δ200*	*URA3::yEGFP* on XIL	*bre1::kanMX*
hERM228	*MAT**a**, lys2Δ202, leu2Δ1, ura3Δ851, his3Δ200*	*URA3::yEGFP* on IIIR	*bre1::kanMX*

[a] All strains were constructed during the course of this study

4.2 Results and Discussion

4.2.1 TPE defects of *sir* mutants

The effect of the four *SIR* genes on silencing at native ends was measured in isogenic strains containing the *URA3-yEGFP* marker adjacent to core X at the repressive XIL or the non-repressive IIIR telomere (Table 4.1). The *sir* deletion mutants were created by transformation of the wild-type strains with *kanMX4* deletion-disruption constructs as described in Chapter 2.

Deletion of *SIR2*, *SIR3* or *SIR4* abrogated silencing at XIL within the limits of this assay (Table 4.2). The strains with *SIR2*, *SIR3* or *SIR4* disrupted were able to express *URA3* due to the loss of TPE, resulting in the lack of growth on FOA media (Fig. 4.1). The *sir4*Δ mutant had only one colony grow on FOA over three independent assays and is therefore considered fully derepressed within the limits of the assay. These results are in agreement with previous studies on the effect of Sirs on TPE at native repressive ends (Pryde and Louis, 1999; Vega-Palas *et al.*, 1998). A slight (~2-fold) decrease in silencing at XIL in *sir1*Δ mutants was observed in previous studies (Pryde and Louis, 1999). However, no reproducible reduction in silencing was observed in the *sir1*Δ mutant in this study (Table 4.2). Although the level of repression at XIL in the *sir1*Δ mutant appears lower than the wild-type repression level (Table 4.2), it was equivalent to the wild-type measurement obtained from the full plate assay used to assess repression in the *sir1*Δ mutant (see Chapter 2). The discrepancy between the study by Pryde *et al.* (1999) and this study on the effect of *sir1*Δ may be a result of the different markers used. In the original study, XIL was marked with *URA3* while this study uses the larger *URA3-yEGFP* marker that moves the *URA3* promoter further from the core X element. The inclusion of the *yEGFP* marker resulted in a moderate reduction in the wild-type level of repression (see Section 3.3.1). The higher levels of repression in the original study likely allowed the small *sir1*Δ effect to be detected.

Since the effect the Sirs on silencing at native non-repressive telomeres has not been previously examined, silencing at IIIR in the *sir* mutants was analyzed. Deletion of *SIR2*, *SIR3* or *SIR4* decreased even the minimal silencing of the wild-type strain at IIIR (Table 4.2), similar to their effect at XIL. The *sir4*Δ mutant was the only one to show any growth on FOA (Fig. 4.1), but it was still reduced compared to wild type. Therefore, although repression at IIIR in wild-type strains is very low, it can still

Table 4.2. Frequency of FOA resistance in *sir* mutants for the *URA3-yEGFP* marker inserted at XIL or IIIR.

Strain	Mutation	Chromosome	%FOA^R	
FEP318-19		XIL	10 – 42	(25)
hERL5	*sir1*Δ	XIL	7 – 12	(10)
hERL7	*sir2*Δ	XIL	0	(0)
hERL9	*sir3*Δ	XIL	0	(0)
hERL11	*sir4*Δ	XIL	0 – 0.027	(0)
FEP318-23		IIIR	0.002 – 1.6	(0.02)
hERL6	*sir1*Δ	IIIR	0.02 – 0.07	(0.05)
hERL8	*sir2*Δ	IIIR	0	(0)
hERL10	*sir3*Δ	IIIR	0	(0)
hERL12	*sir4*Δ	IIIR	0 – 0.004	(0.001)

The range of FOA resistance values from a minimum of three independent measurements is shown with the average value given in parenthesis. The values for the wild-type strains are also shown for comparison. FOA resistance was analyzed as described in Chapter 2.

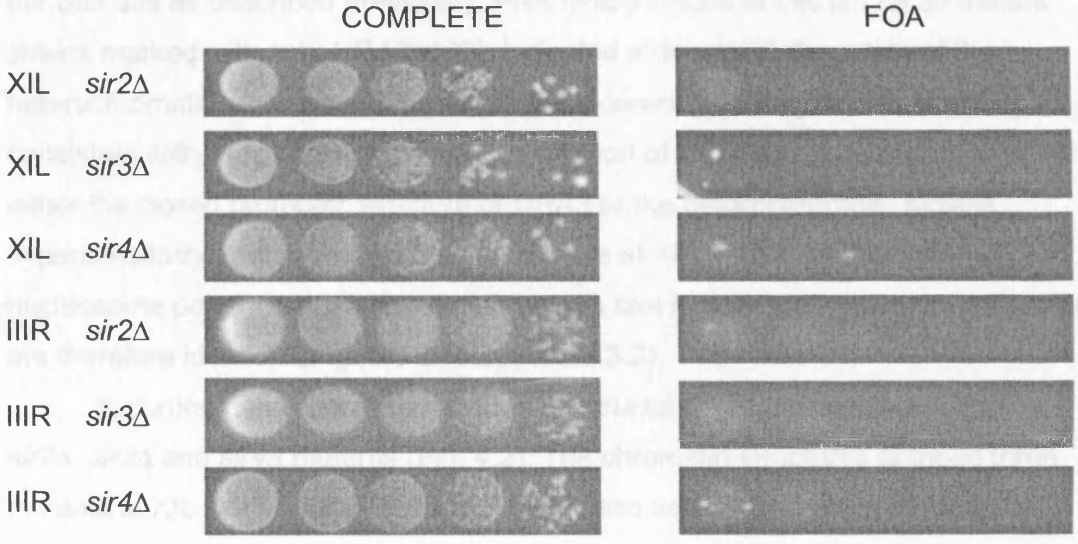

Figure 4.1. Examples of *URA3* repression assays for *sir* deletion mutants. Strains are marked with *URA3-yEGFP* at XIL (hERL7, 9 and 11) and IIIR (hERL8, 10 and 12) are indicated in addition to the relevant gene deletion. Ten-fold serial dilutions of single colonies were plated on complete synthetic media or media containing FOA and grown for three days at 30°C as described in Chapter 2.

be further reduced by deletion of *SIR* genes. Repression at IIIR was unaffected in the *sir1*Δ mutant (Table 4.2).

4.2.2 Deletion of *SIR2*, *SIR3* or *SIR4* disrupts repressive chromatin

The chromatin structure over the *URA3* promoter and native subtelomeric region of XIL was analyzed in the *sir* mutants by MNase and indirect end labeling at the *Stu*I site as described previously. Preliminary results in this lab for *sir* mutant strains marked with only *URA3* at XIL indicated a degree of disruption of the heterochromatic structure (P. Inglis, personal communication). In this study, consistent with its lack of effect on TPE, deletion of *SIR1* had no observable effect on either the closed promoter structure of *URA3* or the heterochromatic MNase hypersensitivity pattern toward the centromere at XIL (Fig. 4.2). The inferred nucleosome positions based on the chromatin blot in both wild-type and *sir1*Δ strains are therefore identical (Fig. 4.3 and Section 3.3.2).

In contrast, the repressive chromatin structure was dramatically altered in *sir2*Δ, *sir3*Δ and *sir4*Δ mutants (Fig. 4.2). The chromatin structures of these three mutants at XIL were nearly identical. The MNase sensitivity pattern of the three promoter-associated bands (black arrows, Fig. 4.2) was very similar to the open promoter structure observed at IIIR (Section 3.3.2). Both the upper and lower bands had increased hypersensitivity in the *sir* mutants compared to the XIL wild-type pattern and the central band was protected in the mutants (Fig. 4.2). This indicates that deletion of *SIR2*, *SIR3* or *SIR4* results in an open *URA3* promoter structure and movement of the nucleosome that protects the TATA box region in the native XIL structure ('b', Fig. 4.3). This correlates with the increased expression of the marker in *sir* mutants.

In addition to the altered promoter structure, the phased pattern of evenly spaced hypersensitive sites in the subtelomeric region of XIL was almost completely disrupted in the three *sir* mutants (grey arrows, Fig. 4.2). A few of the wild-type bands appeared to be faintly present in the mutants but there were variations in the spacing in addition to the dramatically reduced band intensity (Fig. 4.2C). This implies the three phased nucleosomes present in this region of the wild-type strain are either removed or unphased in the *sir* mutants (Fig. 4.3). Similar effects for *sir3*Δ mutants on repressive chromatin structure have been previously observed within the Ty5-1 element at the native IIIR telomere (Vega-Palas *et al.*, 1998), within the promoter of a subtelomeric marker gene (de Bruin *et al.*, 2000) and at the *HM* loci (Ravindra *et al.*,

1999; Weiss and Simpson, 1998). The disruption of heterochromatic structure in the *sir2*Δ, *sir3*Δ and *sir4*Δ mutants observed in this study is consistent with current models in which Sir2p, Sir3p and Sir4p associate in a complex that spreads to adjacent nucleosomes to establish and maintain a phased, repressive structure (reviewed in Rusche, 2002).

Interestingly, further toward the centromere the pattern of MNase digestion in the *sir2*Δ, *sir3*Δ and *sir4*Δ mutants became indistinguishable from that of the wild-type (top two grey arrows, Fig. 4.2). This supports the interpretation that the top two hypersensitive sites indicated by grey arrows do not flank a phased nucleosome and are unrelated to silencing (see Section 3.3.2). The effect of the *sir* mutants on chromatin structure therefore appears to be limited to heterochromatic features.

Figure 4.2. Comparison of chromatin structures toward the centromere at XIL in *sir* mutants. The subtelomeric chromatin structures of the *URA3-yEGFP* marked XIL telomere in the wild-type FEP318-19 (XIL) and *sir* mutants was analyzed by MNase digestion and indirect end labeling at the *Stu*I site as described previously. Black arrows indicate the promoter-associated bands and grey arrows highlight prominent wild-type subtelomeric bands as in Fig. 3.4. Markers (M) are positioned to indicate the *URA3* TATA box and a 100bp ladder (L) is shown as an indication of the distances between hypersensitive sites. A) The chromatin structures toward the XIL centromere in *sir1*Δ and *sir2*Δ mutants. B) The chromatin structures toward the XIL centromere in *sir3*Δ and *sir4*Δ mutants C) Chromatin band intensity profiles of XIL (top), *sir1*Δ (centre) and *sir2*Δ (bottom) were generated using Kodak 1D scan. The black and grey arrows indicate the peaks corresponding to the bands marked by the arrows in (A).

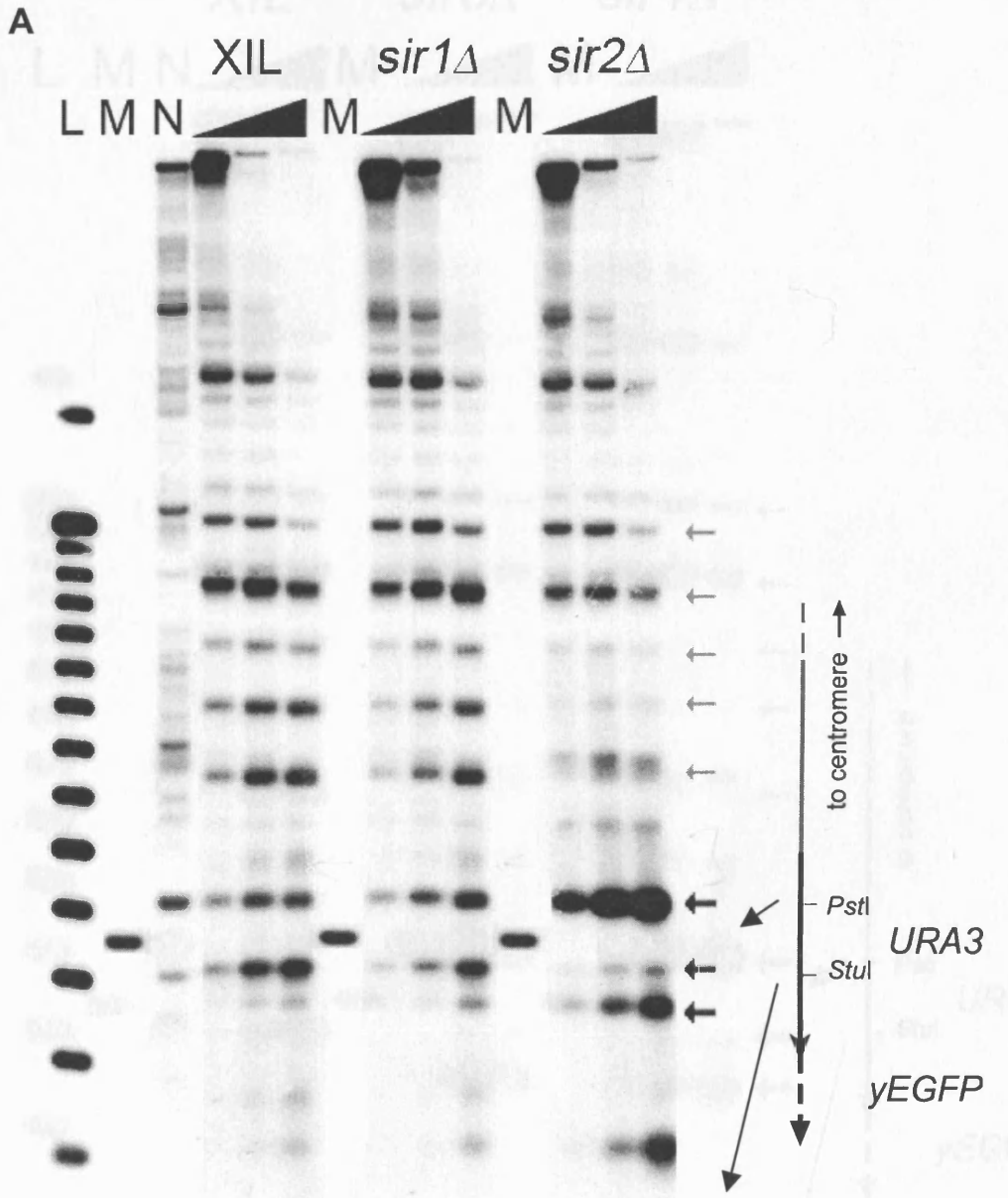

Figure 4.2. Comparison of chromatin structures toward the centromere at XIL in *sir* mutants.

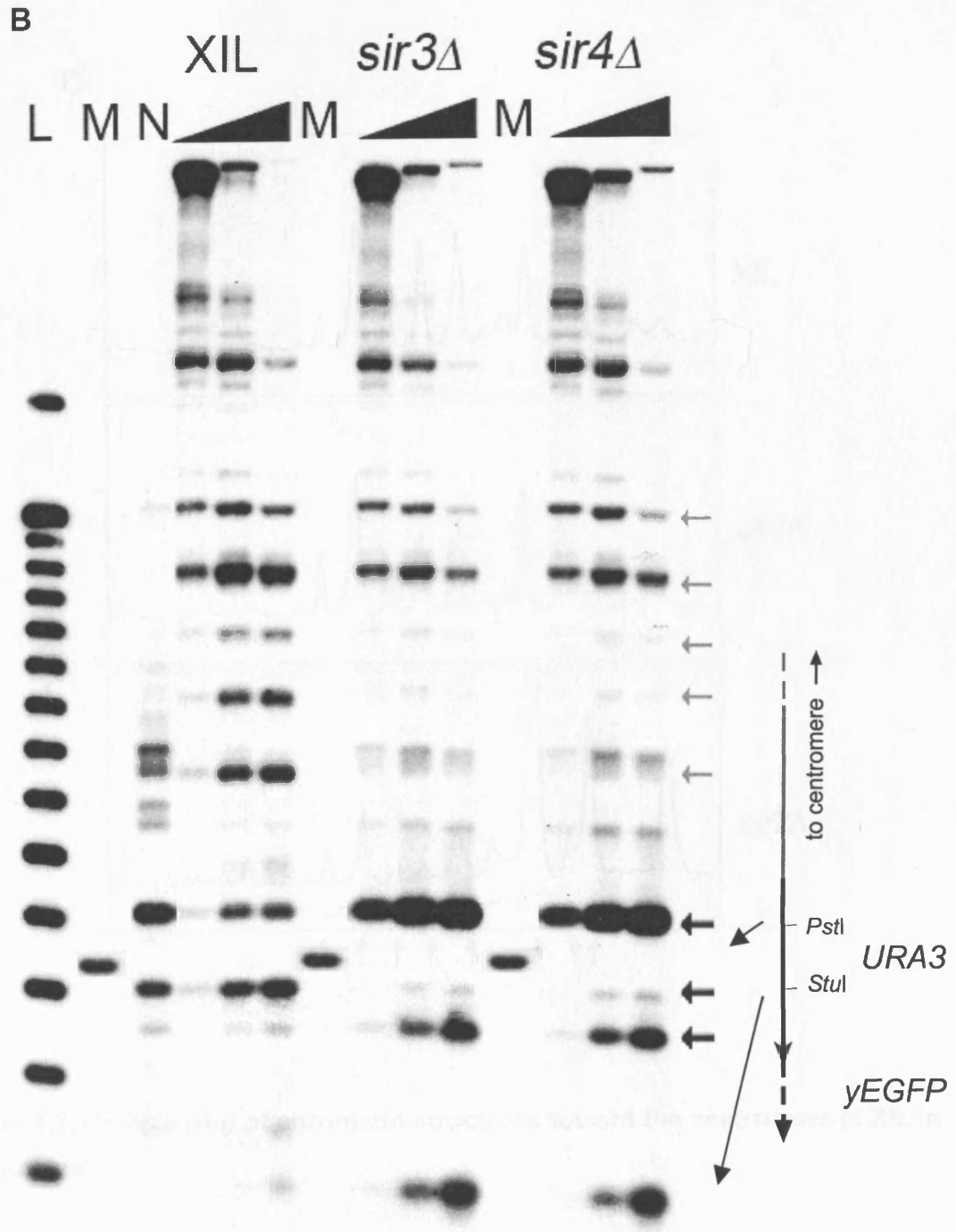

Figure 4.2. Comparison of chromatin structures toward the centromere at XIL in *sir* mutants.

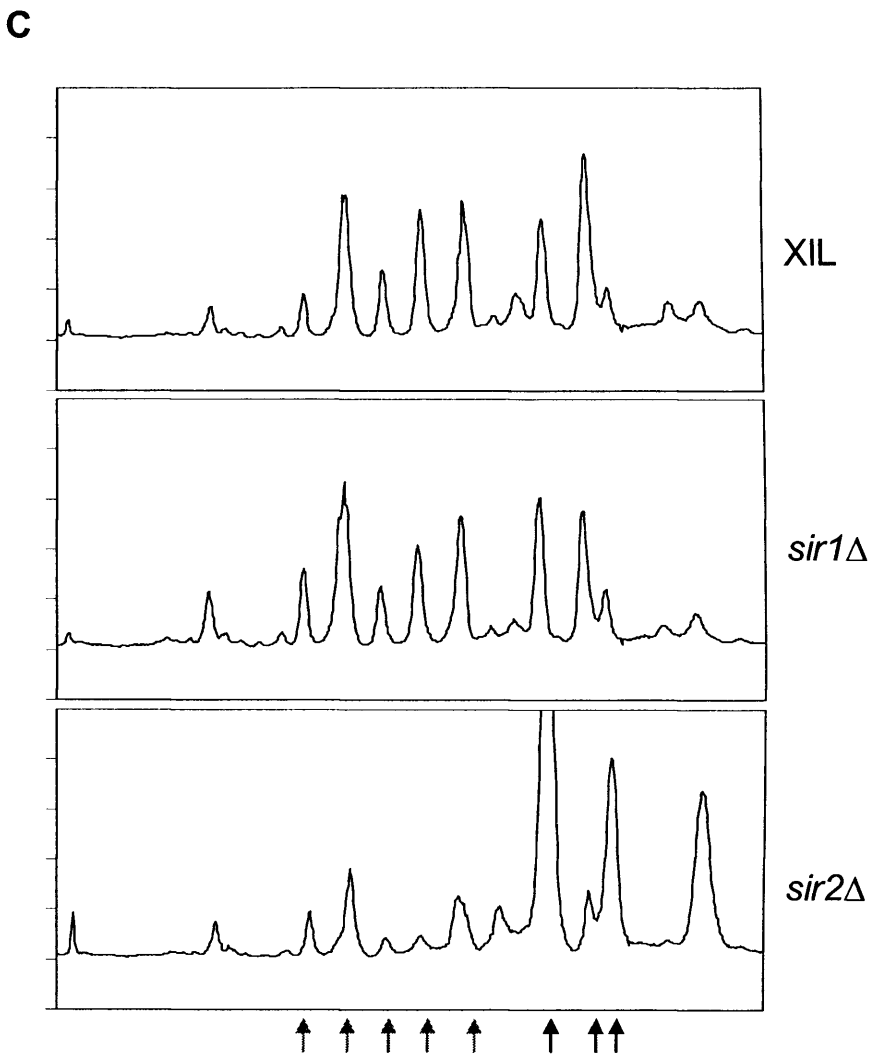

Figure 4.2. Comparison of chromatin structures toward the centromere at XIL in *sir* mutants.

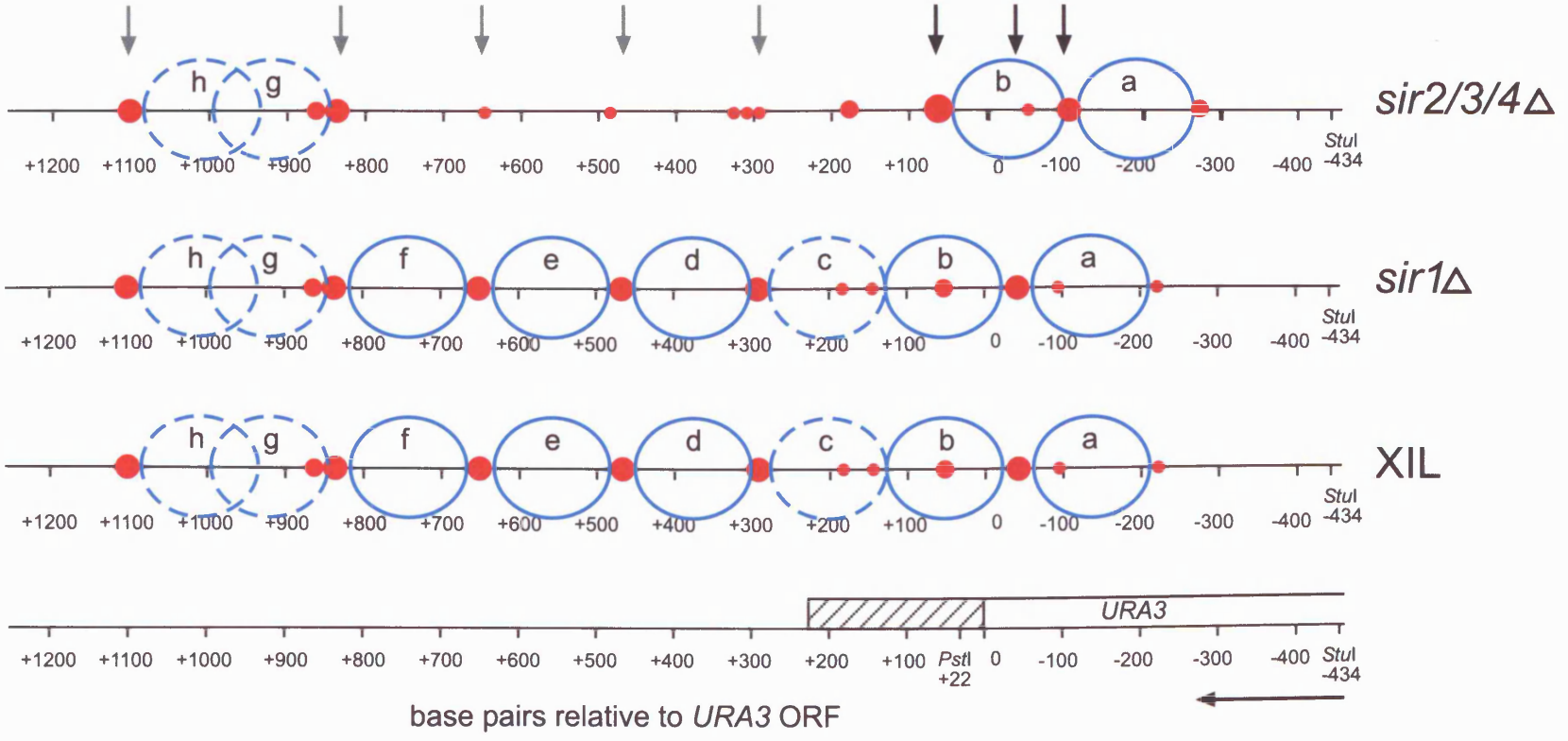

Figure 4.3. Inferred nucleosome positions in *sir* mutants toward the centromere from the XIL telomere. The position of the *URA3* ORF (open rectangle) and *URA3* promoter (diagonal lines) is indicated in the bottom diagram. The *Stu*I and *Pst*I sites are marked and the $URA3_{cen}$ probe is indicated by the black arrow. Sites of MNase digestion within the XIL sequence are indicated by red circles and inferred nucleosome positions are shown by blue circles as in Figure 3.5. Black and grey arrows correspond to those used to highlight MNase hypersensitive sites in Fig. 4.2.The wild-type (XIL) and *sir1*Δ chromatin structures are shown separately while one structure is given for *sir2*Δ, *sir3*Δ and *sir4*Δ mutants as they are indistinguishable.

4.2.3 Euchromatic chromatin is unaffected by *sir* mutations

Consistent with the theory that the Sir proteins only affect heterochromatic structures, MNase analysis toward the centromere of the *URA3-yEGFP* marked IIIR telomere in all four *sir* deletion mutants yielded patterns indistinguishable from wild-type (Fig. 4.4). Deletion of *SIR2*, *SIR3* or *SIR4* did diminish the silencing at IIIR. However, given the low level of silencing and the euchromatic chromatin structure observed in the wild-type strain, no observable chromatin changes were predicted for the *sir* mutants. In all four mutants (*sir1-sir4*Δ), the promoter region of *URA3* was still clearly in the wild-type open structure, with the upper and lower promoter-associated bands exhibiting MNase hypersensitivity (black arrows, Fig. 4.4). The centromere-proximal subtelomeric domain was euchromatic in all *sir* mutants and retained the same features and inferred structure previously described for the wild-type IIIR telomere (see Fig. 3.5). The inability of the Sir proteins to affect chromatin structure at IIIR or establish a repressive domain is in agreement with previous observations that the Sir proteins associate very little with the IIIR telomere in comparison to the XIL telomere (Lieb *et al.*, 2001). Lieb *et al.* reported a similar binding pattern for Rap1p. Rap1p and the Sir complex also exhibited strong associations with other native repressive telomeres and weak associations with non-repressive telomeres. However, there is still no known reason why these proteins associate more strongly with certain telomeres than with others.

Figure 4.4. Comparison of chromatin structures toward the centromere at IIIR in *sir* mutants. The subtelomeric chromatin structure of the *URA3-yEGFP* marked IIIR telomere in wild-type, FEP318-23 (IIIR), and *sir* mutants was analyzed by MNase digestion and indirect end labeling at the *Stu*I site as described previously. Black arrows indicate the promoter-associated bands and grey arrows highlight prominent wild-type subtelomeric bands as in previous figures. Markers (M) are positioned to indicate the *URA3* TATA box and a 100bp ladder (L) is shown as an indication of the distances between hypersensitive sites. A) The chromatin structures toward the IIIR centromere in *sir1*Δ and *sir2*Δ mutants. B) The chromatin structures toward the IIIR centromere in *sir3*Δ and *sir4*Δ mutants. C) Chromatin band intensity profiles of IIIR (top), *sir1*Δ (centre) and *sir2*Δ (bottom) were generated using Kodak 1D scan. The black and grey arrows indicate the peaks corresponding to the bands marked by the arrows in (A).

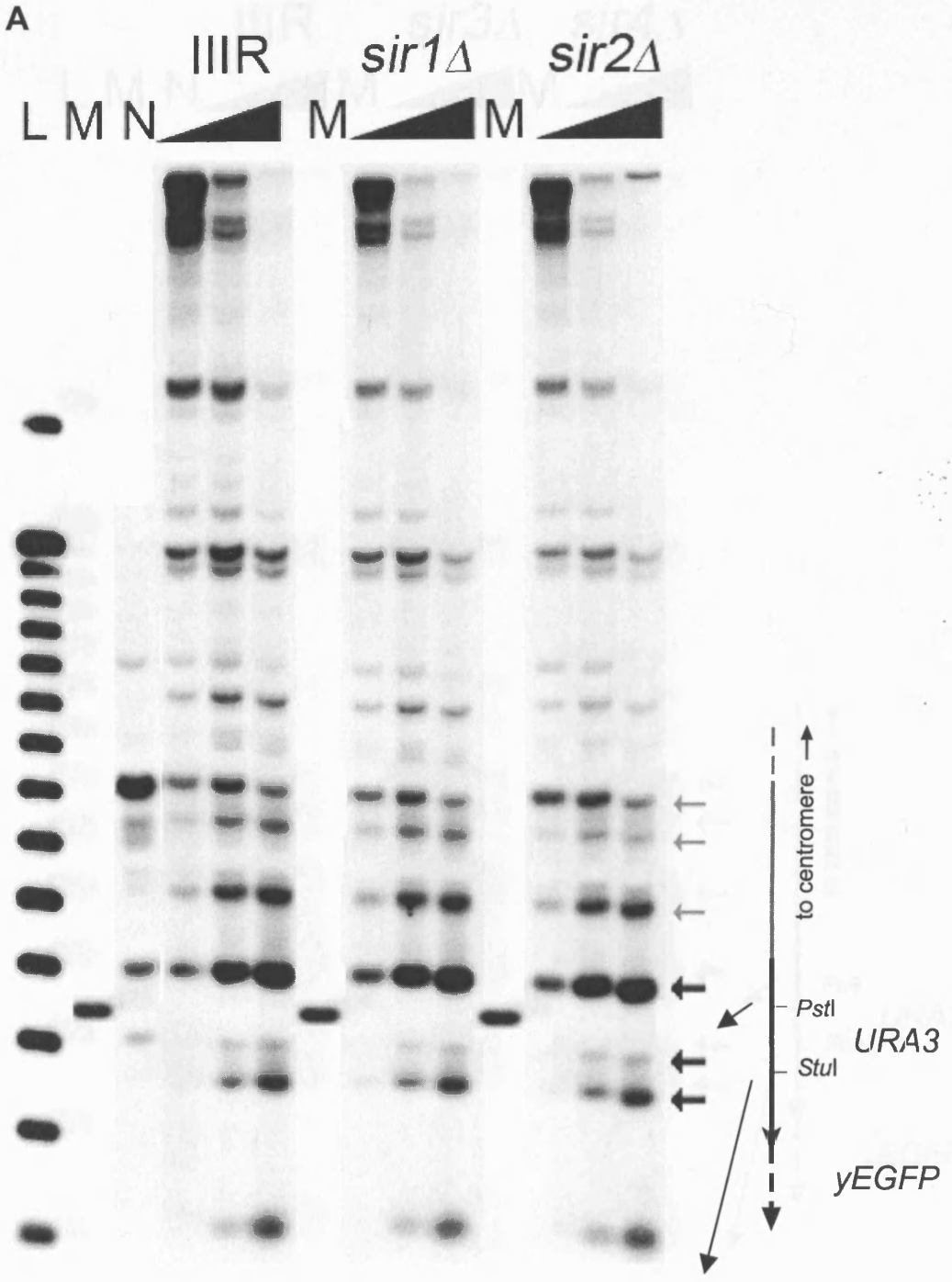

Figure 4.4. Comparison of chromatin structures toward the centromere at IIIR in *sir* mutants.

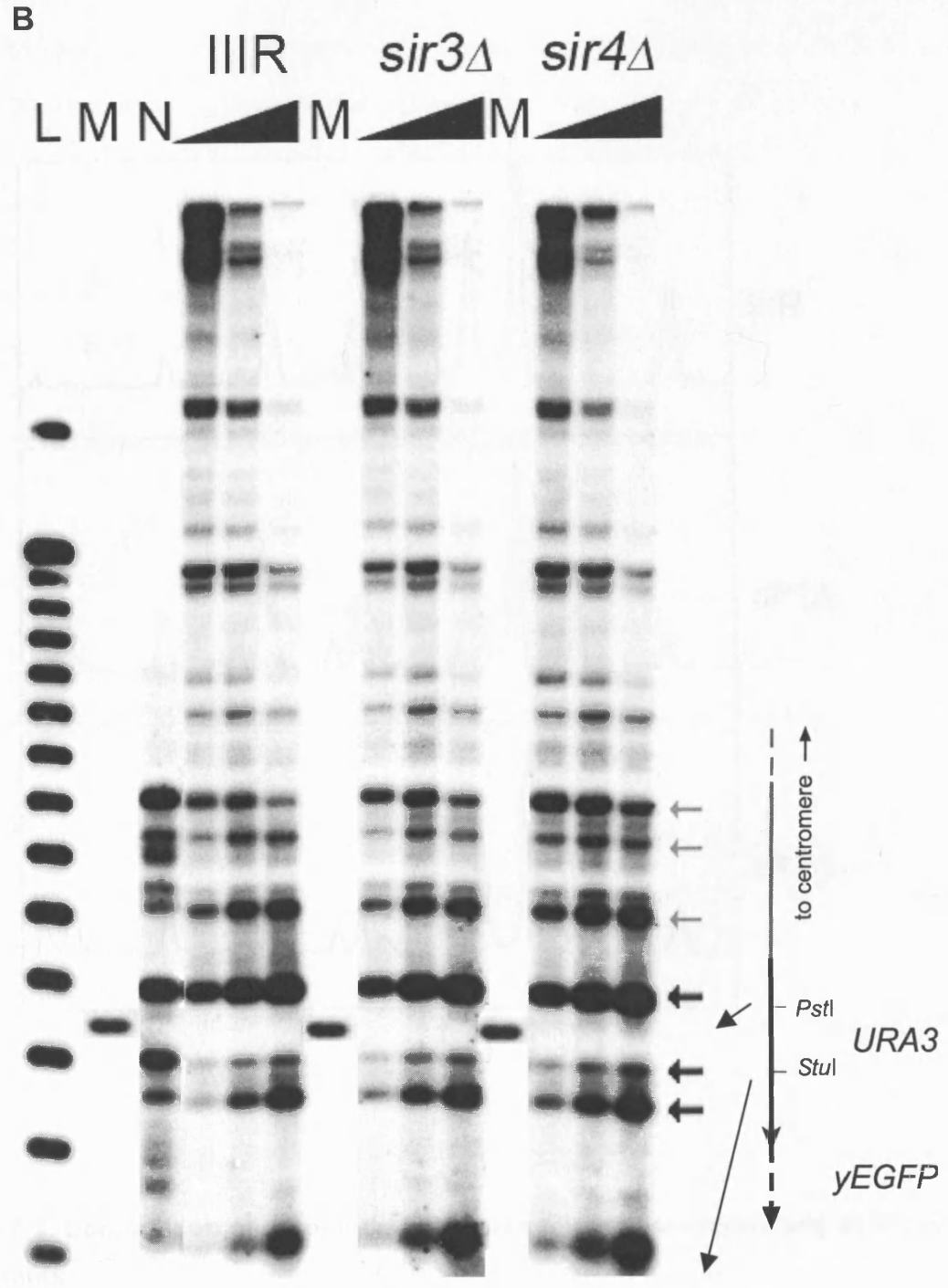

Figure 4.4. Comparison of chromatin structures toward the centromere at IIIR in *sir* mutants.

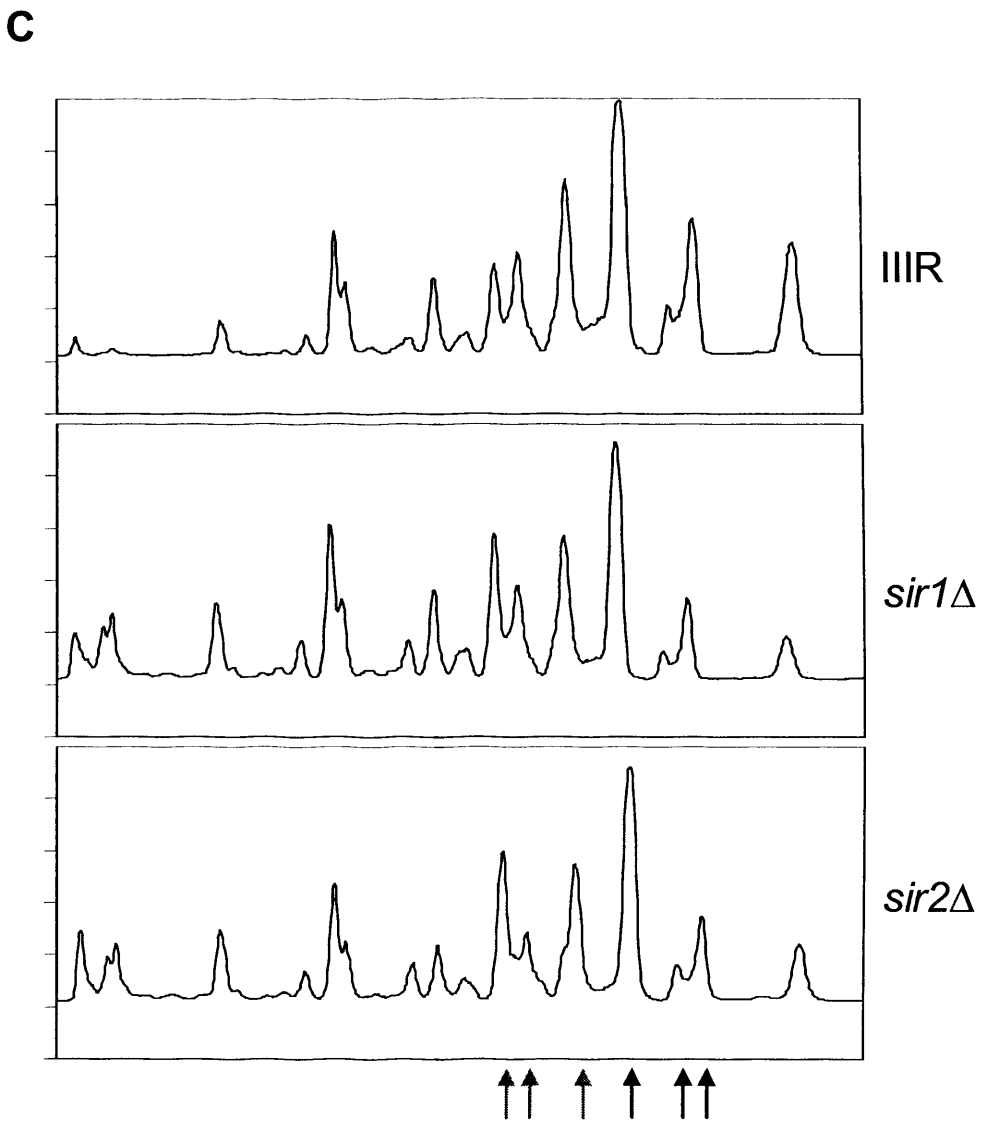

Figure 4.4. Comparison of chromatin structures toward the centromere at IIIR in *sir* mutants.

4.2.4 Sir proteins are not involved in the chromatin structure at core X

The role of the Sir proteins in the specialized chromatin structure observed toward the telomeres of native ends was examined by probing toward the telomere following MNase treatment as previously described. The chromatin structure of core X is believed to arise from the binding of ORC and Abf1p and to be unrelated to the degree of repression (see Section 3.3.3). Therefore, it is not surprising that this structure remained intact in all four *sir* mutants at both the IIIR and XIL telomeres (Fig. 4.5). The structure across the STR repeats in the *sir* mutants was also indistinguishable from the wild-type telomeres. This confirms preliminary results from *sir* deletion strains marked with *URA3* at XIL (P. Inglis, personal communication). Vega-Palas *et al.* (1998) also observed that deletion of *SIR3* did not alter the structure of core X at the native IIIL telomere.

However, in *sir2*Δ, *sir3*Δ and *sir4*Δ strains there was a moderate increase in hypersensitivity at the 3' end of the *URA3-yEGFP* construct within the *URA3* termination sequence (grey arrow, Fig. 4.5). The increased MNase hypersensitivity occurred at both the XIL and IIIR telomeres. A strong hypersensitive site was also observed in this region when the *URA3-yEGFP* construct was present at the native *URA3* locus, suggesting it may be related to the degree of expression of the marker (see Fig. 3.7). However, this region of strong hypersensitivity was not observed at the non-repressive IIIR. Consequently, the hypersensitivity in the *URA3* termination sequence appears to only be present when the *URA3-yEGFP* marker is fully expressed, a phenotype only observed in *sir2*Δ, *sir3*Δ and *sir4*Δ mutants and at the native *URA3* locus. In support of this idea, *sir1*Δ is the only *sir* mutant that neither affected TPE at native ends nor altered the chromatin structure of the *URA3* terminator (Fig. 4.5). Intriguingly, this increased hypersensitivity in the *URA3* terminator was the only observed chromatin alteration at IIIR in the *sir* mutants, toward either the centromere or telomere, despite their silencing defects. This also suggests that this small chromatin change is related to the small increase in expression at IIIR in the *sir* mutants.

Figure 4.5. Comparison of chromatin structures toward the XIL and IIIR telomeres in *sir* mutants. The subtelomeric chromatin structures of the *URA3-yEGFP* marked XIL and IIIR telomeres in the wild-type (XIL and IIIR respectively) and *sir* mutant strains were analyzed by MNase digestion and indirect end labeling at the *Stu*I site as described previously. Black arrows indicate sites of interest close to the ACS and Abf1p binding site in the core X elements and a hypersensitive site within the *URA3* termination sequence. A) The chromatin structures toward the XIL telomere in *sir1*Δ and *sir2*Δ mutants. B) The chromatin structures toward the XIL telomere in *sir3*Δ and *sir4*Δ mutants. C) The chromatin structures toward the IIIR telomere in *sir1*Δ and *sir2*Δ mutants. D) The chromatin structures toward the IIIR telomere in *sir3*Δ and *sir4*Δ mutants.

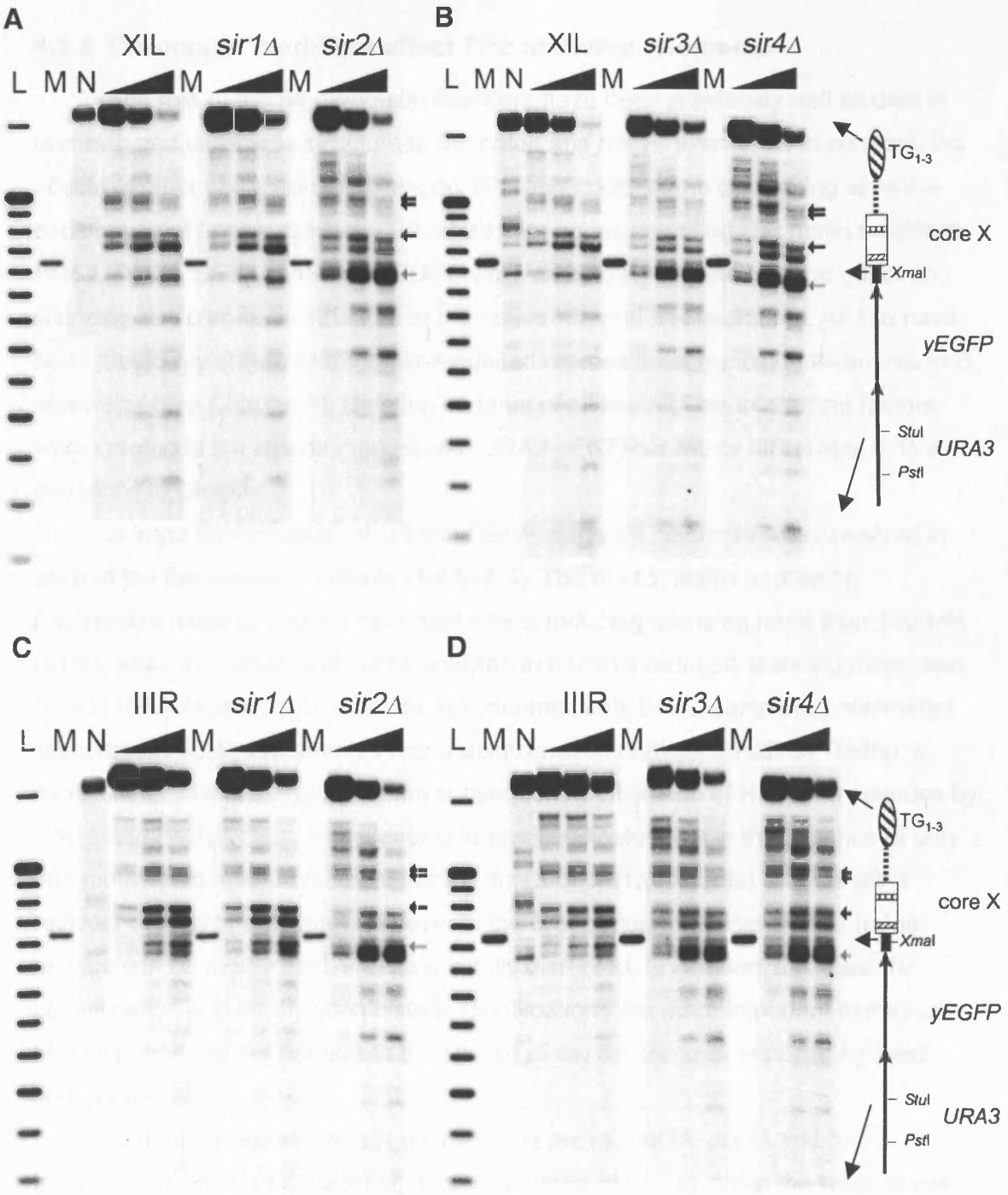

Figure 4.5. Comparison of chromatin structures toward the XIL and IIIR telomeres in *sir* mutants.

4.2.5 Chromatin modifiers affect TPE at native telomeres

The role of the Sir chromatin modifiers have been previously well studied in silencing and chromatin structure at truncated and native telomeres. In contrast, the effects of other chromatin modifiers on TPE and nucleosome positioning at native ends have not been examined. Therefore, five genes encoding chromatin modifiers, *BRE1, DOT1, SET1, SAS2* and *BDF1,* were chosen for analysis of their effect on silencing and chromatin structure at the native XIL and IIIR telomeres. All five have been previously shown to affect Sir-mediated repression at truncated telomeres in *S. cerevisiae* (see Chapter 1). Deletion mutants of all five histone interacting factors were created in the strains marked with *URA3-yEGFP* at XIL or IIIR (Table 4.1), as described in Chapter 2.

A large derepression of *URA3-yEGFP* at the XIL telomere was observed in each of the five deletion mutants (Table 4.3). The *bre1*Δ, *dot1*Δ and *set1*Δ methylation mutants had the strongest effect, reducing silencing more than 100-fold (<1%), while the *sas2*Δ and *bdf1*Δ acetylation mutants reduced silencing more than 5-fold (<5%). Interestingly, of these five mutants, only *bre1*Δ completely eliminated silencing at XIL. Bre1p enables mono-ubiquitination of histone H2B by Rad6p, a modification that is essential for the subsequent methylation of H3 lysine residues by Dot1p and Set1p. Thus, this silencing analysis indicates that in the absence of only one methylated residue (as in either the *dot1*Δ or *set1*Δ mutants) there is still a residual degree of silencing. However in the *bre1*Δ mutant, where neither lysine residue can be methylated, silencing is fully disrupted. In addition, it is clear the ubiquitination and methylation histone modifications are more important to maintain silencing than are the barriers to the spread of the Sir complex imposed by Sas2p and Bdf1p.

At the non-repressive IIIR telomere the *bre1*Δ, *set1*Δ, *dot1*Δ and *bdf1*Δ mutations all eliminated the small degree of native silencing within the limits of this assay (Table 4.3). A reduction in repression also occurred in the *sas2*Δ mutant (Table 4.3). This is similar to the effect of the *sir* mutants on repression at IIIR. The *sas2*Δ mutant also retained the highest degree of silencing of these five histone modifier mutants at XIL, indicating it is not as important for silencing as the other four factors. Representative examples of the FOA assays are shown in Fig. 4.6.

Table 4.3. Frequency of FOA resistance in chromatin modifier mutants for the *URA3-yEGFP* marker inserted at XIL or IIIR.

Strain	Mutation	Chromosome	%FOA^R	
FEP318-19		XIL	10 – 42	(25)
hERM211	*sas2*Δ	XIL	4.4 – 5.5	(4.9)
hERM230	*bdf1*Δ	XIL	1.9 – 6.6	(4.2)
hERM214	*set1*Δ	XIL	0.005 – 0.04	(0.024)
hERM208	*dot1*Δ	XIL	0.16 – 0.05	(0.33)
hERM227	*bre1*Δ	XIL	0	(0)
FEP318-23		IIIR	0.002 – 1.6	(0.02)
hERM212	*sas2*Δ	IIIR	0 – 0.004	(0.002)
hERM231	*bdf1*Δ	IIIR	0	(0)
hERM215	*set1*Δ	IIIR	0	(0)
hERM209	*dot1*Δ	IIIR	0	(0)
hERM228	*bre1*Δ	IIIR	0	(0)

The range of FOA resistance values from a minimum of three independent measurements is shown with the average value given in parenthesis. The values for the wild-type strains are also shown for comparison. FOA resistance was analyzed as described in Chapter 2.

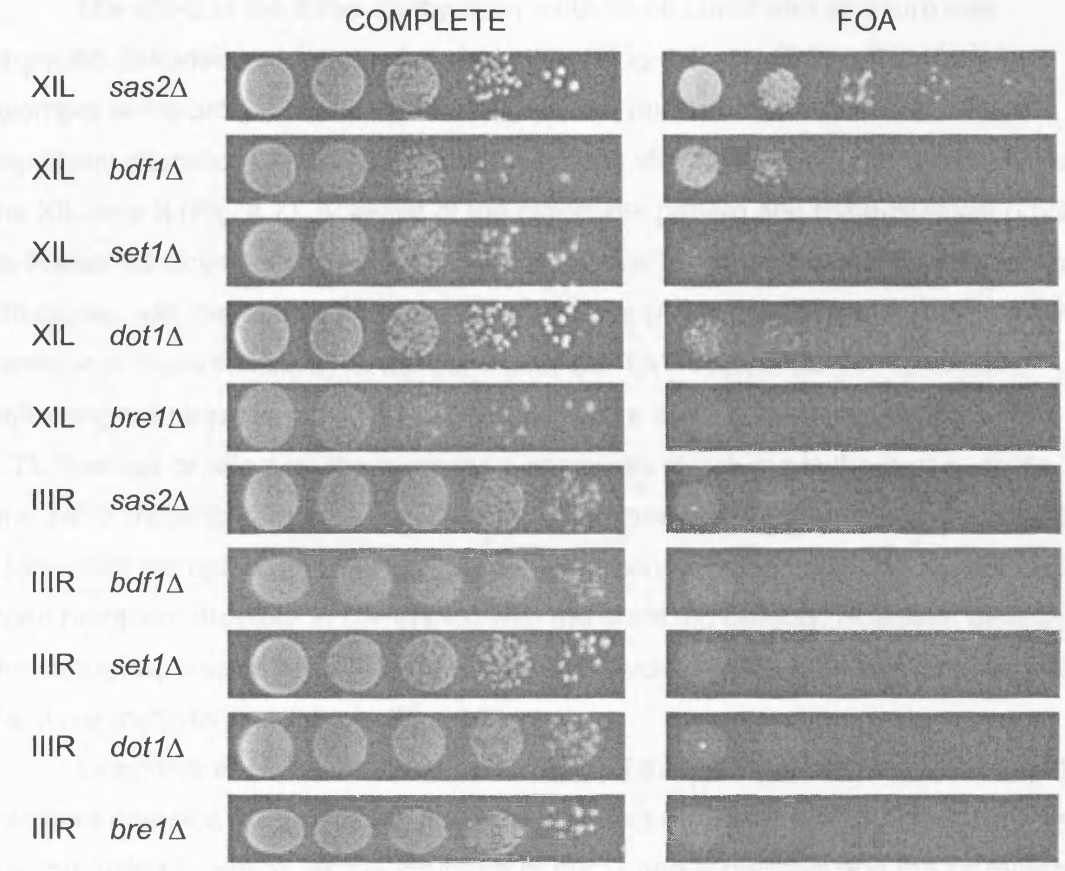

Figure 4.6. Examples of *URA3* repression assays in *sas2*, *bdf1*, *set1*, *dot1* and *bre1* deletion mutants in strains marked at either XIL or IIIR. The marked telomere and mutation in each strain is indicated. Ten-fold serial dilutions of single colonies were plated on complete synthetic media or media containing FOA and grown for three days at 30°C as described in Chapter 2.

4.2.6 Components of the chromatin methylation pathway do not alter nucleosome positioning

The effect of the three methylation mutants on chromatin structure was analyzed. Surprisingly, despite the strong silencing defects observed at the XIL telomere in the *bre1*Δ, *dot1*Δ and *set1*Δ mutants, none of these strains exhibited significant alterations in the repressive chromatin structures centromere-proximal to the XIL core X (Fig. 4.7). Analysis of the chromatin pattern and band intensity profiles by Kodak 1D Scan confirmed the lack of difference between the wild-type and mutant structures, with the exception of the *bre1*Δ mutant (Appendix 2). There was a slight increase in hypersensitivity of the band over the TATA box in the *bre1*Δ mutant, indicating the promoter of *URA3* was slightly more open than in the wild type (Fig. 4.7). The lack of effect on the repressive chromatin structures in the *bre1*Δ, *dot1*Δ and *set1*Δ mutants contrasts with the chromatin analysis of the *sir* mutants. Deletion of the *SIRs* disrupted the heterochromatic nucleosome positioning and resulted in an open promoter structure in correlation with the silencing defects. However, despite the strong expression of *URA3*, the repressive chromatin features were unaffected in the three methylation mutants (Fig. 4.7).

Examination of the chromatin structures of the methylation mutants at the IIIR telomere revealed the mutations also had no effect on this structure (Fig. 4.8). This was predicted however, as the structure of IIIR is non-repressive and the *sir* mutants also did not affect the structure. In addition, none of the methylation mutants altered the chromatin structure of core X or the STRs at either XIL or IIIR (Fig. 4.9). The *sir* and methylation mutants have nearly equivalent silencing defects at both telomeres. Therefore, the increase in hypersensitivity around the marker band in the *URA3* termination sequence that was observed in the *sir* mutants (Fig. 4.5) may also have been predicted to occur in the methylation mutants. However, this hypersensitivity was not observed in the *bre1*Δ, *set1*Δ or *dot1*Δ mutants (Fig. 4.9). It is therefore clear that the histone modifications for which Bre1p, Dot1p and Set1p are responsible are not required for formation of the repressive chromatin structures although they are, intriguingly, still required for the silencing of *URA3*. This implies that the phased nucleosome structure of the native XIL telomere is not sufficient for silencing as discussed more thoroughly in Chapter 7.

Figure 4.7. Analysis of chromatin structure toward the centromere at XIL in methylation mutants. The subtelomeric chromatin structures of the *URA3-yEGFP* marked XIL telomere in *bre1*Δ, *dot1*Δ and *set1*Δ mutants compared to the wild-type FEP318-19 strain (XIL) were analyzed by MNase digestion and indirect end labeling at the *Stu*I site as described previously. Black and grey arrows are as in previous figures. A) The subtelomeric chromatin structures of the XIL telomere in *bre1*Δ and wild-type strains. B) The subtelomeric chromatin structures toward the centromere at XIL in *dot1*Δ and wild-type strains. C) The subtelomeric chromatin structures toward the centromere at XIL in *set1*Δ and wild-type strains.

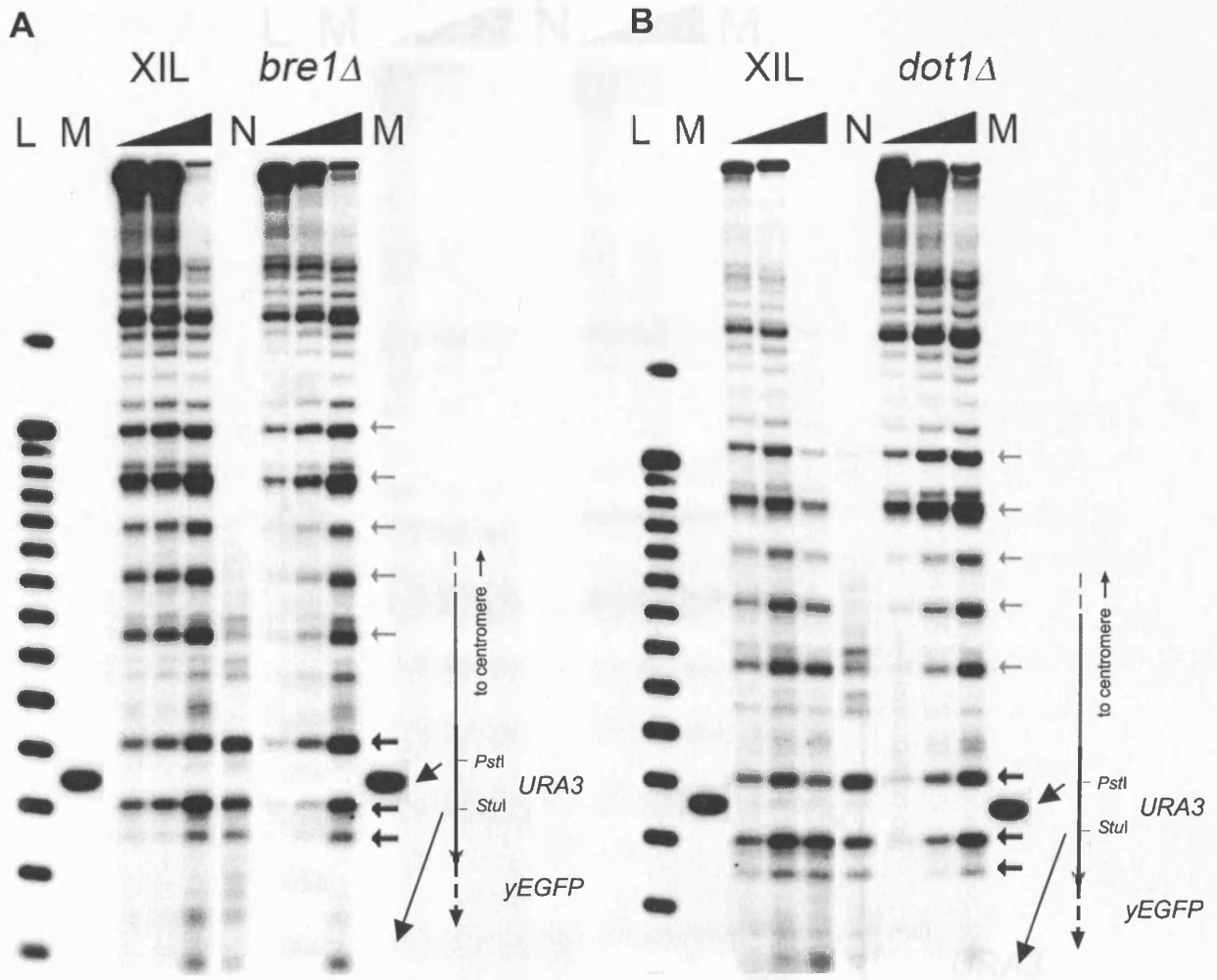

Figure 4.7. Analysis of chromatin structure toward the centromere at XIL in methylation mutants.

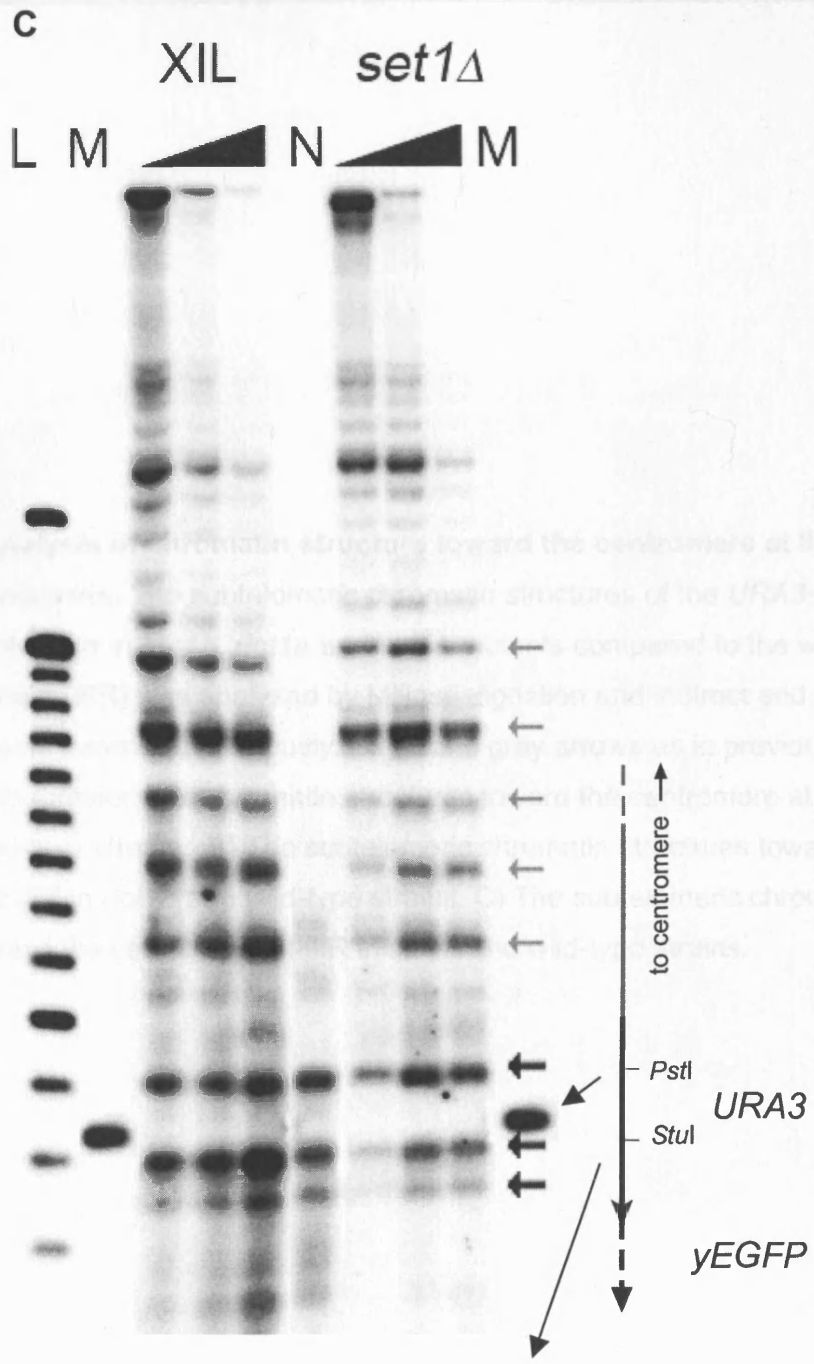

Figure 4.7. Analysis of chromatin structure toward the centromere at XIL in methylation mutants.

Figure 4.8. Analysis of chromatin structure toward the centromere at IIIR in methylation mutants. The subtelomeric chromatin structures of the *URA3-yEGFP* marked IIIR telomere in *bre1Δ, dot1Δ* and *set1Δ* mutants compared to the wild-type FEP318-23 strain (IIIR) was analyzed by MNase digestion and indirect end labeling at the *StuI* site as described previously. Black and grey arrows as in previous figures. A) The subtelomeric chromatin structures toward the centromere at IIIR in *bre1Δ* and wild-type strains. B) The subtelomeric chromatin structures toward the centromere at IIIR in *dot1Δ* and wild-type strains. C) The subtelomeric chromatin structures toward the centromere at IIIR in *set1Δ* and wild-type strains.

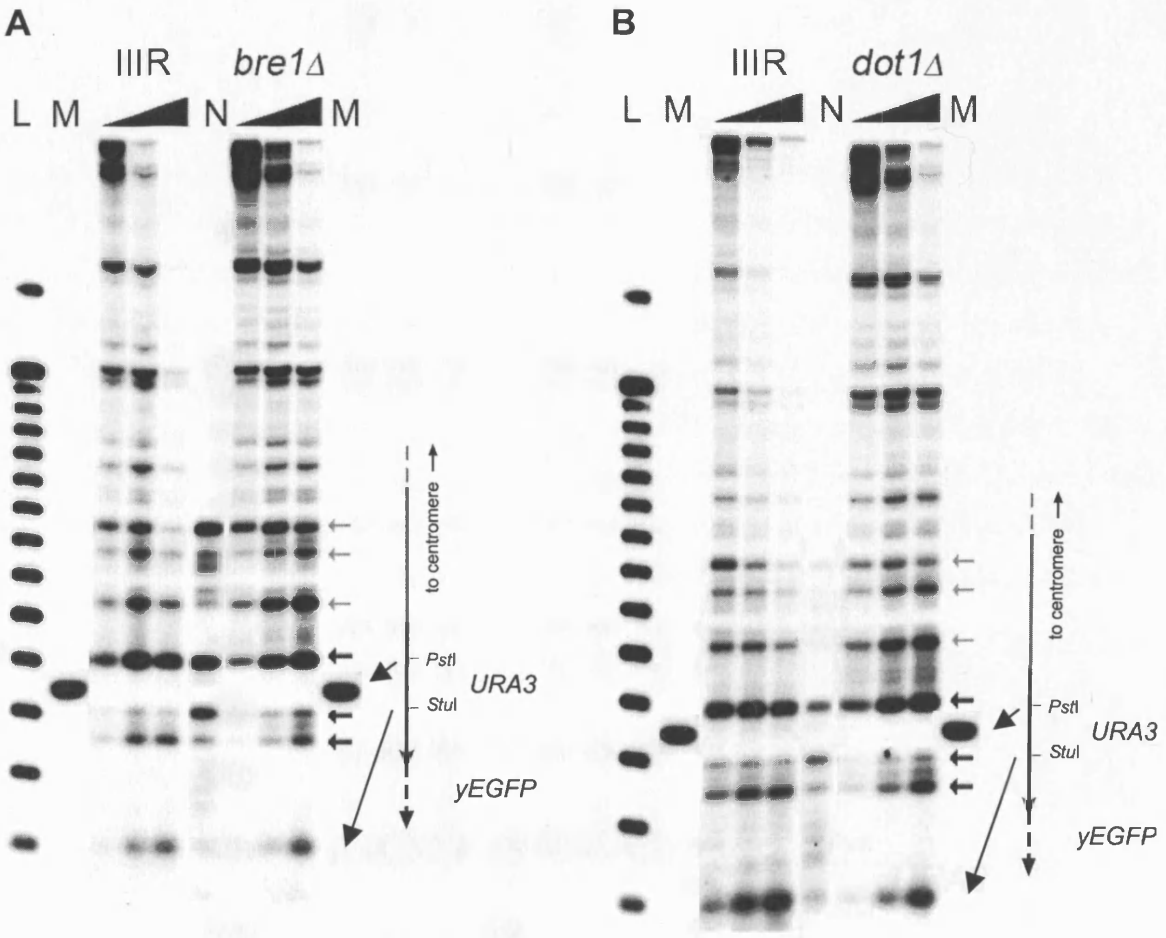

Figure 4.8. Analysis of chromatin structure toward the centromere at IIIR in methylation mutants.

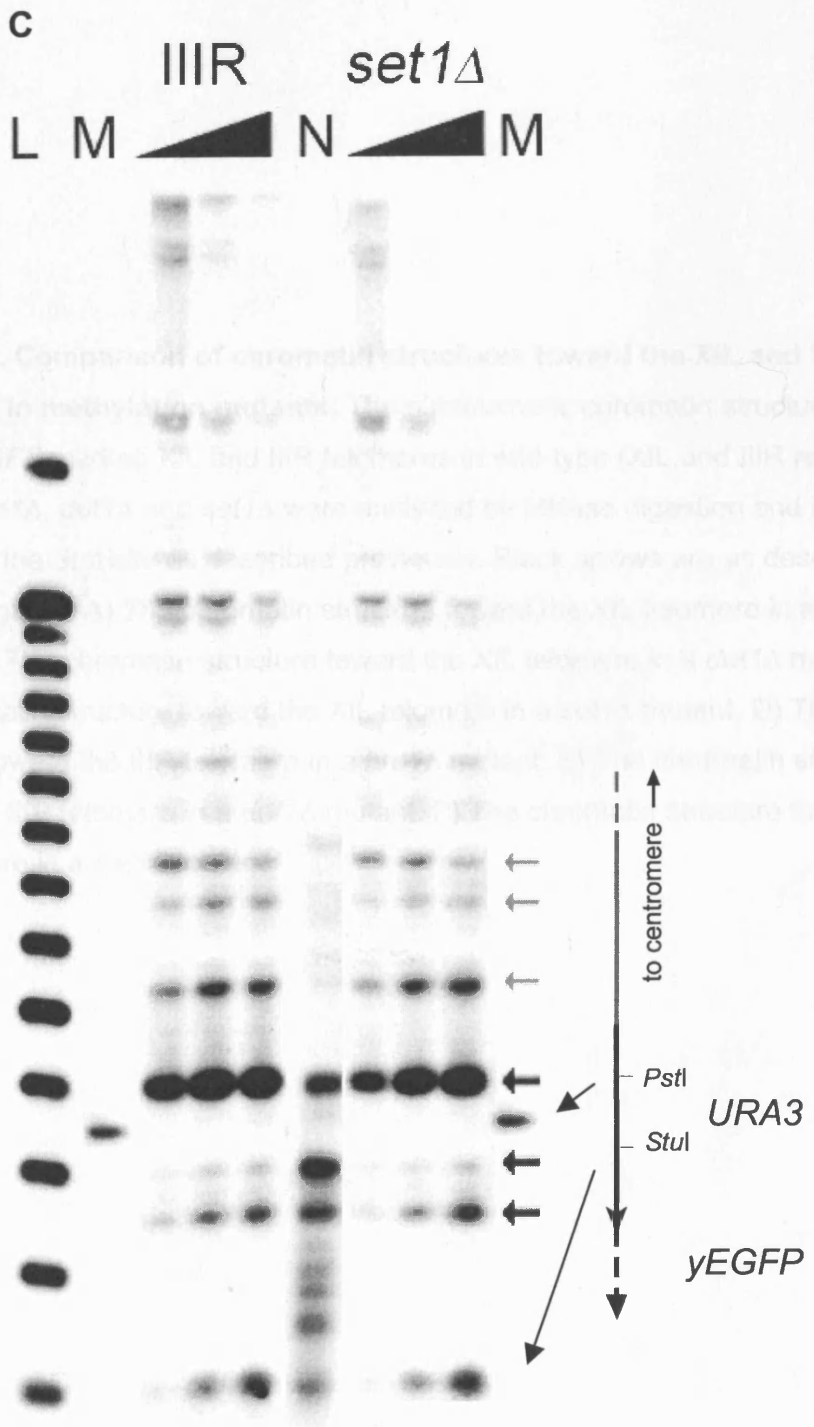

Figure 4.8. Analysis of chromatin structure toward the centromere at IIIR in methylation mutants.

Figure 4.9. Comparison of chromatin structures toward the XIL and IIIR telomeres in methylation mutants. The subtelomeric chromatin structures of the *URA3-yEGFP* marked XIL and IIIR telomeres in wild-type (XIL and IIIR respectively) and the *bre1*Δ, *dot1*Δ and *set1*Δ were analyzed by MNase digestion and indirect end labeling at the *Stu*I site as described previously. Black arrows are as described in previous figures. A) The chromatin structure toward the XIL telomere in a *bre1*Δ mutant. B) The chromatin structure toward the XIL telomere in a *dot1*Δ mutant. C) The chromatin structure toward the XIL telomere in a *set1*Δ mutant. D) The chromatin structure toward the IIIR telomere in a *bre1*Δ mutant. E) The chromatin structure toward the IIIR telomere in a *dot1*Δ mutant. F) The chromatin structure toward the IIIR telomere in a *set1*Δ mutant.

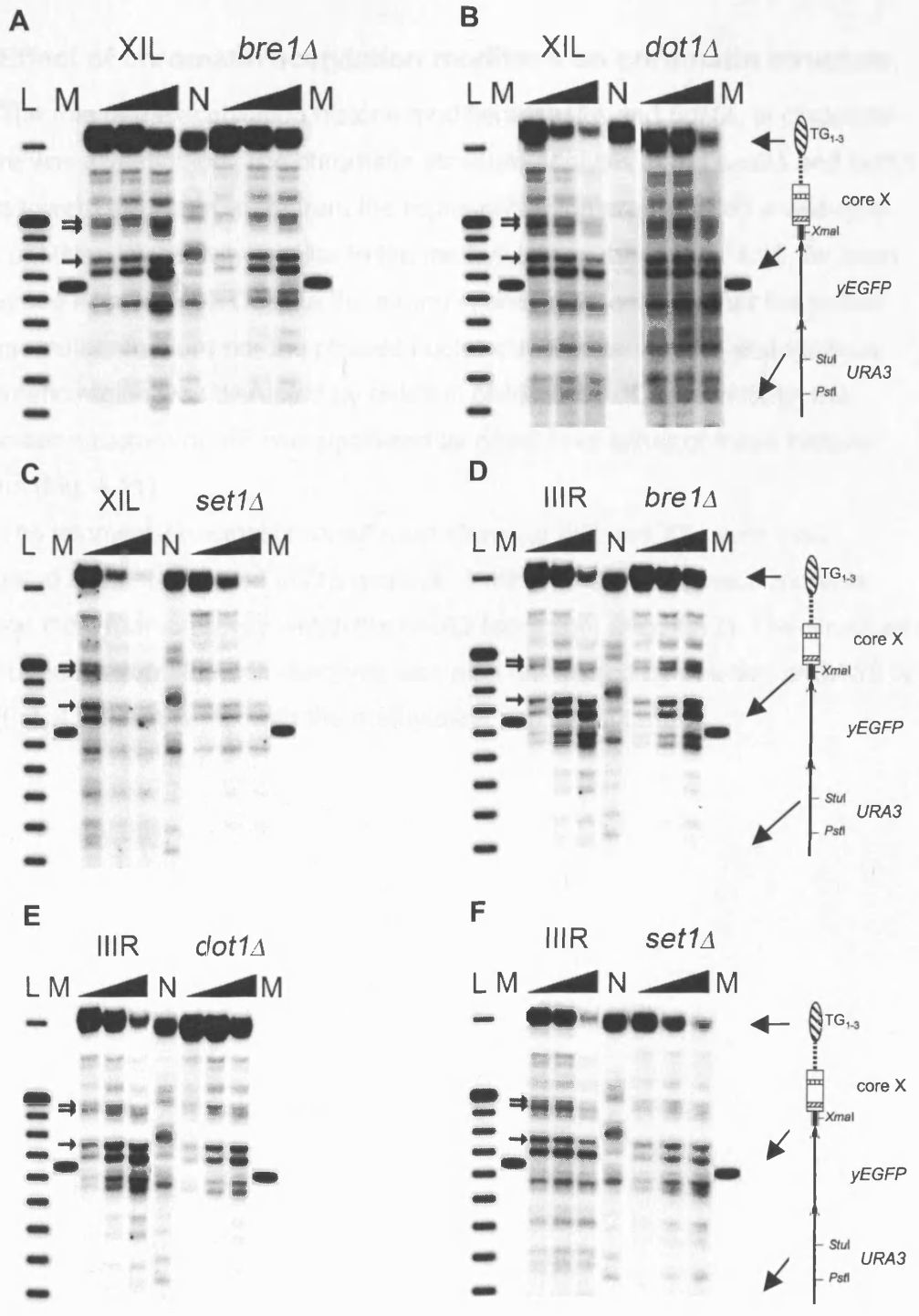

Figure 4.9. Comparison of chromatin structures toward the XIL and IIIR telomeres in methylation mutants.

4.2.7 Effect of chromatin acetylation modifiers on chromatin structure

The role of the acetylation histone modifiers, *sas2*Δ and *bdf1*Δ, in chromatin structure was investigated. The chromatin structure analysis in the *sas2*Δ and *bdf1*Δ mutants toward the centromere from the repressive telomere revealed a wild-type pattern of MNase sensitivity, similar to the methylation mutants (Fig. 4.10, for scan analysis see Appendix 3). Despite the strong silencing defects, neither the closed *URA3* promoter structure nor the phased nucleosome pattern of the endogenous subtelomeric region was disrupted by deletion of *SAS2* or *BDF1*. Similarly, the euchromatic structure of IIIR was unaltered by deletion of either of these histone modifiers (Fig. 4.11).

The telomere-proximal chromatin structures at IIIR and XIL were also investigated in the *sas2*Δ and *bdf1*Δ mutants. Neither of the acetylation mutants increased the hypersensitivity within the *URA3* terminator (Fig. 4.12). The structure of the endogenous subtelomeric elements was also unaffected by deletion of *SAS2* or *BDF1* (Fig. 4.12), similar to both the methylation and *sir* mutants.

Figure 4.10. Analysis of chromatin structures toward the centromere at XIL in acetylation mutants. The subtelomeric chromatin structures of the *URA3-yEGFP* marked XIL telomere in *sas2*Δ and *bdf1*Δ mutants, compared to the wild-type FEP318-19 (XIL), were analyzed by MNase digestion and indirect end labeling at the *Stu*I site as described previously. Black and grey arrows as in previous figures. A) The subtelomeric chromatin structures toward the centromere at XIL in *sas2*Δ and wild-type strains. B) The subtelomeric chromatin structures toward the centromere at XIL in *bdf1*Δ and wild-type strains.

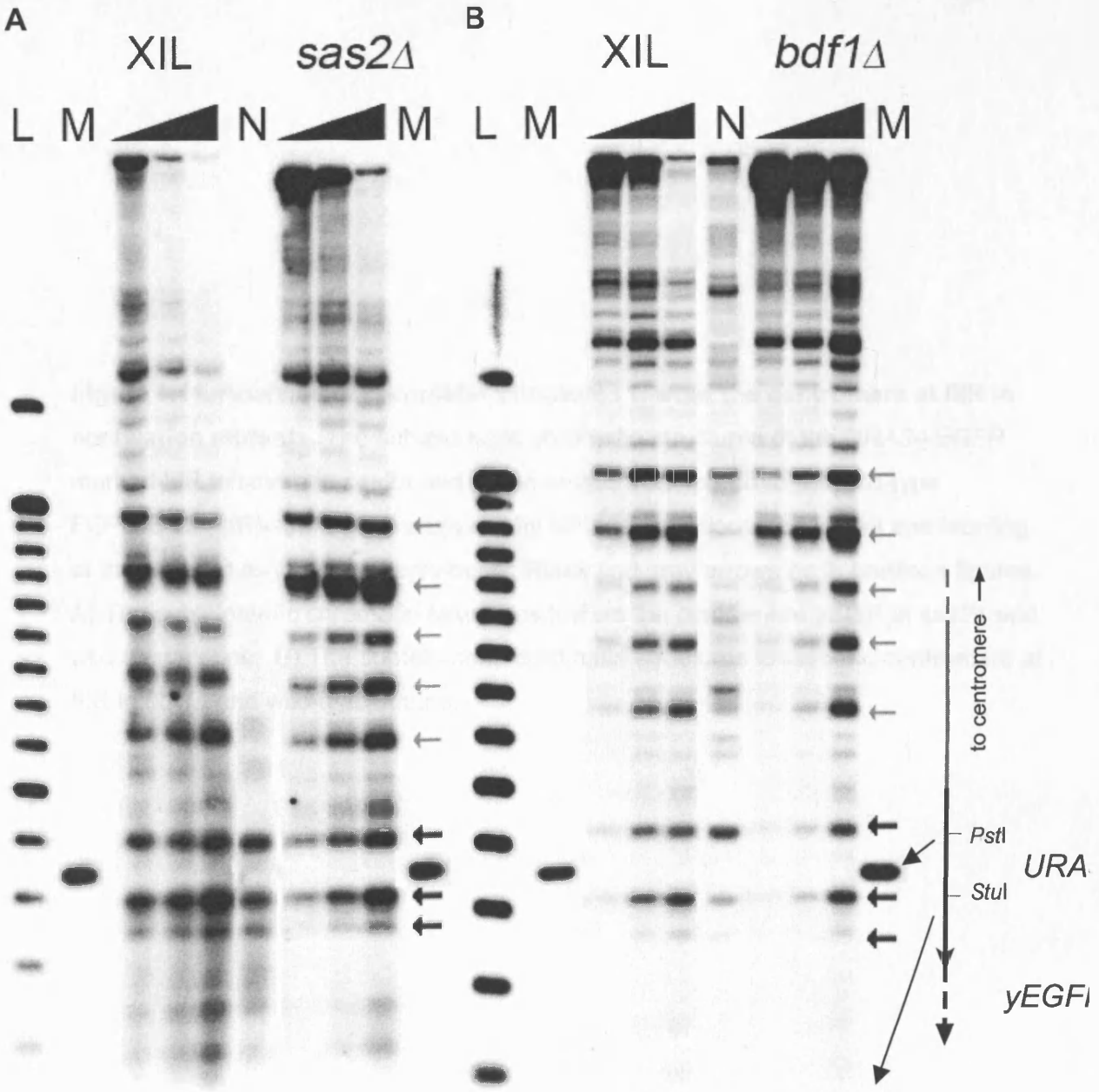

Figure 4.10. Analysis of chromatin structures toward the centromere at XIL in acetylation mutants.

Figure 4.11. Analysis of chromatin structures toward the centromere at IIIR in acetylation mutants. The subtelomeric chromatin structures of the *URA3-yEGFP* marked IIIR telomere in sas2Δ and *bdf1*Δ mutants compared to the wild-type FEP318-23 (IIIR) strain were analyzed by MNase digestion and indirect end labeling at the *Stu*I site as described previously. Black and grey arrows as in previous figures. A) The subtelomeric chromatin structures toward the centromere at IIIR in *sas2*Δ and wild-type strains. B) The subtelomeric chromatin structures toward the centromere at IIIR in *bdf1*Δ and wild-type strains.

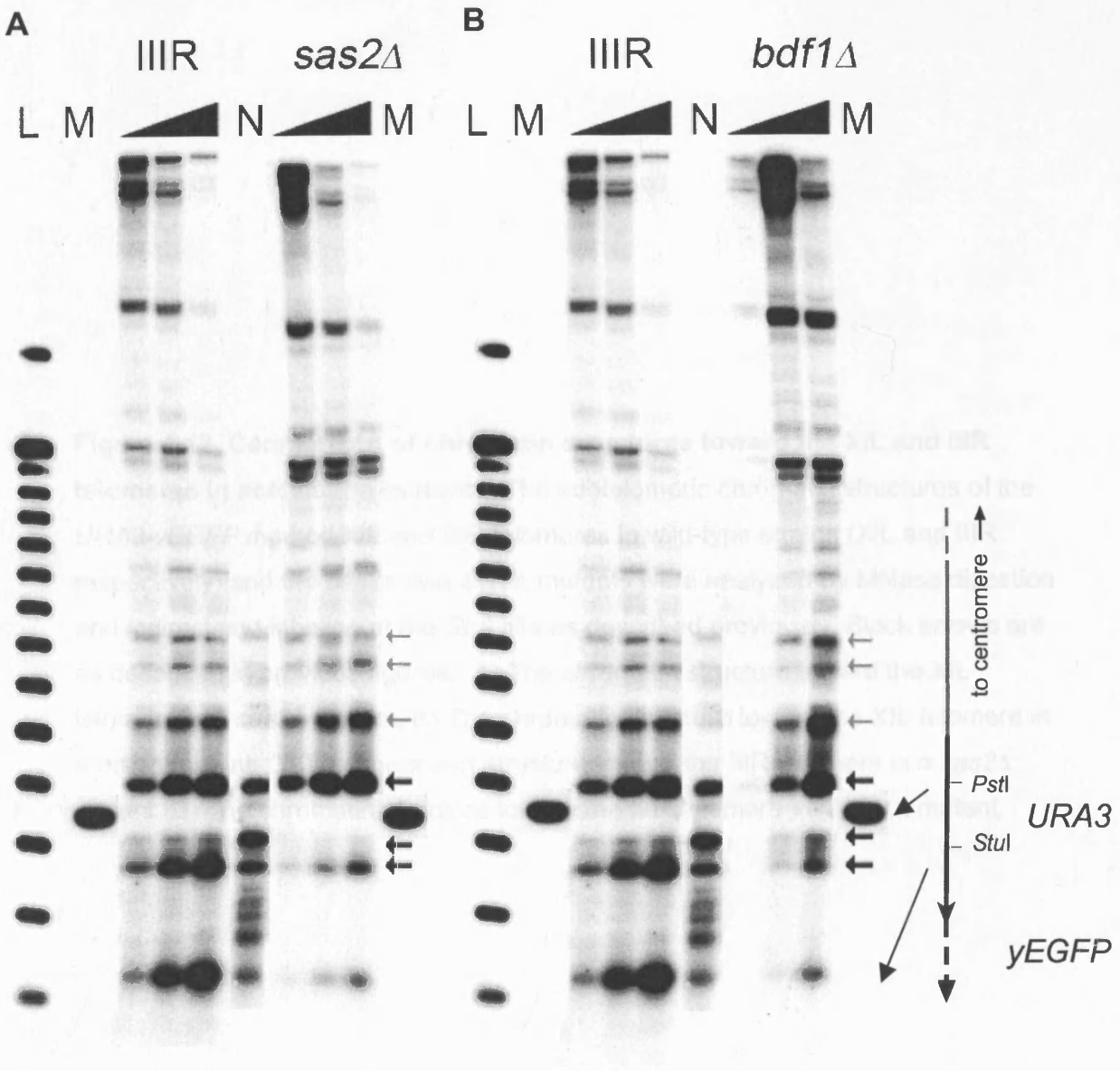

Figure 4.11. Analysis of chromatin structures toward the centromere at IIIR in acetylation mutants.

Figure 4.12. Comparison of chromatin structures toward the XIL and IIIR telomeres in acetylation mutants. The subtelomeric chromatin structures of the *URA3-yEGFP* marked XIL and IIIR telomeres in wild-type strains (XIL and IIIR respectively) and the *sas2*Δ and *bdf1*Δ mutants were analyzed by MNase digestion and indirect end labeling at the *Stu*I site as described previously. Black arrows are as described in previous figures. A) The chromatin structure toward the XIL telomere in a *sas2*Δ mutant. B) The chromatin structure toward the XIL telomere in a *bdf1*Δ mutant. C) The chromatin structure toward the IIIR telomere in a *sas2*Δ mutant. D) The chromatin structure toward the IIIR telomere in a *bdf1*Δ mutant.

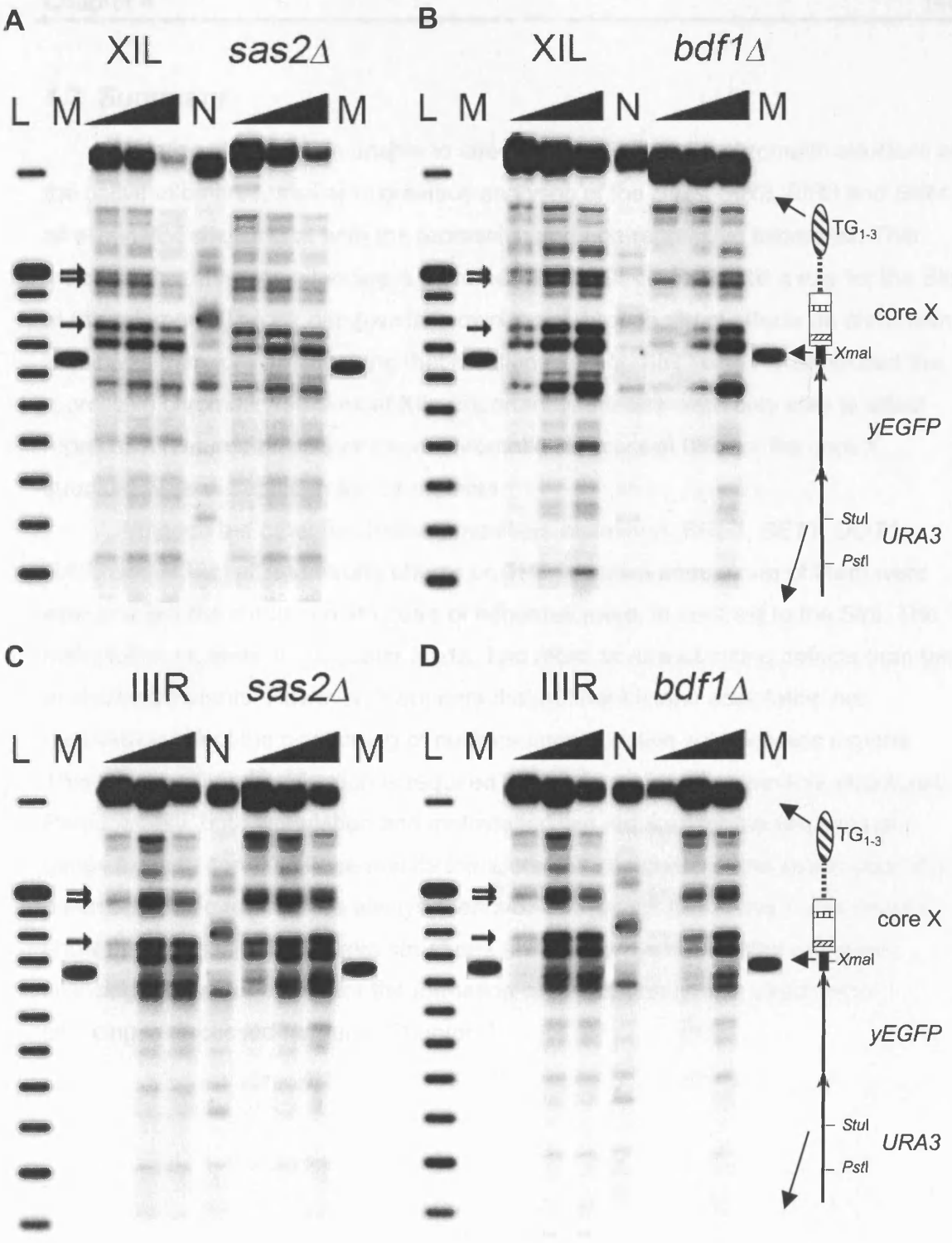

Figure 4.12. Comparison of chromatin structures toward the XIL and IIIR telomeres in acetylation mutants.

4.3 Summary

Deletion of *SIR1* was unable to affect either silencing or chromatin structure at the native telomeres, similar to previous analyses of the *SIRs*. *SIR2, SIR3* and *SIR4* all eliminated silencing at both the repressive and non-repressive telomeres. This indicates that although silencing is extremely low at IIIR there is still a role for the Sirs at this telomere. The Sir complex is known to act through direct effects on chromatin and it was therefore unsurprising that deletion of *SIR2*, *SIR3* or *SIR4* eliminated the repressive chromatin features at XIL. Importantly, the Sirs were only able to affect repressive features as neither the euchromatic structure at IIIR nor the core X structure were disrupted in the *sir* mutants.

Although the other five histone modifiers examined (*BRE1*, *SET1*, *DOT1, SAS2* and *BDF1*) all had strong effects on TPE at native ends, none of them were able to affect the chromatin structure of either telomere, in contrast to the Sirs. The methylation mutants, in particular *bre1*Δ, had more severe silencing defects than the acetylation mutants. However, it appears that neither histone acetylation nor methylation affect the positioning of nucleosomes in native subtelomeric regions. Therefore, neither modification is required for the formation of repressive structures. Paradoxically, both acetylation and methylation are required for the silencing of genes close to core X. These results therefore call into question the assumption that heterochromatic regions are always silenced. The results presented in this chapter show that repressive chromatin structures are not always associated with gene silencing. The requirement for the formation of a heterochromatic structure in silencing is discussed further in Chapter 7.

CHAPTER 5

5 The core X effect

5.1 Introduction

Natural telomeres contain several adjacent repetitive elements that together are termed the subtelomeric region. One of these elements, core X, is found at all ends in *S. cerevisiae* and has a role in natural TPE (Pryde and Louis, 1997; Pryde and Louis, 1999). Similar to the silencers at the *HMR* and *HML* loci, the core X element contains an ORC binding site (ACS) and an Abf1p binding site. Although core X is not required for the silencing of telomere-adjacent genes, it has been shown to have proto-silencer function; the presence of core X facilitates the propagation of silencing from the telomere repeats into the centromere-proximal region and can even promote silencing across anti-silencing, or STAR, elements (Fourel *et al.*, 1999; Pryde and Louis, 1999). This ability of core X elements to interact with telomere repeats is consistent with the loop model of the telomere and TPE at native ends proposed by Pryde and Louis (1999). In this model the core X-telomere interaction forms the tight region of repression observed around core X. Mutation of the core X ACS and Abf1p binding elements at a repressive end reduces the silencing of an adjacent reporter gene confirming the involvement of core X in repression (Pryde and Louis, 1999; this study). At the *HM* loci, Sir1p is recruited by ORC, which binds to the ACS sites in the silencers. In contrast to truncated ends, but similar to *HM* loci silencing, TPE at native ends is affected by the loss of *SIR1* (Fourel *et al.*, 1999; Pryde and Louis, 1999; Vega-Palas *et al.*, 2000), suggesting that ORC and Sir1p have a similar interaction at telomeres. The chromatin structure of core X elements also indicates the presence of a bound ORC and Abf1p (Vega-Palas *et al.*, 1998; Venditti *et al.*, 1999; this study).

This chapter addresses the role of the core X element in formation of the specialized chromatin structure at the repressive end and investigates the role of ORC in TPE and binding to core X elements.

5.2 Materials and Methods

Strains created for the studies in this chapter are listed in Table 5.1. pEL*ORC1*-HA, containing the *ORC1*-HA tagging construct and the *LEU2* selectable marker, was derived from p306-*ORC1*-HA (Stephen Bell) as described in Chapter 2. The *ORC1-HA* tagging construct was integrated at the *ORC1* locus in strains carrying

the *URA3* or *URA3-yEGFP* marker at XIL or IIIR as described in Chapter 2 (Table 5.1). The *ORC1-HA* construct was also integrated into a strain containing a mutated core X element (Table 5.1). The binding of *ORC1* to the core X elements in each strain was analyzed by chromatin immunoprecipitation (ChIP) and quantitative PCR (QPCR) as described in Chapter 2. Primers to the subtelomeric *SEO1* gene at the IL telomere were used to detect the background level of Orc1p-HA association.

Table 5.1. *S. cerevisiae* strains used in Chapter 5.

Strain[a]	Genotype	Relevant Modifications	
hERL37	*MAT**a**, lys2Δ202, leu2Δ1, ura3Δ851, his3Δ200*	*URA3::yEGFP* on XIL	*orc1::ORC1-HA*
hERL38	*MAT**a**, lys2Δ202, leu2Δ1, ura3Δ851, his3Δ200*	*URA3::yEGFP* on IIIR	*orc1::ORC1-HA*
hERL39	*MAT**a**, leu2Δ1, ura3Δ, can1-1, ade2Δ*	*URA3* on XIL	*orc1::ORC1-HA*
hERL40	*MAT**a**, lys2Δ202, leu2Δ1, ura3Δ851, his3Δ200*	*URA3* on XIL, ACS *Nde*I and Abf *Sph*I on XIL	*orc1::ORC1-HA*

[a] Unless indicated otherwise, strains were constructed during the course of this study

5.3 Results and Discussion

5.3.1 Mutations in core X alter silencing at a repressive telomere

The role of the core X ACS and Abf1p binding site in silencing and telomere structure was examined using isogenic strains (other than stated differences) previously constructed in the lab (Table 2.2). PIY180 and FEP270-1 both contain the *URA3* marker inserted adjacent to the core X element of the XIL telomere (see Fig. 3.1B). The XIL core X element is wild-type in PIY180 but contains mutations of the ACS and Abf1p binding site in FEP270-1 (Pryde and Louis, 1999). Repression analysis of PIY180 confirmed that the *URA3* marker was highly silenced, with a higher percentage of repression (39% FOA^R) compared to the *URA3-yEGFP* marker at XIL (25%) in the FEP318-19 strain (see Chapter 3). This is in agreement with previous results from Pryde and Louis (1999).

The mutations of the core X binding elements in the FEP270-1 (core X^{mut}) strain reduced the repression at XIL ~4-fold (13% FOA^R) in comparison to the wild-type PIY180 strain, similar to previous results (Pryde and Louis, 1999). Examples of the FOA analyses are shown in Fig. 5.1. The silencing defect in the core X^{mut} was less severe than in the *sir* or chromatin modifier mutants. However, the moderate reduction in silencing confirms the core X element does facilitate repression in the adjacent subtelomeric region. Therefore the ACS and Abf1p binding sites in core X likely have a similar function in TPE to their role at the *HM* silencers. Mutation of both binding elements in the *HM* silencers eliminates repression of the *HM* loci however (Brand *et al.*, 1987; Kimmerly *et al.*, 1988), while the core X^{mut} had only a moderate silencing defect. The ability of telomeric regions to silence in the absence of the these two binding sites or indeed the whole core X element, as is observed at truncated telomeres, may be related to the high number of Rap1p binding sites present in the telomere repeats (Gilson *et al.*, 1993; Marcand *et al.*, 1997a). The multiple Rap1p factors bound to the telomere may be able to recruit enough Sir proteins to silence in the absence of core X. In contrast, the *HM* silencers have only one Rap1p binding site and therefore require the ORC and/or Abf1p factors to facilitate sufficient Sir complex recruitment.

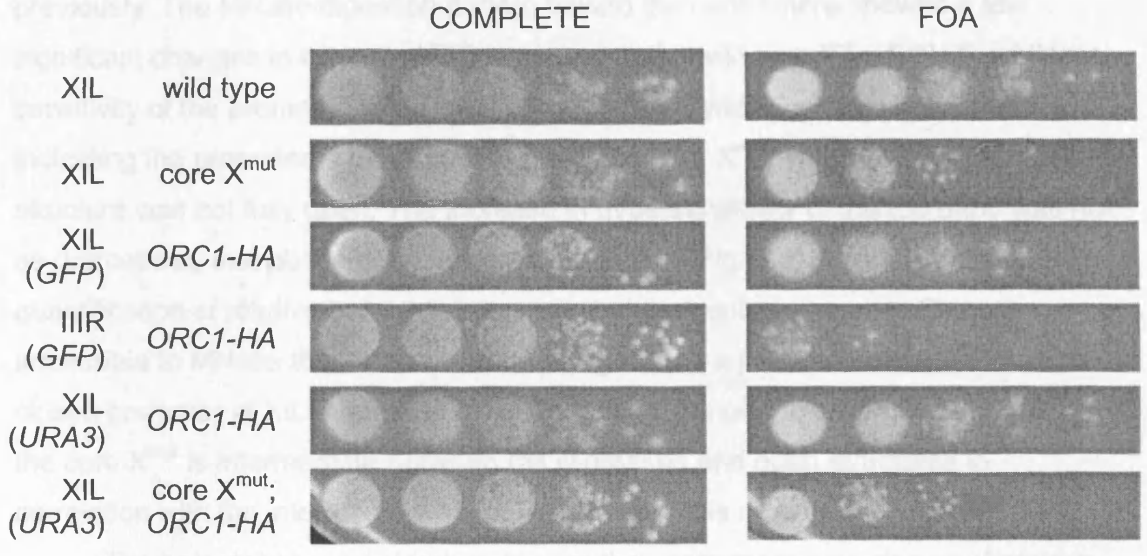

Figure 5.1. Examples of *URA3* repression assays. The wild-type and core X^{mut} strains (PIY180 and FEP270-1 respectively) marked with *URA3* at XIL are shown. Examples of assays for strains containing the HA-tagged *ORC1* construct and the *URA3* or *URA3-yEGFP* (GFP) marker at the indicated telomere are also shown. Ten-fold serial dilutions of single colonies were plated on complete synthetic media or media containing FOA and grown for three days at 30°C as described in Chapter 2.

5.3.2 Mutations in the core X ACS and Abf1p binding sites alter the heterochromatic structure

The chromatin structure of the *URA3*-marked core X^{mut} and wild-type strains were analyzed by MNase digestion and end labeling at the *Stu*I site as described previously. The MNase digestion pattern toward the centromere showed a few significant changes in the core X^{mut} compared to the wild type (Fig. 5.2). The MNase sensitivity of the promoter-associated sites (black arrows, Fig. 5.2) was altered indicating the promoter is more accessible in the core X^{mut}. However, the promoter structure was not fully open. The increase in hypersensitivity of the top band was not as dramatic as that observed in the *sir* mutants (see Fig. 4.2). In addition, quantification of relative band intensity revealed the central site was still more accessible to MNase than the lower band (Fig. 5.2B), a pattern associated with the closed promoter at XIL in the wild type. Therefore, the promoter structure of *URA3* in the core X^{mut} is intermediate between the repressed and open structures in correlation with the intermediate silencing defect of this mutant.

The heterochromatic structure toward the centromere was also weakened in the core X^{mut} strain. The intensity of the bands in the phased nucleosome region (grey arrows, Fig. 5.2) was reduced compared to the wild-type and there was increased MNase digestion between the bands, resulting in a less distinct banding pattern. However, the heterochromatic structure is still largely intact, in contrast to the *sir* mutants. The pattern of digestion suggests the positions of nucleosomes within the *URA3* promoter and the heterochromatic region are similar to wild type but are less strongly positioned in the core X^{mut}. Another possibility is that the heterochromatic structure, and associated silencing, is intact in some cells but not others containing the mutated core X. This would account for both the intermediate silencing and intermediate chromatin defects of this mutant. In addition, a mixture of repressed and non-repressed XIL telomeres carrying the mutated core X would suggest a role for this element in the establishment of TPE (see Chapter 7).

Figure 5.2. Analysis of chromatin structure toward the centromere at XIL in the core X^{mut}. A) The subtelomeric chromatin structures of the *URA3* marked XIL telomere in the FEP270-1 core mutant (X^{mut}) and PIY180 wild-type (XIL) strains were analyzed by MNase digestion and indirect end labeling at the *Stu*I site using the $URA3_{cen}$ probe as described previously. Black and grey arrows are as in previous figures. B) Chromatin band intensity profiles of the wild type (top) and core X^{mut} (bottom) were generated using Kodak 1D scan. The black and grey arrows indicate the peaks corresponding to the bands marked by the arrows in (A).

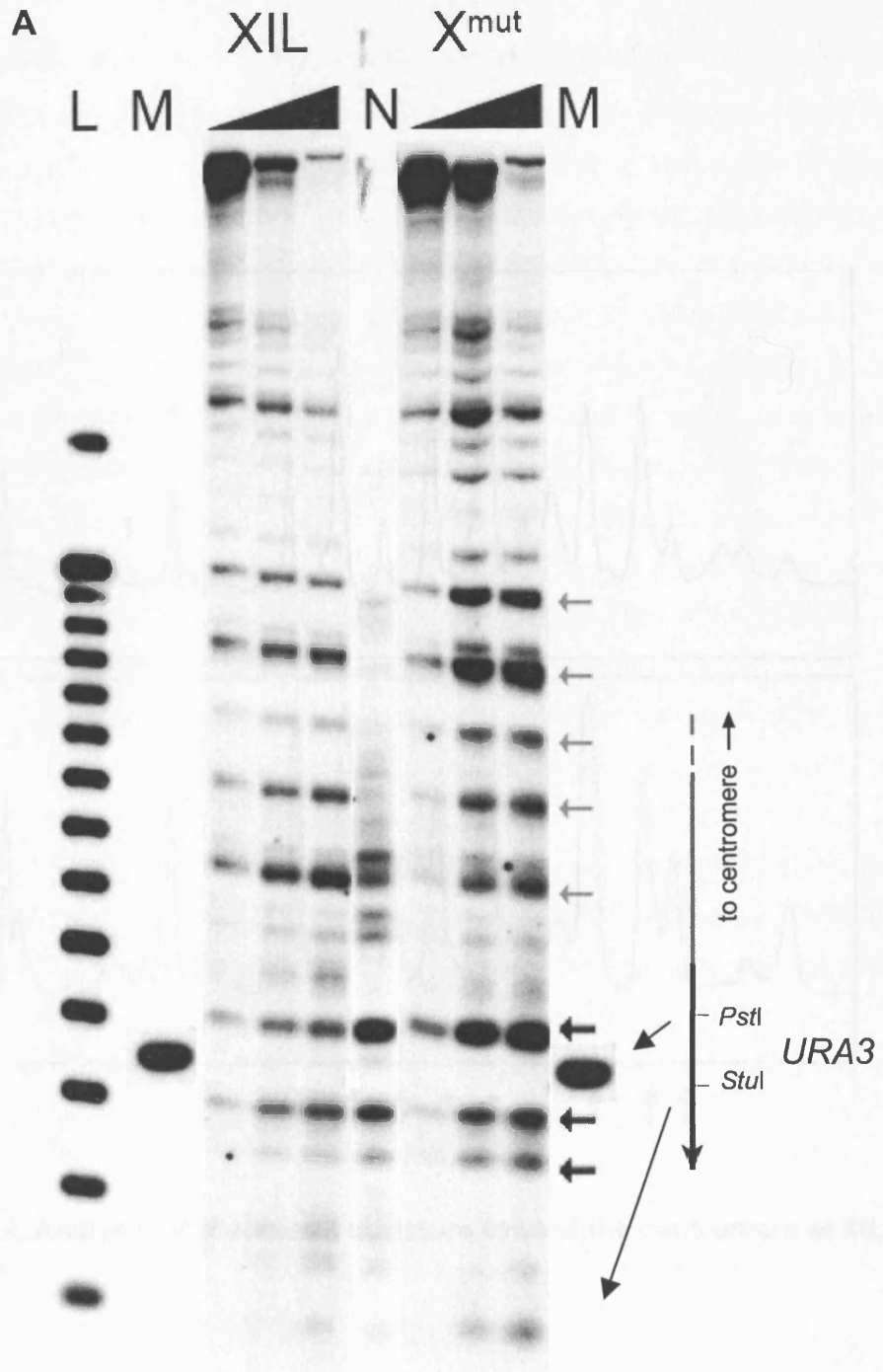

Figure 5.2. Analysis of chromatin structure toward the centromere at XIL in the core X^{mut}.

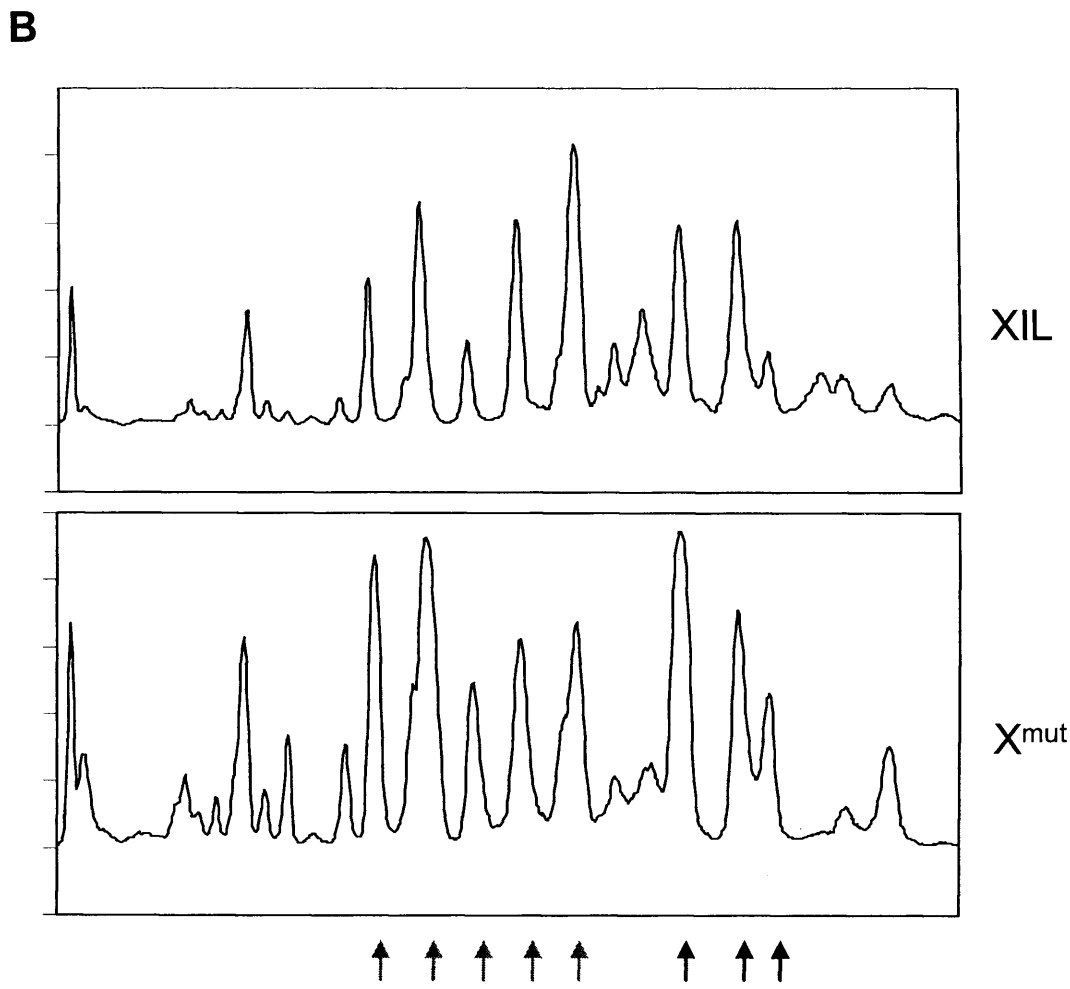

Figure 5.2. Analysis of chromatin structure toward the centromere at XIL in the core X^{mut}.

5.3.3 Mutations in core X disrupt its specialized chromatin structure

Significant changes were observed in the chromatin structure of the core X^{mut} toward the telomere compared to the wild type (Fig. 5.3), in contrast to the moderate centromere-proximal changes. The two strong hypersensitive regions observed in the wild type were missing in the core X^{mut} (black arrows, Fig. 5.3). The MNase pattern in the mutant was, in fact, similar to the pattern generated by digestion of the deproteinized DNA ('N', Fig. 5.3). Therefore, mutation of the two binding elements resulted in loss of the specialized chromatin structure over core X, consistent with the hypothesis that the wild-type structure results from the binding of ORC and Abf1p (as discussed in Section 3.3.3). The chromatin structure of the STR repeats in the core X^{mut} was similar to wild type however, indicating that the structural disruption is localized to core X (Fig. 5.3). In addition, there was a significant increase in hypersensitivity within the *URA3* termination sequence in the core X^{mut}. This increased hypersensitivity was also observed in the *sir* mutants and is believed to be related to the repression of the reporter construct. Therefore, together with the chromatin alterations observed toward the centromere, it appears that binding of ORC and Abf1p to core X is involved in both establishing the core X structure and formation of the centromere-proximal repressive chromatin features. However, the native core X structure is also observed at non-repressive telomeres (see Section 3.3.3), indicating ORC and Abf1p bind core X elements regardless of the silencing status. Thus, these factors are required for full wild-type silencing at the repressive telomere but are insufficient for silencing at telomeres.

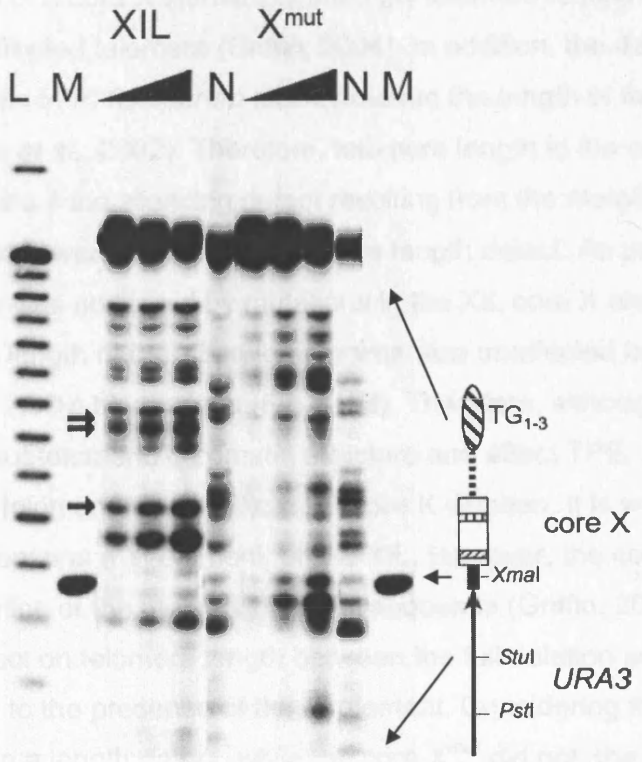

Figure 5.3. Comparison of chromatin structures toward the XIL telomere in the core X^{mut}. The subtelomeric chromatin structures of the *URA3* marked XIL telomere in FEP270-1 (X^{mut}) and the PIY180 wild-type strain (XIL) were analyzed by MNase digestion and indirect end labeling at the *Stu*I site as described previously. MNase-treated naked (N) DNA is shown for both the wild-type (left) and X^{mut} (right) strains. The 445bp markers, generated by digestion with *Stu*I and *Xma*I, are positioned near the *URA3*-core X junction. Black arrows are as described in previous figures. Positions of *Stu*I, *Xma*I and the telomere on the blot relative to the *URA3* marker are indicated by the diagram on the right.

5.3.4 Mutations in core X do not affect telomere length

A full deletion of a core X element at the XVR telomere results in the lengthening of the affected telomere (Griffin, 2004). In addition, the deletion of subtelomeric elements in *P. falciparum* also increased the length of the truncated telomere (Figueiredo *et al.*, 2002). Therefore, telomere length in the core X^{mut} was examined to determine if the silencing defect resulting from the mutation of the ACS and Abf1p binding sites was related to a telomere length defect. As predicted, the bulk telomere length was unaltered by mutations in the XIL core X element (Fig. 5.4A). However, the length of the XIL telomere was also unaffected by mutations in the core X ACS and Abf1p binding site (Fig. 5.4B). Therefore, although these mutations alter the subtelomeric chromatin structure and affect TPE, they do not appear to affect the telomere itself unlike a full core X deletion. It is worth noting that the XVR telomere contains a Y' element, unlike XIL. However, the core X deletion also resulted in deletion of the majority of the Y' sequence (Griffin, 2004). Therefore, the difference in effect on telomere length between the full deletion and the core X^{mut} is unlikely to be due to the presence of the Y' element. Considering that the full core X deletion resulted in a length defect, while the core X^{mut} did not, the role of core X elements in telomere biology must go beyond the recruitment of ORC and Abf1p.

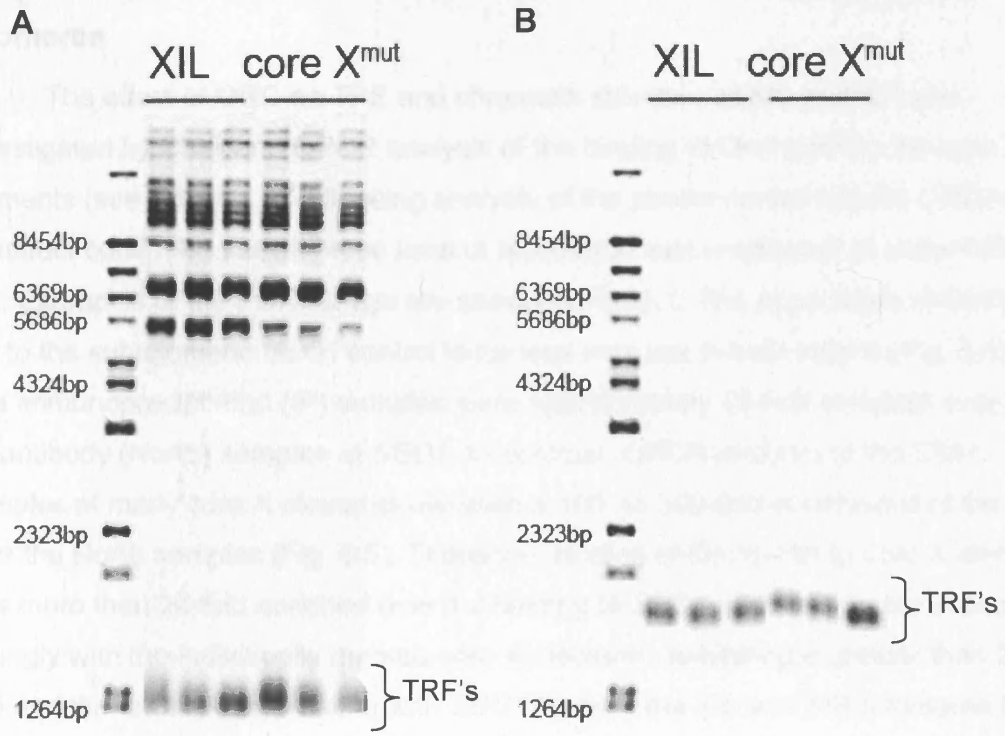

Figure 5.4. Analysis of telomere length in the core X^{mut}. DNA preps from three individual colonies of both strains, the wild-type *URA3* marked PIY180 (XIL) and mutant FEP270-1 (core X^{mut}) strains, were digested with *Xho*I or *Stu*I. Digestion fragments were separated on a 0.5% agarose gel, blotted and probed with a radio-labeled DNA fragment. (A) For analysis of bulk telomere length, the *Xho*I-digested samples were hybridized with a probe corresponding to the telomere-proximal fragment of the Y' element and the TG_{1-3} repeats. The large smeared bands of approximately 1200bp represent the telomere fragments while the other larger bands detected are non-telomeric digestion fragments to which the probe has some homology. (B) For analysis of the XIL telomere lengths, the *Stu*I-digested samples were hybridized with the $URA3_{tel}$ probe. For determination of fragment size the λ*Bst*EII ladder was run on both gels and ladder fragments were detected by probing with labelled lambda DNA. Sizes of the marker bands are indicated on the left.

5.3.5 Orc1p binds to core X at both repressive and non-repressive telomeres

The effect of ORC on TPE and chromatin structure at XIL and IIIR was investigated by ChIP and QPCR analysis of the binding of Orc1p-HA to the core X elements (see Chapter 2). Silencing analysis of the strains containing the *ORC1*-HA construct confirmed the wild-type level of repression was unaffected at either IIIR or XIL. Examples of the FOA assays are shown in Fig. 5.1. The association of Orc1p-HA to the subtelomeric *SEO1* control locus was very low in both strains (Fig. 5.5). The immunoprecipitated (IP) samples were approximately 10-fold enriched over the no-antibody (NoAb) samples at *SEO1.* In contrast, QPCR analysis of the ChIP samples at many core X elements revealed a 100- to 300-fold enrichment of the IP over the NoAb samples (Fig. 5.5). Therefore, binding of Orc1p-HA to core X elements was more than 20-fold enriched over the binding to *SEO1*. Orc1p-HA also associated strongly with the individually marked core X elements, exhibiting a greater than 20-fold enrichment over association with *SEO1* for both the XIL and IIIR telomeres (Fig. 5.5). This indicates the differences in repression at XIL and IIIR do not correlate with differences in ORC association. This work extends a previous study which showed an association of Orc1p with the XIL core X (Geissenhoner *et al.*, 2004).

5.3.6 Orc1p binding is reduced by core X mutations

The disruption of the native core X chromatin structure observed in the core X^{mut} suggests ORC is unable to bind the mutated ACS site. To confirm this hypothesis, QPCR analysis of ChIP samples was performed for *URA3*-marked wild-type and core X^{mut} strains containing the *ORC1*-HA construct (Table 5.1). The *URA3* repression levels in the strains containing *ORC1*-HA were similar to that of the parental strains (Fig. 5.1).

Orc1p-HA bound strongly to most of the core X elements in both the wild-type and core X^{mut} strains, exhibiting ~40-fold and ~20-fold enrichment over binding at the *SEO1* control locus respectively (Fig. 5.5). The binding to the *SEO1* locus was comparable in all four strains containing the tagged *ORC1* construct (Fig. 5.5). In addition, the binding of Orc1p-HA to the *URA3*-marked XIL telomere was similar to the level of binding observed at the *URA3-yEGFP* marked XIL core X (Fig. 5.5). As predicted, binding of Orc1p-HA specifically to the XIL core X element was reduced ~25-fold in the core X^{mut} strain compared to the wild type, and was comparable to the

background level of association at *SEO1* (Fig. 5.5). QPCR amplification of the ChIP input DNA from the wild-type and core X^{mut} strains using the primers specific to the XIL core X was equivalent. Therefore, the reduction in Orc1p-HA binding at the mutated core X is not due to less efficient amplification of the mutated sequence. This confirms ORC association with core X is disrupted by the core X mutations.

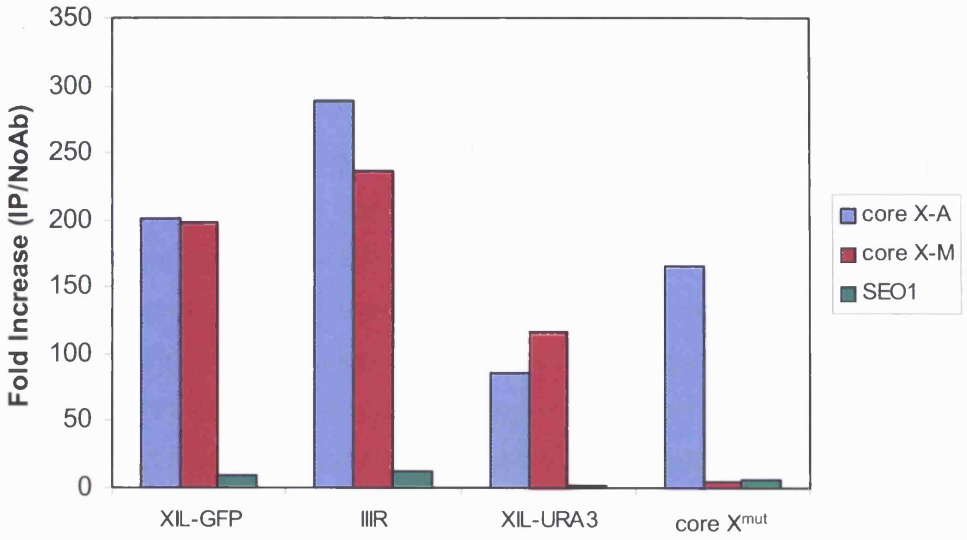

Figure 5.5. Interaction of Orc1p-HA with intact or mutated core X elements assayed by chromatin immunoprecipitation (ChIP). ChIP assays were performed with yeast strains containing the *URA3-yEGFP* construct centromere-proximal to the XIL (XIL-*GFP*) or the IIIR (IIIR) core X elements. Strains containing only the *URA3* reporter at the wild-type (XIL-*URA3*) or mutated (core X^{mut}) XIL core X element were also analyzed. *ORC1* was tagged with HA at its native locus in all strains. The binding of Orc1p-HA to many core X elements (core X-A), the marked core X (core X-M) and *SEO1* was analyzed by quantitative PCR. Histogram indicates the fold increase of DNA amplified in the immunoprecipitated samples (IP) over the samples without antibody (NoAb). Plotted values correspond to the median of three independent experiments.

5.4 Summary

Although the core X element maintains an identical structure at both IIIR and XIL, calling into question its role in silencing, disruption of the ORC and Abf1p binding sites caused a moderate disruption of both the silencing at XIL and the heterochromatic features. Therefore, it is clear that core X and the associated ORC and Abf1p factors do affect TPE at native ends. The inability of these elements to initiate silencing at IIIR, where they are clearly still present, is therefore mysterious. The chromatin alterations of the mutant core X and the lack of Orc1p association with this element confirms that the native core X chromatin structure is formed by the association of ORC and, almost certainly, Abf1p. From this study and the previous study (Griffin, 2004) of telomere length defects in core X mutants it appears the roles of core X in silencing and telomere length regulation are separable. A full core X deletion deregulates telomere length while the mutated core X element does not affect length regulation despite its silencing effects. A more comprehensive understanding of how core X affects the different aspects of telomere biology at different ends will require further investigation.

CHAPTER 6

6 The yKu connection

6.1 Introduction

The Ku heterodimer is comprised of the Ku70p and Ku80p subunits and in mammals is also associated with a DNA kinase catalytic unit, DNA-PK_{cs} to form the DNA-PK complex (Jeggo *et al.*, 1995; Lieber *et al.*, 1997). The Ku proteins provide the DNA-binding ability of this complex to localize in a non-sequence specific manner to double-strand breaks. Ku functions in non-homologous end-joining (NHEJ) and in telomere maintenance and the DNA end-binding function of Ku is likely required for these functions (Lieber *et al.*, 1997). Given its role in NHEJ, a role for Ku in telomere maintenance is counter-intuitive as telomeres must be prevented from binding other free DNA ends. Despite this paradox, yKu is critical for telomere protection and transcriptional repression near both truncated and native telomeres in *S. cerevisiae* and is also important for the peripheral localization of telomeres (Boulton and Jackson, 1998; Hediger *et al.*, 2002; Laroche *et al.*, 1998; Nugent *et al.*, 1998). Ku is also important for telomere protection in mammals (d'Adda di Fagagna *et al.*, 2001; Jaco *et al.*, 2004; Myung *et al.*, 2004).

ChIP and direct immunofluorescence studies have revealed the binding of Ku to telomere repeats in yeast and mammalian cells (d'Adda di Fagagna *et al.*, 2001; Gravel *et al.*, 1998; Hsu *et al.*, 1999; Martin *et al.*, 1999). In addition, yKu is able to bind directly to Sir4p (Roy *et al.*, 2004; Tsukamoto *et al.*, 1997). This association may serve to recruit the Sir complex to the telomeres and allow Sir4p to compete with the Rif (Rap1p interacting factors) telomere length regulators for binding to Rap1p (Mishra and Shore, 1999). yKu is of particular interest in the study of TPE as it is both essential for and specific to silencing at telomeres, unlike most other silencing factors which also affect *HML*/*HMR* silencing (Laroche *et al.*, 1998). Separation-of-function studies have recently revealed that many of the roles of yKu in NHEJ and telomere biology are separable (Bertuch and Lundblad, 2003; Roy *et al.*, 2004; Stellwagen *et al.*, 2003; Taddei *et al.*, 2004). Some of the silencing-defective mutants identified in these studies appear to still possess their ability to interact with the Sir proteins while others cannot, indicating the role of yKu in TPE goes beyond simply recruiting Sir4p to the telomere. Recently, an association of yKu with core X elements has been observed, but yKu does not associate strongly with the Y' element (M. Marvin,

personal communication). This suggests a role for yKu in the loop structure of the telomere, where it may act to stabilize the core X-telomere interaction through its ability to bind to both elements.

The studies presented in this chapter investigated the role of yKu in TPE at native ends, the formation of heterochromatin and the loop structure at both the XIL repressive and IIIR non-repressive telomeres. The effect of full *yku80*Δ mutants and *yku80^{tel}* separation-of-function mutants (Bertuch and Lundblad, 2003) were examined. In addition, the ability of yKU80p and the yku80^{tel}p mutants to interact with core X elements was investigated.

6.2 Materials and Methods

All strains created for the work presented in this chapter are listed in Table 6.1. Strains containing gene deletions, the Myc-tagged *yKU80* at its native locus and the *yku80^{tel}* CEN plasmids were created as described in Chapter 2. Temperature sensitivity in all *yku80* mutants was analyzed by streaking each strain only two plates of the appropriate selective media and growth of one plate at 30°C and the second plate at 37°C for 2-3 days.

Chromatin and ChIP analyses were performed as described in Chapter 2, with the following modifications for strains containing the CEN plasmids. Overnight cultures in YPD were subcultured into 200mls of synthetic media lacking leucine, to select for cells containing the CEN plasmids. The spheroplasting of the cells was carried out for five and a half minutes as cells grown in synthetic media are more resistant to zymolyase. For both PIY133 and all strains containing the *yku80^{tel}* plasmids, chromatin samples were end labeled at with *Bst*XI site using the GFP_{cen} and GFP_{tel} probes adjacent to the *Bst*XI site (Fig. 6.1) to avoid cross-hybridization of the probe with the *ura3-52* allele present in PIY133. Primers used to generate the GFP probes are listed in Chapter 2.

Telomere length, temperature sensitivity and the binding of Myc-tagged yKu80p and yku80^{tel}p proteins were analyzed as described in Chapter 2, with the exception that strains containing the *yku80^{tel}* CEN plasmids were grown in synthetic media lacking leucine.

Table 6.1. *S. cerevisiae* strains used in Chapter 6.

Strain[a]	Genotype	Relevant Modifications	
hERM238	*MAT**a**, lys2Δ202, leu2Δ1, ura3Δ851, his3Δ200*	*URA3::yEGFP* on XIL	*yku70::kanMX*
hERM239	*MAT**a**, lys2Δ202, leu2Δ1, ura3Δ851, his3Δ200*	*URA3::yEGFP* on IIIR	*yku70::kanMX*
hERM247	*MAT**a**, lys2Δ202, leu2Δ1, ura3Δ851, his3Δ200*	*URA3* on XIL, ACS *Nde*I and Abf *Sph*I on XIL	*yku80::kanMX*
hERM244	*MAT**a**, lys2Δ202, leu2Δ1, ura3-52, his3Δ200, yku80Δ*	*URA3::yEGFP* on XIL	*yKU80cmyc::kanMX*
hERM245	*MAT**a**, lys2Δ202, leu2Δ1, ura3Δ851, his3Δ200, yku80Δ*	*URA3::yEGFP* on IIIR	*yKU80cmyc::kanMX*
hERM246	*MAT**a**, leu2Δ1, ura3-52, can1-1, ade2Δ, yku880Δ*	*URA3* on XIL	*yKU80cmyc::kanMX*
hERL4	*MAT**a**, lys2Δ202, leu2Δ1, ura3Δ851, his3Δ200, yku80Δ*	*URA3* on XIL, ACS *Nde*I and Abf *Sph*I on XIL	*yKU80cmyc::kanMX*
hERL13	*MAT**a**, lys2Δ202, leu2Δ1, ura3-52, his3Δ200, yku80Δ*	*URA3::yEGFP* on XIL	pAB109 ($yKU80_{myc18}$)
hERL14	*MAT**a**, lys2Δ202, leu2Δ1, ura3Δ851, his3Δ200, yku80Δ*	*URA3::yEGFP* on IIIR	pAB109 ($yKU80_{myc18}$)
hERL15	*MAT**a**, lys2Δ202, leu2Δ1, ura3-52, his3Δ200, yku80Δ*	*URA3::yEGFP* on XIL	pAB110 ($yku80\text{-}1_{myc18}$)
hERL16	*MAT**a**, lys2Δ202, leu2Δ1, ura3Δ851, his3Δ200, yku80Δ*	*URA3::yEGFP* on IIIR	pAB110 ($yku80\text{-}1_{myc18}$)
hERL17	*MAT**a**, lys2Δ202, leu2Δ1, ura3-52, his3Δ200, yku80Δ*	*URA3::yEGFP* on XIL	pAB111 ($yku80\text{-}4_{myc18}$)
hERL18	*MAT**a**, lys2Δ202, leu2Δ1, ura3Δ851, his3Δ200, yku80Δ*	*URA3::yEGFP* on IIIR	pAB111 ($yku80\text{-}4_{myc18}$)
hERL29	*MAT**a**, lys2Δ202, leu2Δ1, ura3-52, his3Δ200, yku80Δ*	*URA3::yEGFP* on XIL	pAB117 ($yku80\text{-}8_{myc18}$)
hERL30	*MAT**a**, lys2Δ202, leu2Δ1, ura3Δ851, his3Δ200, yku80Δ*	*URA3::yEGFP* on IIIR	pAB117 ($yku80\text{-}8_{myc18}$)

[a] All strains were constructed during the course of this study

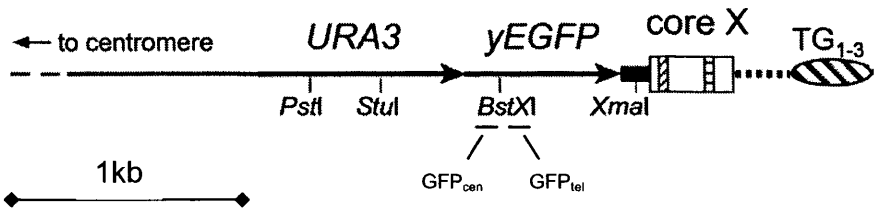

Figure 6.1. Schematic of the *URA3-yEGFP* marked native telomeres with position of the GFP_{cen} and GFP_{tel} probes. The position of *URA3-yEGFP* (black arrows) and the *URA3* terminator (filled black rectangle) relative to core X (large open rectangle) at a native core X-only end. The *Bst*XI site within *yEGFP* and the *Pst*I and *Xma*I sites, used to generate the centromere and telomere-proximal marker bands respectively, are also indicated. Black bars under the *Bst*XI site indicate the positions of the GFP_{cen} and GFP_{tel} probes used for chromatin analysis. The position of the ACS sequence in core X is shown by the diagonal lines while the horizontal lines indicate the Abf1p binding site. All elements are drawn to scale.

6.3 Results and Discussion

6.3.1 Deletion of either yKu subunit disrupts TPE

yKU80 and *yKU70* are both known to decrease silencing at truncation ends. A similar effect for *yKU70* on a *URA3* marked repressive XIL native telomere has also been previously shown (Pryde and Louis, 1999). To further analyze the effect of yKu on silencing and chromatin structure at both the repressive and non-repressive native telomeres, previously constructed *yku80Δ* strains marked with *URA3-yEGFP* at either XIL or IIIR (Table 2.2), were tested for silencing defects. In addition, to confirm that both yKu subunits have a similar effect on TPE and chromatin structure at native ends, *yku70Δ* mutants were generated by *kanMX* gene replacement in the *URA3-yEGFP* marked strains (see Chapter 2) (Table 6.1). Ku-deficient yeast strains are temperature sensitive (Boulton and Jackson, 1996; Feldmann and Winnacker, 1993) and this phenotype was confirmed in the mutants used in this study.

Deletion of either *yKU80* or *yKU70* almost eliminated silencing at XIL (Table 6.2), in agreement with previous results (Pryde and Louis, 1999). Interestingly, the *yku80Δ* mutant appeared to slightly increase silencing at the non-repressive telomere (Table 6.2). This effect may be a result of releasing the Sir complex from the normally repressed loci, allowing them to bind more promiscuously and repress normally expressed loci. yKu mutants are known to result in the delocalization of Sir's from the telomere and increased ectopic silencing (Maillet *et al.*, 2001) and similar effects have been observed in other silencing mutants (Kimura *et al.*, 2002; Ladurner *et al.*, 2003). However, deletion of *yKU70* completely eliminates silencing at the IIIR telomere (Table 6.2), similar to most of the other silencing mutants analyzed in this study. Therefore, there may be slight differences in how the yKu subunits function at telomeres, or perhaps only at non-repressive telomeres. More pronounced telomere effects have been observed for one Ku subunit over the other in studies in *Drosophila* (Melnikova *et al.*, 2005), supporting the idea that the role and effect of the subunits may not always be equal. Examples of all silencing experiments are shown in Fig. 6.2.

Table 6.2. Frequency of FOA resistance in *yKU* deletion and Myc-tagged strains.

Strain	Mutation	Chromosome	%FOA^R	
FEP318-19		XIL	10 – 42	(25)
FEP318-23		IIIR	0.002 – 1.6	(0.02)
PIY133	*yku80Δ*	XIL	0.09 – 0.25	(0.15)
hERM238	*yku70Δ*	XIL	0.03 – 0.07	(0.06)
PIY134	*yku80Δ*	IIIR	0.4 – 2.4	(1.2)
hERM239	*yku70Δ*	IIIR	0	(0)
hERM247	*yku80Δ*, core X^{mut}	XIL	0	(0)
hERM244	*yKU80$_{Myc}$*	XIL	31 – 63	(46)
hERM245	*yKU80$_{Myc}$*	IIIR	0 – 0.03	(0.02)
hERM246	*yKU80$_{Myc}$*	XIL	5 – 5.2	(5)
hERL4	*yKU80$_{Myc}$*, core X^{mut}	XIL	26 – 35	(30)

The range of FOA resistance values from a minimum of three independent measurements is shown with the average value given in parenthesis. The values for the wild-type strains are also shown for comparison. FOA resistance was analyzed as described in Chapter 2.

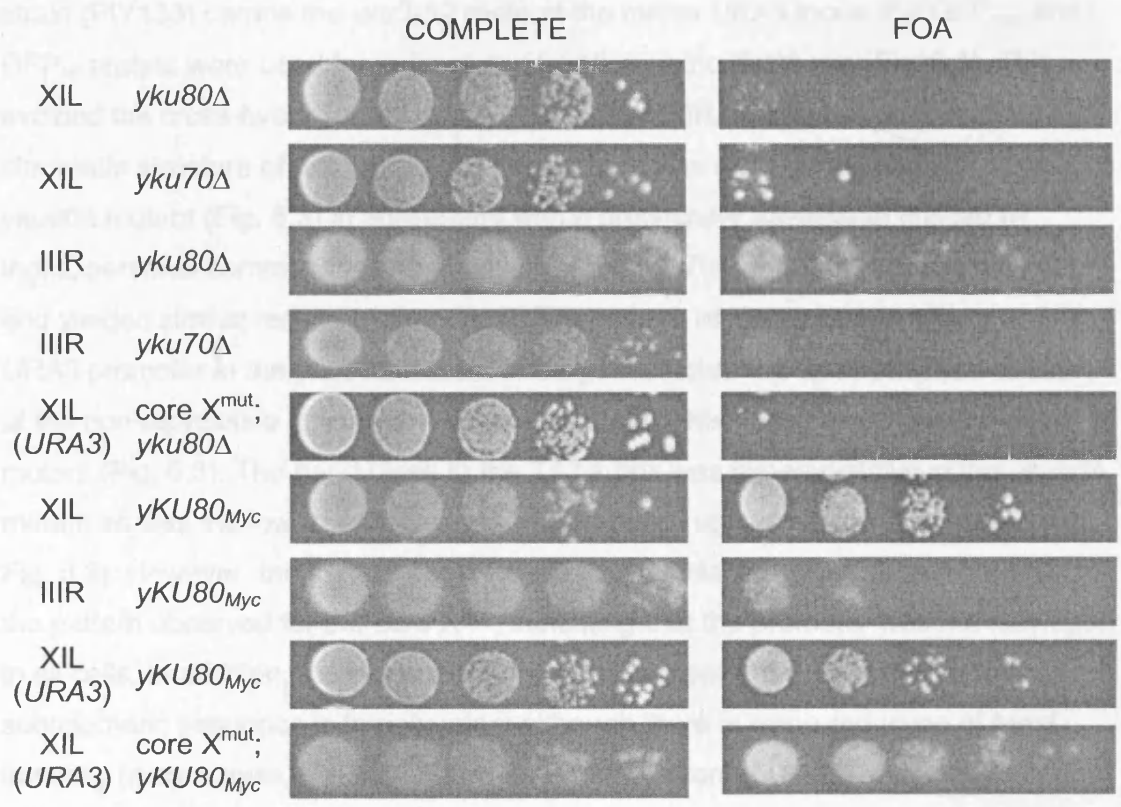

Figure 6.2. Examples of *URA3* repression assays in *yKU* deletion and Myc-tagged strains. The telomeres marked and relevant modifications in each strain are indicated. Those that lack the *yEGFP* ORF are indicated (*URA3*).Ten-fold serial dilutions of single colonies were plated on complete synthetic media or media containing FOA and grown for three days at 30°C as described in Chapter 2.

6.3.2 *yKU80* is involved in the repressive chromatin structure at XIL

The effect of the *yku80*Δ mutation on chromatin structure at XIL was analyzed by MNase digestion as described previously. However, as the XIL-marked *yku80*Δ strain (PIY133) carries the *ura3-52* allele at the native *URA3* locus, the GFP_{cen} and GFP_{tel} probes were used for indirect end labeling at the *BstX*I site (Fig. 6.1). This avoided the cross-hybridization of the $URA3_{cen}$ and $URA3_{tel}$ probes with *ura3-52*. The chromatin structure of XIL toward the centromere was significantly altered in the *yku80*Δ mutant (Fig. 6.3) in agreement with a preliminary analysis in this lab (P. Inglis, personal communication). Analysis of the *yku70*Δ mutant at the marked XIL end yielded similar results (Appendix 4). The pattern of MNase sensitivity near the *URA3* promoter in the *yku80*Δ mutant closely resembled the open structure observed at the non-repressive IIIR telomere, consistent with the strong derepression in this mutant (Fig. 6.3). The band close to the TATA box was hypersensitive in the *yku80*Δ mutant as was the lower promoter-associated band (upper and lower black arrows, Fig. 6.3). However, the central band still exhibited MNase hypersensitivity, similar to the pattern observed for the core X^{mut}, indicating that the promoter was not fully open in all cells. In addition, the heterochromatic banding pattern in the endogenous subtelomeric sequence is largely intact although there is some reduction of band intensity (grey arrows, Fig. 6.3). Therefore, the deletion of *yKU80* weakens but does not fully disrupt the repressive chromatin structure centromere-proximal to the XIL core X.

Due to the use of the *BstX*I probe, more of the *URA3* ORF structure could be observed than in previous analyses. There were some prominent alterations in the MNase sensitivity within the *URA3* ORF in the *yku80*Δ mutant compared to wild type. Notably, there was one strong hypersensitive band 3' of the promoter that was not present in the wild-type pattern and a general increase in accessibility to MNase (Fig. 6.3). This suggests the wild-type chromatin structure of the *URA3* ORF is altered at the repressive XIL telomere. However, a characteristic phased nucleosome array was not clearly observed making nucleosome positions within *URA3* more difficult to infer.

yKU80 therefore appears to affect all aspects of the repressive chromatin structure centromere-proximal to core X but, intriguingly, the repressive structures are not fully disrupted despite the strong silencing defect. Thus the *yku80*Δ phenotype is unique. Similar to the *sir* mutants, *URA3* is derepressed at XIL but,

unlike the *sir* mutants, deletion of *yKU80* does not abrogate the repressive chromatin features. However, the deletion of *yKU80* does moderately disrupt the heterochromatic features; this contrasts with the histone modifier mutants that had similarly severe silencing defects but had little effect on chromatin structure. Therefore, yKU80p may be an intermediary between establishment of the repressive chromatin structure and the subsequent silencing.

Figure 6.3. Analysis of chromatin structure toward the centromere at XIL in a *yku80*Δ mutant. A) The subtelomeric chromatin structure of the *URA3-yEGFP* marked XIL telomere in the wild-type (XIL) and *yku80*Δ mutant strains was analyzed by MNase digestion as described previously. Samples were end labeled at the *Bst*XI site using the GFP_{cen} probe (see Fig. 6.1). The 982bp markers (M), generated by digestion of purified DNA with *Bst*XI, are positioned to indicate the *URA3* TATA box . Black and grey arrows and labels are as in previous figures. B) Chromatin band intensity profiles of the wild-type (top) and *yku80*Δ (bottom) patterns were generated using Kodak 1D scan. The black and grey arrows indicate the peaks corresponding to the bands marked by the arrows in (A).

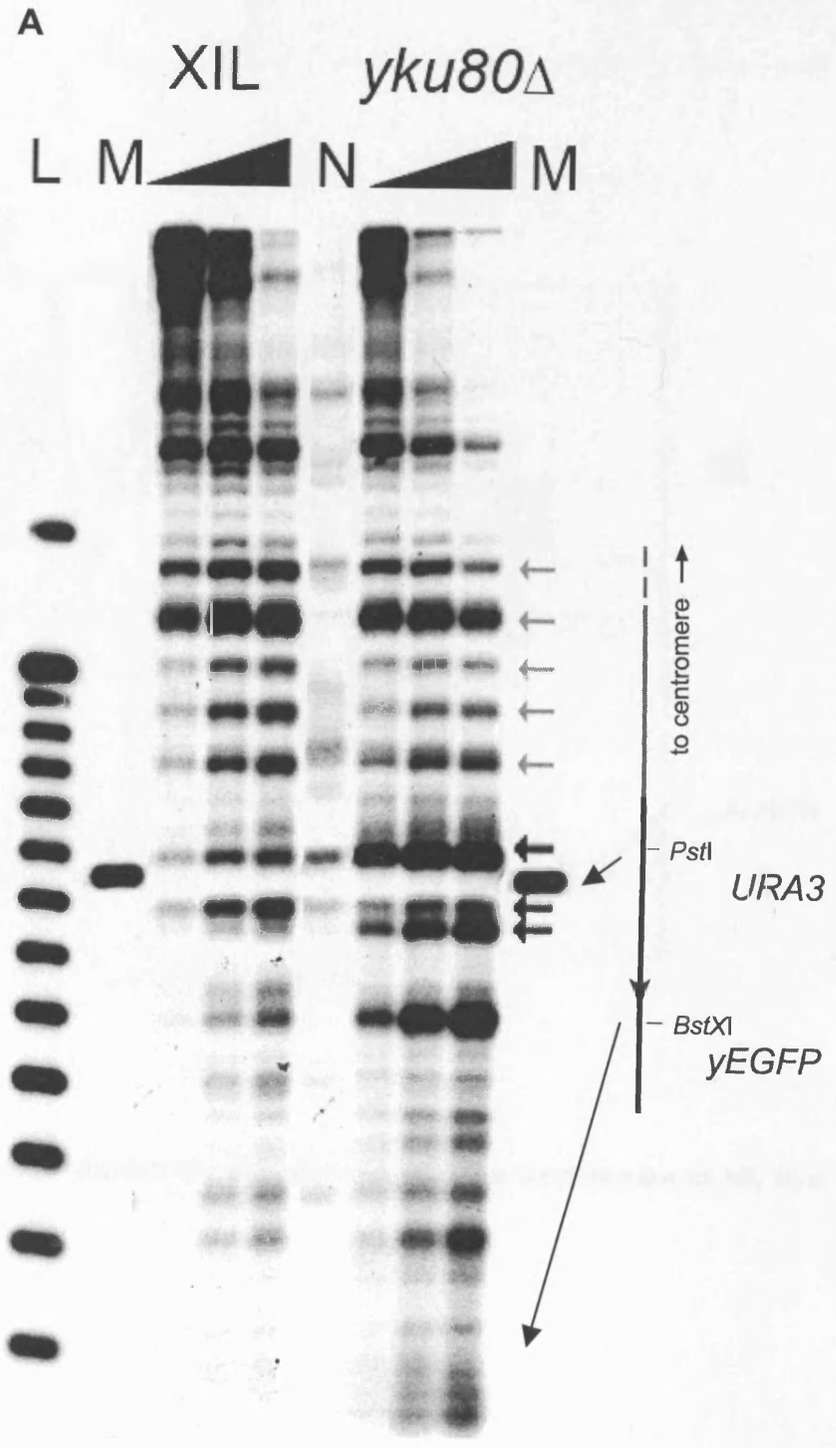

Figure 6.3. Analysis of chromatin structure toward the centromere at XIL in a *yku80*Δ mutant.

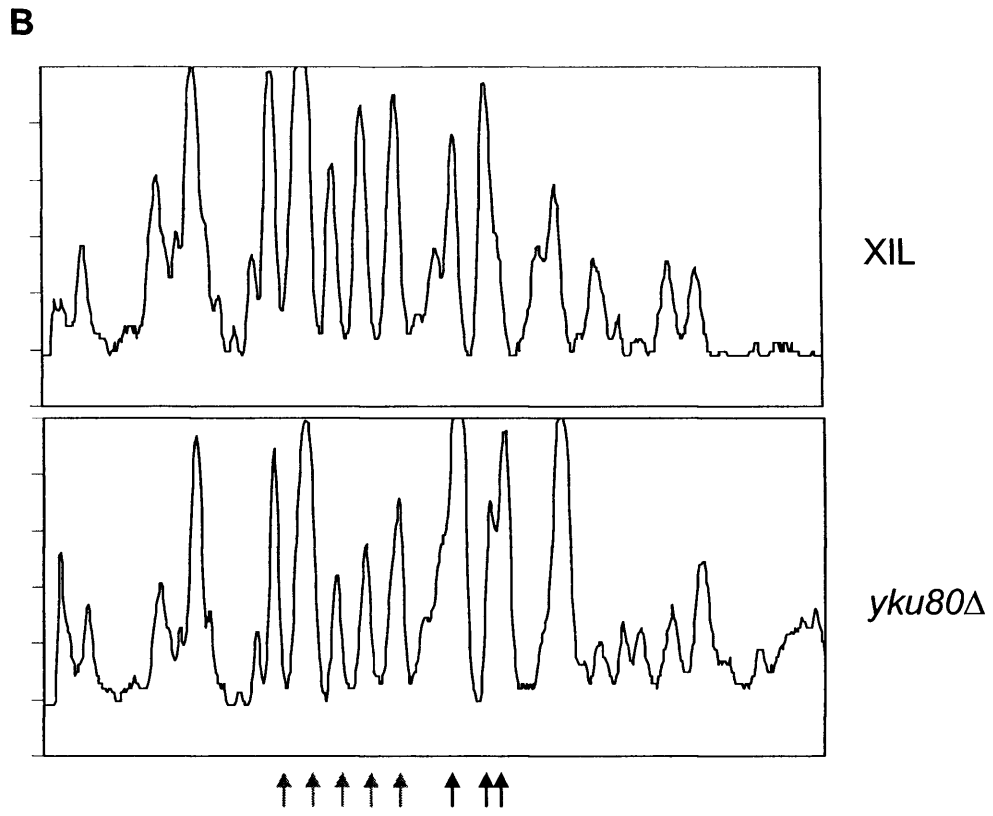

Figure 6.3. Analysis of chromatin structure toward the centromere at XIL in a *yku80Δ* mutant.

6.3.3 Chromatin structure at IIIR and toward the telomere is unaffected by deletion of *yKU80*

Chromatin structure over the *URA3* promoter and subtelomeric DNA centromere-proximal to core X at IIIR was unaffected by deletion of *yKU80* (Fig. 6.4). The promoter structure was still in the open conformation and the subtelomeric region was indistinguishable from wild type. This is consistent with the lack of effect on the IIIR structure of all the silencing factors examined in this study

Consistent with all previous results for gene deletion mutants in this study, deletion of *yKU80* also failed to disrupt the unique structure of the core X element at either the XIL or IIIR telomere (Fig. 6.5). Similar results were obtained in the *yku70*Δ mutant at XIL (Appendix 4). The only observable alteration was the shorter telomere of the *yku* mutants, resulting in the telosome band being smaller in the mutants (large top band, Fig. 6.5). Therefore, the binding of yKu80p to core X elements (M. Marvin, personal communication) does not influence the nucleosome positioning or binding of ORC and Abf1p to core X through indirect interactions with these two factors.

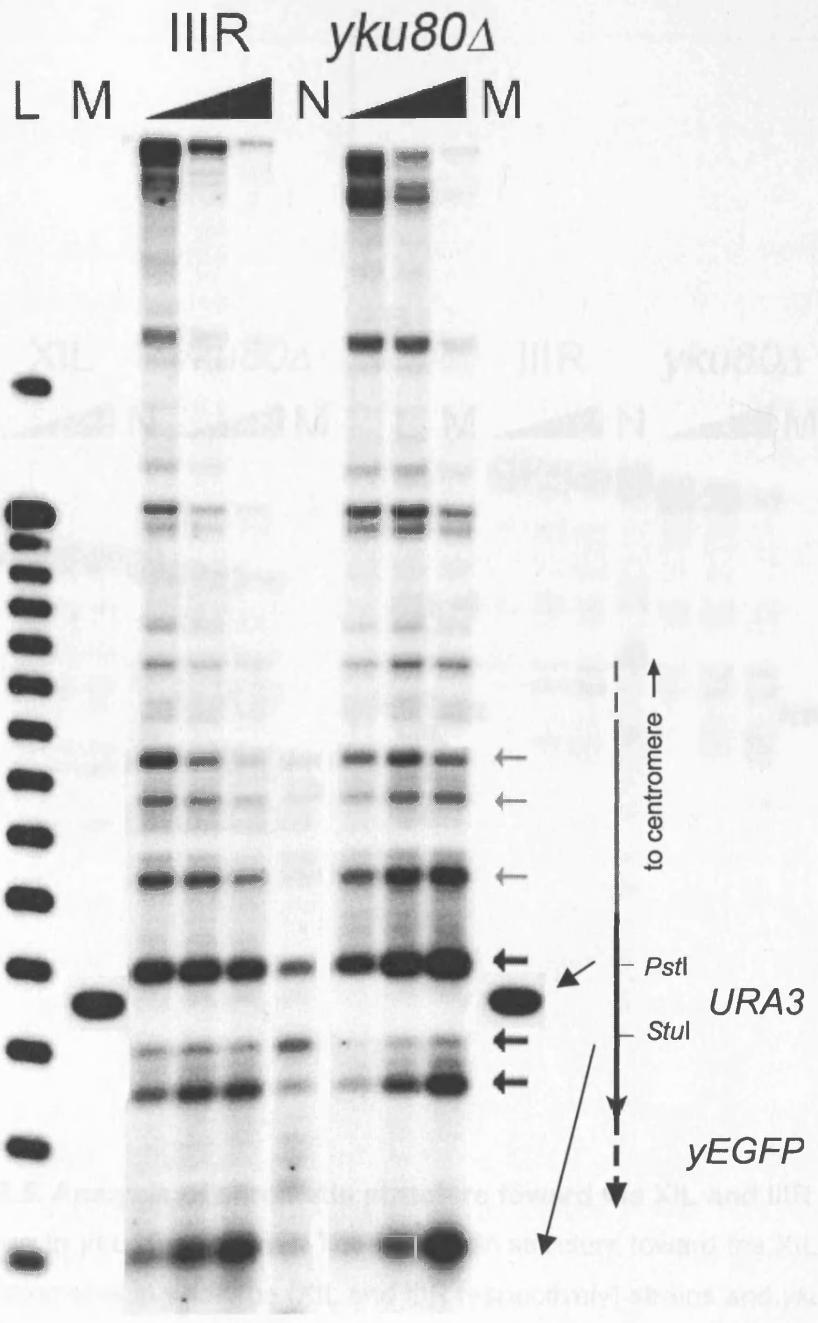

Figure 6.4. Comparison of chromatin structures toward the centromere at IIIR in a *yku80*Δ mutant. The subtelomeric chromatin structures of the *URA3-yEGFP* marked IIIR telomere in the wild-type (IIIR) and *yku80*Δ mutant strains were analyzed by MNase digestion and indirect end labeling at the *Stu*I site as described previously. Black and grey arrows are as in previous figures.

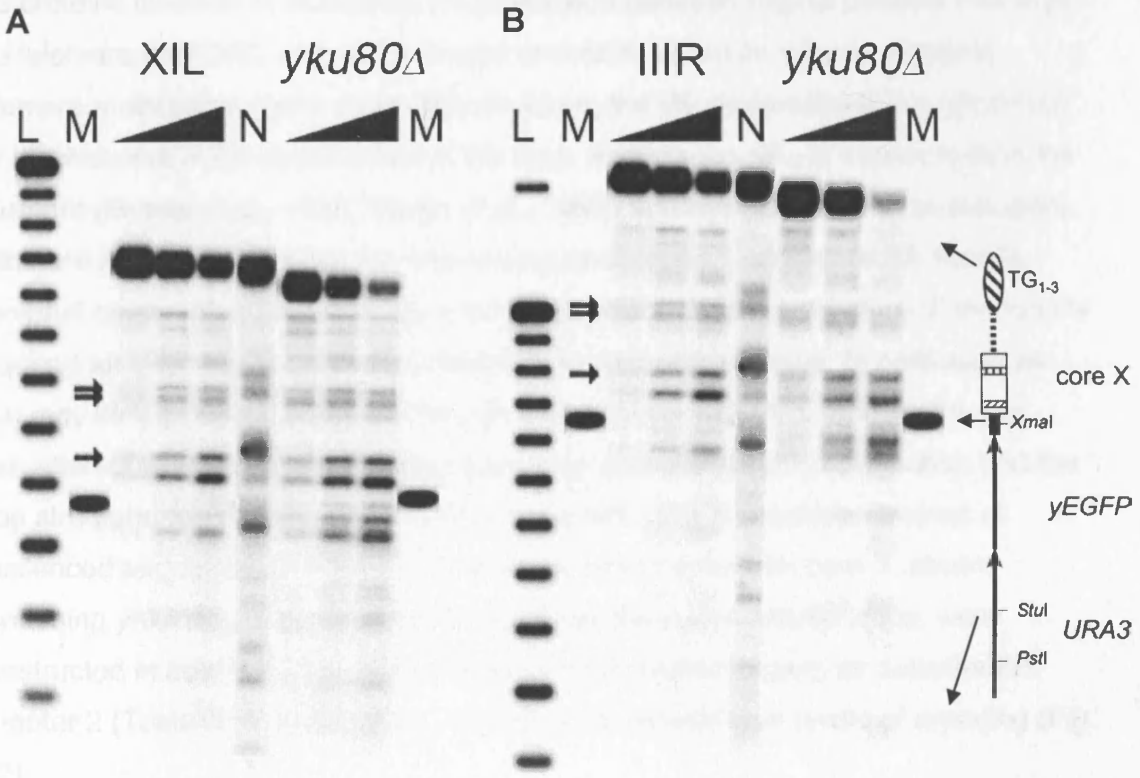

Figure 6.5. Analysis of chromatin structure toward the XIL and IIIR telomeres in *yku80*Δ mutants. The chromatin structure toward the XIL (A) and IIIR (B) telomeres in wild-type (XIL and IIIR respectively) strains and *yku80*Δ mutants were analyzed by MNase digestion and indirect end labeling as described previously. The XIL-marked strains were end labeled at the *Bst*XI site using the GFP_{tel} probe (see Fig. 6.1). The 645bp marker bands (M), generated by digestion with *Bst*XI and *Xma*I, are positioned to indicate the *URA3*-core X junction. The IIIR-marked strains were end-labeled at the *Stu*I site. Labels and arrows are as previously described.

6.3.4 The binding of *yKU80* to core X is not disrupted in the core X^{mut} strain

The looping model for the stabilization of native silencing proposes that there are proteins involved in stabilizing the interaction between Rap1p proteins bound at the telomere and ORC and Abf1p bound at core X. Given its roles in silencing, telomere maintenance and chromatin structure, the yKu heterodimer is a candidate for involvement in the stabilization of the loop. Importantly, yKu is known to bind the telomere (Gravel *et al.*, 1998; Martin *et al.*, 1999) and has been shown to associate with core X elements but not the intervening unsilenced Y' elements (M. Marvin, personal communication), strongly implicating yKu in the loop structure. If the loop is required for silencing, it should be disrupted in silencing mutants. In particular, as yKu may bind at core X indirectly though associations with ORC and Abf1p, the disruption of their respective binding sites may also disrupt yKu association and the loop structure. In addition, association of yKu with core X should be weaker at unsilenced telomeres. In order to study yKu's interactions with core X, strains containing $yKU80_{Myc}$, tagged at the C-termini at the native *yKU80* locus, were constructed in both the *URA3-yEGFP* and *URA3* marked strains as described in Chapter 2 (Table 6.1). All $yKU80_{Myc}$ strains retained wild-type levels of silencing (Fig. 6.2).

The relative binding of yKu80p-Myc to core X elements at XIL was compared to IIIR in the *URA3-yEGFP* marked strains using QPCR analysis of ChIP samples. Similar to the analysis of Orc1p binding to core X, several primer sets were used to compare the binding of yKu80p-Myc to all core X elements, to the specific core X elements marked with *URA3-yEGFP* in each strain and to the *SEO1* control locus as a measurement of the background level of yKu80p-Myc association. yKu80p-Myc showed very little association with the *SEO1* locus. The IP samples were less than 10-fold enriched over the NoAb samples at *SEO1* (Fig. 6.6), similar to the enrichment observed at other loci at which yKu has no affect (M. Marvin, personal communication). A strong association of yKu80p-Myc with most core X elements was observed in both the XIL and IIIR-marked strains (Fig. 6.6). Intriguingly, the marked IIIR and XIL core X elements were precipitated by the anti-Myc antibodies with similar efficiency, showing ~43-fold and ~70-fold enrichments over the NoAb samples respectively (Fig. 6.6). This result is consistent with the model in which yKu80p provides a link between the telomere repeats and core X to stabilize the loop.

However, it also indicates that both repressive and non-repressive telomeres form the loop structure, raising the question of whether or not the loop is involved in the silencing.

The association of yKu80p-Myc with the native and mutant core X elements at XIL was analyzed in the *URA3*-marked strains. In both the wild-type and core X^{mut} strains, yKu80p-Myc associated strongly with most core X elements, but weakly with *SEO1* control locus (Fig. 6.6).The strong association of yKu80p-Myc with the XIL core X element was not disrupted by ORC and Abf1p binding site mutations in the core X^{mut} (Fig. 6.6). Therefore, yKu associates with core X independently of ORC and Abf1p. This implies the association of yKu with core X may also be independent of the Sir proteins, as the Sirs are believed to bind at core X through interactions with ORC and Abf1p. In addition, the ability of yKu to bind the mutated core X implies the loop may remain intact despite the silencing defect and suggests that ORC and Abf1p may not be required for loop formation. Taken together with the ability of yKu to bind core X at IIIR, these results indicate the loop is insufficient for silencing.

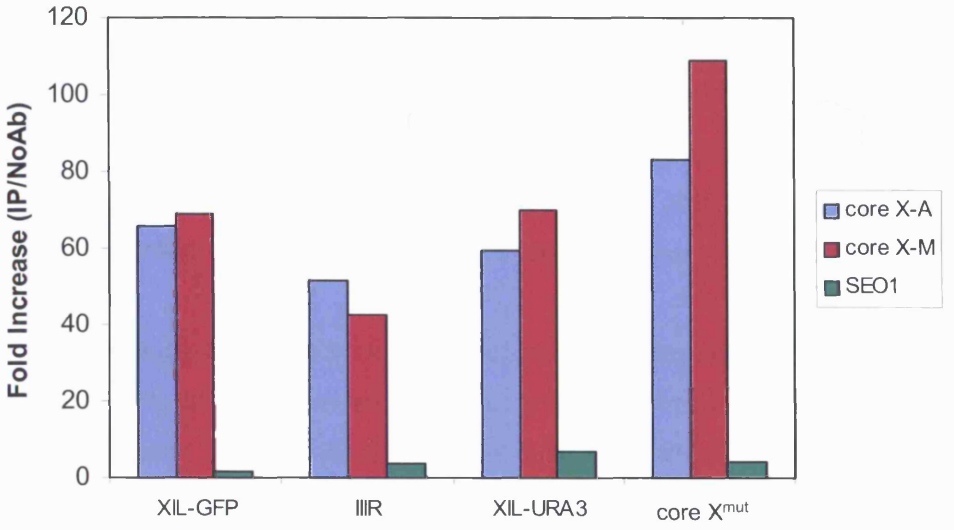

Figure 6.6. Interaction of yKu80p-Myc with intact or mutated core X elements as assayed by chromatin immunoprecipitation (ChIP). ChIP assays were performed with yeast strains containing the *URA3-yEGFP* construct centromere-proximal to the XIL (XIL-GFP) or the IIIR (IIIR) core X elements. Strains containing only the *URA3* reporter at the wild-type (XIL-URA3) or mutated (core X^{mut}) XIL core X element were also analyzed. *yKU80* was tagged with Myc at its native locus in all strains. The binding of $yKu80p_{Myc}$ to many core X elements (core X-A), the marked core X (core X-M) and *SEO1* was analyzed by quantitative PCR. Histogram indicates the fold increase of DNA amplified in the immunoprecipitated samples (IP) over the samples without antibody (NoAb). Plotted values correspond to the median of three independent experiments.

6.3.5 Effect of *yku80*Δ in a core X^{mut} strain

The intermediate chromatin defects of both the core X^{mut} and *yku80*Δ mutants at XIL and the ability of yKu80p to bind both the wild-type and mutant core X elements raises the possibility that these factors act independently to promote silencing and heterochromatin formation. To determine if the effects of these two mutations were additive, *yKU80* was deleted in the core X^{mut} to generate a core X^{mut}, *yku80*Δ double mutant (Table 6.1). Analysis of *URA3* silencing in the double mutant strain indicated a complete disruption of repression (Table 6.2, Fig. 6.2). This was a more severe effect than that previously observed for the *yku80*Δ mutation alone (Table 6.2).

Examination of the combined effect of the two mutations on chromatin structure toward the centromere from XIL by MNase digestion revealed a chromatin structure that was significantly different from either of the single mutants (Fig. 6.7). The structure of the *URA3* promoter was fully open, unlike the intermediate structures of the single mutants (black arrows, Fig. 6.7). In addition, the heterochromatic banding pattern was almost completely disrupted in the core X^{mut}, *yku80*Δ double mutant, as observed in both the chromatin analysis and the band intensity quantification, (grey arrows, Fig. 6.7). This contrasts with the single mutants in which the heterochromatic pattern remained largely intact. Significantly, the chromatin structure of the double mutant is indistinguishable from the structures of the *sir2*Δ, *sir3*Δ and *sir4*Δ mutants (Fig. 6.8, also see Section 4.2.2). This suggests that the core X element and *yKU80* may have partially redundant and independent roles in recruiting the Sir complex. Either single mutation results in a minor disruption of the chromatin structure as Sir proteins can still be recruited, although at a lower frequency. However, simultaneous disruption of both core X and yKu mimics the deletion of the *SIRs* as the Sir complex can no longer be recruited to the telomere. The stronger silencing defect observed for the *yku80*Δ mutant compared with the core X^{mut} strain suggests the Sir-recruitment pathway involving *yKU80* is more important. Similar to the effect observed for the histone modifier mutants, a sufficient proportion of Sir complexes can be recruited to XIL in both the core X^{mut} and *yku80*Δ mutants to form the heterochromatin, but an insufficient number of Sir complexes are present to subsequently establish wild-type levels of silencing. It is also possible that core X is involved in the establishment of silencing at its locus while yKu is important for establishment and maintenance of silencing near telomeres (see Chapter 7).

The chromatin structure of the double mutant was also examined toward the XIL telomere in comparison to the wild type. A shortened telomere could be observed in the core X^{mut}, *yku80*Δ strain, due to the deletion of *yKU80*, but the chromatin structure was otherwise identical to the core X^{mut} pattern (Fig. 6.9). This confirms that deletion of *yKU80* does not affect the chromatin structure toward the telomere.

Figure 6.7. Analysis of chromatin structure toward the centromere at XIL in a core X^{mut}, *yku80*Δ double mutant. A) The subtelomeric chromatin structures of the *URA3* marked XIL telomere in the PIY180 wild-type (XIL) strain and the hERM247 strain (X^{mut}, *yku*Δ) , which carries both the mutated XIL core X and a *yKU80* deletion, were analyzed by MNase digestion as described previously. Samples were end labeled at the *Stu*I site. The marker was generated by digestion of purified DNA with *Stu*I and *Pst*I, and is positioned near the *URA3* TATA box. The chromatin structures of the core X^{mut} and *yku80*Δ mutants (from Fig. 5.2 and Fig. 6.3 respectively) are shown for comparison. The *yku80*Δ pattern was produced by end labeling at the *Bst*XI site. Black and grey arrows and labels are as in previous figures. B) Chromatin band intensity profiles of the wild type (top) and core X^{mut}, *yku80*Δ double mutant (bottom) were generated using Kodak 1D scan. The black and grey arrows indicate the peaks corresponding to the bands marked by the arrows in (A).

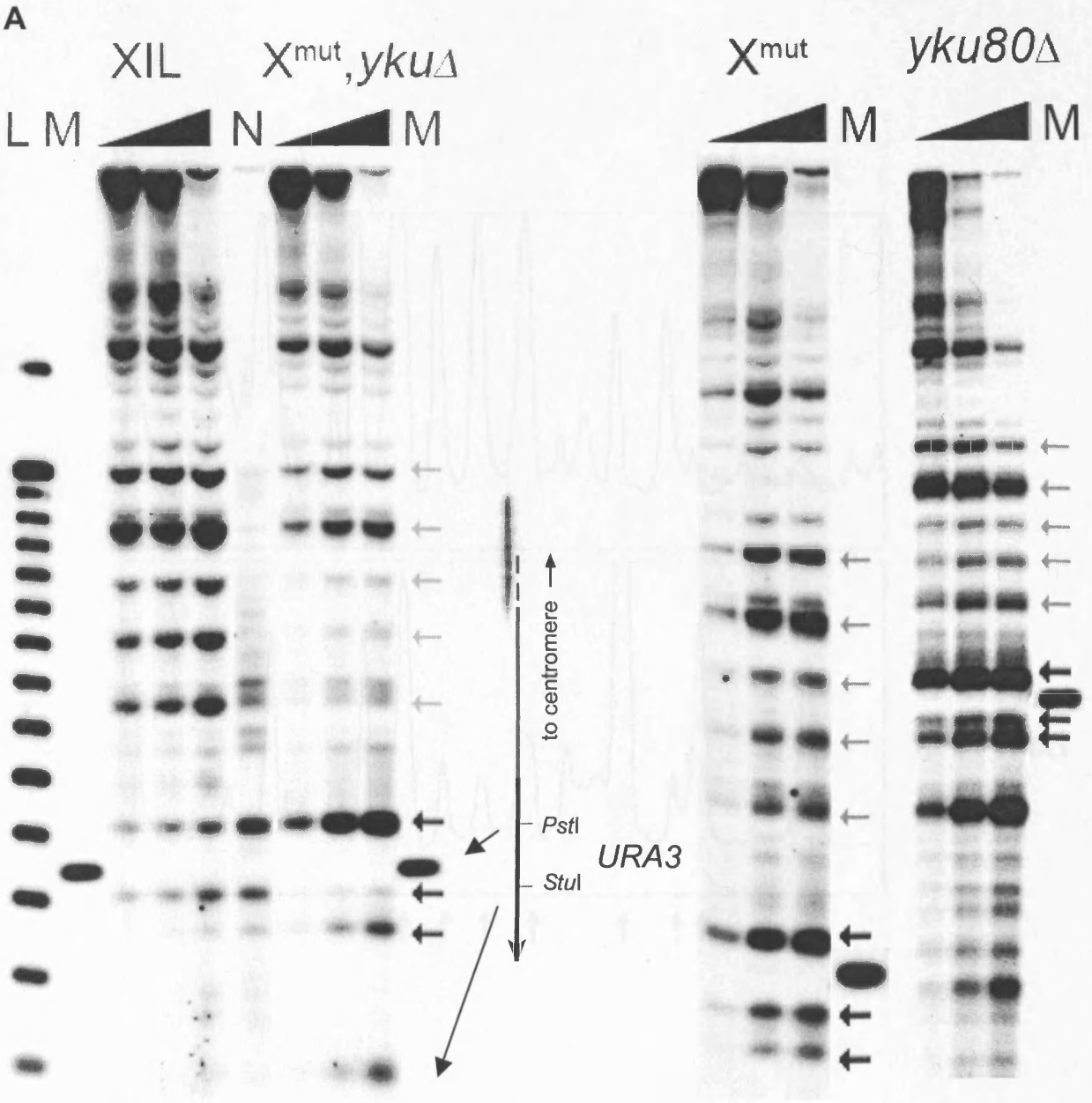

Figure 6.7. Analysis of chromatin structure toward the centromere at XIL in a coreX^{mut}, *yku80*△ double mutant.

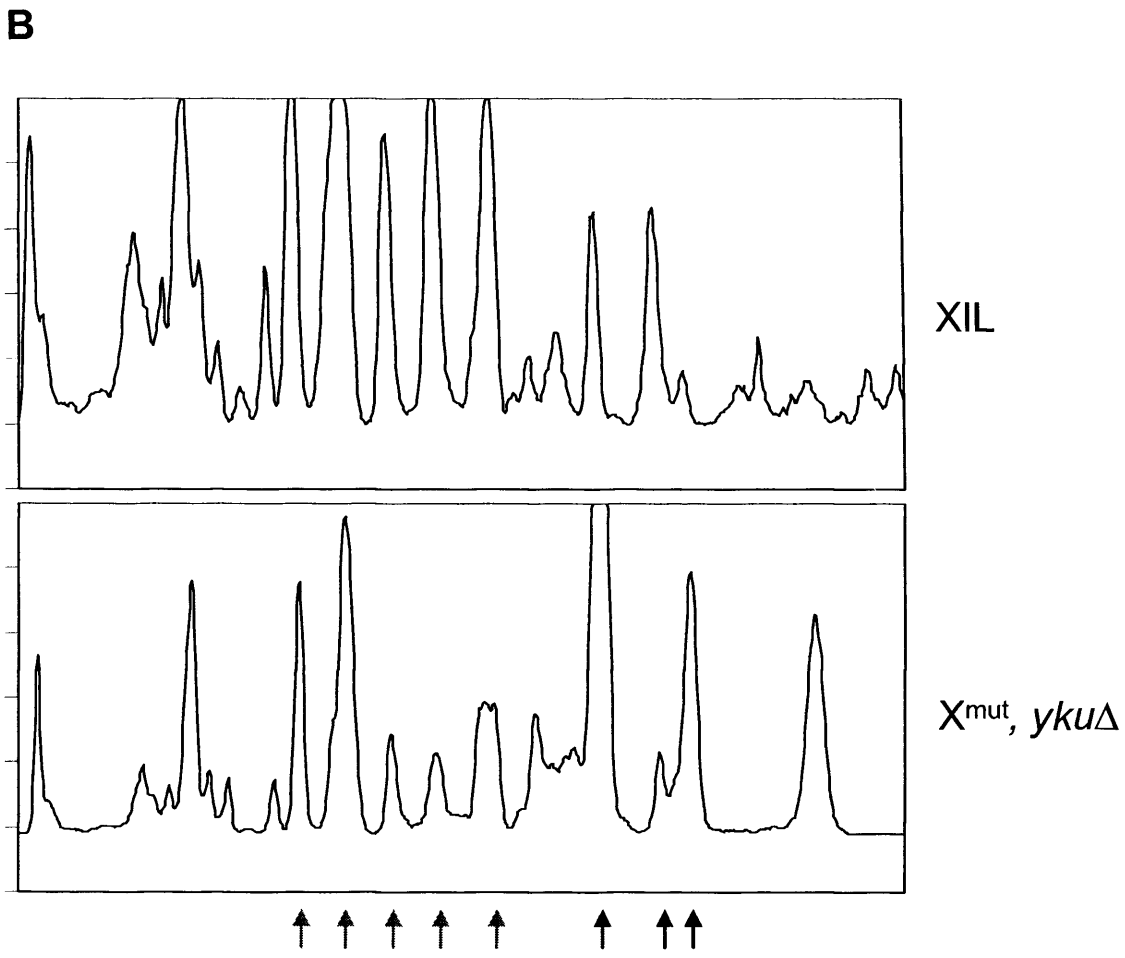

Figure 6.7. Analysis of chromatin structure toward the centromere at XIL in a coreX^{mut}, *yku80*Δ double mutant.

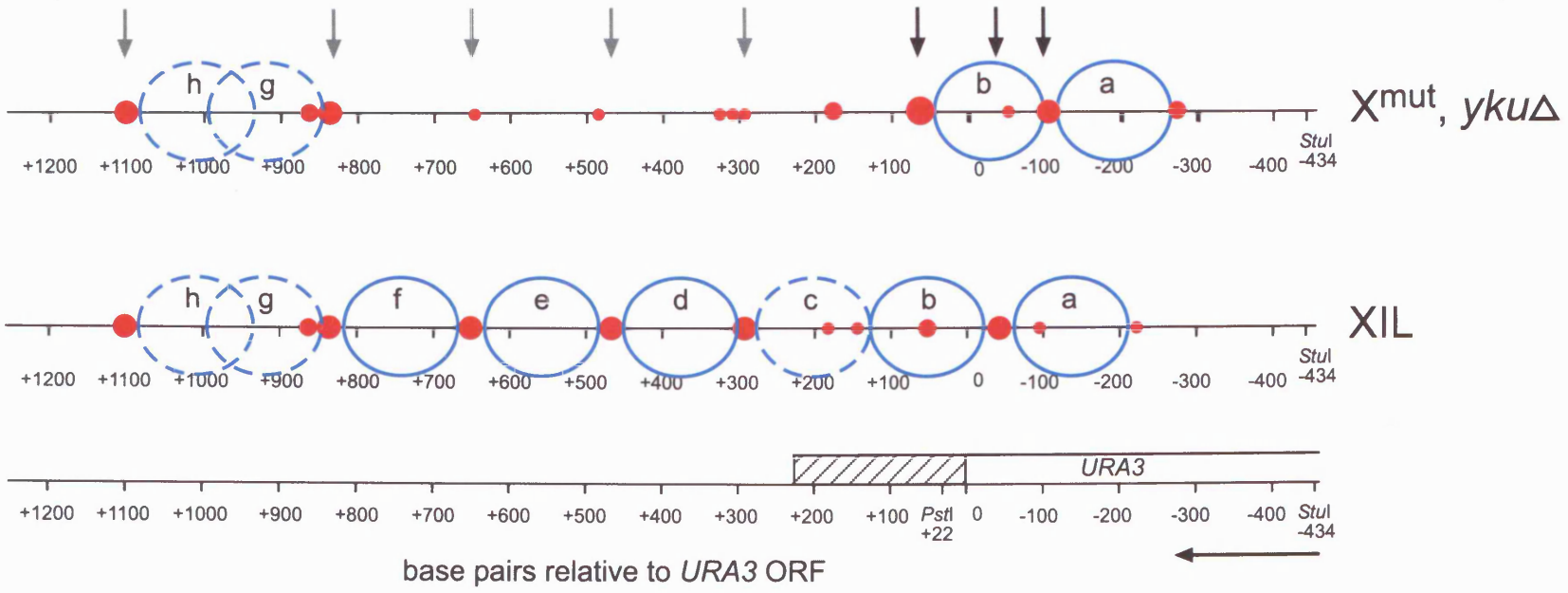

Figure 6.8. Inferred nucleosome positions in the core X^{mut}, *yku80*Δ double mutant toward the centromere from XIL. The position of the *URA3* ORF (open rectangle) and *URA3* promoter (diagonal lines) is indicated in the bottom diagram. The *Stu*I and *Pst*I sites are marked and the URA3$_{cen}$ probe is indicated by the black arrow. Sites of MNase digestion within the XIL sequence are indicated by red circles and inferred nucleosome positions are shown by blue circles. Dashed lines indicate a lower certainty of nucleosome placement. Black and grey arrows correspond to those used to highlight MNase hypersensitive sites in Fig. 6.7. Both the wild-type (XIL) and mutant (X^{mut}, *yku*Δ) chromatin structures are shown.

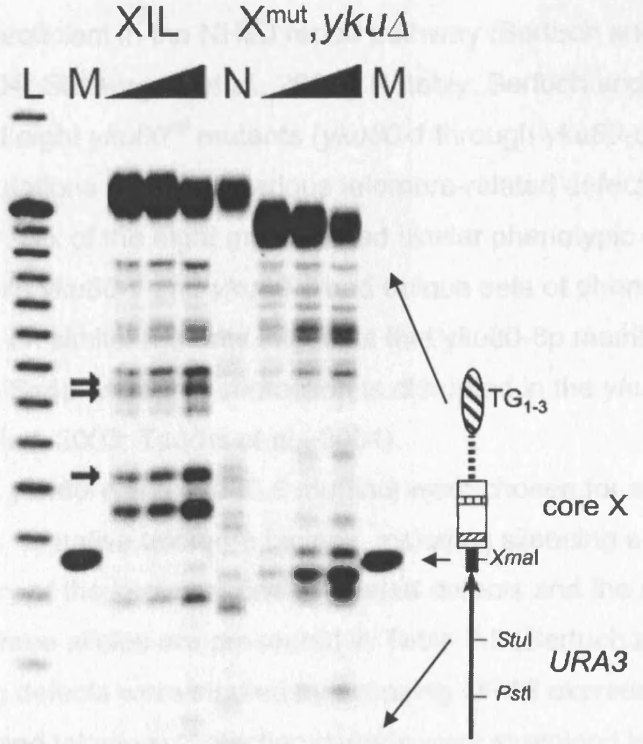

Figure 6.9. Analysis of chromatin structure toward the telomere at XIL in a core X^{mut}, *yku80*∆ double mutant. The subtelomeric chromatin structures toward the telomere of the *URA3* marked XIL telomere in the PIY180 wild-type (XIL) strain and the hERM247 strain (X^{mut}, *yku*∆) , which carries both the mutated XIL core X and a *yKU80* deletion, were analyzed by MNase digestion as described previously. Samples were end labeled at the *Stu*I site. The markers (M), generated by digestion of purified DNA with *Stu*I and *Xma*I, are positioned at the *URA3*-core X junction. Black arrows and labels are as in previous figures.

6.3.6 *yKU80* NHEJ-proficient mutants

One of the difficulties in studying the effect of the yKu heterodimer using full gene deletions are the myriad roles of this complex in diverse cellular processes. In particular, deletions of *yKU80*, as used in this study, affect not only the telomere-related processes under study but also disrupt DNA repair. Recently a variety of yKu separation-of-function mutants have been described that have telomere-related defects but are still proficient in the NHEJ repair pathway (Bertuch and Lundblad, 2003; Roy *et al.*, 2004; Stellwagen *et al.*, 2003). Notably, Bertuch and Lundblad (2003) characterized eight *yku80*^{tel} mutants (*yku80-1* through *yku80-8*), most of which carry single point mutations and have various telomere-related defects but little to no defect in DNA repair. Six of the eight mutants had similar phenotypic defects in telomere biology while *yku80-1* and *yku80-8* had unique sets of phenotypes. Work from several groups on similar mutants suggests that yku80-8p maintains the wild-type interaction with Sir4p while this interaction is disrupted in the *yku80-4* mutant (Bertuch and Lundblad, 2003; Taddei *et al.*, 2004).

The *yku80-1*, *yku80-4* and *yku80-8* mutants were chosen for analysis in this study of their effects on native telomere biology, including silencing and chromatin structure. A summary of the known telomere related defects and the specific mutations of these three alleles are presented in Table 6.3 (Bertuch and Lundblad, 2003). The silencing defects were studied by assaying *URA3* expression at a truncated telomere and telomere protection defects were examined by telomere length measurements and assessing the length of the single-stranded G-rich overhang (G-tail) of the telomeres. A full *yKU80* deletion mutant shows a strong increase in the length of the G-tail, together with a shorter telomere, indicating a severe end-protection defect (Table 6.3).

All three *yku80*^{tel} alleles and the wild-type *yKU80* gene were transformed separately into strains marked with *URA3-yEGFP* at XIL or IIIR (Table 6.1). Both parental strains contained full deletions of the endogenous *yKU80* ORF. The wild-type and mutant alleles were carried on CEN plasmids also encoding the *LEU2* selectable marker and were expressed under the control of the native *yKU80* promoter. In addition, each allele was tagged at the C-terminus with 18 copies of the Myc tag for use in ChIP assays.

Table 6.3. Summary of telomere properties of *yku80^{tel}* mutants

Allele	Mutation	G-tail defect	Telomere length (bp)	Silencing at a truncated end
yKU80	None	wild type	~320	wild type
yku80-1	L240S	moderately severe	~270	Abolished
yku80-4	P437L	moderate	~270	Impaired
yku80-8	L149R	slight	~285	Impaired
yku80Δ	None	severe	~145	Abolished

Phenotypes of the wild type and full *yKU80* deletion are shown for comparison. Data reproduced from Bertuch and Lundblad (2003).

6.3.7 Temperature sensitivity in *yku80^{tel}* mutants

The temperature sensitivity observed in *yku80Δ* strains is also thought to be related to an end-protection defect (Boulton and Jackson, 1996; Feldmann and Winnacker, 1993). At lower temperatures, *yku80Δ* strains are viable despite the end-protection defects resulting in shorter telomeres. However, in the absence of yKu80p higher temperatures appear to destabilize a protective telomere structure resulting in the temperature sensitivity. This role in stabilizing a structure required for telomere protection is similar to yKu80p's proposed role in stabilization of the loop structure of the telomere in silencing. The temperature sensitivity of the *yku80^{tel}* mutants was assessed to examine their ability to stabilize the proposed protective structure. In agreement with the different degrees of loss of end-protection observed by Bertuch and Lundblad (2003) (Table 6.3), *yku80-1* and *yku80-4* mutants showed significantly reduced growth at 37°C, while *yku80-8* remained viable (Fig. 6.10). The mutants in strains marked at XIL and IIIR were tested. Only the XIL-marked strains are shown as results were identical to the IIIR-marked strains.

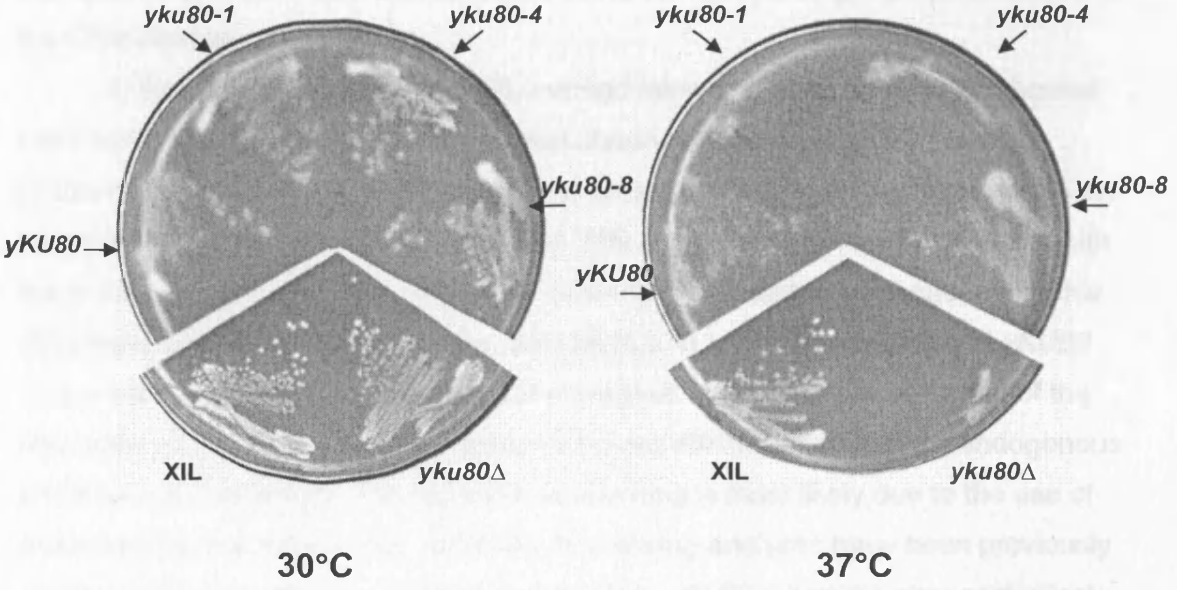

Figure 6.10. Temperature sensitivity in *yku80^{tel}* mutants. The temperature sensitivity of hERL13 (*yKU80*), hERL15 (*yku80-1*), hERL17 (*yku80-4*) and hERL29 (*yku80-8*) was assayed by growth at 30°C (A) and 37°C (B) as described in Chapter 2. The growth of the wild-type FEP318-19 (XIL) strain and PIY133 (*yku80Δ*) at both temperatures are also shown.

6.3.8 Effects of *yku80^{tel}* mutants on TPE at native ends

The silencing defects of the *yku80^{tel}* mutants at both the repressive and non-repressive telomeres were analyzed. A similar method to that described previously was used with the exception that both the complete and FOA media also lacked leucine to maintain selection for the plasmids carrying the mutants. In addition, the wild-type level of silencing was assessed using the full *yKU80* gene expressed from the CEN plasmid.

In the strains containing the XIL-marked telomere, all three mutants showed reductions in silencing consistent with that observed for the full *yKU80* deletion (Table 6.4). However, the wild-type level of silencing in the strain carrying *yKU80* on the plasmid was only 6% compared to the 30% observed in the wild-type strain with the endogenous *yKU80* gene. There are a number of possible explanations for this difference. The reduction in silencing may be due to variable expression of *yKU80* from a plasmid rather than its native chromosomal locus, or to the presence of the Myc epitopes. However, the Myc epitopes did not effect silencing at the endogenous *yKU80* locus (Table 6.2). The reduction in silencing is most likely due to the use of plates lacking leucine as plate variability in silencing analyses have been previously observed (data not shown). Of the three mutants, *yku80-1* had the strongest effect, completely abolishing silencing, while *yku80-8* had the weakest effect, reducing repression ~15-fold (Table 6.4). These data are consistent with the relative defects of these mutants in silencing at a truncated telomere (Table 6.3) (Bertuch and Lundblad, 2003).

The wild-type level of silencing at IIIR in the strain expressing *yKU80* from the plasmid was similar to that of the wild-type strain with the endogenous *yKU80* gene (Table 6.4). The *yku80-1* mutant showed no effect on repression at IIIR while *yku80-8* slightly increased the repression of the marker. Interestingly, the *yku80-4* mutant exhibited an increase in silencing at IIIR comparable to that previously observed for a full *yku80Δ* mutant (Table 6.4). This may indicate the increase in repression at IIIR in *yku80-4*, *yku80-8* and *yku80Δ* mutants is related to disruption of a specific function of *yKU80* that is unaffected in the *yku80-1* mutant. This idea is also supported by the fact that a *yku70Δ* mutant did not increase silencing at IIIR (see Table 6.2), confirming the increase is not due to a general disruption of the yKu heterodimer and is instead specific to the yKu80p subunit. Examples of the silencing assays are shown in Fig. 6.11.

Table 6.4. Frequency of FOA resistance in *yku80^{tel}* mutants for the *URA3-yEGFP* marker inserted at XIL or IIIR.

Strain	Mutation	Chromosome	%FOA^R	
hERL13	*yKU80$_{Myc18}$*	XIL	4 – 8	(6)
hERL15	*yku80-1$_{Myc18}$*	XIL	0	(0)
hERL17	*yku80-4$_{Myc18}$*	XIL	0 – 0.03	(0.01)
hERL29	*yku80-8$_{Myc18}$*	XIL	0.3 – 0.6	(0.4)
hERL14	*yKU80$_{Myc18}$*	IIIR	0.01 – 0.05	(0.03)
hERL16	*yku80-1$_{Myc18}$*	IIIR	0.05 – 0.06	(0.056)
hERL18	*yku80-4$_{Myc18}$*	IIIR	0.75 – 1.83	(1.15)
hERL30	*yku80-8$_{Myc18}$*	IIIR	0.1 – 0.14	(0.12)
FEP318-19		XIL	10 – 42	(25)
FEP318-23		IIIR	0.002 – 1.6	(0.02)
PIY133	*yku80Δ*	XIL	0.09 – 0.25	(0.15)
PIY134	*yku80Δ*	IIIR	0.4 – 2.4	(1.2)

The range of FOA resistance values from a minimum of three independent measurements is shown with the average value given in parenthesis. Cells were plated on complete synthetic media and FOA media lacking leucine to maintain selection for the plasmids encoding the *yku80^{tel}* mutants. The values for the wild-type and full yku80 deletion strains are also shown for comparison. FOA resistance was analyzed as described in Chapter 2.

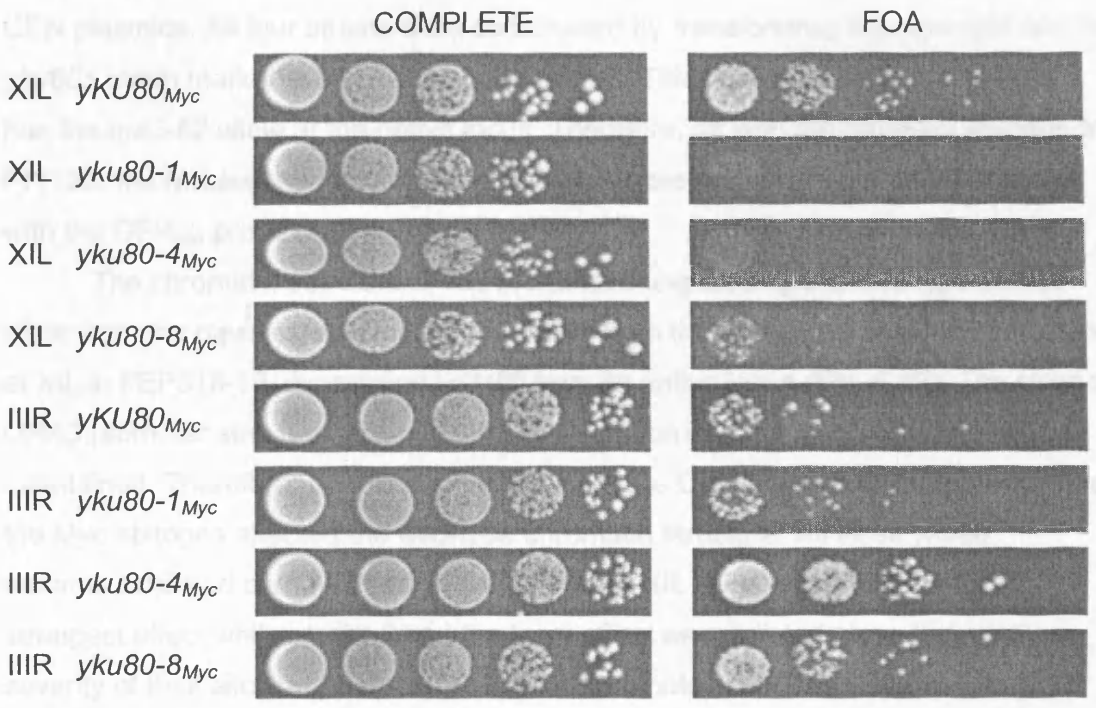

Figure 6.11. Examples of *URA3* repression assays in *yku80^{tel}* mutants. The growth of strains expressing the wild-type *yKU80* or *yku80^{tel}* alleles from a CEN plasmid in strains marked at either XIL or IIIR are shown. Ten-fold serial dilutions of single colonies were plated on complete synthetic media or media containing FOA and grown for three days at 30°C as described in Chapter 2.

6.3.9 *yku80^{tel}* mutants have intermediate effects on repressive chromatin structure

Chromatin structure toward the centromere at XIL was analyzed in strains containing each of the *yku80^{tel}* mutants or the wild-type *yKU80* gene expressed from CEN plasmids. All four strains were constructed by transforming the plasmids into the *yku80Δ* strain marked with *URA3-yEGFP* at XIL. This parental strain (PIY133) also has the *ura3-52* allele at the native locus. Therefore, as with the previous analysis of PIY133, the MNase treated chromatin samples were end labeled at the *Bst*XI site with the GFP_{cen} probe (Fig. 6.1).

The chromatin structure of XIL in hERL13, expressing the wild-type *yKU80* allele from the plasmid, was indistinguishable from the previously observed structure at XIL in FEP318-19, expressing *yKU80* from its native locus (Fig. 6.12). The closed *URA3* promoter structure and wild-type heterochromatic banding pattern were both maintained. Therefore, neither expression from the CEN plasmid nor the presence of the Myc epitopes affected the wild-type chromatin structure. All three *yku80^{tel}* mutants exhibited chromatin structure defects at XIL (Fig 6.12). *yku80-1* had the strongest effect while *yku80-8* had the least effect as predicted given the relative severity of their silencing defects. The *URA3* promoter structure was intermediate between the open and closed state in all three mutants, similar to the phenotype of *yku80Δ*. The MNase hypersensitive site close to the TATA box (top black arrows, Fig. 6.12) showed increased digestion, indicative of more open promoters. In the *yku80-4* mutant the lower two promoter-associated bands were of approximately equally intensity (two black arrows below the marker band, Fig. 6.12). The central band was slightly more intense than the lower one in *yku80-8*, while the opposite was observed for *yku80-1* (Fig. 6.12). Therefore, the promoter was closer to the open conformation in *yku80-1* and closer to the closed structure in *yku80-4* and *yku80-8*. In addition, the intensity of the heterochromatic bands was clearly reduced in the *yku80-1* mutant (grey arrows, Fig 6.12). There was an increase in MNase digestion between the hypersensitive sites in the *yku80-4* and *yku80-8* mutants, but the intensity of the bands was close to wild-type (grey arrows, Fig. 6.12). Therefore, the chromatin structure at XIL in the *yku80-1* mutant was very similar to that observed in a *yku80Δ* strain, while *yku80-4* and *yku80-8* mutants exhibited more moderate disruptions of the repressive chromatin structures.

Figure 6.12. Analysis of chromatin structure toward the centromere at XIL in *yku80^{tel}* mutants. A) The subtelomeric chromatin structure of the *URA3-yEGFP* marked XIL telomere in hERL13 (XIL), hERL15 (*yku80-1*), hERL17 (*yku80-4*) or hERL29 (*yku80-8*) was analyzed by MNase digestion as described previously. Samples were end labeled at the *Bst*XI site using the GFP_{cen} probe. The 982bp markers, generated by digestion of purified DNA with *Bst*XI and *Pst*I, are positioned to indicate the *URA3* TATA box. Labels and arrows are as in previous figures. B) Chromatin band intensity profiles of all strains were generated using Kodak 1D scan. The black and grey arrows indicate the peaks corresponding to the bands marked by the arrows in (A).

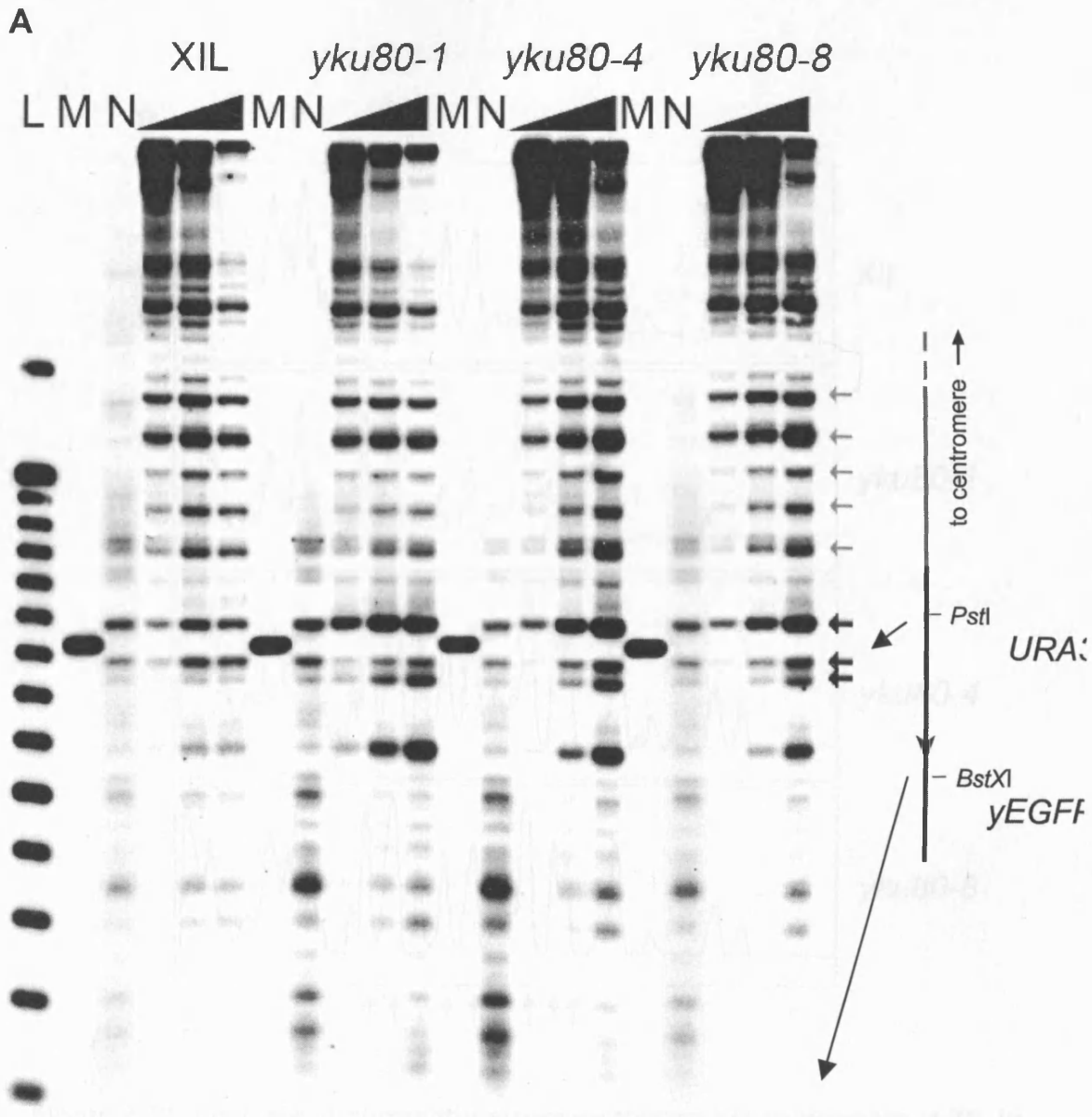

Figure 6.12. Analysis of chromatin structure toward the centromere at XIL in *yku80^{tel}* mutants.

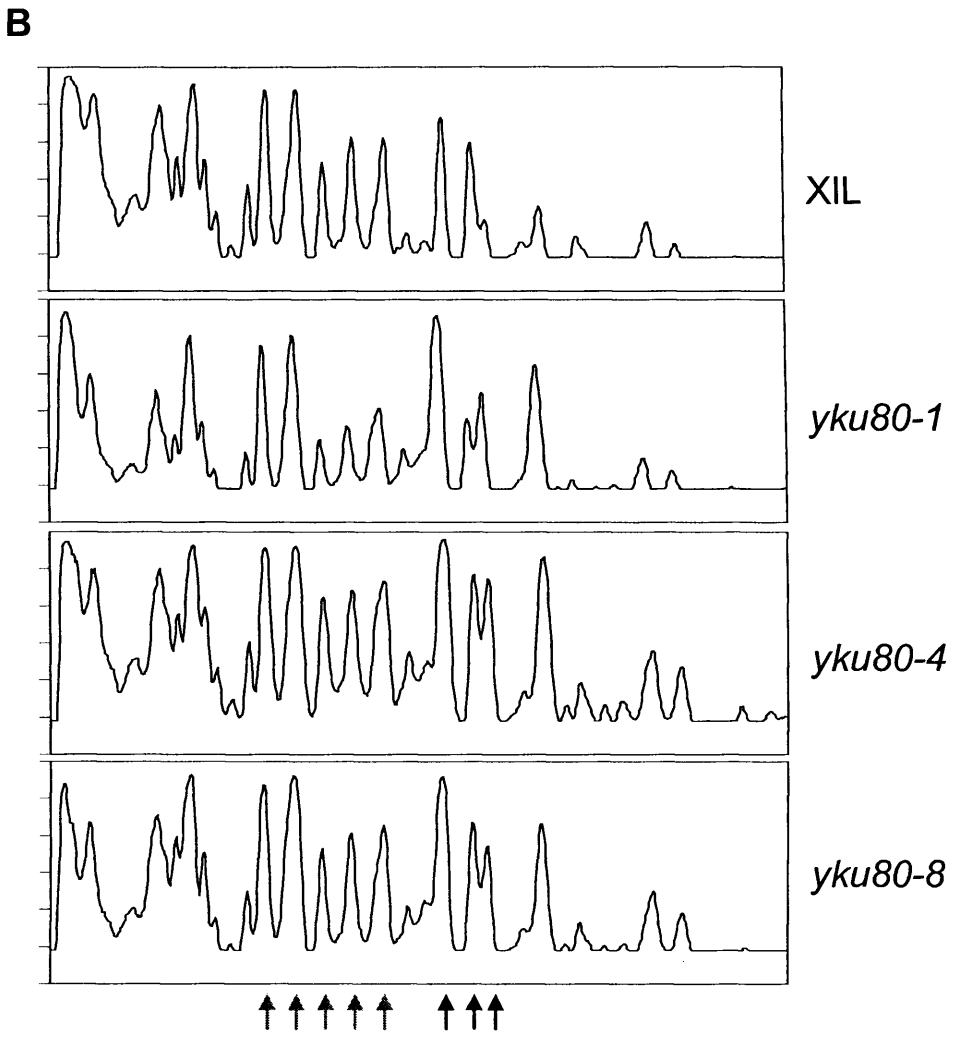

Figure 6.12. Analysis of chromatin structure toward the centromere at XIL in *yku80^{tel}* mutants.

6.3.10 Non-repressive chromatin is unaltered in *yku80*^{tel} mutants

None of the *yku80*^{tel} mutants had a significant effect on the chromatin structure toward the centromere of the IIIR telomere (Fig.6.13), as predicted from the results of the full *yKU80* deletion. For consistency between the XIL and IIIR analyses of these mutants, the chromatin samples from the strains marked with *URA3-yEGFP* at IIIR were also end labeled at the *Bst*XI site. In all three mutants and the *yKU80* wild-type strain, the promoter was clearly maintained in the open conformation of the non-repressive telomere and the euchromatic structure was also unaffected (Fig. 6.13). The apparent differences in band intensity in some of the mutants compared to the wild-type strain are a result of slight differences in the amount of DNA digested by MNase due the increased difficulty in spheroplasting the cells after growth in synthetic media. However, the overall profile of band intensity was almost identical in the mutants and wild-type as shown in Fig. 6.13B.

Figure 6.13. Analysis of chromatin structure toward the centromere at IIIR in *yku80^{tel}* mutants. A) The subtelomeric chromatin structure of the *URA3-yEGFP* marked IIIR telomere in hERL14 (IIIR), hERL16 (*yku80-1*), hERL18 (*yku80-4*) or hERL30 (*yku80-8*) was analyzed by MNase digestion as described previously. Samples were end labeled at the *Bst*XI site using the GFP_{cen} probe. The 982bp markers, generated by digestion of purified DNA with *Bst*XI and *Pst*I, are positioned to indicate the *URA3* TATA box. Labels and arrows are as in previous figures. B) Chromatin band intensity profiles of all strains were generated using Kodak 1D scan. The black and grey arrows indicate the peaks corresponding to the bands marked by the arrows in (A).

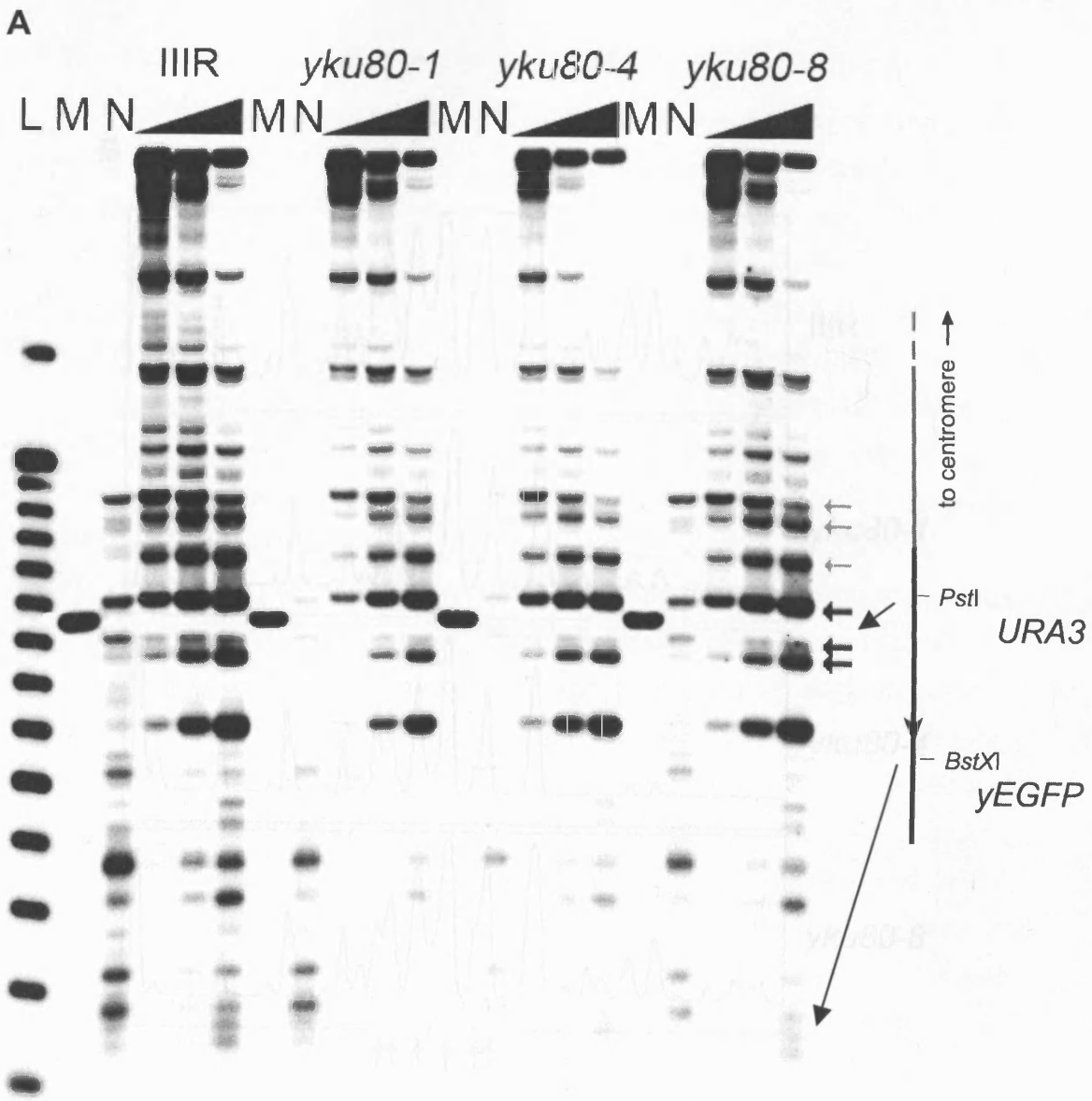

Figure 6.13. Analysis of chromatin structure toward the centromere at IIIR in *yku80^{tel}* mutants.

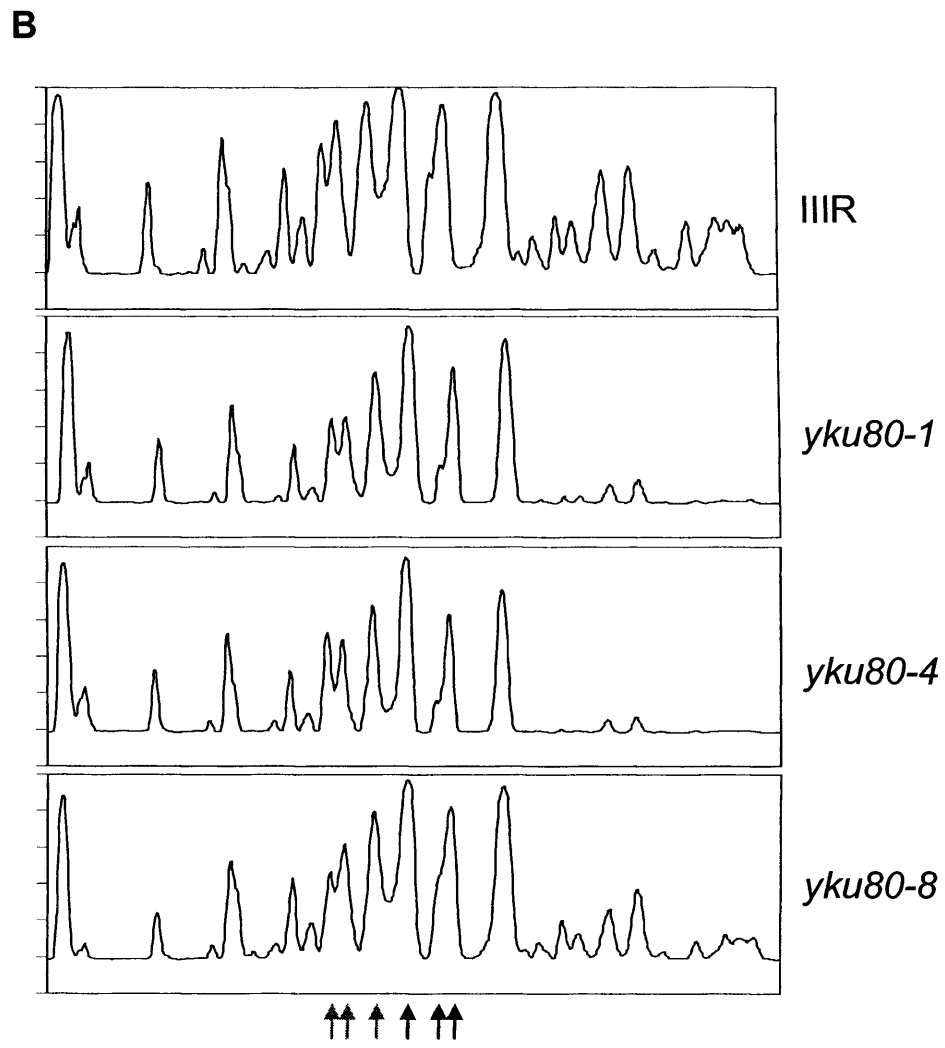

Figure 6.13. Analysis of chromatin structure toward the centromere at IIIR in *yku80^{tel}* mutants.

6.3.11 Effect of *yku80Δ* and *yku80^{tel}* mutants on telomere length

The effect of the *yku80Δ* and *yku80^{tel}* mutants on the telomere length of the XIL and IIIR telomeres was examined for a relationship with the silencing defects in these mutants. Deletion of either yKu subunit is known to result in stably shortened telomeres (Peterson *et al.*, 2001; Porter *et al.*, 1996). The effect of the *yku80^{tel}* mutants on bulk telomere length in the YPH275 strain background has been previously analyzed as shown in Table 6.3 (Bertuch and Lundblad, 2003). The average telomere lengths of both the full *yku80* deletion and the *yku80^{tel}* mutants were analyzed to confirm their effect on bulk telomere length in the S288C strains used in this study. The *yku80Δ* strains, with either the XIL or IIIR telomere marked, both showed the expected reduction in telomere length of ~180bp (Fig. 6.14). Reintroduction of the full *yKU80* gene on the CEN plasmid restored the telomeres to almost wild-type length in both strains (Fig 6.14). Although Bertuch and Lundblad reported only a small reduction in telomere length for the *yku80^{tel}* mutants, both the XIL and IIIR marked *yku80-1* and *yku80-4* strains exhibited a similar telomere length defect to the full deletion mutant. The *yku80-8* mutant however had only a mild length defect, reducing telomere length by ~70bp (Fig. 6.14).

To assess the effect of the *yku80^{tel}* mutants on core X-only ends and, in particular, to determine if any length defects can be related to the degree of silencing, the lengths of the individually marked IIIR and XIL telomeres in the *yku80^{tel}* mutants were examined. Both the IIIR and XIL telomeres in the wild-type strains had similar telomere lengths (Fig. 6.15), in agreement with the length analysis in Chapter 3. Although probing with the *URA3* specific probe should yield a single telomere band, there was a second smaller band of ~1500bp present for the *yku80Δ* and *yku80^{tel}* mutants containing the XIL marked telomere (Fig. 6.15). These strains all contain the *ura3-52* allele that hybridizes to the URA3$_{tel}$ probe to yield this second band. At XIL, the full *yku80Δ* mutant had a similar telomere length defect (Fig. 6.15) to that observed in the bulk analysis (Fig. 6.14). Reintroduction of *yKU80* on the plasmid restored the wild-type telomere length. The *yku80-1* and *yku80-4* mutants had telomere length defects similar to the full deletion and *yku80-8* had an intermediate length reduction (Fig. 6.15).

Comparison of telomere lengths in the strains marked at IIIR revealed a different pattern, most notably in the effect of the *yku80-4* mutant (Fig. 6.15). The full *yku80Δ* mutant reduced the length of the IIIR telomere dramatically, and expression

of *yKU80* from the plasmid restored the native length (Fig. 6.15), similar to results at XIL and in the bulk telomere analysis. The *yku80-1* mutant did not reduce telomere length as much as the *yku80Δ* mutant, unlike its effect at XIL. Interestingly, the length of IIIR was increased by ~150bp in the *yku80-8* mutant and strikingly, the *yku80-4* mutant increased the length of the IIIR telomere by over 2kb (Fig. 6.15). Therefore, the *yku80^{tel}* mutants have varying effects on telomere length both between the different mutants and between different telomeres.

Similar end-specific length defects have been previously observed in *tel1 rif1* and *kem1* mutants (Craven and Petes, 1999; Liu *et al.*, 1995). Craven and Petes (1999) observed differences in length regulation both between Y' and core-X only telomeres and between different core-X only ends. In addition, large increases in telomere length of 2-3kb were observed at particular core X-only ends in some transformants, but were shown to be the result of *de novo* insertion of a Y' element (Craven and Petes, 1999). It is therefore possible the same explanation applies to the increase in length observed at IIIR in the *yku80-4* mutant. All *yku80-4* subclones used in the analysis were derived from a single transformant that may have contained a Y' insertion at IIIR. In addition, Y' elements contain a *Stu*I site approximately 2kb from the centromere-proximal end. Therefore, the digestion with *Stu*I would cut within both *URA3* and the inserted Y' element to yield an approximately 4kb band as observed in the *yku80-4* mutant. However, given that the *yku80-8* mutant also showed an increase in the length of IIIR, albeit a much smaller one, the effect of the *yku80-4* mutant may be genuine. Further analysis of separate transformants is therefore required to confirm these preliminary results.

Figure 6.14. Analysis of bulk telomere lengths in *yku80*Δ and *yku80*^{tel} mutants. DNA extracts from three individual colonies of each strain were digested with *Xho*I. Digestion fragments were separated on a 0.5% agarose gel, blotted and probed with a radio-labeled DNA fragment corresponding to the telomere-proximal fragment of the Y' element and the TG_{1-3} repeats. The large smeared bands of approximately 1200bp represent the TRF's while the other larger bands detected are *Xho*I digestion fragments to which the probe has some homology. For determination of fragment size the λ*Bst*EII ladder (L) was also run on the gel and ladder fragments were detected by probing with labeled lambda DNA. Sizes of the marker bands are indicated on the left. A) Analysis of telomere lengths in strains containing the *URA3-yEGFP* marker at XIL including the parental FEP318-19 (XIL) and PIY133 (*yku80*Δ) strains and four strains containing either a wild-type copy of *yKU80* or one of the *yku80*^{tel} mutants, as marked, expressed from a plasmid in PIY133. B) Analysis of telomere lengths in strains containing the *URA3-yEGFP* marker at IIIR including the parental FEP318-23 (IIIR) and PIY134 (*yku80*Δ) strains and four strains containing either a wild-type copy of *yKU80* or one of the *yku80*^{tel} mutants, as marked, expressed from a plasmid in PIY134.

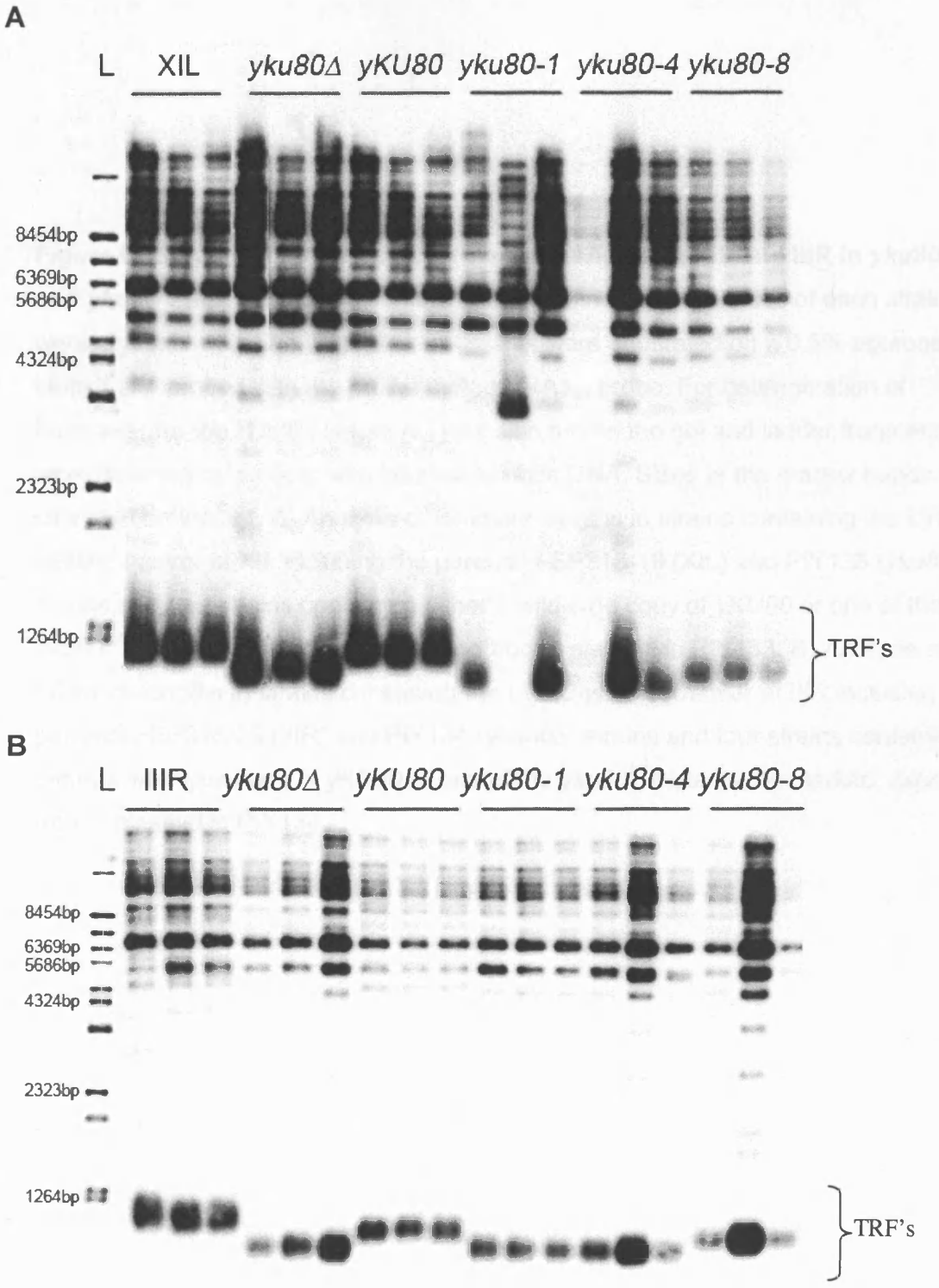

Figure 6.14. Analysis of bulk telomere lengths in *yku80Δ* and *yku80^{tel}* mutants.

Figure 6.15. Analysis of individual telomere lengths at XIL and IIIR in *yku80*Δ and *yku80*^{tel} mutants. DNA extracts from three individual colonies of each strain were digested with *Stu*I. Digestion fragments were separated on a 0.5% agarose gel, blotted and probed with the radio-labeled $URA3_{tel}$ probe. For determination of fragment size the λ*Bst*EII ladder (L) was also run on the gel and ladder fragments were detected by probing with labelled lambda DNA. Sizes of the marker bands are indicated on the left. A) Analysis of telomere lengths in strains containing the *URA3-yEGFP* marker at XIL including the parental FEP318-19 (XIL) and PIY133 (*yku80*Δ) strains and four strains containing either a wild-type copy of *yKU80* or one of the *yku80*^{tel} mutants, as marked, expressed from a plasmid in PIY133. B) Analysis of telomere lengths in strains containing the *URA3-yEGFP* marker at IIIR including the parental FEP318-23 (IIIR) and PIY134 (*yku80*Δ) strains and four strains containing either a wild-type copy of *yKU80* or one of the *yku80*^{tel} mutants, as marked, expressed from a plasmid in PIY134.

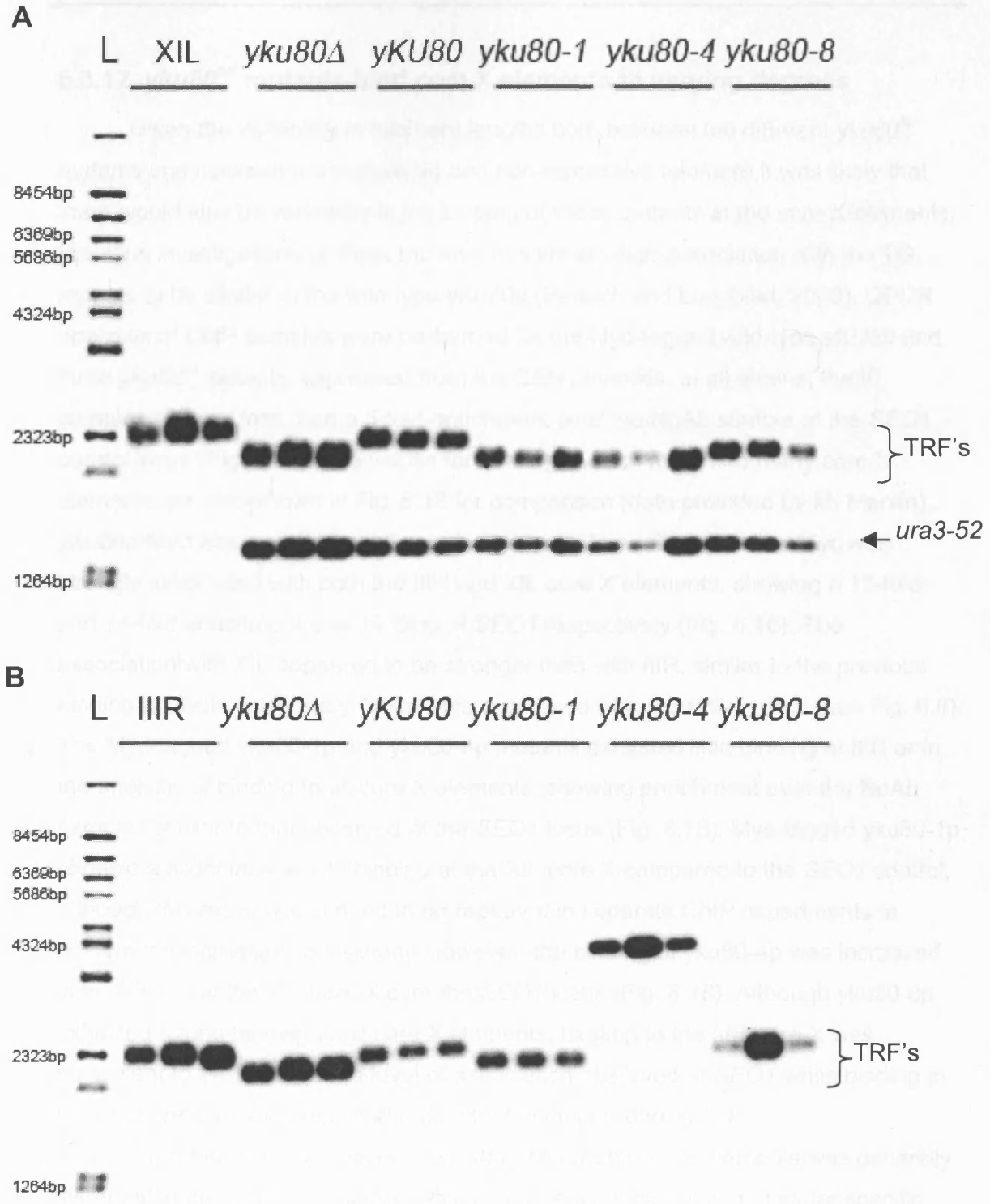

Figure 6.15. Analysis of individual telomere lengths at XIL and IIIR in *yku80*Δ and *yku80*^{tel} mutants.

6.3.12 *yku80^{tel}* mutants bind core X elements to varying degrees

Given the variability in telomere lengths both between the different *yku80^{tel}* mutants and between the repressive and non-repressive telomere it was likely that there would also be variability in the binding of these mutants at the core X elements. Previous investigations of these mutants has shown their association with the TG_{1-3} repeats to be similar to the wild-type yKu80p (Bertuch and Lundblad, 2003). QPCR analyses of ChIP samples were performed for the Myc-tagged wild-type *yKU80* and three *yku80^{tel}* mutants, expressed from the CEN plasmids. In all strains, the IP samples showed less than a 5-fold enrichment over the NoAb sample at the *SEO1* control locus (Fig. 6.16). The values for binding of each mutant to many core X elements are also shown in Fig. 6.16 for comparison (data provided by M. Marvin). yKu80p-Myc was enriched at all core X elements. In addition yKu80p-Myc was strongly associated with both the IIIR and XIL core X elements, showing a 13-fold and 24-fold enrichment over binding at *SEO1* respectively (Fig. 6.16). The association with XIL appeared to be stronger than with IIIR, similar to the previous binding analysis using the yKu80p-Myc expressed from its native locus (see Fig. 6.6). The Myc-tagged yku80-1p and yku80-4p mutants exhibited little binding at IIIR or in the analysis of binding to all core X elements, showing enrichment over the NoAb samples similar to that observed at the *SEO1* locus (Fig. 6.16). Myc-tagged yku80-1p showed a slight increase to binding at the XIL core X compared to the *SEO1* control, although this result would need to be repeated in separate ChIP experiments to confirm the increase is consistent. However, the binding of yku80-4p was increased almost 8-fold at the XIL core X over the *SEO1* locus (Fig. 6.16). Although yku80-8p exhibited strong binding to all core X elements, binding to the IIIR core X was equivalent to the background level of association observed at *SEO1* while binding to the XIL core X was increased almost 18-fold compared to *SEO1*.

Therefore, the association of yKu80p-Myc with core X elements was generally disrupted in the yku80-1p mutant, which showed little association at either specific ends or to most core X elements. yku80-4p exhibited a general inability to bind core X elements but still retained a degree of binding to the XIL core X (Fig. 6.16). yku80-8p had the least binding defect of the three mutants. yku80-8p still retained wild-type levels of association with core X elements and the XIL association was only moderately disrupted compared to wild type. These results could be consistent with the ability of *yku80-4* and *yku80-8* mutants to retain a degree of *URA3* silencing at

XIL as *yku80-8* showed both the least silencing and the least binding defects at XIL. In addition, the *yku80-1* mutant completely abrogated silencing at XIL and had the greatest defect in binding to the XIL core X. However, correlating the binding and silencing phenotypes at IIIR is more difficult. The strain expressing yku80-4p exhibited an increase in silencing over wild-type at IIIR and yet, like yku80-1p and yku80-8p, yku80-4p did not appear to associate with the IIIR core X. Therefore, the effect of the different binding efficiencies at the two core X elements on aspects of telomere biology will require further investigation. The variations in the effects of these mutants on silencing, telomere length and core X association may provide clues to the differences between repressive and non-repressive ends and the role of yKu at both types of telomeres.

Figure 6.16. Interaction of Myc-tagged yKu80p and yku80^{tel}p mutants with the XIL and IIIR core X elements. ChIP assays were performed with yeast strains containing the *yKU80*, *yku80-1*, *yku80-4* or *yku80-8* and marked with *URA3-yEGFP* at XIL (A) or IIIR (B). All alleles of *yKU80* were C-terminally tagged with Myc and expressed from CEN plasmids under the native *yKU80* promoter. The binding of yKu80p-Myc and the yku80^{tel}p-Myc mutants to many core X elements (core X-A) [data provided by M. Marvin], the marked core X (core X-M) and *SEO1* was analyzed by quantitative PCR. Histograms indicate the fold increase of DNA amplified in the immunoprecipitated samples (IP) over the samples without antibody (NoAb). Plotted values correspond to the median of three independent experiments.

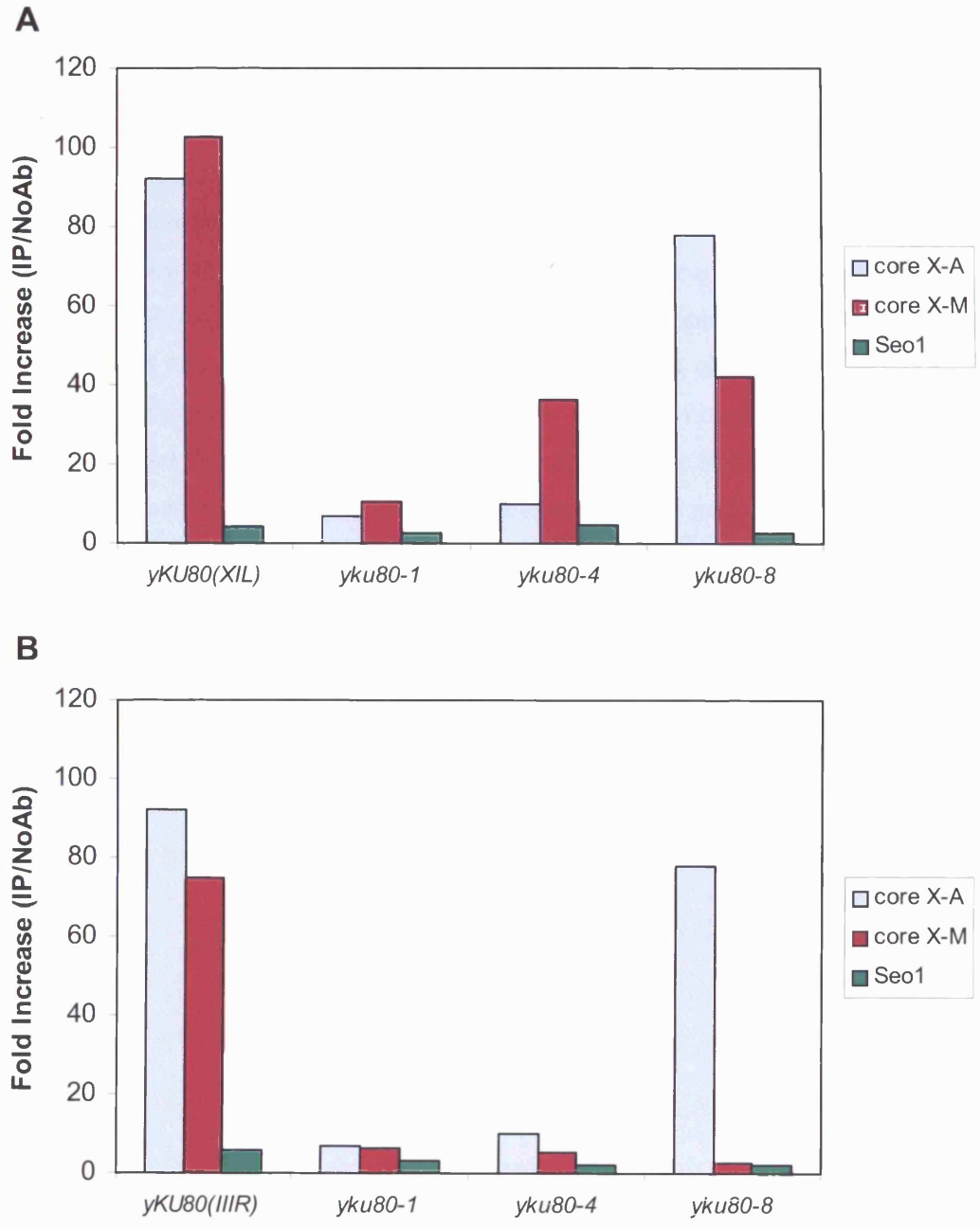

Figure 6.16. Interaction of Myc-tagged yKu80p and yku80^{tel}p mutants with the XIL and IIIR core X elements.

6.4 Summary

The yKu heterodimer is clearly of vital importance in telomere maintenance. The full yKu deletions and the *yku80*^{tel} mutants all exhibited loss of end-protection to varying degrees as shown by their telomere length defects and temperature sensitivity. In addition all the mutants severely disrupted TPE at native ends in conjunction with mild to moderate disruptions of the repressive chromatin structures at XIL. Therefore, in addition to its known roles in NHEJ, telomere length maintenance and silencing, yKu is also important for the assembly of heterochromatin at the telomeres, a function that is separable from its DNA repair function. In this role, yKu acts together with the core X element to establish and maintain the repressive chromatin structure, a function most likely mediated through the recruited Sir complex. Interestingly, yKu80p is able to associate strongly with wild-type and mutant core X elements and at silenced and unsilenced ends, indicating this association does not require ORC or Abf1p and is largely unrelated to silencing. The association of yKu with core X is believed to be indicative of the presence of the loop structure. Therefore, it appears the primary role of the loop is not in silencing, in contrast to the original model. Given the other defects of the yKu mutants in telomere protection, the loop structure may be primarily required for end-protection.

CHAPTER 7

7 Discussion

Heterochromatin is traditionally thought to cause transcriptional repression and silenced domains are believed to be heterochromatic. By this model, disruptions in silencing should be accompanied by disruptions in the heterochromatic structure of the region. However, the data reported in this study challenges this model. Disruptions in silencing were not always accompanied by disruptions in the heterochromatic structure. However, significant silencing was only observed in a heterochromatic region, defined in this study as a region capable of repression in the wild-type state that exhibits compact, phased nucleosome spacing.

Several models involving the looping or folding back of the telomere upon itself or the subtelomeric elements have been proposed to explain many aspects of telomere biology. In particular, Louis and Pryde (1999) have previously proposed the loop model of the telomere as the mechanism of discontinuous silencing centred at the core X element. Unsilenced ends were proposed to not form this loop or to be unable to recruit major factors believed to be important for loop formation, such as ORC or yKu. However, this study suggests the loop is present at native repressive and non-repressive ends. Therefore, revised models for silencing and the role of the loop in telomere biology are proposed below.

7.1 Heterochromatin and silencing

The correlation between silencing at native telomeres and chromatin structure was confirmed by investigations of repressive and non-repressive ends. Both repressive ends exhibited a regular array of translationally phased nucleosomes in the native subtelomeric sequence, similar to previously observed structures at other silenced regions (Ravindra *et al.*, 1999; Vega-Palas *et al.*, 2000; Vega-Palas *et al.*, 1998; Weiss and Simpson, 1998). In contrast, the non-repressive ends examined had distinctly euchromatic structures. This heterochromatic structure was dependent on Sir2p, Sir3p and Sir4p but not Sir1p, in agreement with their respective silencing defects and observations at other heterochromatic loci (Chapter 4) (Ravindra *et al.*, 1999; Vega-Palas *et al.*, 1998; Weiss and Simpson, 1998). Surprisingly, although deletion strains of each of the five chromatin modifiers (*BRE1, DOT1, SET1*, *SAS2* and *BDF1*) showed significant reductions in the silencing of *URA3* at native telomeres, none of them affected the heterochromatic structure of XIL (Chapter 4).

Therefore, in contrast to current models, silencing can be fully disrupted without an accompanying disruption of the repressive chromatin features. Intriguingly, a recent study reported an alteration in the chromatin structure of the *HML* α2 transcriptional start site in a *sas2Δ sir1Δ* mutant similar to the disruption observed in a *sir4Δ* mutant (Osada *et al.*, 2005). The *yku80Δ* mutant had a unique phenotype; repression of *URA3* at XIL was fully disrupted, accompanied by a partial disruption of the heterochromatic structure (Chapter 6, Section 6.3.1-6.3.2). The Sirs are required for the formation of the heterochromatic structure (Section 4.2.2) and yKu is known to be involved in the recruitment of the Sir complex to the telomeres (Martin *et al.*, 1999; Mishra and Shore, 1999; Roy *et al.*, 2004; Tsukamoto *et al.*, 1997). Thus the disruption in silencing and chromatin structure observed in the *yku80Δ* mutant is likely caused by a significant decrease in recruitment of the Sir complex to the telomere. However, as the heterochromatic structure is not fully disrupted, some Sir complexes must still be recruited by a pathway not requiring yKu80p.

These results have significant implications. The regular nucleosomal array observed in heterochromatic regions, while indicative of a silenced domain, is not sufficient for silencing. This suggests the need for a model of heterochromatin formation and silencing in which heterochromatin formation precedes silencing (Fig. 7.1). In addition, the phenotypes of the histone modifier, core X^{mut}, and *yku80* mutants indicate the heterochromatic structure can be formed at a lower concentration of Sir factors than required for silencing. All five histone modifiers examined in this study are involved in maintaining euchromatin or the barrier between euchromatic and heterochromatic regions. The *sas2Δ, dot1Δ* and *bdf1Δ* mutants allow the Sir complex to bind promiscuously (Kimura *et al.*, 2002; Ladurner *et al.*, 2003; San-Segundo and Roeder, 2000; Suka *et al.*, 2002; van Leeuwen *et al.*, 2002), suggesting deletion of *bre1Δ* or *set1Δ* would also allow the Sirs to spread away from silenced domains. In the mutants examined in these studies, Sir association at telomeres is reduced compared to the wild-type but a significant proportion of Sirs are still bound near telomeres (50% or more of the wild-type level of association) (Kimura *et al.*, 2002; San-Segundo and Roeder, 2000; Suka *et al.*, 2002; van Leeuwen *et al.*, 2002). Therefore, this level of Sir association is sufficient to establish the heterochromatic structure but insufficient for silencing.

Deletion of *yKU80*, which is actively required for Sir association at telomeres, presumably decreases the Sir association to a much greater extent than the histone modifier mutants. Therefore, in the *yku80Δ* mutant an insufficient concentration of Sir

factors are present for stabilization of the phased nucleosome structure. This results in the full silencing defect and moderate disruption of the heterochromatic structure. The lesser chromatin defects of some of the *yku80*^{tel} mutants (Section 6.3.9) may indicate these mutants were still able to recruit Sir factors, albeit less efficiently than the wild-type yKu80p. Georgel *et al.* (2001) have proposed that the multiple interactions of the Sir proteins form a highly compact higher order chromatin structure that is inaccessible to transcription. Thus it is reasonable that at a lower level of Sir association, the first order heterochromatin structures can be formed (ie. phased nucleosomes), but the multiple interactions needed to form the fully repressive higher order structures require an increased concentration of Sir factors (Fig. 7.1).

However, in light of this model the phenotype of the core X^{mut} is more difficult to interpret because the core X^{mut} exhibited only a moderate silencing defect but there was also a moderate disruption of the chromatin structure. This conflicts with the model proposed above in which the heterochromatic structure is fully formed prior to silencing. However, as shown in Chapter 5, the core X^{mut} prevents the association of ORC. At the *HM* silencers, ORC recruits Sir1p which is required for establishment but not maintenance of repression. In the absence of Sir1p, silencing can still be established in a subset of cells where it is then maintained by the remaining Sir proteins. This results in the variegated repression of genes, similar to TPE at truncated telomeres. In this study (Section 3.3.2) the chromatin structure of the truncated telomere appeared to be a mixture of the repressive and non-repressive structure, correlating with the variegated repression. The core X^{mut} had a similarly mixed chromatin structure (Section 5.3.2) suggesting variegated repression may also occur in this mutant. Therefore, core X is proposed to be important for establishing silencing within the subtelomeric region, similar to the role of Sir1p at the *HM* loci. In addition, core X is unlikely to be necessary for the maintenance of silencing as repression appears to be maintained in a subset of cells in the core X^{mut}. This proposed role of core X in the establishment of silencing is in agreement with its protosilencer function in which it is known to promote (ie. establish) silencing at a distance from the telomere and across the STAR elements that lie between core X and the telomere.(Fourel *et al.*, 2002; Lebrun *et al.*, 2001). Deletion of Sir1p, however, did not have a similar effect to the core X^{mut} on the heterochromatic structure. Therefore, ORC may have other functions in TPE in addition to the recruitment of Sir1p, in contrast to silencing at the *HM* loci. Perhaps ORC is able to bind other silencing or telosome elements directly to facilitate propagation of the Sir

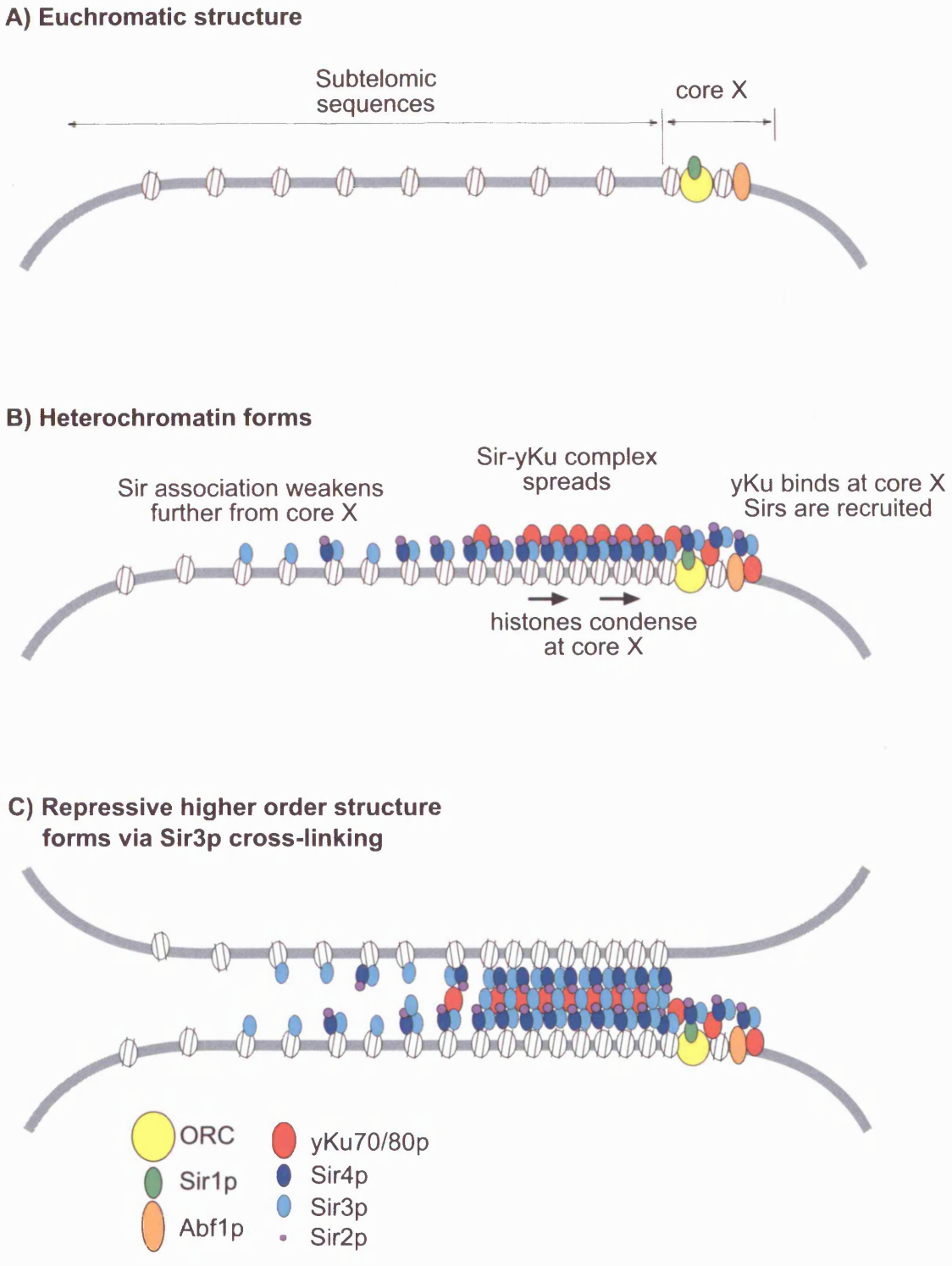

Figure 7.1. Two-step model of the formation of silenced domains near core X. A) ORC and Abf1p are bound at core X. B) Association of yKu with core X helps recruit the Sirs. Spreading of the Sirs results in formation of a compact nucleosome structure near core X. C) Multiple Sir3p factors bind and cross-link heterochromatic regions into a higher order, repressive domain.

complex. The core X^{mut} is also disrupted for the Abf1p binding site and it is likely that the coordinated effects of ORC and Abf1p are required to establish silencing near core X. Indeed, the ACS and Abf1p binding site are known to have additive effects on silencing (Pryde and Louis, 1999).

Intriguingly, combining the deletion of *yKU80* with the core X mutations mimicked the effect of the Sir mutants on the heterochromatic structure. This suggests core X and yKu are both required, and act independently, to recruit and stabilize the Sir complex. Given the strong silencing defect of the *yku80Δ* mutant, yKu is likely important for both establishment and maintenance of silencing. Perhaps yKu acts to recruit the Sir's to the telomere, followed by association of the recruited complex with core X via it's protosilencer function. Once silencing is established at core X by interactions with ORC and Abf1p, the Sir complex spreads to the centromere-proximal region. Silencing across the region is maintained by stabilization of the Sir complex by association with yKu (Fig. 7.1). This model is supported by work demonstrating that tethering yKu70p next to *URA3* at an internal location results in silencing even in the absence of cis-acting silencers (Martin *et al.*, 1999). This shows yKu is able to both establish and maintain silencing. In addition, yKu is known to spread several kilobases into the subtelomere in a Sir-dependent manner (Martin *et al.*, 1999), indicating an association of yKu with the Sir complex.

7.2 The role of the loop structure

The original model, proposed to explain the observations that Rap1p and yKu interacted with the subtelomeric elements in the absence of binding sites, hypothesized a folded telomere structure as described in Chapter 1 (see Fig. 1.6). The folded structure was thought to create a continuous silenced region of core heterochromatin from the telomere (reviewed in Grunstein, 1998; Ray and Runge, 1999). Work by Pryde and Louis (1999) demonstrated that silencing at native telomeres was discontinuous. This led to a modified loop structure of the telomere in which the telomere repeats interacted with the core X element, generating the regions of repression observed at these loci (see Fig 1.6). The non-repressed elements in between the telomere and core X were looped out in a non-heterochromatic structure (Pryde and Louis, 1999). It was originally thought that non-repressive native ends lacked this telomere-core X interaction. As originally proposed, the formation of the loop was thought to be stabilized at core X by interactions between telomere-bound factors such as Rap1p, yKu and the Sir

complex with ORC and Abf1p at core X (Pryde and Louis, 1999). yKu is known to associate strongly with telomeres (Gravel *et al.*, 1998; Martin *et al.*, 1999). The further observation that yKu associates strongly with core X, but only weakly with Y' elements (this study; M. Marvin, personal communication), similar to the binding pattern of Sir factors (van Leeuwen *et al.*, 2002), provided further support for this proposed role of yKu in stabilizing the loop.

However, in contrast to the original model of telomere looping, this study revealed an association of yKu80p with core X at native non-repressive ends, strongly suggesting the telomere-core X interaction is maintained. Deletion of either yKu subunit, in addition to defects in TPE, also leads to defects in telomere length and end protection. Therefore, the role of the loop appears to be primarily for protection of the telomere rather than silencing, similar to the function proposed for the folded telomere structure (Ray and Runge, 1999). This model is supported by the synthetic lethality of yKu mutants with elevated temperatures (Fellerhoff *et al.*, 2000), implying that in yKu mutants an unstable loop is formed that cannot be maintained at elevated temperatures. Therefore yKu is essential for stabilization of the loop but there must also be other factors involved in the loop formation as it is unlikely that Rap1p is solely responsible for the interaction of the telomere with core X in the absence of yKu.

The ORC, Abf1p and Sir factors are not essential for formation of the loop. Disruption of the ORC and Abf1p binding sites did not result in either telomere length defects (Section 5.3.4) or disruption of the yKu association with the mutated core X element (Section 6.3.4). The association of Rap1p with subtelomeric regions was similarly unaffected in a *sir3*Δ mutant (de Bruin *et al.*, 2000). In addition, deletion of *SIR4* does not disrupt yKu binding to core X elements (M. Marvin, personal communication). However, the proposed folding of the telomere in the study by de Bruin *et al.* (2001), detected by transcriptional activation at a truncated telomere by interaction of a downstream UAS with the gene promoter (see Section 1.5.1), was shown to be dependent on Sir3p. However, the telomere in this study lacked the core X element with which yKu interacts. Therefore in the absence of core X, interactions between the telomere and subtelomeric regions may become Sir-dependent. The core X element itself does appear to be required for loop formation and the associated telomere length maintenance as deletion of core X resulted in a longer telomere (Griffin, 2004). Deletion of subtelomeric elements in *P. falciparum* also results in longer telomeres (Figueiredo *et al.*, 2002). This suggests the dependence

of telomere length regulation on subtelomeric elements is not specific to *S. cerevisiae*.

How yKu binds at core X is still unresolved. Intriguingly, in a recent study in humans, deletion of one *KU80* allele decreased the recruitment of ORC subunits to replication origins (Sibani *et al.*, 2005), suggesting Ku may have the ability to associate directly near ACS sites. An earlier study also demonstrated a requirement for yKu70p in ORC assembly at yeast replication origins (Shakibai *et al.*, 1996). This raises the possibility that ORC association with core X may be facilitated by yKu. Although yKu is not essential for silencing at the *HM* loci, it is bound near both *HMR* and *HML* silencers (M. Marvin, personal communication), which may indicate yKu is also able bind the silencer ACS sites.

In the model of telomere looping proposed here, the loop is formed at all ends by interactions between telomere-bound factors and the core X element and is required to maintain and protect the telomeres (Fig. 7.2). The silencing observed close to core X is a secondary effect of the juxtaposition of many strong silencing factors at core X including Rap1p, yKu, ORC and Abf1p, that are all known to recruit the Sir complex. Thus, as with the formation of the heterochromatic nucleosome structure, formation of the loop is required but insufficient for silencing.

The phenotypes of the *yku80*^{tel} mutants, in the context of this model, can be explained by the effects of the specific mutations. Based on a structural analysis, the mutations in *yku80-1* and *yku80-4* are believed to be located in regions important for the heterodimerization of yKu (Bertuch and Lundblad, 2003). These mutants would therefore be predicted to disrupt the loop stabilization function of the yKu heterodimer resulting in the length, telomere protection and silencing defects observed in these mutants. The mutation in *yku80-8*, in contrast, does not appear to affect heterodimerization (Bertuch and Lundblad, 2003). The yku80-8p mutant retained the ability to associate with core X (Section 6.3.12). In addition, similar yku80p mutants were shown to retain their ability to bind the telomere repeats, suggesting yku80-8p may also retain an interaction with the telomere (Roy *et al.*, 2004). This indicates yku80-8p is able to stabilize the telomere-core X interaction in agreement with the modest telomere length and protection defects of this mutant (Section 6.3.7 and 6.3.11). However, despite the presumed formation of the loop, silencing is still significantly reduced in the *yku80-8* mutant. This may be due to the fact that yku80-8p cannot interact with Sir4p (A. Bertuch, personal communication). Thus the TPE defect is due to decreased recruitment of the Sir factors to the telomere.

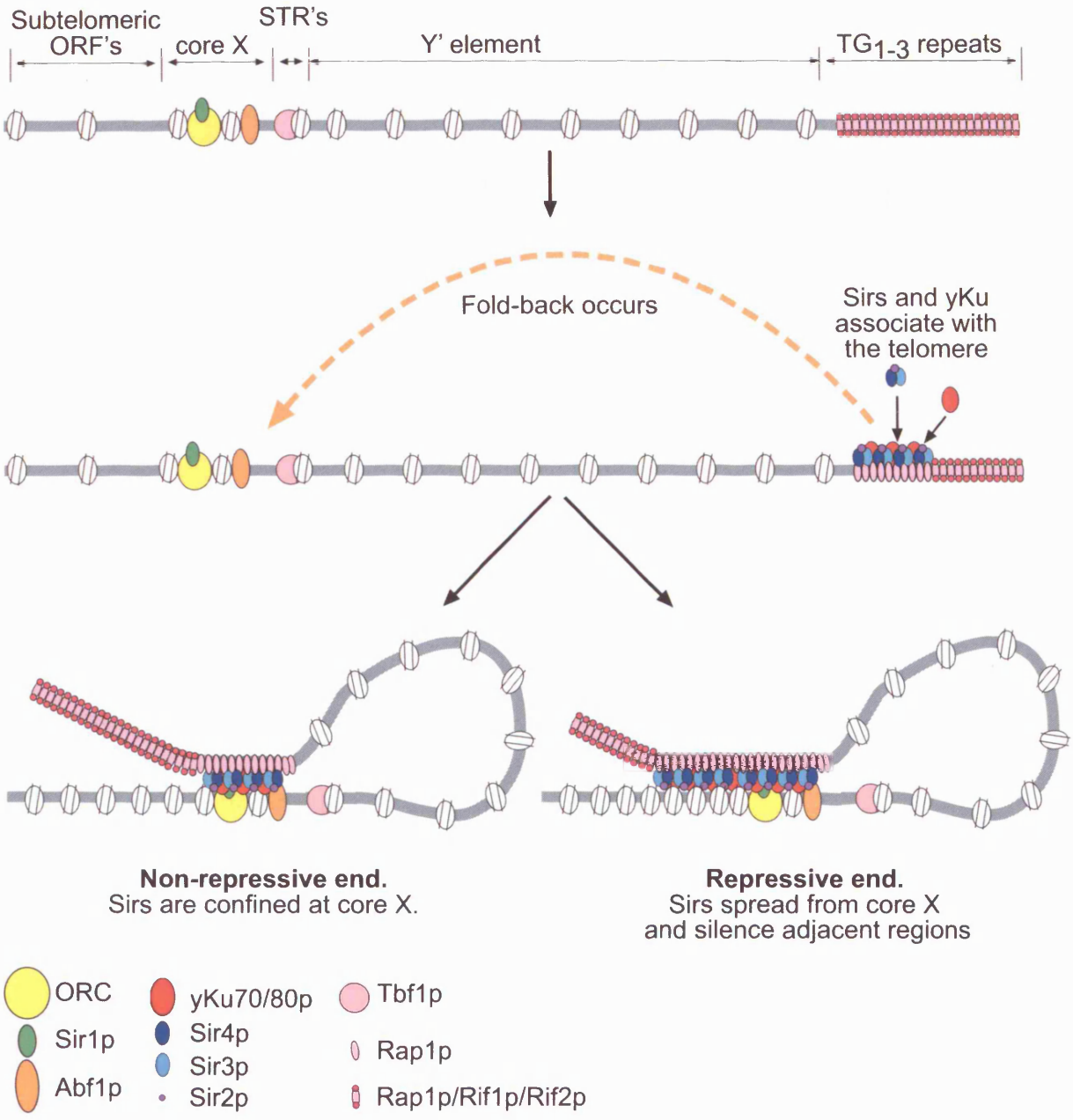

Figure 7.2. Loop model of chromosome ends. Association of yKu with Rap1p at the telomeres facilitates recruitment of the Sir complex. The telomere folds back to interact at the core X element through interactions with yKu at both loci. At non-repressive telomeres the Sirs are confined to core X. At repressive ends the Sirs are able to spread and form a heterochromatic structure adjacent to core X. Symbols are as given in Fig. 7.1.

It is worth noting that the *yku80*^{tel} mutants believed to disrupt the loop (including *yku80-1* and *yku80-4*) also exhibit strong hyper-recombination between telomeres and internal loci (M. Marvin, personal communication). The inhibition on this recombination in wild-type strains is believed to be related to the localization and tethering of telomeres to the nuclear periphery. This is disrupted in yKu deletion mutants (Hediger *et al.*, 2002; Laroche *et al.*, 1998; Taddei *et al.*, 2004). Therefore, it is possible that formation of the loop at telomeres is important for the peripheral localization, as previously proposed by de Bruin *et al.* (2000). However, as these mutants are also thought to be deficient in the ability to form a stable complex with yKu70p, it is possible that the loop formation and peripheral localization roles of yKu are separable but both require formation of the yKu70p/80p heterodimer.

7.3 Silenced or not?

The question of why some ends are silenced, while other seemingly identical ends are not, remains a perplexing one. Tbf1p, which binds the STR elements telomere-proximal to core X, is proposed to have an insulator function suggesting there may be differences in the number of Tbf1p binding sites between the two types of ends. However, previous work by F. Pryde (1999) demonstrated there were no obvious differences in sequence or number of Tbf1p binding sites between repressive and non-repressive ends. Perhaps there are as yet unidentified STAR elements centromere-proximal to the core X element at unsilenced telomeres that prevent the spread of the Sir complex (Fig. 7.2).

The ability of yKu80p and ORC to bind core X at both repressive and non-repressive telomeres suggests the Sir complex should be recruited equally to both types of ends. However, the ChIP on chip study by Lieb *et al.* (2001) indicated a very low association of Sir and Rap1p proteins with non-repressive telomeres. An intriguing possibility is that the unsilenced ends may not be localized to the peripheral telomere clusters and associated silencing foci. However, the yKu heterodimer is known to be one of the major factors in enabling peripheral localization (Hediger *et al.*, 2002; Laroche *et al.*, 1998) and this study has shown it to associate strongly with non-repressive ends. Perhaps additional, and as yet unidentified factors, are required for peripheral localization that are absent at the non-repressive ends. However, the differences in silencing may not be due to differences in peripheral localization.

7.4 The silencing function

Vega-Palas *et al.* (2000) showed that only one of several endogenous ORF's centromere-proximal to core X elements exhibited repression, suggesting that silencing is unlikely to be a general mechanism at telomeres for control of gene expression. Similar to many of the other factors that associate with telomeres, including yKu and the Rad50p/Mre11p/Xrs2p complex, it is more likely that the telomeric foci serve to sequester the Sir silencing factors from the rest of the genome to ensure that inappropriate repression and/or chromatin-remodelling does not occur. These sequestered factors often have additional roles in telomere maintenance. The Sir's also appear to have active functions in length maintenance and chromosome stability as part of the telosome (Bourns *et al.*, 1998; Palladino *et al.*, 1993a). It has therefore been suggested that the primary role of the Sirs at the telomere is to maintain and protect the chromosome end with the silencing of adjacent regions being a secondary effect (Huang, 2002).

7.5 Future directions

There are a wide variety of experiments that would further the understanding of the structure and function of the telomere loop and the nature of silencing at native ends. In particular, as this study dealt exclusively with core X-only ends, similar studies of specifically marked Y' ends would be of great interest. Investigation of yKu association with core X elements at Y' ends would yield insight into the nature of the loop at Y' ends. Perhaps the interaction between core X and the telomere is weakened due to the presence of the Y' element, resulting in the low levels of silencing observed. Alternatively, the Y' elements may prevent the association of the Sir complex despite the presence of a very stable core X-telomere interaction.

It would also be very interesting to examine the effect of various mutants (eg. *sirs*, *bre1*Δ, *dot1*Δ, *sas2*Δ) on the loop structure by assaying the association of yKu and Rap1p with subtelomeric loci in mutant strains. The association of Rap1p and the Sirs with subtelomeric regions in a *yku80*Δ strain would be of particular interest. If the loop is indeed compromised in the absence of yKu80p, the association of Rap1p and the Sirs with core X and other subtelomeric regions should be similarly disrupted. The wild-type yKu80p associated strongly with both types of ends. However, the *yku80*^{tel} mutants exhibited significant differences in both core X association and telomere length defects at the two types of ends, indicating there may be differences in the loop structure and role of yKu at different types of ends. Therefore, further

investigations of the yku80^{tel}p mutants, including their ability to bind the mutated core X element, may also provide further insight into the function of both core X and yKu in silencing and loop formation.

Variegation of repression has traditionally been studied using the *ADE2* reporter gene. Cells in which *ADE2* is repressed are red in colour and strains which are able to switch the repression status of *ADE2* give rise to red and white sectored colonies. Therefore, the role of core X in the establishment versus maintenance of TPE could be examined by replacing the *URA3* reporter gene with *ADE2* in the core X^{mut}. If, as proposed in this study, core X is primarily involved in establishment this strain would be expected to give rise to sectored colonies.

More concrete evidence for the existence of the loop and for the effect of various mutants on the ability of the loop to form could be generated using the 3C (Chromosome Conformation Capture) technique (Dekker *et al.*, 2002). This technique would allow a more direct observation of the structure of chromosome ends and facilitate investigation of the role of various factors in formation of the loop.

Finally, the work presented in this thesis has furthered the understanding of heterochromatin formation and its requirement in silencing and the function of higher order telomere structure. In particular, insight has been gained into the roles of cis- and trans-acting factors in various aspects of telomere biology and the similarities and differences in the effects of these factors at silenced and non-silenced native telomeres. The questions remaining following this work will be addressed by further studies in the months and years ahead.

Appendix 1

Supplementary data for Figure 3.11

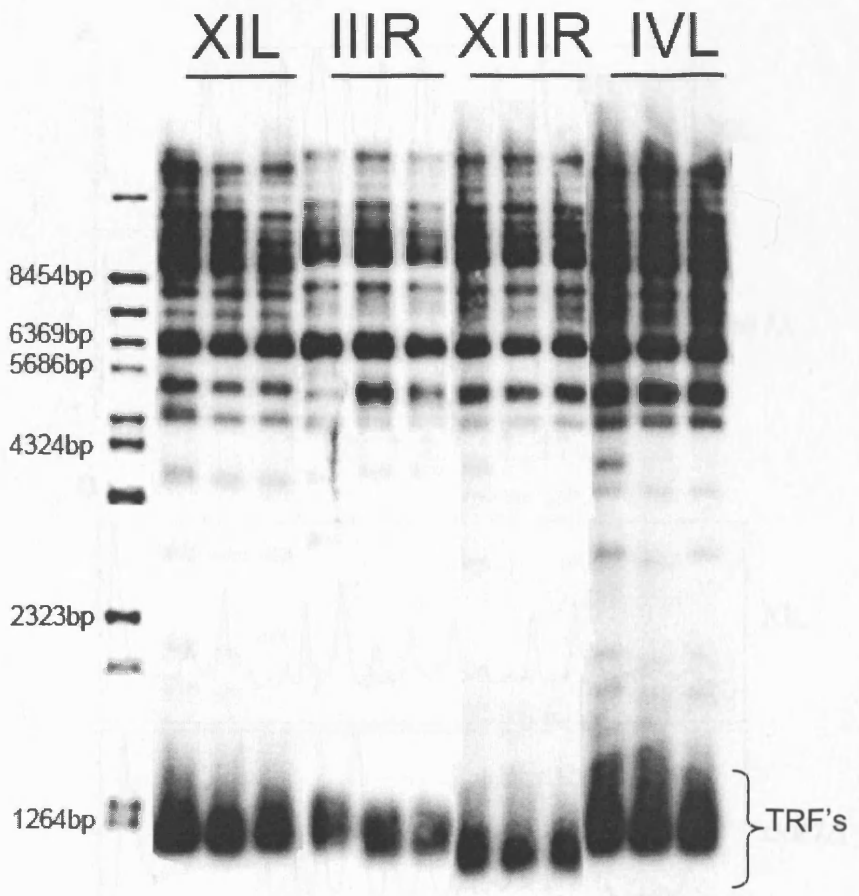

Analysis of bulk telomere length in four *S. cerevisiae* strains. DNA preps from three individual colonies each of the four strains FEP318-19, FEP318-23, FEP100-40 and FEP229-4 (indicated by XIL, IIIR, XIIIR and IVL respectively) were digested with *Xho*I. Digestion fragments were separated on a 0.5% agarose gel, blotted and probed with a radio-labeled DNA fragment corresponding to the telomere-proximal fragment of the Y' element and the TG_{1-3} repeats. The large smeared bands of approximately 1200bp represent the telomere fragments while the majority of the larger bands detected are non-telomeric digestion fragments to which the probe has some homology. For determination of fragment size the _*Bst*EII ladder was also run on the gel and ladder fragments were detected by probing with labelled lambda DNA.

Appendix 2

Supplementary data for Figure 4.7

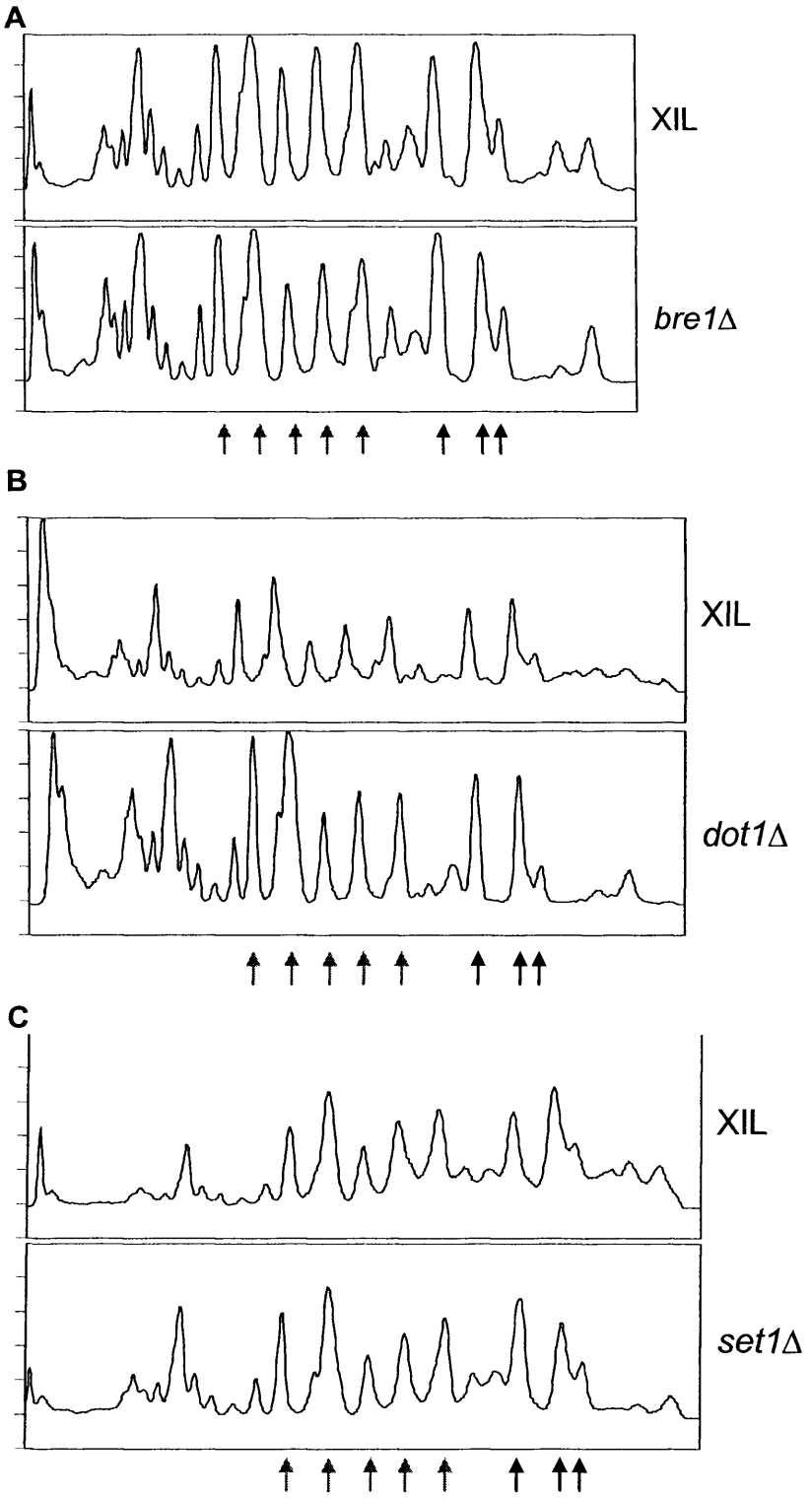

Chromatin band intensity profiles of the methylation mutants. Profiles of the wild-type at XIL and the *bre1Δ* (A), *dot1Δ* (B) and *set1Δ* (C) methylation mutants were generated using Kodak 1D scan. The black and grey arrows indicate the peaks corresponding to the bands marked by the arrows in Figure 4.7.

Appendix 3

Supplementary data for Figure 4.10

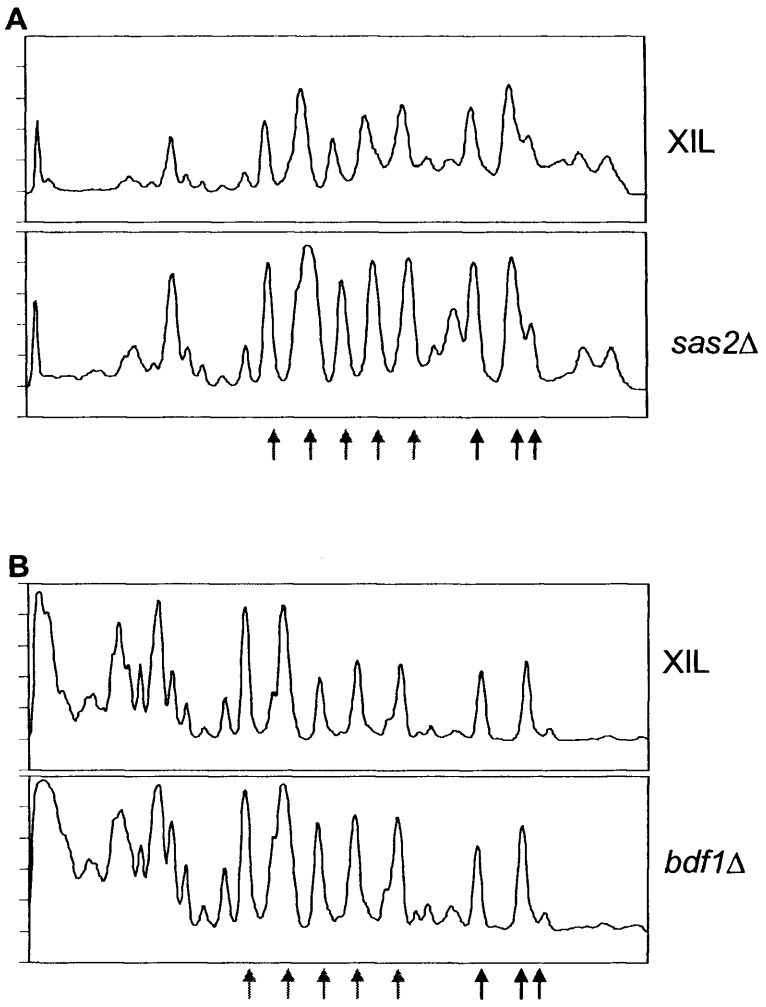

Chromatin band intensity profiles of the acetylation mutants. Profiles of the wild-type at XIL and the *sas2*Δ (A) and *bdf1*Δ (B) mutants were generated using Kodak 1D scan. The black and grey arrows indicate the peaks corresponding to the bands marked by the arrows in Figure 4.10.

Appendix 4

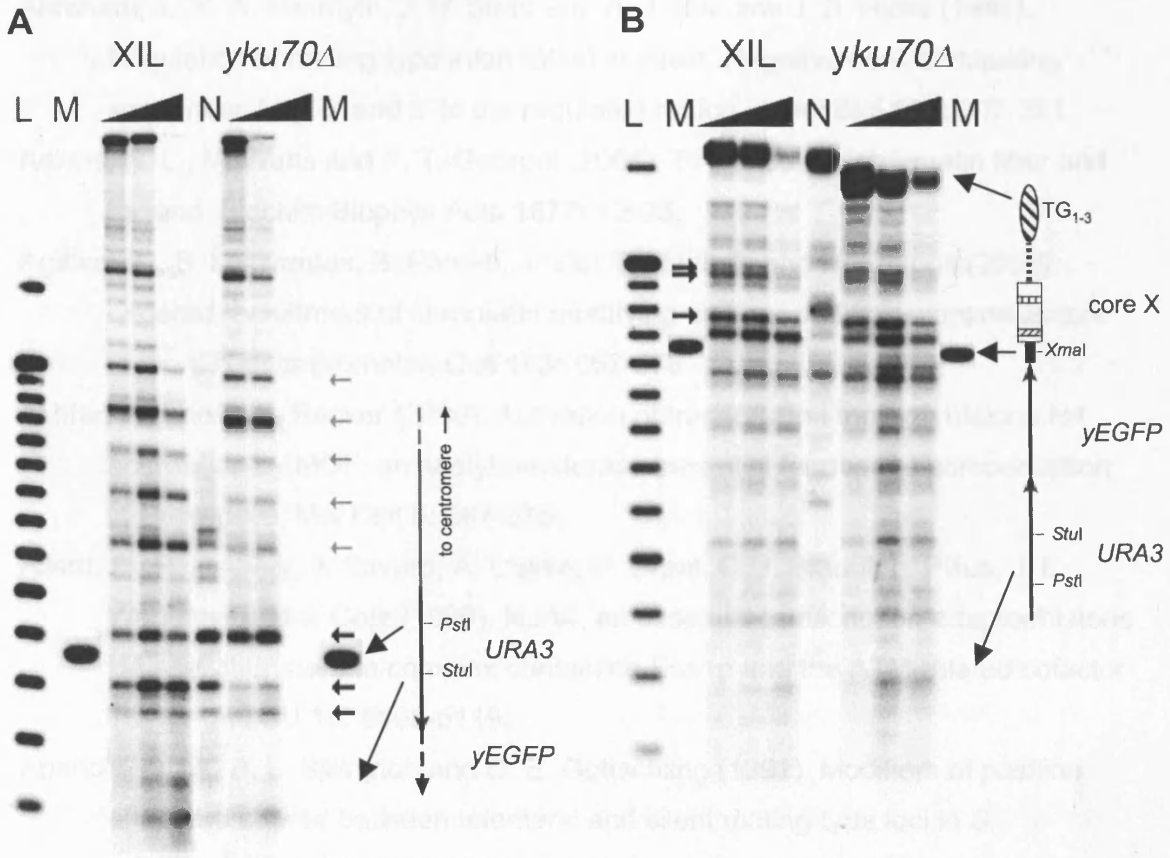

Comparison of chromatin structures at XIL in a *yku70*Δ mutant. A) The subtelomeric chromatin structures of the *URA3-yEGFP* marked XIL telomere in hERM238 (*yku70*Δ) and the wild-type FEP318-19 (XIL) strain were analyzed by MNase digestion and indirect end labeling at the *Stu*I site as described previously. Black and grey arrows are as previously described. A) The chromatin structure toward the XIL centromere. B) The chromatin structure toward the XIL telomere.

9 References

Abraham, J., K. A. Nasmyth, J. N. Strathern, A. J. Klar and J. B. Hicks (1984). Regulation of mating-type information in yeast. Negative control requiring sequences both 5' and 3' to the regulated region. J Mol Biol **176:** 307-331.

Adkins, N. L., M. Watts and P. T. Georgel (2004). To the 30-nm chromatin fiber and beyond. Biochim Biophys Acta **1677:** 12-23.

Agalioti, T., S. Lomvardas, B. Parekh, J. Yie, T. Maniatis and D. Thanos (2000). Ordered recruitment of chromatin modifying and general transcription factors to the IFN-beta promoter. Cell **103:** 667-678.

Akhtar, A., and P. B. Becker (2000). Activation of transcription through histone H4 acetylation by MOF, an acetyltransferase essential for dosage compensation in *Drosophila*. Mol Cell **5:** 367-375.

Allard, S., R. T. Utley, J. Savard, A. Clarke, P. Grant, C. J. Brandl, L. Pillus, J. L. Workman and J. Cote (1999). NuA4, an essential transcription adaptor/histone H4 acetyltransferase complex containing Esa1p and the ATM-related cofactor Tra1p. Embo J **18:** 5108-5119.

Aparicio, O. M., B. L. Billington and D. E. Gottschling (1991). Modifiers of position effect are shared between telomeric and silent mating-type loci in *S. cerevisiae*. Cell **66:** 1279-1287.

Astrom, S. U., S. M. Okamura and J. Rine (1999). Yeast cell-type regulation of DNA repair. Nature **397:** 310.

Bailey, S. M., J. Meyne, D. J. Chen, A. Kurimasa, G. C. Li, B. E. Lehnert and E. H. Goodwin (1999). DNA double-strand break repair proteins are required to cap the ends of mammalian chromosomes. Proc Natl Acad Sci U S A **96:** 14899-14904.

Balajee, A. S., I. Dominguez, V. A. Bohr and A. T. Natarajan (1996). Immunofluorescent analysis of the organization of telomeric DNA sequences and their involvement in chromosomal aberrations in hamster cells. Mutat Res **372:** 163-172.

Bannister, A. J., P. Zegerman, J. F. Partridge, E. A. Miska, J. O. Thomas, R. C. Allshire and T. Kouzarides (2001). Selective recognition of methylated lysine 9 on histone H3 by the HP1 chromo domain. Nature **410:** 120-124.

Barry, J. D., M. L. Ginger, P. Burton and R. McCulloch (2003). Why are parasite contingency genes often associated with telomeres? Int J Parasitol **33:** 29-45.

Barsoum, J., and A. Varshavsky (1985). Preferential localization of variant nucleosomes near the 5'-end of the mouse dihydrofolate reductase gene. J Biol Chem **260:** 7688-7697.

Bartolomei, M. S., and S. M. Tilghman (1997). Genomic imprinting in mammals. Annu Rev Genet **31:** 493-525.

Baumann, P., and T. R. Cech (2000). Protection of telomeres by the Ku protein in fission yeast. Mol Biol Cell **11:** 3265-3275.

Baur, J. A., Y. Zou, J. W. Shay and W. E. Wright (2001). Telomere position effect in human cells. Science **292:** 2075-2077.

Becker, P. B. (1994). The establishment of active promoters in chromatin. Bioessays **16:** 541-547.

Bell, A. C., and G. Felsenfeld (2000). Methylation of a *CTCF*-dependent boundary controls imprinted expression of the *Igf2* gene. Nature **405:** 482-485.

Bell, S. P., and A. Dutta (2002). DNA replication in eukaryotic cells. Annu Rev Biochem **71:** 333-374.

Bell, S. P., R. Kobayashi and B. Stillman (1993). Yeast origin recognition complex functions in transcription silencing and DNA replication. Science **262:** 1844-1849.

Bellard, M., G. Dretzen, A. Giangrande and P. Ramain (1989). Nuclease digestion of transcriptionally active chromatin. Methods Enzymol **170:** 317-346.

Bernstein, B. E., E. L. Humphrey, R. L. Erlich, R. Schneider, P. Bouman, J. S. Liu, T. Kouzarides and S. L. Schreiber (2002). Methylation of histone H3 Lys 4 in coding regions of active genes. Proc Natl Acad Sci U S A **99:** 8695-8700.

Bertuch, A., and V. Lundblad (1998). Telomeres and double-strand breaks: trying to make ends meet. Trends Cell Biol **8:** 339-342.

Bertuch, A. A., and V. Lundblad (2003). The Ku heterodimer performs separable activities at double-strand breaks and chromosome termini. Mol Cell Biol **23:** 8202-8215.

Bi, X., M. Braunstein, G. J. Shei and J. R. Broach (1999). The yeast *HML* I silencer defines a heterochromatin domain boundary by directional establishment of silencing. Proc Natl Acad Sci U S A **96:** 11934-11939.

Bi, X., and J. R. Broach (1999). UASrpg can function as a heterochromatin boundary element in yeast. Genes Dev **13:** 1089-1101.

Bianchi, A., and T. de Lange (1999). Ku binds telomeric DNA *in vitro*. J Biol Chem **274:** 21223-21227.

Bianchi, A., S. Smith, L. Chong, P. Elias and T. de Lange (1997). *TRF1* is a dimer and bends telomeric DNA. Embo J **16:** 1785-1794.

Biessmann, H., and J. M. Mason (1997). Telomere maintenance without telomerase. Chromosoma **106:** 63-69.

Bitterman, K. J., R. M. Anderson, H. Y. Cohen, M. Latorre-Esteves and D. A. Sinclair (2002). Inhibition of silencing and accelerated aging by nicotinamide, a putative negative regulator of yeast *sir2* and human *SIRT1*. J Biol Chem **277:** 45099-45107.

Blackburn, E. H., and C. W. Greider (Editors), 1995 Telomeres. Cold Spring Harbor Laboratory Press, Cold Spring Harbor, New York.

Boeke, J. D., F. LaCroute and G. R. Fink (1984). A positive selection for mutants lacking orotidine-5'-phosphate decarboxylase activity in yeast: 5-fluoro-orotic acid resistance. Mol Gen Genet **197:** 345-346.

Boivin, A., and J. M. Dura (1998). *In vivo* chromatin accessibility correlates with gene silencing in *Drosophila*. Genetics **150:** 1539-1549.

Borst, P., G. Rudenko, M. C. Taylor, P. A. Blundell, F. Van Leeuwen, W. Bitter, M. Cross and R. McCulloch (1996). Antigenic variation in trypanosomes. Arch Med Res **27:** 379-388.

Boscheron, C., L. Maillet, S. Marcand, M. Tsai-Pflugfelder, S. M. Gasser and E. Gilson (1996). Cooperation at a distance between silencers and proto-silencers at the yeast *HML* locus. Embo J **15:** 2184-2195.

Bose, M. E., K. H. McConnell, K. A. Gardner-Aukema, U. Muller, M. Weinreich, J. L. Keck and C. A. Fox (2004). The origin recognition complex and Sir4 protein recruit Sir1p to yeast silent chromatin through independent interactions requiring a common Sir1p domain. Mol Cell Biol **24:** 774-786.

Boulton, S. J., and S. P. Jackson (1996). Identification of a *Saccharomyces cerevisiae* Ku80 homologue: roles in DNA double strand break rejoining and in telomeric maintenance. Nucleic Acids Res **24:** 4639-4648.

Boulton, S. J., and S. P. Jackson (1998). Components of the Ku-dependent non-homologous end-joining pathway are involved in telomeric length maintenance and telomeric silencing. Embo J **17:** 1819-1828.

Bourns, B. D., M. K. Alexander, A. M. Smith and V. A. Zakian (1998). Sir proteins, Rif proteins, and Cdc13p bind Saccharomyces telomeres *in vivo*. Mol Cell Biol **18:** 5600-5608.

Brachmann, C. B., J. M. Sherman, S. E. Devine, E. E. Cameron, L. Pillus and J. D. Boeke (1995). The *SIR2* gene family, conserved from bacteria to humans, functions in silencing, cell cycle progression, and chromosome stability. Genes Dev **9:** 2888-2902.

Brand, A. H., G. Micklem and K. Nasmyth (1987). A yeast silencer contains sequences that can promote autonomous plasmid replication and transcriptional activation. Cell **51:** 709-719.

Brasher, S. V., B. O. Smith, R. H. Fogh, D. Nietlispach, A. Thiru, P. R. Nielsen, R. W. Broadhurst, L. J. Ball, N. V. Murzina and E. D. Laue (2000). The structure of mouse HP1 suggests a unique mode of single peptide recognition by the shadow chromo domain dimer. Embo J **19:** 1587-1597.

Braunstein, M., A. B. Rose, S. G. Holmes, C. D. Allis and J. R. Broach (1993). Transcriptional silencing in yeast is associated with reduced nucleosome acetylation. Genes Dev **7:** 592-604.

Braunstein, M., R. E. Sobel, C. D. Allis, B. M. Turner and J. R. Broach (1996). Efficient transcriptional silencing in *Saccharomyces cerevisiae* requires a heterochromatin histone acetylation pattern. Mol Cell Biol **16:** 4349-4356.

Briggs, S. D., M. Bryk, B. D. Strahl, W. L. Cheung, J. K. Davie, S. Y. Dent, F. Winston and C. D. Allis (2001). Histone H3 lysine 4 methylation is mediated by Set1 and required for cell growth and rDNA silencing in *Saccharomyces cerevisiae.* Genes Dev **15:** 3286-3295.

Briggs, S. D., T. Xiao, Z. W. Sun, J. A. Caldwell, J. Shabanowitz, D. F. Hunt, C. D. Allis and B. D. Strahl (2002). Gene silencing: trans-histone regulatory pathway in chromatin. Nature **418:** 498.

Broccoli, D., A. Smogorzewska, L. Chong and T. de Lange (1997). Human telomeres contain two distinct Myb-related proteins, TRF1 and TRF2. Nat Genet **17:** 231-235.

Brockdorff, N. (2002). X-chromosome inactivation: closing in on proteins that bind Xist RNA. Trends Genet **18:** 352-358.

Brockdorff, N., and S. M. Duthie (1998). X chromosome inactivation and the Xist gene. Cell Mol Life Sci **54:** 104-112.

Bryan, T. M., A. Englezou, L. Dalla-Pozza, M. A. Dunham and R. R. Reddel (1997). Evidence for an alternative mechanism for maintaining telomere length in human tumors and tumor-derived cell lines. Nat Med **3:** 1271-1274.

Bryk, M., M. Banerjee, M. Murphy, K. E. Knudsen, D. J. Garfinkel and M. J. Curcio (1997). Transcriptional silencing of Ty1 elements in the *RDN1* locus of yeast. Genes Dev **11:** 255-269.

Bryk, M., S. D. Briggs, B. D. Strahl, M. J. Curcio, C. D. Allis and F. Winston (2002). Evidence that Set1, a factor required for methylation of histone H3, regulates rDNA silencing in *S. cerevisiae* by a Sir2-independent mechanism. Curr Biol **12:** 165-170.

Buck, S. W., and D. Shore (1995). Action of a RAP1 carboxy-terminal silencing domain reveals an underlying competition between *HMR* and telomeres in yeast. Genes Dev **9:** 370-384.

Bystricky, K., T. Laroche, G. van Houwe, M. Blaszczyk and S. M. Gasser (2005). Chromosome looping in yeast: telomere pairing and coordinated movement reflect anchoring efficiency and territorial organization. J Cell Biol **168:** 375-387.

Carmen, A. A., L. Milne and M. Grunstein (2002). Acetylation of the yeast histone H4 N terminus regulates its binding to heterochromatin protein SIR3. J Biol Chem **277:** 4778-4781.

Cavalli, G., and R. Paro (1998). Chromo-domain proteins: linking chromatin structure to epigenetic regulation. Curr Opin Cell Biol **10:** 354-360.

Chai, W., L. P. Ford, L. Lenertz, W. E. Wright and J. W. Shay (2002). Human Ku70/80 associates physically with telomerase through interaction with hTERT. J Biol Chem **277:** 47242-47247.

Chan, C. S., and B. K. Tye (1983a). A family of *Saccharomyces cerevisiae* repetitive autonomously replicating sequences that have very similar genomic environments. J Mol Biol **168:** 505-523.

Chan, C. S., and B. K. Tye (1983b). Organization of DNA sequences and replication origins at yeast telomeres. Cell **33:** 563-573.

Chen, T. A., M. M. Smith, S. Y. Le, R. Sternglanz and V. G. Allfrey (1991). Nucleosome fractionation by mercury affinity chromatography. Contrasting distribution of transcriptionally active DNA sequences and acetylated histones in nucleosome fractions of wild-type yeast cells and cells expressing a histone H3 gene altered to encode a cysteine 110 residue. J Biol Chem **266:** 6489-6498.

Chen-Cleland, T. A., M. M. Smith, S. Le, R. Sternglanz and V. G. Allfrey (1993). Nucleosome structural changes during derepression of silent mating-type loci in yeast. J Biol Chem **268:** 1118-1124.

Chien, C. T., S. Buck, R. Sternglanz and D. Shore (1993). Targeting of SIR1 protein establishes transcriptional silencing at *HM* loci and telomeres in yeast. Cell **75:** 531-541.

Chong, L., B. van Steensel, D. Broccoli, H. Erdjument-Bromage, J. Hanish, P. Tempst and T. de Lange (1995). A human telomeric protein. Science **270:** 1663-1667.

Chua, P., and G. S. Roeder (1995). Bdf1, a yeast chromosomal protein required for sporulation. Mol Cell Biol **15:** 3685-3696.

Chung, H. M., C. Shea, S. Fields, R. N. Taub, L. H. Van der Ploeg and D. B. Tse (1990). Architectural organization in the interphase nucleus of the protozoan Trypanosoma brucei: location of telomeres and mini-chromosomes. Embo J **9:** 2611-2619.

Cockell, M., M. Gotta, F. Palladino, S. G. Martin and S. M. Gasser (1998a). Targeting Sir proteins to sites of action: a general mechanism for regulated repression. Cold Spring Harb Symp Quant Biol. **63:** 401-412.

Cockell, M., F. Palladino, T. Laroche, G. Kyrion, C. Liu, A. J. Lustig and S. M. Gasser (1995). The carboxy termini of Sir4 and Rap1 affect Sir3 localization: evidence for a multicomponent complex required for yeast telomeric silencing. J Cell Biol **129:** 909-924.

Cockell, M., H. Renauld, P. Watt and S. M. Gasser (1998b). Sif2p interacts with Sir4p amino-terminal domain and antagonizes telomeric silencing in yeast. Curr Biol **8:** 787-790.

Cockell, M., D. Rhodes and A. Klug (1983). Location of the primary sites of micrococcal nuclease cleavage on the nucleosome core. J Mol Biol **170:** 423-446.

Cohen, D. E., and J. T. Lee (2002). X-chromosome inactivation and the search for chromosome-wide silencers. Curr Opin Genet Dev **12:** 219-224.

Coleman, J., D. M. Baird and N. J. Royle (1999). The plasticity of human telomeres demonstrated by a hypervariable telomere repeat array that is located on some copies of 16p and 16q. Hum Mol Genet **8:** 1637-1646.

Conrad, M. N., J. H. Wright, A. J. Wolf and V. A. Zakian (1990). RAP1 protein interacts with yeast telomeres in vivo: overproduction alters telomere structure and decreases chromosome stability. Cell **63:** 739-750.

Conway, C., R. McCulloch, M. L. Ginger, N. P. Robinson, A. Browitt and J. D. Barry (2002). Ku is important for telomere maintenance, but not for differential expression of telomeric VSG genes, in African trypanosomes. J Biol Chem **277:** 21269-21277.

Cooper, J. P. (2000). Telomere transitions in yeast: the end of the chromosome as we know it. Curr Opin Genet Dev **10:** 169-177.

Corda, Y., V. Schramke, M. P. Longhese, T. Smokvina, V. Paciotti, V. Brevet, E. Gilson and V. Geli (1999). Interaction between Set1p and checkpoint protein Mec3p in DNA repair and telomere functions. Nat Genet **21:** 204-208.

Craven, R. J., and T. D. Petes (1999). Dependence of the regulation of telomere length on the type of subtelomeric repeat in the yeast *Saccharomyces cerevisiae*. Genetics **152:** 1531-1541.

Cryderman, D. E., E. J. Morris, H. Biessmann, S. C. Elgin and L. L. Wallrath (1999). Silencing at *Drosophila* telomeres: nuclear organization and chromatin structure play critical roles. Embo J **18:** 3724-3735.

Csink, A. K., and S. Henikoff (1996). Genetic modification of heterochromatic association and nuclear organization in *Drosophila*. Nature **381:** 529-531.

d'Adda di Fagagna, F., M. P. Hande, W. M. Tong, D. Roth, P. M. Lansdorp, Z. Q. Wang and S. P. Jackson (2001). Effects of DNA nonhomologous end-joining factors on telomere length and chromosomal stability in mammalian cells. Curr Biol **11:** 1192-1196.

de Bruin, D., S. M. Kantrow, R. A. Liberatore and V. A. Zakian (2000). Telomere folding is required for the stable maintenance of telomere position effects in yeast. Mol Cell Biol **20:** 7991-8000.

de Bruin, D., Z. Zaman, R. A. Liberatore and M. Ptashne (2001). Telomere looping permits gene activation by a downstream UAS in yeast. Nature **409:** 109-113.

de Lange, T. (1992). Human telomeres are attached to the nuclear matrix. Embo J **11:** 717-724.

DeChiara, T. M., E. J. Robertson and A. Efstratiadis (1991). Parental imprinting of the mouse insulin-like growth factor II gene. Cell **64:** 849-859.

Dekker, J., K. Rippe, M. Dekker and N. Kleckner (2002). Capturing chromosome conformation. Science **295:** 1306-1311.

Dhalluin, C., J. E. Carlson, L. Zeng, C. He, A. K. Aggarwal and M. M. Zhou (1999). Structure and ligand of a histone acetyltransferase bromodomain. Nature **399:** 491-496.

Dillin, A., and J. Rine (1997). Separable functions of *ORC5* in replication initiation and silencing in *Saccharomyces cerevisiae*. Genetics **147:** 1053-1062.

Dingwall, C., G. P. Lomonossoff and R. A. Laskey (1981). High sequence specificity of micrococcal nuclease. Nucleic Acids Res **9:** 2659-2673.

Donze, D., C. R. Adams, J. Rine and R. T. Kamakaka (1999). The boundaries of the silenced *HMR* domain in *Saccharomyces cerevisiae*. Genes Dev **13:** 698-708.

Donze, D., and R. T. Kamakaka (2001). RNA polymerase III and RNA polymerase II promoter complexes are heterochromatin barriers in *Saccharomyces cerevisiae*. Embo J **20:** 520-531.

Dover, J., J. Schneider, M. A. Tawiah-Boateng, A. Wood, K. Dean, M. Johnston and A. Shilatifard (2002). Methylation of histone H3 by COMPASS requires ubiquitination of histone H2B by Rad6. J Biol Chem **277:** 28368-28371.

Downs, J. A., and S. P. Jackson (2004). A means to a DNA end: the many roles of Ku. Nat Rev Mol Cell Biol **5:** 367-378.

Dresser, M. E., and C. N. Giroux (1988). Meiotic chromosome behavior in spread preparations of yeast. J Cell Biol **106:** 567-573.

Drewell, R. A., C. J. Goddard, J. O. Thomas and M. A. Surani (2002). Methylation-dependent silencing at the *H19* imprinting control region by MeCP2. Nucleic Acids Res **30:** 1139-1144.

Dunham, M. A., A. A. Neumann, C. L. Fasching and R. R. Reddel (2000). Telomere maintenance by recombination in human cells. Nat Genet **26:** 447-450.

Ehrenhofer-Murray, A. E., D. H. Rivier and J. Rine (1997). The role of Sas2, an acetyltransferase homologue of *Saccharomyces cerevisiae*, in silencing and ORC function. Genetics **145:** 923-934.

Eid, J. E., and B. Sollner-Webb (1995). ST-1, a 39-kilodalton protein in Trypanosoma brucei, exhibits a dual affinity for the duplex form of the 29-base-pair subtelomeric repeat and its C-rich strand. Mol Cell Biol **15:** 389-397.

Eissenberg, J. C., T. C. James, D. M. Foster-Hartnett, T. Hartnett, V. Ngan and S. C. Elgin (1990). Mutation in a heterochromatin-specific chromosomal protein is associated with suppression of position-effect variegation in *Drosophila melanogaster*. Proc Natl Acad Sci U S A **87:** 9923-9927.

Ekwall, K., E. R. Nimmo, J. P. Javerzat, B. Borgstrom, R. Egel, G. Cranston and R. Allshire (1996). Mutations in the fission yeast silencing factors *clr4+* and *rik1+* disrupt the localisation of the chromo domain protein Swi6p and impair centromere function. J Cell Sci **109 (Pt 11):** 2637-2648.

Emre, N. C., K. Ingvarsdottir, A. Wyce, A. Wood, N. J. Krogan, K. W. Henry, K. Li, R. Marmorstein, J. F. Greenblatt, A. Shilatifard and S. L. Berger (2005). Maintenance of low histone ubiquitylation by Ubp10 correlates with telomere-proximal Sir2 association and gene silencing. Mol Cell **17:** 585-594.

Enomoto, S., and J. Berman (1998). Chromatin assembly factor I contributes to the maintenance, but not the re-establishment, of silencing at the yeast silent mating loci. Genes Dev **12:** 219-232.

Eyre, D. E. (2001). A genetic screen for the disruption of the nuclear architecture of yeast telomeres, based on ectopic recombination. D. Phil Thesis, Wolfson College.

Feldmann, H., L. Driller, B. Meier, G. Mages, J. Kellermann and E. L. Winnacker (1996). HDF2, the second subunit of the Ku homologue from *Saccharomyces cerevisiae*. J Biol Chem **271:** 27765-27769.

Feldmann, H., and E. L. Winnacker (1993). A putative homologue of the human autoantigen Ku from *Saccharomyces cerevisiae*. J Biol Chem **268:** 12895-12900.

Fellerhoff, B., F. Eckardt-Schupp and A. A. Friedl (2000). Subtelomeric repeat amplification is associated with growth at elevated temperature in yku70 mutants of *Saccharomyces cerevisiae*. Genetics **154:** 1039-1051.

Feng, Q., H. Wang, H. H. Ng, H. Erdjument-Bromage, P. Tempst, K. Struhl and Y. Zhang (2002). Methylation of H3-lysine 79 is mediated by a new family of HMTases without a SET domain. Curr Biol **12:** 1052-1058.

Ferrari, S., K. C. Simmen, Y. Dusserre, K. Muller, G. Fourel, E. Gilson and N. Mermod (2004). Chromatin domain boundaries delimited by a histone-binding protein in yeast. J Biol Chem **279:** 55520-55530.

Ferreiro, J. A., N. G. Powell, N. Karabetsou, N. A. Kent, J. Mellor and R. Waters (2004). Cbf1p modulates chromatin structure, transcription and repair at the *Saccharomyces cerevisiae* MET16 locus. Nucleic Acids Res **32:** 1617-1626.

Figueiredo, L. M., L. H. Freitas-Junior, E. Bottius, J. C. Olivo-Marin and A. Scherf (2002). A central role for Plasmodium falciparum subtelomeric regions in spatial positioning and telomere length regulation. Embo J **21:** 815-824.

Fingerman, I. M., C. L. Wu, B. D. Wilson and S. D. Briggs (2005). Global loss of Set1-mediated H3 Lys4 trimethylation is associated with silencing defects in *Saccharomyces cerevisiae*. J Biol Chem.

Fischer, G., S. A. James, I. N. Roberts, S. G. Oliver and E. J. Louis (2000). Chromosomal evolution in *Saccharomyces*. Nature **405:** 451-454.

Fisher, A. G., and M. Merkenschlager (2002). Gene silencing, cell fate and nuclear organisation. Curr Opin Genet Dev **12:** 193-197.

Flint, J., G. P. Bates, K. Clark, A. Dorman, D. Willingham, B. A. Roe, G. Micklem, D. R. Higgs and E. J. Louis (1997). Sequence comparison of human and yeast telomeres identifies structurally distinct subtelomeric domains. Hum Mol Genet **6:** 1305-1313.

Foss, M., F. J. McNally, P. Laurenson and J. Rine (1993). Origin recognition complex (ORC) in transcriptional silencing and DNA replication in *S. cerevisiae*. Science **262:** 1838-1844.

Fourel, G., E. Lebrun and E. Gilson (2002). Protosilencers as building blocks for heterochromatin. Bioessays. **24:** 828-835.

Fourel, G., E. Revardel, C. E. Koering and E. Gilson (1999). Cohabitation of insulators and silencing elements in yeast subtelomeric regions. Embo J **18:** 2522-2537.

Fox, C. A., A. E. Ehrenhofer-Murray, S. Loo and J. Rine (1997). The origin recognition complex, *SIR1*, and the S phase requirement for silencing. Science **276:** 1547-1551.

Fox, C. A., S. Loo, A. Dillin and J. Rine (1995). The origin recognition complex has essential functions in transcriptional silencing and chromosomal replication. Genes Dev **9:** 911-924.

Fox, C. A., S. Loo, D. H. Rivier, M. A. Foss and J. Rine (1993). A transcriptional silencer as a specialized origin of replication that establishes functional domains of chromatin. Cold Spring Harb Symp Quant Biol **58:** 443-455.

Freitas-Junior, L. H., E. Bottius, L. A. Pirrit, K. W. Deitsch, C. Scheidig, F. Guinet, U. Nehrbass, T. E. Wellems and A. Scherf (2000). Frequent ectopic recombination of virulence factor genes in telomeric chromosome clusters of *P. falciparum.* Nature **407:** 1018-1022.

Freitas-Junior, L. H., R. Hernandez-Rivas, S. A. Ralph, D. Montiel-Condado, O. K. Ruvalcaba-Salazar, A. P. Rojas-Meza, L. Mancio-Silva, R. J. Leal-Silvestre, A. M. Gontijo, S. Shorte and A. Scherf (2005). Telomeric heterochromatin

propagation and histone acetylation control mutually exclusive expression of antigenic variation genes in malaria parasites. Cell **121:** 25-36.

Frye, R. A. (2000). Phylogenetic classification of prokaryotic and eukaryotic Sir2-like proteins. Biochem Biophys Res Commun **273:** 793-798.

Funabiki, H., I. Hagan, S. Uzawa and M. Yanagida (1993). Cell cycle-dependent specific positioning and clustering of centromeres and telomeres in fission yeast. J Cell Biol **121:** 961-976.

Galy, V., J. C. Olivo-Marin, H. Scherthan, V. Doye, N. Rascalou and U. Nehrbass (2000). Nuclear pore complexes in the organization of silent telomeric chromatin. Nature **403:** 108-112.

Gardner, K. A., and C. A. Fox (2001). The Sir1 protein's association with a silenced chromosome domain. Genes Dev **15:** 147-157.

Gardner, K. A., J. Rine and C. A. Fox (1999). A region of the Sir1 protein dedicated to recognition of a silencer and required for interaction with the Orc1 protein in *Saccharomyces cerevisiae.* Genetics **151:** 31-44.

Gartenberg, M. R. (2000). The Sir proteins of *Saccharomyces cerevisiae*: mediators of transcriptional silencing and much more. Curr Opin Microbiol. **3:** 132-137.

Gavin, A. C., M. Bosche, R. Krause, P. Grandi, M. Marzioch, A. Bauer, J. Schultz, J. M. Rick, A. M. Michon, C. M. Cruciat, M. Remor, C. Hofert, M. Schelder, M. Brajenovic, H. Ruffner, A. Merino, K. Klein, M. Hudak, D. Dickson, T. Rudi, V. Gnau, A. Bauch, S. Bastuck, B. Huhse, C. Leutwein, M. A. Heurtier, R. R. Copley, A. Edelmann, E. Querfurth, V. Rybin, G. Drewes, M. Raida, T. Bouwmeester, P. Bork, B. Seraphin, B. Kuster, G. Neubauer and G. Superti-Furga (2002). Functional organization of the yeast proteome by systematic analysis of protein complexes. Nature **415:** 141-147.

Geissenhoner, A., C. Weise and A. E. Ehrenhofer-Murray (2004). Dependence of ORC silencing function on NatA-mediated Nalpha acetylation in *Saccharomyces cerevisiae*. Mol Cell Biol **24:** 10300-10312.

Georgel, P. T., M. A. Palacios DeBeer, G. Pietz, C. A. Fox and J. C. Hansen (2001). Sir3-dependent assembly of supramolecular chromatin structures *in vitro.* Proc Natl Acad Sci U S A **98:** 8584-8589.

Ghidelli, S., D. Donze, N. Dhillon and R. T. Kamakaka (2001). Sir2p exists in two nucleosome-binding complexes with distinct deacetylase activities. Embo J **20:** 4522-4535.

Gietz, D., A. St Jean, R. A. Woods and R. H. Schiestl (1992). Improved method for high efficiency transformation of intact yeast cells. Nucleic Acids Res **20:** 1425.

Gilson, E., M. Roberge, R. Giraldo, D. Rhodes and S. M. Gasser (1993). Distortion of the DNA double helix by RAP1 at silencers and multiple telomeric binding sites. J Mol Biol **231:** 293-310.

Glusman, G., I. Yanai, I. Rubin and D. Lancet (2001). The complete human olfactory subgenome. Genome Res **11:** 685-702.

Goldstein, A. L., and J. H. McCusker (1999). Three new dominant drug resistance cassettes for gene disruption in *Saccharomyces cerevisiae*. Yeast **15:** 1541-1553.

Gotta, M., T. Laroche, A. Formenton, L. Maillet, H. Scherthan and S. M. Gasser (1996). The clustering of telomeres and colocalization with Rap1, Sir3, and Sir4 proteins in wild-type *Saccharomyces cerevisiae*. J Cell Biol **134:** 1349-1363.

Gotta, M., S. Strahl-Bolsinger, H. Renauld, T. Laroche, B. K. Kennedy, M. Grunstein and S. M. Gasser (1997). Localization of Sir2p: the nucleolus as a compartment for silent information regulators. Embo J **16:** 3243-3255.

Gottlieb, T. M., and S. P. Jackson (1993). The DNA-dependent protein kinase: requirement for DNA ends and association with Ku antigen. Cell **72:** 131-142.

Gottschling, D. E., O. M. Aparicio, B. L. Billington and V. A. Zakian (1990). Position effect at *S. cerevisiae* telomeres: reversible repression of Pol II transcription. Cell **63:** 751-762.

Graham, I. R., R. A. Haw, K. G. Spink, K. A. Halden and A. Chambers (1999). *In vivo* analysis of functional regions within yeast Rap1p. Mol Cell Biol **19:** 7481-7490.

Gravel, S., M. Larrivee, P. Labrecque and R. J. Wellinger (1998). Yeast Ku as a regulator of chromosomal DNA end structure. Science **280:** 741-744.

Grewal, S. I., and S. C. Elgin (2002). Heterochromatin: new possibilities for the inheritance of structure. Curr Opin Genet Dev **12:** 178-187.

Grewal, S. I., and A. J. Klar (1997). A recombinationally repressed region between *mat2* and *mat3* loci shares homology to centromeric repeats and regulates directionality of mating-type switching in fission yeast. Genetics **146:** 1221-1238.

Grewal, S. I., and D. Moazed (2003). Heterochromatin and epigenetic control of gene expression. Science **301:** 798-802.

Griffin, C. D. (2004). Genome recombination studies. D. Phil Thesis, University of Leicester.

Griffith, J. D., L. Comeau, S. Rosenfield, R. M. Stansel, A. Bianchi, H. Moss and T. de Lange (1999). Mammalian telomeres end in a large duplex loop. Cell **97:** 503-514.

Grigoryev, S. A. (2004). Keeping fingers crossed: heterochromatin spreading through interdigitation of nucleosome arrays. FEBS Lett **564:** 4-8.

Gruenbaum, Y., M. Hochstrasser, D. Mathog, H. Saumweber, D. A. Agard and J. W. Sedat (1984). Spatial organization of the *Drosophila* nucleus: a three-dimensional cytogenetic study. J Cell Sci Suppl **1:** 223-234.

Grunstein, M. (1997). Histone acetylation in chromatin structure and transcription. Nature **389:** 349-352.

Guarente, L., and C. Kenyon (2000). Genetic pathways that regulate ageing in model organisms. Nature **408:** 255-262.

Hardy, C. F., L. Sussel and D. Shore (1992). A RAP1-interacting protein involved in transcriptional silencing and telomere length regulation. Genes Dev **6:** 801-814.

Hassan, A. H., P. Prochasson, K. E. Neely, S. C. Galasinski, M. Chandy, M. J. Carrozza and J. L. Workman (2002). Function and selectivity of bromodomains in anchoring chromatin-modifying complexes to promoter nucleosomes. Cell **111:** 369-379.

Hayashi, N., T. Nomura, N. Sakumoto, Y. Mukai, Y. Kaneko, S. Harashima and S. Murakami (2005). The *SIT4* gene, which encodes protein phosphatase 2A, is required for telomere function in *Saccharomyces cerevisiae*. Curr Genet **47:** 359-367.

Heard, E. (2004). Recent advances in X-chromosome inactivation. Curr Opin Cell Biol **16:** 247-255.

Hecht, A., T. Laroche, S. Strahl-Bolsinger, S. M. Gasser and M. Grunstein (1995). Histone H3 and H4 N-termini interact with SIR3 and SIR4 proteins: a molecular model for the formation of heterochromatin in yeast. Cell **80:** 583-592.

Hecht, A., S. Strahl-Bolsinger and M. Grunstein (1996). Spreading of transcriptional repressor SIR3 from telomeric heterochromatin. Nature **383:** 92-96.

Hediger, F., and S. M. Gasser (2002). Nuclear organization and silencing: putting things in their place. Nat Cell Biol **4:** E53-55.

Hediger, F., F. R. Neumann, G. Van Houwe, K. Dubrana and S. M. Gasser (2002). Live Imaging of Telomeres. yKu and Sir Proteins Define Redundant Telomere-Anchoring Pathways in Yeast. Curr Biol **12:** 2076-2089.

Hemann, M. T., M. A. Strong, L. Y. Hao and C. W. Greider (2001). The shortest telomere, not average telomere length, is critical for cell viability and chromosome stability. Cell **107:** 67-77.

Heun, P., T. Laroche, K. Shimada, P. Furrer and S. M. Gasser (2001a). Chromosome dynamics in the yeast interphase nucleus. Science **294:** 2181-2186.

Heun, P., A. Taddei and S. M. Gasser (2001b). From snapshots to moving pictures: new perspectives on nuclear organization. Trends Cell Biol **11:** 519-525.

Hild, M., and R. Paro (2003). Anti-silencing from the core: a histone H2A variant protects euchromatin. Nat Cell Biol **5:** 278-280.

Hishida, T., T. Ohno, H. Iwasaki and H. Shinagawa (2002). *Saccharomyces cerevisiae* MGS1 is essential in strains deficient in the RAD6-dependent DNA damage tolerance pathway. Embo J **21:** 2019-2029.

Hopfner, K. P., C. D. Putnam and J. A. Tainer (2002). DNA double-strand break repair from head to tail. Curr Opin Struct Biol **12:** 115-122.

Hoppe, G. J., J. C. Tanny, A. D. Rudner, S. A. Gerber, S. Danaie, S. P. Gygi and D. Moazed (2002). Steps in assembly of silent chromatin in yeast: Sir3-independent binding of a Sir2/Sir4 complex to silencers and role for Sir2-dependent deacetylation. Mol Cell Biol **22:** 4167-4180.

Hsu, H. C., B. Stillman and R. M. Xu (2005). Structural basis for origin recognition complex 1 protein-silence information regulator 1 protein interaction in epigenetic silencing. Proc Natl Acad Sci U S A **102:** 8519-8524.

Hsu, H. L., D. Gilley, E. H. Blackburn and D. J. Chen (1999). Ku is associated with the telomere in mammals. Proc Natl Acad Sci U S A **96:** 12454-12458.

Huang, H., A. Kahana, D. E. Gottschling, L. Prakash and S. W. Liebman (1997). The ubiquitin-conjugating enzyme Rad6 (Ubc2) is required for silencing in *Saccharomyces cerevisiae*. Mol Cell Biol **17:** 6693-6699.

Huang, P., F. E. Pryde, D. Lester, R. L. Maddison, R. H. Borts, I. D. Hickson and E. J. Louis (2001). SGS1 is required for telomere elongation in the absence of telomerase. Curr Biol **11:** 125-129.

Huang, Y. (2002). Transcriptional silencing in *Saccharomyces cerevisiae* and *Schizosaccharomyces pombe*. Nucleic Acids Res **30:** 1465-1482.

Hudson, B. P., M. A. Martinez-Yamout, H. J. Dyson and P. E. Wright (2000). Solution structure and acetyl-lysine binding activity of the GCN5 bromodomain. J Mol Biol **304:** 355-370.

Ikeda, K., D. J. Steger, A. Eberharter and J. L. Workman (1999). Activation domain-specific and general transcription stimulation by native histone acetyltransferase complexes. Mol Cell Biol **19:** 855-863.

Imai, S., C. M. Armstrong, M. Kaeberlein and L. Guarente (2000a). Transcriptional silencing and longevity protein Sir2 is an NAD-dependent histone deacetylase. Nature **403:** 795-800.

Imai, S., F. B. Johnson, R. A. Marciniak, M. McVey, P. U. Park and L. Guarente (2000b). Sir2: an NAD-dependent histone deacetylase that connects chromatin silencing, metabolism, and aging. Cold Spring Harb Symp Quant Biol **65:** 297-302.

Ivanova, A. V., M. J. Bonaduce, S. V. Ivanov and A. J. Klar (1998). The chromo and SET domains of the Clr4 protein are essential for silencing in fission yeast. Nat Genet **19:** 192-195.

Jackson, J. P., A. M. Lindroth, X. Cao and S. E. Jacobsen (2002). Control of CpNpG DNA methylation by the KRYPTONITE histone H3 methyltransferase. Nature **416:** 556-560.

Jaco, I., P. Munoz and M. A. Blasco (2004). Role of human Ku86 in telomere length maintenance and telomere capping. Cancer Res **64:** 7271-7278.

Jacobs, S. A., S. D. Taverna, Y. Zhang, S. D. Briggs, J. Li, J. C. Eissenberg, C. D. Allis and S. Khorasanizadeh (2001). Specificity of the HP1 chromo domain for the methylated N-terminus of histone H3. Embo J **20:** 5232-5241.

Jacobson, R. H., A. G. Ladurner, D. S. King and R. Tjian (2000). Structure and function of a human TAFII250 double bromodomain module. Science **288:** 1422-1425.

Jason, L. J., S. C. Moore, J. D. Lewis, G. Lindsey and J. Ausio (2002). Histone ubiquitination: a tagging tail unfolds? Bioessays **24:** 166-174.

Jeanmougin, F., J. M. Wurtz, B. Le Douarin, P. Chambon and R. Losson (1997). The bromodomain revisited. Trends Biochem Sci **22:** 151-153.

Jeggo, P. A., G. E. Taccioli and S. P. Jackson (1995). Menage a trois: double strand break repair, V(D)J recombination and DNA-PK. Bioessays **17:** 949-957.

Jentsch, S., J. P. McGrath and A. Varshavsky (1987). The yeast DNA repair gene *RAD6* encodes a ubiquitin-conjugating enzyme. Nature **329:** 131-134.

Jenuwein, T. (2001). Re-SET-ting heterochromatin by histone methyltransferases. Trends Cell Biol **11:** 266-273.

Jenuwein, T., and C. D. Allis (2001). Translating the histone code. Science **293:** 1074-1080.

Jenuwein, T., G. Laible, R. Dorn and G. Reuter (1998). SET domain proteins modulate chromatin domains in eu- and heterochromatin. Cell Mol Life Sci **54:** 80-93.

Johnson, L. M., P. S. Kayne, E. S. Kahn and M. Grunstein (1990). Genetic evidence for an interaction between *SIR3* and histone H4 in the repression of the silent mating loci in *Saccharomyces cerevisiae*. Proc Natl Acad Sci U S A **87:** 6286-6290.

Kaeberlein, M., M. McVey and L. Guarente (1999). The *SIR2/3/4* complex and *SIR2* alone promote longevity in *Saccharomyces cerevisiae* by two different mechanisms. Genes Dev **13:** 2570-2580.

Kaffer, C. R., M. Srivastava, K. Y. Park, E. Ives, S. Hsieh, J. Batlle, A. Grinberg, S. P. Huang and K. Pfeifer (2000). A transcriptional insulator at the imprinted *H19/Igf2* locus. Genes Dev **14:** 1908-1919.

Kamakaka, R. T., and J. Rine (1998). Sir- and silencer-independent disruption of silencing in Saccharomyces by Sas10p. Genetics **149:** 903-914.

Kang, X. L., F. Yadao, R. D. Gietz and B. A. Kunz (1992). Elimination of the yeast RAD6 ubiquitin conjugase enhances base-pair transitions and G.C----T.A transversions as well as transposition of the Ty element: implications for the control of spontaneous mutation. Genetics **130:** 285-294.

Karlseder, J. (2003). Telomere repeat binding factors: keeping the ends in check. Cancer Lett **194:** 189-197.

Karlseder, J., L. Kachatrian, H. Takai, K. Mercer, S. Hingorani, T. Jacks and T. de Lange (2003). Targeted deletion reveals an essential function for the telomere length regulator Trf1. Mol Cell Biol **23:** 6533-6541.

Karpen, G. H., and A. C. Spradling (1992). Analysis of subtelomeric heterochromatin in the *Drosophila* minichromosome Dp1187 by single P element insertional mutagenesis. Genetics **132:** 737-753.

Kass-Eisler, A., and C. W. Greider (2000). Recombination in telomere-length maintenance. Trends Biochem Sci **25:** 200-204.

Kaufman, P. D., R. Kobayashi and B. Stillman (1997). Ultraviolet radiation sensitivity and reduction of telomeric silencing in *Saccharomyces cerevisiae* cells lacking chromatin assembly factor-I. Genes Dev **11:** 345-357.

Kennedy, B. K., M. Gotta, D. A. Sinclair, K. Mills, D. S. McNabb, M. Murthy, S. M. Pak, T. Laroche, S. M. Gasser and L. Guarente (1997). Redistribution of silencing proteins from telomeres to the nucleolus is associated with extension of life span in *S. cerevisiae*. Cell **89:** 381-391.

Kent, N. A., L. E. Bird and J. Mellor (1993). Chromatin analysis in yeast using NP-40 permeabilised sphaeroplasts. Nucleic Acids Res **21:** 4653-4654.

Kent, N. A., S. M. Eibert and J. Mellor (2004). Cbf1p is required for chromatin remodeling at promoter-proximal CACGTG motifs in yeast. J Biol Chem **279:** 27116-27123.

Kent, N. A., and J. Mellor (1995). Chromatin structure snap-shots: rapid nuclease digestion of chromatin in yeast. Nucleic Acids Res **23:** 3786-3787.

Kimmerly, W., A. Buchman, R. Kornberg and J. Rine (1988). Roles of two DNA-binding factors in replication, segregation and transcriptional repression mediated by a yeast silencer. Embo J **7:** 2241-2253.

Kimura, A., T. Umehara and M. Horikoshi (2002). Chromosomal gradient of histone acetylation established by Sas2p and Sir2p functions as a shield against gene silencing. Nature Genetics.

Klar, A. J. (1992). Developmental choices in mating-type interconversion in fission yeast. Trends Genet **8:** 208-213.

Klein, F., T. Laroche, M. E. Cardenas, J. F. Hofmann, D. Schweizer and S. M. Gasser (1992). Localization of RAP1 and topoisomerase II in nuclei and meiotic chromosomes of yeast. J Cell Biol **117:** 935-948.

Kornberg, R. D., and Y. Lorch (1999). Twenty-five years of the nucleosome, fundamental particle of the eukaryote chromosome. Cell **98:** 285-294.

Kota, R. S., and K. W. Runge (1999). Tel2p, a regulator of yeast telomeric length in vivo, binds to single-stranded telomeric DNA in vitro. Chromosoma **108:** 278-290.

Krogan, N. J., J. Dover, S. Khorrami, J. F. Greenblatt, J. Schneider, M. Johnston and A. Shilatifard (2002). COMPASS, a histone H3 (Lysine 4) methyltransferase required for telomeric silencing of gene expression. J Biol Chem **277:** 10753-10755.

Krogan, N. J., J. Dover, A. Wood, J. Schneider, J. Heidt, M. A. Boateng, K. Dean, O. W. Ryan, A. Golshani, M. Johnston, J. F. Greenblatt and A. Shilatifard (2003). The Paf1 complex is required for histone H3 methylation by COMPASS and Dot1p: linking transcriptional elongation to histone methylation. Mol Cell **11:** 721-729.

Kuo, M. H., and C. D. Allis (1998). Roles of histone acetyltransferases and deacetylases in gene regulation. Bioessays **20:** 615-626.

Kupiec, M., and G. Simchen (1986). Regulation of the *RAD6* gene of *Saccharomyces cerevisiae* in the mitotic cell cycle and in meiosis. Mol Gen Genet **203:** 538-543.

Kyrion, G., K. Liu, C. Liu and A. J. Lustig (1993). *RAP1* and telomere structure regulate telomere position effects in *Saccharomyces cerevisiae*. Genes Dev **7:** 1146-1159.

Lachner, M., and T. Jenuwein (2002). The many faces of histone lysine methylation. Curr Opin Cell Biol **14:** 286-298.

Lachner, M., D. O'Carroll, S. Rea, K. Mechtler and T. Jenuwein (2001). Methylation of histone H3 lysine 9 creates a binding site for HP1 proteins. Nature **410:** 116-120.

Lacoste, N., R. T. Utley, J. M. Hunter, G. G. Poirier and J. Cote (2002). Disruptor of telomeric silencing-1 is a chromatin-specific histone H3 methyltransferase. J Biol Chem **277:** 30421-30424.

Ladurner, A. G., C. Inouye, R. Jain and R. Tjian (2003). Bromodomains mediate an acetyl-histone encoded antisilencing function at heterochromatin boundaries. Mol Cell **11:** 365-376.

Lahue, E., J. Heckathorn, Z. Meyer, J. Smith and C. Wolfe (2005). The *Saccharomyces cerevisiae* Sub2 protein suppresses heterochromatic silencing at telomeres and subtelomeric genes. Yeast **22:** 537-551.

Landry, J., A. Sutton, S. T. Tafrov, R. C. Heller, J. Stebbins, L. Pillus and R. Sternglanz (2000). The silencing protein SIR2 and its homologs are NAD-dependent protein deacetylases. Proc Natl Acad Sci U S A **97:** 5807-5811.

Lanzer, M., K. Fischer and S. M. Le Blancq (1995). Parasitism and chromosome dynamics in protozoan parasites: is there a connection? Mol Biochem Parasitol **70:** 1-8.

Laroche, T., S. G. Martin, M. Gotta, H. C. Gorham, F. E. Pryde, E. J. Louis and S. M. Gasser (1998). Mutation of yeast Ku genes disrupts the subnuclear organization of telomeres. Curr Biol **8:** 653-656.

Laurenson, P., and J. Rine (1992). Silencers, silencing, and heritable transcriptional states. Microbiol Rev **56:** 543-560.

Lebrun, E., E. Revardel, C. Boscheron, R. Li, E. Gilson and G. Fourel (2001). Protosilencers in *Saccharomyces cerevisiae* subtelomeric regions. Genetics **158:** 167-176.

Lee, J. T. (2003). Molecular links between X-inactivation and autosomal imprinting: X-inactivation as a driving force for the evolution of imprinting? Curr Biol **13:** R242-254.

Lee, S. E., F. Paques, J. Sylvan and J. E. Haber (1999). Role of yeast *SIR* genes and mating type in directing DNA double-strand breaks to homologous and non-homologous repair paths. Curr Biol **9:** 767-770.

Leighton, P. A., R. S. Ingram, J. Eggenschwiler, A. Efstratiadis and S. M. Tilghman (1995). Disruption of imprinting caused by deletion of the *H19* gene region in mice. Nature **375:** 34-39.

Lejnine, S., V. L. Makarov and J. P. Langmore (1995). Conserved nucleoprotein structure at the ends of vertebrate and invertebrate chromosomes. Proc Natl Acad Sci U S A **92:** 2393-2397.

Levis, R., T. Hazelrigg and G. M. Rubin (1985). Effects of genomic position on the expression of transduced copies of the white gene of *Drosophila*. Science **229:** 558-561.

Levy, D. L., and E. H. Blackburn (2004). Counting of Rif1p and Rif2p on *Saccharomyces cerevisiae* telomeres regulates telomere length. Mol Cell Biol **24:** 10857-10867.

Li, B., and T. de Lange (2003). Rap1 affects the length and heterogeneity of human telomeres. Mol Biol Cell **14:** 5060-5068.

Li, B., S. Oestreich and T. de Lange (2000). Identification of human Rap1: implications for telomere evolution. Cell **101:** 471-483.

Li, E. (2002). Chromatin modification and epigenetic reprogramming in mammalian development. Nat Rev Genet **3:** 662-673.

Lieb, J. D., X. Liu, D. Botstein and P. O. Brown (2001). Promoter-specific binding of Rap1 revealed by genome-wide maps of protein-DNA association. Nat Genet **28:** 327-334.

Lieber, M. R., U. Grawunder, X. Wu and M. Yaneva (1997). Tying loose ends: roles of Ku and DNA-dependent protein kinase in the repair of double-strand breaks. Curr Opin Genet Dev **7:** 99-104.

Lingner, J., and T. R. Cech (1998). Telomerase and chromosome end maintenance. Curr Opin Genet Dev **8:** 226-232.

Lingner, J., T. R. Hughes, A. Shevchenko, M. Mann, V. Lundblad and T. R. Cech (1997). Reverse transcriptase motifs in the catalytic subunit of telomerase. Science **276:** 561-567.

Liou, G. G., J. C. Tanny, R. G. Kruger, T. Walz and D. Moazed (2005). Assembly of the SIR complex and its regulation by O-acetyl-ADP-ribose, a product of NAD-dependent histone deacetylation. Cell **121:** 515-527.

Litt, M. D., M. Simpson, M. Gaszner, C. D. Allis and G. Felsenfeld (2001). Correlation between histone lysine methylation and developmental changes at the chicken beta-globin locus. Science **293:** 2453-2455.

Liu, C., and A. J. Lustig (1996). Genetic analysis of Rap1p/Sir3p interactions in telomeric and HML silencing in *Saccharomyces cerevisiae*. Genetics **143:** 81-93.

Liu, Z., A. Lee and W. Gilbert (1995). Gene disruption of a G4-DNA-dependent nuclease in yeast leads to cellular senescence and telomere shortening. Proc Natl Acad Sci U S A **92:** 6002-6006.

Liu, Z. P., and B. K. Tye (1991). A yeast protein that binds to vertebrate telomeres and conserved yeast telomeric junctions. Genes Dev **5:** 49-59.

Loayza, D., and T. De Lange (2003). *POT1* as a terminal transducer of *TRF1* telomere length control. Nature **423:** 1013-1018.

Longtine, M. S., A. McKenzie, 3rd, D. J. Demarini, N. G. Shah, A. Wach, A. Brachat, P. Philippsen and J. R. Pringle (1998). Additional modules for versatile and economical PCR-based gene deletion and modification in *Saccharomyces cerevisiae*. Yeast **14:** 953-961.

Loo, S., C. A. Fox, J. Rine, R. Kobayashi, B. Stillman and S. Bell (1995a). The origin recognition complex in silencing, cell cycle progression, and DNA replication. Mol Biol Cell **6:** 741-756.

Loo, S., P. Laurenson, M. Foss, A. Dillin and J. Rine (1995b). Roles of *ABF1*, *NPL3*, and *YCL54* in silencing in *Saccharomyces cerevisiae*. Genetics **141:** 889-902.

Loo, S., and J. Rine (1994). Silencers and domains of generalized repression. Science **264:** 1768-1771.

Lopez, C. C., L. Nielsen and J. E. Edstrom (1996). Terminal long tandem repeats in chromosomes form *Chironomus pallidivittatus*. Mol Cell Biol **16:** 3285-3290.

Lorentz, A., K. Ostermann, O. Fleck and H. Schmidt (1994). Switching gene swi6, involved in repression of silent mating-type loci in fission yeast, encodes a homologue of chromatin-associated proteins from *Drosophila* and mammals. Gene **143:** 139-143.

Louis, E. J. (1995). The chromosome ends of *Saccharomyces cerevisiae*. Yeast **11:** 1553-1573.

Louis, E. J., 1998 Whole Chromosome Analysis, pp. 15-31 in Methods in Microbiology: Yeast Gene Analysis, edited by M. F. TUITE and A. J. P. BROWN. Academic Press.

Louis, E. J., and J. E. Haber (1990). Mitotic recombination among subtelomeric Y' repeats in *Saccharomyces cerevisiae*. Genetics **124:** 547-559.

Louis, E. J., and J. E. Haber (1992). The structure and evolution of subtelomeric Y' repeats in *Saccharomyces cerevisiae*. Genetics **131:** 559-574.

Louis, E. J., E. S. Naumova, A. Lee, G. Naumov and J. E. Haber (1994). The chromosome end in yeast: its mosaic nature and influence on recombinational dynamics. Genetics **136:** 789-802.

Lu, B. Y., P. C. Emtage, B. J. Duyf, A. J. Hilliker and J. C. Eissenberg (2000). Heterochromatin protein 1 is required for the normal expression of two heterochromatin genes in *Drosophila*. Genetics **155:** 699-708.

Luger, K., A. W. Mader, R. K. Richmond, D. F. Sargent and T. J. Richmond (1997). Crystal structure of the nucleosome core particle at 2.8 A resolution. Nature **389:** 251-260.

Luger, K., and T. J. Richmond (1998). The histone tails of the nucleosome. Curr Opin Genet Dev **8:** 140-146.

Lundblad, V., and E. H. Blackburn (1993). An alternative pathway for yeast telomere maintenance rescues *est1-* senescence. Cell **73:** 347-360.

Luo, K., M. A. Vega-Palas and M. Grunstein (2002). Rap1-Sir4 binding independent of other Sir, yKu, or histone interactions initiates the assembly of telomeric heterochromatin in yeast. Genes Dev **16:** 1528-1539.

Lustig, A. J. (1998). Mechanisms of silencing in *Saccharomyces cerevisiae*. Curr Opin Genet Dev **8:** 233-239.

Lustig, A. J., C. Liu, C. Zhang and J. P. Hanish (1996). Tethered Sir3p nucleates silencing at telomeres and internal loci in *Saccharomyces cerevisiae*. Mol Cell Biol **16:** 2483-2495.

Lustig, A. J., and T. D. Petes (1986). Identification of yeast mutants with altered telomere structure. Proc Natl Acad Sci U S A **83:** 1398-1402.

Lygerou, Z., C. Conesa, P. Lesage, R. N. Swanson, A. Ruet, M. Carlson, A. Sentenac and B. Seraphin (1994). The yeast *BDF1* gene encodes a transcription factor involved in the expression of a broad class of genes including snRNAs. Nucleic Acids Res **22:** 5332-5340.

Macina, R. A., D. G. Negorev, C. Spais, L. A. Ruthig, X. L. Hu and H. C. Riethman (1994). Sequence organization of the human chromosome 2q telomere. Hum Mol Genet **3:** 1847-1853.

Maillet, L., C. Boscheron, M. Gotta, S. Marcand, E. Gilson and S. M. Gasser (1996). Evidence for silencing compartments within the yeast nucleus: a role for telomere proximity and Sir protein concentration in silencer-mediated repression. Genes and Development **10:** 1796-1811.

Maillet, L., F. Gaden, V. Brevet, G. Fourel, S. G. Martin, K. Dubrana, S. M. Gasser and E. Gilson (2001). Ku-deficient yeast strains exhibit alternative states of silencing competence. EMBO Rep **2:** 203-210.

Makarov, V. L., S. Lejnine, J. Bedoyan and J. P. Langmore (1993). Nucleosomal organization of telomere-specific chromatin in rat. Cell **73:** 775-787.

Manolis, K. G., E. R. Nimmo, E. Hartsuiker, A. M. Carr, P. A. Jeggo and R. C. Allshire (2001). Novel functional requirements for non-homologous DNA end joining in *Schizosaccharomyces pombe*. Embo J **20:** 210-221.

Marcand, S., S. W. Buck, P. Moretti, E. Gilson and D. Shore (1996). Silencing of genes at nontelomeric sites in yeast is controlled by sequestration of silencing factors at telomeres by Rap 1 protein. Genes Dev **10:** 1297-1309.

Marcand, S., E. Gilson and D. Shore (1997a). A protein-counting mechanism for telomere length regulation in yeast. Science **275:** 986-990.

Marcand, S., D. Wotton, E. Gilson and D. Shore (1997b). Rap1p and telomere length regulation in yeast. Ciba Found Symp **211:** 76-93; discussion 93-103.

Marciniak, R. A., D. Cavazos, R. Montellano, Q. Chen, L. Guarente and F. B. Johnson (2005). A novel telomere structure in a human alternative lengthening of telomeres cell line. Cancer Res **65:** 2730-2737.

Marshall, W. F. (2002). Order and disorder in the nucleus. Curr Biol **12:** R185-192.

Marshall, W. F., A. F. Dernburg, B. Harmon, D. A. Agard and J. W. Sedat (1996). Specific interactions of chromatin with the nuclear envelope: positional determination within the nucleus in *Drosophila melanogaster*. Mol Biol Cell **7:** 825-842.

Martin, S. G., T. Laroche, N. Suka, M. Grunstein and S. M. Gasser (1999). Relocalization of telomeric Ku and SIR proteins in response to DNA strand breaks in yeast. Cell **97:** 621-633.

Martinez-Campa, C., P. Politis, J. L. Moreau, N. Kent, J. Goodall, J. Mellor and C. R. Goding (2004). Precise nucleosome positioning and the TATA box dictate requirements for the histone H4 tail and the bromodomain factor Bdf1. Mol Cell **15:** 69-81.

Matangkasombut, O., R. M. Buratowski, N. W. Swilling and S. Buratowski (2000). Bromodomain factor 1 corresponds to a missing piece of yeast TFIID. Genes Dev **14:** 951-962.

Matangkasombut, O., and S. Buratowski (2003). Different sensitivities of bromodomain factors 1 and 2 to histone H4 acetylation. Mol Cell **11:** 353-363.

McCulloch, R., G. Rudenko and P. Borst (1997). Gene conversions mediating antigenic variation in *Trypanosoma brucei* can occur in variant surface glycoprotein expression sites lacking 70-base-pair repeat sequences. Mol Cell Biol **17:** 833-843.

McNally, F. J., and J. Rine (1991). A synthetic silencer mediates *SIR*-dependent functions in *Saccharomyces cerevisiae*. Mol Cell Biol **11:** 5648-5659.

Mefford, H. C., E. Linardopoulou, D. Coil, G. van den Engh and B. J. Trask (2001). Comparative sequencing of a multicopy subtelomeric region containing olfactory receptor genes reveals multiple interactions between non-homologous chromosomes. Hum Mol Genet **10:** 2363-2372.

Meijsing, S. H., and A. E. Ehrenhofer-Murray (2001). The silencing complex SAS-I links histone acetylation to the assembly of repressed chromatin by CAF-I and Asf1 in *Saccharomyces cerevisiae*. Genes Dev **15:** 3169-3182.

Melnikova, L., H. Biessmann and P. Georgiev (2005). The ku protein complex is involved in length regulation of *Drosophila* telomeres. Genetics **170:** 221-235.

Meluh, P. B., and J. R. Broach (1999). Immunological analysis of yeast chromatin. Methods Enzymol **304:** 414-430.

Michels, C. A., E. Read, K. Nat and M. J. Charron (1992). The telomere-associated MAL3 locus of *Saccharomyces* is a tandem array of repeated genes. Yeast **8:** 655-665.

Micklem, G., A. Rowley, J. Harwood, K. Nasmyth and J. F. Diffley (1993). Yeast origin recognition complex is involved in DNA replication and transcriptional silencing. Nature **366:** 87-89.

Migeon, B. R. (1994). X-chromosome inactivation: molecular mechanisms and genetic consequences. Trends Genet **10:** 230-235.

Mills, K. D., D. A. Sinclair and L. Guarente (1999). MEC1-dependent redistribution of the Sir3 silencing protein from telomeres to DNA double-strand breaks. Cell **97:** 609-620.

Milne, G. T., S. Jin, K. B. Shannon and D. T. Weaver (1996). Mutations in two Ku homologs define a DNA end-joining repair pathway in *Saccharomyces cerevisiae*. Mol Cell Biol **16:** 4189-4198.

Min, J., Q. Feng, Z. Li, Y. Zhang and R. M. Xu (2003). Structure of the catalytic domain of human *DOT1L*, a non-SET domain nucleosomal histone methyltransferase. Cell **112:** 711-723.

Mishra, K., and D. Shore (1999). Yeast Ku protein plays a direct role in telomeric silencing and counteracts inhibition by rif proteins. Curr Biol **9:** 1123-1126.

Moazed, D., A. Kistler, A. Axelrod, J. Rine and A. D. Johnson (1997). Silent information regulator protein complexes in *Saccharomyces cerevisiae*: a SIR2/SIR4 complex and evidence for a regulatory domain in SIR4 that inhibits its interaction with SIR3. Proc Natl Acad Sci U S A **94:** 2186-2191.

Moazed, D., A. D. Rudner, J. Huang, G. J. Hoppe and J. C. Tanny (2004). A model for step-wise assembly of heterochromatin in yeast. Novartis Found Symp **259:** 48-56; discussion 56-62, 163-169.

Monson, E. K., D. de Bruin and V. A. Zakian (1997). The yeast Cac1 protein is required for the stable inheritance of transcriptionally repressed chromatin at telomeres. Proc Natl Acad Sci U S A **94:** 13081-13086.

Moretti, P., K. Freeman, L. Coodly and D. Shore (1994). Evidence that a complex of SIR proteins interacts with the silencer and telomere-binding protein RAP1. Genes Dev **8:** 2257-2269.

Moretti, P., and D. Shore (2001). Multiple interactions in Sir protein recruitment by Rap1p at silencers and telomeres in yeast. Mol Cell Biol **21:** 8082-8094.

Morse, R. H. (2000). RAP, RAP, open up! New wrinkles for *RAP1* in yeast. Trends Genet **16:** 51-53.

Mukai, T., and M. Sekiguchi (2002). Gene silencing in phenomena related to DNA repair. Oncogene **21:** 9033-9042.

Muller, J. (1995). Transcriptional silencing by the Polycomb protein in *Drosophila* embryos. Embo J **14:** 1209-1220.

Muller, J., S. Gaunt and P. A. Lawrence (1995). Function of the Polycomb protein is conserved in mice and flies. Development **121:** 2847-2852.

Munoz-Jordan, J. L., G. A. Cross, T. de Lange and J. D. Griffith (2001). t-loops at trypanosome telomeres. Embo J **20:** 579-588.

Muren, E., M. Oyen, G. Barmark and H. Ronne (2001). Identification of yeast deletion strains that are hypersensitive to brefeldin A or monensin, two drugs that affect intracellular transport. Yeast **18:** 163-172.

Murti, K. G., and D. M. Prescott (1999). Telomeres of polytene chromosomes in a ciliated protozoan terminate in duplex DNA loops. Proc Natl Acad Sci U S A **96:** 14436-14439.

Myung, K., G. Ghosh, F. J. Fattah, G. Li, H. Kim, A. Dutia, E. Pak, S. Smith and E. A. Hendrickson (2004). Regulation of telomere length and suppression of genomic instability in human somatic cells by Ku86. Mol Cell Biol **24:** 5050-5059.

Nagy, P. L., J. Griesenbeck, R. D. Kornberg and M. L. Cleary (2002). A trithorax-group complex purified from *Saccharomyces cerevisiae* is required for methylation of histone H3. Proc Natl Acad Sci U S A **99:** 90-94.

Nakayama, J., A. J. Klar and S. I. Grewal (2000). A chromodomain protein, Swi6, performs imprinting functions in fission yeast during mitosis and meiosis. Cell **101:** 307-317.

Nakayama, J., J. C. Rice, B. D. Strahl, C. D. Allis and S. I. Grewal (2001). Role of histone H3 lysine 9 methylation in epigenetic control of heterochromatin assembly. Science **292:** 110-113.

Naumov, G. I., E. S. Naumova, E. D. Sancho and M. P. Korhola (1996). Polymeric SUC genes in natural populations of *Saccharomyces cerevisiae*. FEMS Microbiol Lett **135:** 31-35.

Ng, H. H., Q. Feng, H. Wang, H. Erdjument-Bromage, P. Tempst, Y. Zhang and K. Struhl (2002a). Lysine methylation within the globular domain of histone H3 by

Dot1 is important for telomeric silencing and Sir protein association. Genes Dev **16:** 1518-1527.

Ng, H. H., R. M. Xu, Y. Zhang and K. Struhl (2002b). Ubiquitination of histone H2B by Rad6 is required for efficient Dot1-mediated methylation of histone H3 lysine 79. J Biol Chem **277:** 34655-34657.

Nielsen, S. J., R. Schneider, U. M. Bauer, A. J. Bannister, A. Morrison, D. O'Carroll, R. Firestein, M. Cleary, T. Jenuwein, R. E. Herrera and T. Kouzarides (2001). Rb targets histone H3 methylation and HP1 to promoters. Nature **412:** 561-565.

Nishioka, K., S. Chuikov, K. Sarma, H. Erdjument-Bromage, C. D. Allis, P. Tempst and D. Reinberg (2002). Set9, a novel histone H3 methyltransferase that facilitates transcription by precluding histone tail modifications required for heterochromatin formation. Genes Dev **16:** 479-489.

Nislow, C., E. Ray and L. Pillus (1997). *SET1*, a yeast member of the trithorax family, functions in transcriptional silencing and diverse cellular processes. Mol Biol Cell **8:** 2421-2436.

Noma, K., and S. I. Grewal (2002). Histone H3 lysine 4 methylation is mediated by Set1 and promotes maintenance of active chromatin states in fission yeast. Proc Natl Acad Sci U S A **99 Suppl 4:** 16438-16445.

North, B. J., B. L. Marshall, M. T. Borra, J. M. Denu and E. Verdin (2003). The human Sir2 ortholog, SIRT2, is an NAD+-dependent tubulin deacetylase. Mol Cell **11:** 437-444.

Nugent, C. I., G. Bosco, L. O. Ross, S. K. Evans, A. P. Salinger, J. K. Moore, J. E. Haber and V. Lundblad (1998). Telomere maintenance is dependent on activities required for end repair of double-strand breaks. Curr Biol **8:** 657-660.

O'Connor, M. S., A. Safari, D. Liu, J. Qin and Z. Songyang (2004). The human Rap1 protein complex and modulation of telomere length. J Biol Chem **279:** 28585-28591.

Oki, M., and R. T. Kamakaka (2002). Blockers and barriers to transcription: competing activities? Curr Opin Cell Biol **14:** 299-304.

Orlando, V., and R. Paro (1995). Chromatin multiprotein complexes involved in the maintenance of transcription patterns. Curr Opin Genet Dev **5:** 174-179.

Ornaghi, P., P. Ballario, A. M. Lena, A. Gonzalez and P. Filetici (1999). The bromodomain of Gcn5p interacts in vitro with specific residues in the N terminus of histone H4. J Mol Biol **287:** 1-7.

Osada, S., M. Kurita, J. Nishikawa and T. Nishihara (2005). Chromatin assembly factor Asf1p-dependent occupancy of the SAS histone acetyltransferase complex at the silent mating-type locus *HMLalpha*. Nucleic Acids Res **33:** 2742-2750.

Owen, D. J., P. Ornaghi, J. C. Yang, N. Lowe, P. R. Evans, P. Ballario, D. Neuhaus, P. Filetici and A. A. Travers (2000). The structural basis for the recognition of acetylated histone H4 by the bromodomain of histone acetyltransferase gcn5p. Embo J **19:** 6141-6149.

Pak, D. T., M. Pflumm, I. Chesnokov, D. W. Huang, R. Kellum, J. Marr, P. Romanowski and M. R. Botchan (1997). Association of the origin recognition complex with heterochromatin and HP1 in higher eukaryotes. Cell **91:** 311-323.

Palladino, F., T. Laroche, E. Gilson, A. Axelrod, L. Pillus and S. M. Gasser (1993a). SIR3 and SIR4 proteins are required for the positioning and integrity of yeast telomeres. Cell **75:** 543-555.

Palladino, F., T. Laroche, E. Gilson, L. Pillus and S. M. Gasser (1993b). The positioning of yeast telomeres depends on *SIR3*, *SIR4*, and the integrity of the nuclear membrane. Cold Spring Harb Symp Quant Biol **58:** 733-746.

Pamblanco, M., A. Poveda, R. Sendra, S. Rodriguez-Navarro, J. E. Perez-Ortin and V. Tordera (2001). Bromodomain factor 1 (Bdf1) protein interacts with histones. FEBS Lett **496:** 31-35.

Park, E. C., and J. W. Szostak (1990). Point mutations in the yeast histone H4 gene prevent silencing of the silent mating type locus *HML*. Mol Cell Biol **10:** 4932-4934.

Park, J. H., M. S. Cosgrove, E. Youngman, C. Wolberger and J. D. Boeke (2002a). A core nucleosome surface crucial for transcriptional silencing. Nat Genet **32:** 273-279.

Park, M. J., Y. K. Jang, E. S. Choi, H. S. Kim and S. D. Park (2002b). Fission yeast Rap1 homolog is a telomere-specific silencing factor and interacts with Taz1p. Mol Cells **13:** 327-333.

Park, Y., and A. J. Lustig (2000). Telomere structure regulates the heritability of repressed subtelomeric chromatin in *Saccharomyces cerevisiae*. Genetics **154:** 587-598.

Paro, R. (2000). Chromatin regulation. Formatting genetic text. Nature **406:** 579-580.

Parsons, X. H., S. N. Garcia, L. Pillus and J. T. Kadonaga (2003). Histone deacetylation by Sir2 generates a transcriptionally repressed nucleoprotein complex. Proc Natl Acad Sci U S A **100:** 1609-1614.

Perez-Morga, D., A. Amiguet-Vercher, D. Vermijlen and E. Pays (2001). Organization of telomeres during the cell and life cycles of *Trypanosoma brucei.* J Eukaryot Microbiol **48:** 221-226.

Peterson, S. E., A. E. Stellwagen, S. J. Diede, M. S. Singer, Z. W. Haimberger, C. O. Johnson, M. Tzoneva and D. E. Gottschling (2001). The function of a stem-loop in telomerase RNA is linked to the DNA repair protein Ku. Nat Genet **27:** 64-67.

Pich, U., J. Fuchs and I. Schubert (1996). How do *Alliaceae* stabilize their chromosome ends in the absence of TTTAGGG sequences? Chromosome Res **4:** 207-213.

Pillus, L., and J. Rine (1989). Epigenetic inheritance of transcriptional states in *S. cerevisiae*. Cell **59:** 637-647.

Pina, B., J. Fernandez-Larrea, N. Garcia-Reyero and F. Z. Idrissi (2003). The different (sur)faces of Rap1p. Mol Genet Genomics **268:** 791-798.

Pirrotta, V. (1997). Chromatin-silencing mechanisms in *Drosophila* maintain patterns of gene expression. Trends Genet **13:** 314-318.

Pirrotta, V. (1998). Polycombing the genome: PcG, trxG, and chromatin silencing. Cell **93:** 333-336.

Pirrotta, V. (1999). Polycomb silencing and the maintenance of stable chromatin states. Results Probl Cell Differ **25:** 205-228.

Pirrotta, V., and D. S. Gross (2005). Epigenetic silencing mechanisms in budding yeast and fruit fly: different paths, same destinations. Mol Cell **18:** 395-398.

Polotnianka, R. M., J. Li and A. J. Lustig (1998). The yeast Ku heterodimer is essential for protection of the telomere against nucleolytic and recombinational activities. Curr Biol **8:** 831-834.

Porter, S. E., P. W. Greenwell, K. B. Ritchie and T. D. Petes (1996). The DNA-binding protein Hdf1p (a putative Ku homologue) is required for maintaining normal telomere length in *Saccharomyces cerevisiae*. Nucleic Acids Res **24:** 582-585.

Pryde, F. E., H. C. Gorham and E. J. Louis (1997). Chromosome ends: all the same under thier caps. Curr Opin Genet Dev **7:** 822-828.

Pryde, F. E., T. C. Huckle and E. J. Louis (1995). Sequence analysis of the right end of chromosome XV in *Saccharomyces cerevisiae*: an insight into the structural and functional significance of sub-telomeric repeat sequences. Yeast **11:** 371-382.

Pryde, F. E., and E. J. Louis (1997). *Saccharomyces cerevisiae* telomeres. A review. Biochemistry (Mosc) **62:** 1232-1241.

Pryde, F. E., and E. J. Louis (1999). Limitations of silencing at native yeast telomeres. Embo J **18:** 2538-2550.

Ravindra, A., K. Weiss and R. T. Simpson (1999). High-resolution structural analysis of chromatin at specific loci: *Saccharomyces cerevisiae* silent mating-type locus *HMRa*. Mol Cell Biol **19:** 7944-7950.

Rawlins, D. J., and P. J. Shaw (1990). Localization of ribosomal and telomeric DNA sequences in intact plant nuclei by in-situ hybridization and three-dimensional optical microscopy. J Microsc **157 (Pt 1):** 83-89.

Ray, A., and K. W. Runge (1999). The yeast telomere length counting machinery is sensitive to sequences at the telomere-nontelomere junction. Mol Cell Biol **19:** 31-45.

Razin, A., and H. Cedar (1994). DNA methylation and genomic imprinting. Cell **77:** 473-476.

Rea, S., F. Eisenhaber, D. O'Carroll, B. D. Strahl, Z. W. Sun, M. Schmid, S. Opravil, K. Mechtler, C. P. Ponting, C. D. Allis and T. Jenuwein (2000). Regulation of chromatin structure by site-specific histone H3 methyltransferases. Nature **406:** 593-599.

Recillas-Targa, F. (2002). DNA methylation, chromatin boundaries, and mechanisms of genomic imprinting. Arch Med Res **33:** 428-438.

Reddel, R. R. (2003). Alternative lengthening of telomeres, telomerase, and cancer. Cancer Lett **194:** 155-162.

Reifsnyder, C., J. Lowell, A. Clarke and L. Pillus (1996). Yeast SAS silencing genes and human genes associated with AML and HIV-1 Tat interactions are homologous with acetyltransferases. Nat Genet **14:** 42-49.

Renauld, H., O. M. Aparicio, P. D. Zierath, B. L. Billington, S. K. Chhablani and D. E. Gottschling (1993). Silent domains are assembled continuously from the telomere and are defined by promoter distance and strength, and by *SIR3* dosage. Genes Dev **7:** 1133-1145.

Richards, E. J., and S. C. Elgin (2002). Epigenetic codes for heterochromatin formation and silencing: rounding up the usual suspects. Cell **108:** 489-500.

Riethman, H., A. Ambrosini, C. Castaneda, J. Finklestein, X. L. Hu, U. Mudunuri, S. Paul and J. Wei (2004). Mapping and initial analysis of human subtelomeric sequence assemblies. Genome Res **14:** 18-28.

Riha, K., and D. E. Shippen (2003a). Ku is required for telomeric C-rich strand maintenance but not for end-to-end chromosome fusions in *Arabidopsis*. Proc Natl Acad Sci U S A **100:** 611-615.

Riha, K., and D. E. Shippen (2003b). Telomere structure, function and maintenance in *Arabidopsis*. Chromosome Res **11:** 263-275.

Rine, J., and I. Herskowitz (1987). Four genes responsible for a position effect on expression from *HML* and *HMR* in *Saccharomyces cerevisiae*. Genetics **116:** 9-22.

Robzyk, K., J. Recht and M. A. Osley (2000). Rad6-dependent ubiquitination of histone H2B in yeast. Science **287:** 501-504.

Rockmill, B., and G. S. Roeder (1998). Telomere-mediated chromosome pairing during meiosis in budding yeast. Genes Dev **12:** 2574-2586.

Roguev, A., D. Schaft, A. Shevchenko, W. W. Pijnappel, M. Wilm, R. Aasland and A. F. Stewart (2001). The *Saccharomyces cerevisiae* Set1 complex includes an Ash2 homologue and methylates histone 3 lysine 4. Embo J **20:** 7137-7148.

Ronsseray, S., T. Josse, A. Boivin and D. Anxolabehere (2003). Telomeric transgenes and trans-silencing in *Drosophila*. Genetica **117:** 327-335.

Roy, R., B. Meier, A. D. McAinsh, H. M. Feldmann and S. P. Jackson (2004). Separation-of-function mutants of yeast Ku80 reveal a Yku80p-Sir4p interaction involved in telomeric silencing. J Biol Chem **279:** 86-94.

Rubio, J. P., J. K. Thompson and A. F. Cowman (1996). The *var* genes of *Plasmodium falciparum* are located in the subtelomeric region of most chromosomes. Embo J **15:** 4069-4077.

Rundlett, S. E., A. A. Carmen, N. Suka, B. M. Turner and M. Grunstein (1998). Transcriptional repression by *UME6* involves deacetylation of lysine 5 of histone H4 by RPD3. Nature **392:** 831-835.

Rusche, L. N., A. L. Kirchmaier and J. Rine (2002). Ordered nucleation and spreading of silenced chromatin in *Saccharomyces cerevisiae*. Mol Biol Cell **13:** 2207-2222.

Rusche, L. N., A. L. Kirchmaier and J. Rine (2003). The establishment, inheritance, and function of silenced chromatin in *Saccharomyces cerevisiae*. Annu Rev Biochem **72:** 481-516.

Sambrook, J., E. Fritsch and e. al (1989). Molecular cloning; a laboratory manual. Cold Spring Harbor Laboratory, Cold Spring Harbor, New York.

Samper, E., F. A. Goytisolo, P. Slijepcevic, P. P. van Buul and M. A. Blasco (2000). Mammalian Ku86 protein prevents telomeric fusions independently of the length of TTAGGG repeats and the G-strand overhang. EMBO Rep **1:** 244-252.

Sanders, S. L., J. Jennings, A. Canutescu, A. J. Link and P. A. Weil (2002). Proteomics of the eukaryotic transcription machinery: identification of proteins associated with components of yeast TFIID by multidimensional mass spectrometry. Mol Cell Biol **22:** 4723-4738.

San-Segundo, P. A., and G. S. Roeder (2000). Role for the silencing protein Dot1 in meiotic checkpoint control. Mol Biol Cell **11:** 3601-3615.

Santos-Rosa, H., A. J. Bannister, P. M. Dehe, V. Geli and T. Kouzarides (2004). Methylation of H3 lysine 4 at euchromatin promotes Sir3p association with heterochromatin. J Biol Chem **279:** 47506-47512.

Schlichter, A., and B. R. Cairns (2005). Histone trimethylation by Set1 is coordinated by the RRM, autoinhibitory, and catalytic domains. Embo J **24:** 1222-1231.

Schotta, G., A. Ebert, R. Dorn and G. Reuter (2003a). Position-effect variegation and the genetic dissection of chromatin regulation in *Drosophila*. Semin Cell Dev Biol **14:** 67-75.

Schotta, G., A. Ebert and G. Reuter (2003b). *SU(VAR)3-9* is a conserved key function in heterochromatic gene silencing. Genetica **117:** 149-158.

Schultz, J., R. R. Copley, T. Doerks, C. P. Ponting and P. Bork (2000). SMART: a web-based tool for the study of genetically mobile domains. Nucleic Acids Res **28:** 231-234.

Seum, C., M. Delattre, A. Spierer and P. Spierer (2001). Ectopic HP1 promotes chromosome loops and variegated silencing in *Drosophila*. Embo J **20:** 812-818.

Shakibai, N., V. Kumar and S. Eisenberg (1996). The Ku-like protein from *Saccharomyces cerevisiae* is required *in vitro* for the assembly of a stable multiprotein complex at a eukaryotic origin of replication. Proc Natl Acad Sci U S A **93:** 11569-11574.

Shampay, J., and E. H. Blackburn (1988). Generation of telomere-length heterogeneity in *Saccharomyces cerevisiae*. Proc Natl Acad Sci U S A **85:** 534-538.

Shankaranarayana, G. D., M. R. Motamedi, D. Moazed and S. I. Grewal (2003). Sir2 regulates histone H3 lysine 9 methylation and heterochromatin assembly in fission yeast. Curr Biol **13:** 1240-1246.

Sherman, J. M., and L. Pillus (1997). An uncertain silence. Trends Genet **13:** 308-313.

Shi, Y., F. Lan, C. Matson, P. Mulligan, J. R. Whetstine, P. A. Cole and R. A. Casero (2004). Histone demethylation mediated by the nuclear amine oxidase homolog LSD1. Cell **119:** 941-953.

Shia, W. J., S. Osada, L. Florens, S. K. Swanson, M. P. Washburn and J. L. Workman (2005). Characterization of the yeast trimeric-SAS acetyltransferase complex. J Biol Chem **280:** 11987-11994.

Shore, D. (2001). Telomeric chromatin: replicating and wrapping up chromosome ends. Curr Opin Genet Dev **11:** 189-198.

Sibani, S., G. B. Price and M. Zannis-Hadjopoulos (2005). Ku80 binds to human replication origins prior to the assembly of the ORC complex. Biochemistry **44:** 7885-7896.

Sigrist, C. J., and V. Pirrotta (1997). Chromatin insulator elements block the silencing of a target gene by the *Drosophila* polycomb response element (PRE) but allow trans interactions between PREs on different chromosomes. Genetics **147:** 209-221.

Singer, M. S., and D. E. Gottschling (1994). TLC1: template RNA component of *Saccharomyces cerevisiae* telomerase. Science **266:** 404-409.

Singer, M. S., A. Kahana, A. J. Wolf, L. L. Meisinger, S. E. Peterson, C. Goggin, M. Mahowald and D. E. Gottschling (1998). Identification of high-copy disruptors of telomeric silencing in *Saccharomyces cerevisiae*. Genetics **150:** 613-632.

Smith, C. M., Z. W. Haimberger, C. O. Johnson, A. J. Wolf, P. R. Gafken, Z. Zhang, M. R. Parthun and D. E. Gottschling (2002). Heritable chromatin structure: mapping "memory" in histones H3 and H4. Proc Natl Acad Sci U S A **99 Suppl 4:** 16454-16461.

Smith, E. R., A. Pannuti, W. Gu, A. Steurnagel, R. G. Cook, C. D. Allis and J. C. Lucchesi (2000a). The *drosophila* MSL complex acetylates histone H4 at

lysine 16, a chromatin modification linked to dosage compensation. Mol Cell Biol **20:** 312-318.

Smith, J. S., and J. D. Boeke (1997). An unusual form of transcriptional silencing in yeast ribosomal DNA. Genes Dev **11:** 241-254.

Smith, J. S., C. B. Brachmann, I. Celic, M. A. Kenna, S. Muhammad, V. J. Starai, J. L. Avalos, J. C. Escalante-Semerena, C. Grubmeyer, C. Wolberger and J. D. Boeke (2000b). A phylogenetically conserved NAD+-dependent protein deacetylase activity in the Sir2 protein family. Proc Natl Acad Sci U S A **97:** 6658-6663.

Smith, J. S., C. B. Brachmann, L. Pillus and J. D. Boeke (1998). Distribution of a limited Sir2 protein pool regulates the strength of yeast rDNA silencing and is modulated by Sir4p. Genetics **149:** 1205-1219.

Smogorzewska, A., and T. de Lange (2004). Regulation of telomerase by telomeric proteins. Annu Rev Biochem **73:** 177-208.

Stellwagen, A. E., Z. W. Haimberger, J. R. Veatch and D. E. Gottschling (2003). Ku interacts with telomerase RNA to promote telomere addition at native and broken chromosome ends. Genes Dev **17:** 2384-2395.

Strahl, B. D., and C. D. Allis (2000). The language of covalent histone modifications. Nature **403:** 41-45.

Strahl, B. D., R. Ohba, R. G. Cook and C. D. Allis (1999). Methylation of histone H3 at lysine 4 is highly conserved and correlates with transcriptionally active nuclei in *Tetrahymena*. Proc Natl Acad Sci U S A **96:** 14967-14972.

Strahl-Bolsinger, S., A. Hecht, K. Luo and M. Grunstein (1997). SIR2 and SIR4 interactions differ in core and extended telomeric heterochromatin in yeast. Genes Dev **11:** 83-93.

Straight, A. F., W. Shou, G. J. Dowd, C. W. Turck, R. J. Deshaies, A. D. Johnson and D. Moazed (1999). Net1, a Sir2-associated nucleolar protein required for rDNA silencing and nucleolar integrity. Cell **97:** 245-256.

Struhl, K. (1998). Histone acetylation and transcriptional regulatory mechanisms. Genes Dev **12:** 599-606.

Strutt, H., G. Cavalli and R. Paro (1997). Co-localization of Polycomb protein and GAGA factor on regulatory elements responsible for the maintenance of homeotic gene expression. Embo J **16:** 3621-3632.

Suka, N., K. Luo and M. Grunstein (2002). Sir2p and Sas2p opposingly regulate acetylation of yeast histone H4 lysine16 and spreading of heterochromatin. Nat Genet **32:** 378-383.

Suka, N., Y. Suka, A. A. Carmen, J. Wu and M. Grunstein (2001). Highly specific antibodies determine histone acetylation site usage in yeast heterochromatin and euchromatin. Mol Cell **8:** 473-479.

Sun, Z. W., and C. D. Allis (2002). Ubiquitination of histone H2B regulates H3 methylation and gene silencing in yeast. Nature **418:** 104-108.

Sussel, L., and D. Shore (1991). Separation of transcriptional activation and silencing functions of the *RAP1*-encoded repressor/activator protein 1: isolation of viable mutants affecting both silencing and telomere length. Proc Natl Acad Sci U S A **88:** 7749-7753.

Taddei, A., M. R. Gartenberg, F. R. Neumann, F. Hediger and S. M. Gasser (2005). Multiple pathways tether telomeres and silent chromatin at the nuclear periphery: functional implications for sir-mediated repression. Novartis Found Symp **264:** 140-156; discussion 156-165, 227-130.

Taddei, A., F. Hediger, F. R. Neumann, C. Bauer and S. M. Gasser (2004). Separation of silencing from perinuclear anchoring functions in yeast Ku80, Sir4 and Esc1 proteins. Embo J **23:** 1301-1312.

Tamaru, H., and E. U. Selker (2001). A histone H3 methyltransferase controls DNA methylation in *Neurospora crassa*. Nature **414:** 277-283.

Tamkun, J. W., R. Deuring, M. P. Scott, M. Kissinger, A. M. Pattatucci, T. C. Kaufman and J. A. Kennison (1992). brahma: a regulator of *Drosophila* homeotic genes structurally related to the yeast transcriptional activator SNF2/SWI2. Cell **68:** 561-572.

Tan, M., C. Wei and C. M. Price (2003). The telomeric protein Rap1 is conserved in vertebrates and is expressed from a bidirectional promoter positioned between the *Rap1* and *KARS* genes. Gene **323:** 1-10.

Tanaka, S., M. Livingstone-Zatchej and F. Thoma (1996). Chromatin structure of the yeast *URA3* gene at high resolution provides insight into structure and positioning of nucleosomes in the chromosomal context. J Mol Biol **257:** 919-934.

Tate, P. H., and A. P. Bird (1993). Effects of DNA methylation on DNA-binding proteins and gene expression. Curr Opin Genet Dev **3:** 226-231.

Teixeira, M. T., M. Arneric, P. Sperisen and J. Lingner (2004). Telomere length homeostasis is achieved via a switch between telomerase- extendible and -nonextendible states. Cell **117:** 323-335.

Teo, S. H., and S. P. Jackson (2001). Telomerase subunit overexpression suppresses telomere-specific checkpoint activation in the yeast *yku80* mutant. EMBO Rep **2:** 197-202.

Tham, W. H., J. S. Wyithe, P. Ko Ferrigno, P. A. Silver and V. A. Zakian (2001). Localization of yeast telomeres to the nuclear periphery is separable from transcriptional repression and telomere stability functions. Mol Cell **8:** 189-199.

Thoma, F. (1986). Protein-DNA interactions and nuclease-sensitive regions determine nucleosome positions on yeast plasmid chromatin. J Mol Biol **190:** 177-190.

Thoma, F., G. Cavalli and S. Tanaka, 1993 Structural and functional organisation of yeast chromatin, pp. 43-72 in The Eukaryotic Genome, edited by P. M. A. BRODA, S. G. OLIVER and P. I. G. SIMS. Cambridge University Press, Cambridge.

Thompson, J. S., X. Ling and M. Grunstein (1994). Histone H3 amino terminus is required for telomeric and silent mating locus repression in yeast. Nature **369:** 245-247.

Ting, N. S., Y. Yu, B. Pohorelic, S. P. Lees-Miller and T. L. Beattie (2005). Human Ku70/80 interacts directly with hTR, the RNA component of human telomerase. Nucleic Acids Res **33:** 2090-2098.

Tissenbaum, H. A., and L. Guarente (2001). Increased dosage of a *sir-2* gene extends lifespan in *Caenorhabditis elegans*. Nature **410:** 227-230.

Trask, B. J., C. Friedman, A. Martin-Gallardo, L. Rowen, C. Akinbami, J. Blankenship, C. Collins, D. Giorgi, S. Iadonato, F. Johnson, W. L. Kuo, H. Massa, T. Morrish, S. Naylor, O. T. Nguyen, S. Rouquier, T. Smith, D. J. Wong, J. Youngblom and G. van den Engh (1998). Members of the olfactory receptor gene family are contained in large blocks of DNA duplicated polymorphically near the ends of human chromosomes. Hum Mol Genet **7:** 13-26.

Travers, A. A., and A. Klug (1987). The bending of DNA in nucleosomes and its wider implications. Philos Trans R Soc Lond B Biol Sci **317:** 537-561.

Trelles-Sticken, E., J. Loidl and H. Scherthan (1999). Bouquet formation in budding yeast: initiation of recombination is not required for meiotic telomere clustering. J Cell Sci **112 (Pt 5):** 651-658.

Triolo, T., and R. Sternglanz (1996). Role of interactions between the origin recognition complex and *SIR1* in transcriptional silencing. Nature **381:** 251-253.

Tsukamoto, Y., J. Kato and H. Ikeda (1997). Silencing factors participate in DNA repair and recombination in *Saccharomyces cerevisiae*. Nature **388:** 900-903.

Tuteja, R., and N. Tuteja (2000). Ku autoantigen: a multifunctional DNA-binding protein. Crit Rev Biochem Mol Biol **35:** 1-33.

Underwood, A. P., E. J. Louis, R. H. Borts, J. R. Stringer and A. E. Wakefield (1996). *Pneumocystis carinii* telomere repeats are composed of TTAGGG and the subtelomeric sequence contains a gene encoding the major surface glycoprotein. Mol Microbiol **19:** 273-281.

Utley, R. T., K. Ikeda, P. A. Grant, J. Cote, D. J. Steger, A. Eberharter, S. John and J. L. Workman (1998). Transcriptional activators direct histone acetyltransferase complexes to nucleosomes. Nature **394:** 498-502.

van Dekken, H., D. Pinkel, J. Mullikin, B. Trask, G. van den Engh and J. Gray (1989). Three-dimensional analysis of the organization of human chromosome domains in human and human-hamster hybrid interphase nuclei. J Cell Sci **94 (Pt 2):** 299-306.

van Holde, K. E. (1988). Chromatin. Springer-Verlag, New York.

van Leeuwen, F., P. R. Gafken and D. E. Gottschling (2002). Dot1p modulates silencing in yeast by methylation of the nucleosome core. Cell **109:** 745-756.

van Leeuwen, F., and D. E. Gottschling (2002). Genome-wide histone modifications: gaining specificity by preventing promiscuity. Curr Opin Cell Biol **14:** 756-762.

Varley, H., H. A. Pickett, J. L. Foxon, R. R. Reddel and N. J. Royle (2002). Molecular characterization of inter-telomere and intra-telomere mutations in human ALT cells. Nat Genet **30:** 301-305.

Vega-Palas, M. A., E. Martin-Figueroa and F. J. Florencio (2000). Telomeric silencing of a natural subtelomeric gene. Mol Gen Genet **263:** 287-291.

Vega-Palas, M. A., S. Venditti and E. Di Mauro (1997). Telomeric transcriptional silencing in a natural context. Nat Genet **15:** 232-233.

Vega-Palas, M. A., S. Venditti and E. Di Mauro (1998). Heterochromatin organization of a natural yeast telomere. Changes of nucleosome distribution driven by the absence of Sir3p. J Biol Chem **273:** 9388-9392.

Venditti, S., M. A. Vega-Palas and E. Di Mauro (1999a). Heterochromatin organization of a natural yeast telomere. Recruitment of Sir3p through interaction with histone H4 N terminus is required for the establishment of repressive structures. J Biol Chem **274:** 1928-1933.

Venditti, S., M. A. Vega-Palas, G. Di Stefano and E. Di Mauro (1999b). Imbalance in dosage of the genes for the heterochromatin components Sir3p and histone H4 results in changes in the length and sequence organization of yeast telomeres. Mol Gen Genet **262:** 367-377.

Verona, R. I., M. R. Mann and M. S. Bartolomei (2003). Genomic imprinting: intricacies of epigenetic regulation in clusters. Annu Rev Cell Dev Biol **19:** 237-259.

Wach, A., A. Brachat, R. Pohlmann and P. Philippsen (1994). New heterologous modules for classical or PCR-based gene disruptions in *Saccharomyces cerevisiae*. Yeast **10:** 1793-1808.

Wada, M., and Y. Nakamura (1996). Unique telomeric expression site of major-surface-glycoprotein genes of *Pneumocystis carinii*. DNA Res **3:** 55-64.

Wahlin, J., M. Rosen and M. Cohn (2003). DNA binding and telomere length regulation of yeast *RAP1* homologues. J Mol Biol **332:** 821-833.

Walker, J. R., R. A. Corpina and J. Goldberg (2001). Structure of the Ku heterodimer bound to DNA and its implications for double-strand break repair. Nature **412:** 607-614.

Wallrath, L. L., and S. C. Elgin (1995). Position effect variegation in *Drosophila* is associated with an altered chromatin structure. Genes Dev **9:** 1263-1277.

Wang, H., R. Cao, L. Xia, H. Erdjument-Bromage, C. Borchers, P. Tempst and Y. Zhang (2001). Purification and functional characterization of a histone H3-lysine 4-specific methyltransferase. Mol Cell **8:** 1207-1217.

Weiler, K. S., and B. T. Wakimoto (1995). Heterochromatin and gene expression in *Drosophila*. Annu Rev Genet **29:** 577-605.

Weiss, K., and R. T. Simpson (1998). High-resolution structural analysis of chromatin at specific loci: *Saccharomyces cerevisiae* silent mating type locus *HMLalpha*. Mol Cell Biol **18:** 5392-5403.

White, C. L., R. K. Suto and K. Luger (2001). Structure of the yeast nucleosome core particle reveals fundamental changes in internucleosome interactions. Embo J **20:** 5207-5218.

Winston, F., and C. D. Allis (1999). The bromodomain: a chromatin-targeting module? Nat Struct Biol **6:** 601-604.

Winston, F., C. Dollard and S. L. Ricupero-Hovasse (1995). Construction of a set of convenient *Saccharomyces cerevisiae* strains that are isogenic to S288C. Yeast **11:** 53-55.

Wood, A., N. J. Krogan, J. Dover, J. Schneider, J. Heidt, M. A. Boateng, K. Dean, A. Golshani, Y. Zhang, J. F. Greenblatt, M. Johnston and A. Shilatifard (2003a). Bre1, an E3 ubiquitin ligase required for recruitment and substrate selection of Rad6 at a promoter. Mol Cell **11:** 267-274.

Wood, A., J. Schneider, J. Dover, M. Johnston and A. Shilatifard (2003b). The Paf1 complex is essential for histone monoubiquitination by the Rad6-Bre1 complex, which signals for histone methylation by COMPASS and Dot1p. J Biol Chem **278:** 34739-34742.

Workman, J. L., and R. E. Kingston (1998). Alteration of nucleosome structure as a mechanism of transcriptional regulation. Annu Rev Biochem **67:** 545-579.

Wotton, D., and D. Shore (1997). A novel Rap1p-interacting factor, Rif2p, cooperates with Rif1p to regulate telomere length in *Saccharomyces cerevisiae*. Genes Dev **11:** 748-760.

Wright, J. H., D. E. Gottschling and V. A. Zakian (1992). *Saccharomyces* telomeres assume a non-nucleosomal chromatin structure. Genes Dev **6:** 197-210.

Wright, J. H., and V. A. Zakian (1995). Protein-DNA interactions in soluble telosomes from *Saccharomyces cerevisiae*. Nucleic Acids Res **23:** 1454-1460.

Wu, C. (1980). The 5' ends of Drosophila heat shock genes in chromatin are hypersensitive to DNase I. Nature **286:** 854-860.

Wu, L., and F. Winston (1997). Evidence that Snf-Swi controls chromatin structure over both the TATA and UAS regions of the SUC2 promoter in *Saccharomyces cerevisiae*. Nucleic Acids Res **25:** 4230-4234.

Yamada, M., N. Hayatsu, A. Matsuura and F. Ishikawa (1998). Y'-Help1, a DNA helicase encoded by the yeast subtelomeric Y' element, is induced in survivors defective for telomerase. J Biol Chem **273:** 33360-33366.

Yu, Q., R. Qiu, T. B. Foland, D. Griesen, C. S. Galloway, Y. H. Chiu, J. Sandmeier, J. R. Broach and X. Bi (2003). Rap1p and other transcriptional regulators can

function in defining distinct domains of gene expression. Nucleic Acids Res **31:** 1224-1233.

Zakian, V. A. (1996). Structure, function, and replication of *Saccharomyces cerevisiae* telomeres. Annu Rev Genet **30:** 141-172.

Zhang, W., Y. Hayashizaki and B. C. Kone (2004). Structure and regulation of the mDot1 gene, a mouse histone H3 methyltransferase. Biochem J **377:** 641-651.

Zhang, Z., M. K. Hayashi, O. Merkel, B. Stillman and R. M. Xu (2002). Structure and function of the BAH-containing domain of Orc1p in epigenetic silencing. Embo J **21:** 4600-4611.